TESIS DE LA UNIVERSIDAD DE ZARAGOZA

2018 109

Filiberto Ares Asensio

Entanglement entropy in homogeneus, fermionic chains: some results and some conjectures

Departamento
Física Teórica

Director/es
GARCÍA ESTEVE, JOSÉ
FALCETO BLECUA, FERNANDO

ISSN 2254-7606

Prensas de la Universidad
Universidad Zaragoza

ISSN 2254-7606

Universidad Zaragoza
1542

Tesis Doctoral

ENTANGLEMENT ENTROPY IN HOMOGENEUS, FERMIONIC CHAINS: SOME RESULTS AND SOME CONJECTURES

Autor

Filiberto Ares Asensio

Director/es

GARCÍA ESTEVE, JOSÉ
FALCETO BLECUA, FERNANDO

UNIVERSIDAD DE ZARAGOZA

Física Teórica

2018

Departamento de Física Teórica
Facultad de Ciencias, Universidad de Zaragoza

Entanglement entropy in homogeneous, fermionic chains: some results and some conjectures

Filiberto Ares Asensio

PhD thesis supervised by

Dr. Fernando Falceto Blecua and Dr. José V. García Esteve

July 2018

Contents

Agradecimientos

Esta tesis no hubiera sido posible sin la enorme dedicación y ayuda de mis directores, Fernando y Pepe. La gran mayoría de las ideas, al menos las buenas, que aquí se exponen se deben a ellos. Agradezco la guía y la confianza que siempre me han prestado y sus valiosas enseñanzas, no solo en esto de hacer Física, sino en muchas otras cosas; así como la libertad y el ánimo que me han brindado para explorar e investigar nuevos temas fuera del nido familiar. He disfrutado mucho aprendiendo y trabajando codo con codo con vosotros durante estos años y espero seguir haciéndolo, desde donde sea, muchos más.

De igual manera, este agradecimiento es extensible a Amílcar de Queiroz, coautor de buena parte de los artículos en los que se basa esta tesis, cuasisupervisor en el extranjero y compañero de viajes y congresos. Las infinitas y encendidas discusiones delante de una pizarra, o de la barra del bar, han sido claves para entender muchos puntos de la investigación que aquí se presenta. También he de agradecer, a él y a su familia, su hospitalidad durante mis fructíferas estancias en la Universidade de Brasília.

Me gustaría aprovechar estas líneas para dar las gracias a todos y cada uno de los miembros del pasillo de Física Teórica de la Universidad de Zaragoza, lugar donde se ha realizado esta tesis y donde siempre me han hecho sentir como en casa desde que entré como precario. Ha sido un privilegio compartir trabajo y buenos momentos con vosotros. Muy especialmente, a los profesores Manuel Asorey y José Luis Alonso, por sus cualidades tanto humanas como científicas y su generosidad, preocupación e interés. También a Víctor Gopar, Eduardo Follana y Eduardo Royo. Por supuesto, a Pierpaolo Bruscolini y Jesús Clemente, por la confianza que me han dado para ayudarles con la docencia de su asignatura, y a nuestros secretarios, a los que están y a los que han tenido que irse, por su siempre buena sintonía y predisposición.

Thanks to this thesis I have met many wonderful people. Science is a collaborative task and I would like to express my gratitude to all those who have been interested and have discussed with us this work. I really appreciate all the opportunities given to present our research in seminars and workshops. Specially, I thank Zoltán Zimborás very much for his invitation to visit the University College London, and for the crucial role that he played in the first steps of the work presented in Chapter 7 of this thesis. I have to acknowledge the support of Prof. Vladimir Korepin and his hospitality during my stay at Simons Center for Geometry and Physics. I also thank Erik Tonni for his interest and discussions each time that we have met in this small World and for the opportunity to visit SISSA, that sadly I had to cancel because I was immersed in finishing this dissertation.

Finalmente, y no por ello menos importante, a mi familia porque sin su incondicional apoyo todo esto solo hubiera sido sueño.

Esta tesis ha sido realizada gracias al contrato predoctoral para la formación de personal investigador concedido por el Gobierno de Aragón con referencia C070/2014 y cofinanciado por el Fondo Social Europeo. Asimismo, la investigación que aquí se presenta también ha sido parcialmente financiada por los proyectos de investigación FPA2012-35453 y FPA2015-65745-P del Ministerio de Economía y Competitividad (España) y por el Grupo Teórico de Altas Energías (referencias E24/2 y E21_17R) reconocido por el Gobierno de Aragón.

Resumen

El objetivo de esta tesis es el estudio de la entropía de entrelazamiento de Rényi en los estados estacionarios de cadenas de fermiones sin spin descritas por un Hamiltoniano cuadrático general con invariancia translacional y posibles acoplos a larga distancia.

Nuestra investigación se basa en la relación que existe entre la matriz densidad de los estados estacionarios y la correspondiente matriz de correlaciones entre dos puntos. Esta propiedad reduce la complejidad de calcular numéricamente la entropía de entrelazamiento y permite expresar esta magnitud en términos del determinante del resolvente de la matriz de correlaciones.

Dado que la cadena es invariante translacional, la matriz de correlaciones es una matriz *block* Toeplitz. En vista de este hecho, la filosofía que seguimos en esta tesis es la de aprovecharnos de las propiedades asintóticas de este tipo de determinantes para investigar la entropía de entrelazamiento de Rényi en el límite termodinámico. Un aspecto interesante es que los resultados conocidos sobre el comportamiento asintótico de los determinantes *block* Toeplitz no son válidos para algunas de las matrices de correlaciones que consideraremos. Intentando llenar esta laguna, obtenemos algunos resultados originales sobre el comportamiento asintótico de los determinantes de matrices de Toeplitz y *block* Toeplitz.

Estos nuevos resultados combinados con los ya previamente conocidos nos permiten obtener analíticamente el término dominante en la expansión de la entropía de entrelazamiento, tanto para un único intervalo de puntos o *sites* contiguos de la cadena como para subsistemas formados por varios intervalos disjuntos. En particular, descubrimos que los acoplos de largo alcance dan lugar a nuevas propiedades del comportamiento asintótico de la entropía tales como la aparición de un término logarítmico no universal fuera de los puntos críticos cuando los términos de *pairing* decaen siguiendo una ley de potencias o un crecimiento sublogarítmico cuando dichos acoplos decaen logarítmicamente.

El estudio de la entropía de entrelazamiento a través de los determinantes *block* Toeplitz también nos ha llevado a descubrir una nueva simetría de la entropía de entrelazamiento bajo transformaciones de Möbius que pueden verse como transformaciones de los acoplos de la teoría. En particular, encontramos que para teorías críticas esta simetría presenta un intrigante paralelismo con las transformaciones conformes en el espacio-tiempo.

La tesis está organizada de la siguiente manera:

- En el Capítulo 1 introducimos el concepto de entrelazamiento, revisando breve-

mente algunos aspectos históricos así como su relevancia en diferentes áreas de la Física. También definimos la entropía de entrelazamiento de Rényi, examinando sus propiedades más importantes y sus aplicaciones.

- En el Capítulo 2 presentamos los sistemas objeto de nuestra investigación: cadenas fermiónicas cuadráticas y homogéneas. Los resolvemos, obteniendo el espectro y los autoestados del Hamiltoniano. Derivamos la relación entre la entropía de entrelazamiento de Rényi y la matriz de correlaciones entre dos puntos. También calculamos esta última para los estados estacionarios de la cadena.

- El Capítulo 3 se centra en cadenas que no tienen acoplos de *pairing* y, por tanto, el número de partículas en el estado está bien definido. En este caso, la matriz de correlaciones es Toeplitz. Aplicamos la conjetura de Fisher-Hartwig para obtener la expansión asintótica de la entropía de entrelazamiento para un intervalo de la cadena en un estado estacionario cualquiera. Generalizamos este resultado para calcular la entropía de entrelazamiento de un fragmento de una escalera fermiónica.

- En el Capítulo 4 consideramos el caso más general, en el que la cadena contiene términos de *pairing*, y estamos obligados a lidiar con determinantes *block* Toeplitz. Tras revisar los principales resultados conocidos sobre el comportamiento asintótico de este tipo de determinantes, estudiamos el caso de símbolos con discontinuidades de salto, deduciendo su contribución dominante en el determinante. Aplicamos estos resultados al cálculo de la entropía de entrelazamiento para un intervalo en el estado fundamental de la cadena. Como ejemplos particulares, realizamos un análisis detallado de la entropía de entrelazamiento en la cadena de spines XY con acoplo de Dzyaloshinski-Moriya y en una cadena de Kitaev con acoplos de *pairing* de largo alcance.

- En el Capítulo 5 estudiamos la simetría de Möbius de la entropía de entrelazamiento para un único intervalo. Demostramos que para teorías no críticas con acoplos de alcance finito la entropía de entrelazamiento de Rényi del estado fundamental es asintóticamente invariante bajo estas transformaciones. En teorías críticas, encontramos que la entropía no es invariante pero su ley de transformación puede relacionarse con la de un producto de campos homogéneos insertados en los ceros de la relación de dispersión del Hamiltoniano. También extendemos estos resultados a teorías con acoplos de alcance infinito. Finalmente, aplicamos la simetría de Möbius en la cadena de spines XY, descubriendo el origen geométrico de algunas dualidades y relaciones de la entropía de entrelazamiento en este modelo y obteniendo algunas nuevas.

- El Capítulo 6 está dedicado al análisis de la entropía de entrelazamiento para subsistemas de varios intervalos de *sites* disjuntos. Repasamos los resultados que la Teoría de Campos Conforme predice en este caso. A partir de ellos, conjeturamos una expresión asintótica para el determinante de una submatriz principal de una matriz *block* Toeplitz. Aplicando esta conjetura encontramos la expansión de la entropía de entrelazamiento para varios intervalos disjuntos en un estado estacionario cualquiera. También extendemos la simetría de Möbius al caso de varios intervalos y la comparamos con las transformaciones conformes globales en el espacio real.

- En el Capítulo 7 exploramos la posibilidad de que la entropía de entrelazamiento muestre un crecimiento sublogarítmico con la longitud del intervalo en una cadena de

Kitaev con términos de *pairing* que decaen logarítmicamente. Para ello, estudiamos el comportamiento asintótico de determinantes de Toeplitz cuyo símbolo es un caso intermedio entre aquellos que dan lugar a un límite finito y aquellos que inducen un crecimiento lineal con el logaritmo de la dimensión. Para este tipo de símbolos conjeturamos un nuevo comportamiento en el que el logaritmo del determinante diverge a un ritmo inferior que el logaritmo de la dimensión.

- En el Capítulo 8 reunimos y resumimos los principales resultados de la tesis.

También incluimos varios apéndices. En particular, en el Apéndice A damos los detalles sobre los cálculos numéricos que hemos realizado para comprobar las conjeturas analíticas propuestas. El resto de los apéndices tratan sobre algunos puntos que requieren una discusión más técnica que no es necesaria para seguir el texto principal.

Summary

This dissertation is devoted to the study of the Rényi entanglement entropy in the stationary states of chains of spinless fermions described by general, quadratic, translational invariant Hamiltonians with possible long-range couplings.

Our investigation is based on the relation that exists between the density matrix of the stationary states and the two-point correlation matrix. This property reduces the complexity of computing numerically the entanglement entropy and allows to express it in terms of the determinant of the resolvent of the correlation matrix.

Due to the translational invariance of the chain, the correlation matrix is a block Toeplitz matrix. In the light of this fact, the philosophy of the thesis is to take advantage of the asymptotic properties of this kind of determinants to investigate the Rényi entanglement entropy in the thermodynamic limit. An interesting point is that the known results about the asymptotic behaviour of block Toeplitz determinants are not valid for some of the correlation matrices under consideration. We try to fill this gap, obtaining several original results on the asymptotics of Toeplitz and block Toeplitz determinants.

These new results combined with those previously known allow us to determine analytically the leading term in the expansion of the entanglement entropy, both for a single interval of contiguous sites of the chain and for subsystems with disjoint intervals. In particular, we discover that the long-range interactions give rise to some new properties for the asymptotic behaviour of the entropy such as the appearance of a non universal logarithmic term outside the critical points when the pairing couplings decay with a power law or a sublogarithmic growth when they decay logarithmically.

The study of the entanglement entropy in terms of block Toeplitz determinants also leads us to discover a new symmetry of the entanglement entropy under Möbius transformations, that can be viewed as transformations in the couplings of the theory. In particular, we find that, for critical chains, this symmetry shows an intriguing parallelism with conformal transformations in space-time.

The thesis is organized as follows:

- In Chapter 1, we introduce the notion of entanglement, reviewing briefly some historical aspects as well as its relevance in different areas. We also define the Rényi entanglement entropy, examining its main properties and applications.
- In Chapter 2, we present the systems that will be the object of our investigation: quadratic, homogeneous fermionic chains. We solve them, obtaining the spectrum

and the eigenstates of the Hamiltonian. We derive the relation between the Rényi entanglement entropy and the two-point correlation matrix. We also calculate the latter for the stationary states of the chain.

- In Chapter 3, we focus on chains that do not have pairing couplings and, therefore, the number of particles in the state is well-defined. For them, the correlation matrix is Toeplitz. We apply the Fisher-Hartwig conjecture to obtain the asymptotic expansion of the Rényi entanglement entropy for an interval of the chain in any stationary state. We generalize this result to compute the entanglement entropy for a fragment of a fermionic ladder.

- In Chapter 4, we consider the full general situation in which the chain contains pairing couplings and one is forced to deal with block Toeplitz determinants. After reviewing the main known results on the asymptotics of this kind of determinants, we study the case of symbols with jump discontinuities, deriving their leading contribution to the determinant. We apply these results to the computation of the ground state entanglement entropy for an interval. As particular examples, we perform an exhaustive analysis of the entanglement entropy in the XY spin chain with a Dzyaloshinski-Moriya coupling and in a Kitaev chain with long-range pairing.

- In Chapter 5, we study the Möbius symmetry of the entanglement entropy for a single interval. We show that for non critical chains with finite-range coupling the ground state Rényi entanglement entropy is asymptotically invariant under these transformations. For critical theories, we find that the entropy is not invariant but its transformation law can be related to that of a product of homogeneous fields inserted at the zeros of the dispersion relation of the Hamiltonian. We extend these results to theories with infinite-range couplings. We apply the Möbius symmetry in the XY spin chain, uncovering the geometrical origin of some dualities and relations for the entanglement entropy in this model and obtaining new ones.

- Chapter 6 is dedicated to the analysis of the entanglement entropy for subsystems made up of several disjoint intervals. We recall the results that Conformal Field Theory predicts in this case. Using them, we conjecture an asymptotic expression for the determinant of a principal submatrix of a block Toeplitz matrix. We apply it to obtain the expansion of the entanglement entropy for several disjoint intervals in any stationary state of the chain. We extend the Möbius symmetry to several disjoint intervals, comparing it with global conformal transformations in real space.

- In Chapter 7, we explore the possibility that the entanglement entropy displays a sublogarithmic growth with the length of the interval in a Kitaev chain with logarithmic decaying pairing. For this purpose, we study the asymptotics of Toeplitz determinants whose symbol is intermediate between those that provide a finite asymptotic limit and those that induce a linear growth with the logarithm of the dimension. We conjecture that a new behaviour emerges in which the logarithm of the determinant diverges at a rate smaller than the logarithm of the dimension.

- In Chapter 8, we collect and summarize the main results of the thesis.

We also include several appendices. In particular, in Appendix A we describe the details about the numerical calculations performed to give support to our analytical conjectures.

The rest of appendices refer to some points that require a more technical discussion that is not necessary to follow the main text.

Part of the research presented in this dissertation has been published in the following articles:

- F. Ares, J. G. Esteve, F. Falceto, E. Sánchez-Burillo,
  Excited state entanglement in homogeneous fermionic chains,
  J. Phys. A: Math. Theor. 47 245301 (2014), arXiv: 1401.5922 [quant-ph]
- F. Ares, J. G. Esteve, F. Falceto,
  Entanglement of several blocks in fermionic chains,
  Phys. Rev. A 90, 062321 (2014), arXiv: 1406.1668 [quant-ph]
- F. Ares, J. G. Esteve, F. Falceto,
  Rényi entanglement entropy in fermionic chains,
  Int. J. Geom. Methods Mod. Phys. 12, 1560002 (2015)
- F. Ares, J. G. Esteve, F. Falceto, A. R. de Queiroz,
  Entanglement in fermionic chains with finite range coupling and broken symmetries,
  Phys. Rev. A 92, 042334 (2015), arXiv: 1506.06665 [quant-ph]
- F. Ares, J. G. Esteve, F. Falceto, A. R. de Queiroz,
  On the Möbius transformation in the entanglement entropy of fermionic chains,
  J. Stat. Mech. 043106 (2016), arXiv: 1511.02382 [math-ph]
- F. Ares, J. G. Esteve, F. Falceto, A. R. de Queiroz,
  Complex Geometry in the Entanglement Entropy of Fermionic Chains,
  Int. J. Geom. Methods Mod. Phys. 14, 1740010 (2017)
- F. Ares, J. G. Esteve, F. Falceto, A. R. de Queiroz,
  Entanglement entropy and Möbius transformations for critical fermionic chains,
  J. Stat. Mech. 063104 (2017), arXiv: 1612.07319 [quant-ph]
- F. Ares, J. G. Esteve, F. Falceto, A. R. de Queiroz,
  Entanglement entropy in the Long-Range Kitaev chain,
  Phys. Rev. A 97, 062301 (2018), arXiv: 1801.07043 [quant-ph]

Chapter 1

Introduction

Quantum Mechanics describes Nature at the most fundamental level. It was born a century ago to account for some experimental results that Classical Physics could not explain. So far it has had an outstanding success, from the Standard Model to the transistor, representing the theoretical paradigm for Physics at small scales. The development of Quantum Mechanics implied a radical change. It modified completely our way of understanding and explaining the natural phenomena with respect to the vision given by Classical Physics, introducing notions that defy our intuition.

The crucial property that makes the quantum world different from the classical one is *entanglement*. As Schrödinger already recognized in [1, 2], entanglement *is not one but rather the characteristic trait of Quantum Mechanics, the one that enforces its entire departure from the classical lines of thought*. It is Schrödinger himself who introduced in the mentioned works the German term *Verschränkung* (entanglement) to account for the apparently paradoxical fact that in Quantum Mechanics *the best possible knowledge of a whole does not necessarily include the best possible knowledge of its parts*.

We can see this property considering two different particles X and Y of spin $1/2$. Regarding their spin, the space of states of each particle is $\mathbb{C}^2$. Then the space of states of the full system is the tensor product of the space for each particle, $\mathbb{C}^2 \otimes \mathbb{C}^2$. Let $|\uparrow\rangle_j$, $|\downarrow\rangle_j$ be respectively the states of the particle j, with $j = X, Y$, for which the third component of the spin is $+1/2$ and $-1/2$ (in units of $\hbar$).

A possible state of the total system is

$$|\uparrow\rangle_X \otimes |\downarrow\rangle_Y .$$

Here we know that the spin third component of the particle X is $+1/2$ while that of the particle Y is $-1/2$. This is a non entangled or *separable state*. It is the product of the state up for the first spin and the state down for the second one. In this case we have a full knowledge of the whole and also of the parts.

But, since the space of states admits the superposition principle, the full system can also be described by

$$\frac{1}{\sqrt{2}} \left(|\uparrow\rangle_X \otimes |\downarrow\rangle_Y + |\downarrow\rangle_X \otimes |\uparrow\rangle_Y \right) , \tag{1.1}$$

which means that, in spite of a complete knowledge of the state for the whole system, we have not the slightest idea of the state for the parts. This is an example of an *entangled state* which cannot be expressed as the product of a state for the particle X and a state for the particle Y.

A striking feature of entangled states is the following: if we measure the spin third component of the particle X in a system described by the state in (1.1), the possible outcomes after the measurement are

$$|\uparrow\rangle_X \otimes |\downarrow\rangle_Y , \quad \text{or} \quad |\downarrow\rangle_X \otimes |\uparrow\rangle_Y ,$$

and the result is completely random, each one with a 50% probability. But observe that there is a correlation between the result of measuring the spin third component of X and that of Y. In fact, whenever we obtain $+1/2$ for the spin of X, the result of the eventual measurement of the spin of Y will be necessarily $-1/2$ and viceversa. Therefore, the value obtained when we measure the spin of X determines instantaneously the value that we will obtain for the spin of the particle Y. To add more mystery to the theory (and make events in Nature causally related), it can be shown [3] that this instantaneous effect cannot be employed to transmit any information.

A qubit of History

Schrödinger introduced the term entanglement in a response to the famous paper [4] by Einstein, Podolski and Rosen. The correlation that entanglement establishes between particles that can be separated even by a space-like interval bothered Einstein, for whom this was *a spooky action at a distance* in his own words. In the article with Podolski and Rosen, they employed these correlations to argue that Quantum Mechanics gives an incomplete description of physical reality, defending the necessity of a theory that removes the intrinsic indeterminism of the quantum theory.

This work motivated the development of the so called hidden-variable theories. These theories try to get rid of quantum indeterminism adding some extra parameters (hidden variables). Then the randomness of the result after a measurement would arise because these extra parameters are actually ignored by the experimentalist. Therefore, according to these theories, quantum probabilities should be treated as a statistical ensemble, like in classical statistical mechanics.

The study of entanglement was relegated to this kind of works on the foundations of quantum theory during most of the XXth century. A milestone was the paper [5] that Bell published in 1964. He found that in the theories with local hidden variables the correlations between observables must satisfy some inequalities (Bell inequalities) that are violated by entangled states. This result enforced entanglement as the distinctive feature of quantum theory as Schrödinger stated, and opened the way for an experimental test of its fundamental principles. A measurement of the violation of the Bell inequalities with entangled states would discard the local hidden-variable theories in favour of Quantum Mechanics.

In 1972 Freedman and Clauser [6] gave the first strong experimental evidence against local hidden-variable theories measuring the linear polarization correlation between the en-

tangled photons emitted in an atomic cascade of calcium. During the subsequent decade, the group of Aspect [7] improved the experimental set-up, obtaining convincing results on the violation of Bell inequalities. Later, more complex and refined experiments have arrived at the same conclusions. However, one could pose arguments (loopholes) about the experimental set-up or the design of the experiment that would affect the validity of the results, opening a window to maintain the hidden variables. In 2015, three independent experiments [8, 9, 10] claimed to be loophole-free, imposing strong restrictions to a possible hidden-variable theory. The sophistication reached by this kind of experiments is such that, last year, a Chinese group led by Pan performed a successful Bell test [11] between entangled photons sent from a satellite to two stations separated 1200 km.

The importance of entanglement

Since the 90s, entanglement is not a mere issue on the foundations of the theory but it has become one of the main characters of the Physics scene. The inflection point was to recognise that entanglement is a fundamental physical resource as real as energy [12]. It is the essential ingredient to perform tasks that are classically impossible or very inefficient. For instance the simulation of quantum systems. As Feynman pointed out in 1982 [13], *Nature is not classical, and if you want to make a simulation of Nature, you would better make it quantum mechanical*, rather than with a classical computer.

A prominent research field in this direction is Quantum Information and Computation [14]. It studies the transmission and processing of information using the laws of Quantum Mechanics. Entanglement is precisely the property that makes the quantum computation to overtake the classical one. It provides the computational speed-up in quantum algorithms as compared to algorithms based on the processes of Classical Physics [15]. It is also present in processes like quantum teleportation, quantum cryptography, quantum error correction, or superdense coding to cite some of them [12, 16]. As a sample of the rapid development of this area we can mention the experiment [17] of Zeilinger's group in 2012 in which they were able to teleportate a state between two entangled photons separated 143 km.

The relevance of entanglement as well as the methods to deal with it have spread from quantum information to other areas of Physics such as quantum optics, condensed matter or high energy physics. It has been recognised as a crucial concept in many fields. Specially in the arena of strongly correlated quantum many-body systems. See for instance the reviews [18, 19] and the special issue [20] of *Journal of Physics A* on this topic. The ground state of these systems is often highly entangled. The presence of entanglement gives rise to complex correlations between the parts of the system. The form of these correlations leads to different phases and collective phenomena such as topological order, quantum spin liquids, superconductivity, quantum Hall effect, disordered systems, etc. Some of these phases, for instance the topological ones, cannot be distinguished by any local order parameter. As Kitaev and Preskill showed for topological order in Ref. [21], the study of entanglement provides appropriate tools that can detect the global features that distinguish one phase from another.

In addition, quantum many-body systems may undergo a quantum phase transition in

which the ground state of the system qualitatively changes. These transitions are induced by the variation of a parameter of the Hamiltonian at zero temperature. While classical phase transitions are governed by thermal fluctuations, quantum phase transitions are driven by fluctuations of quantum nature. At the quantum critical point the correlation length of the system may diverge. As the pioneer works [22, 23, 24] found, the increasing of the entanglement in the ground state is a signal of long-range correlations at criticality. Subsequent works have shown that entanglement can be used as a suitable order parameter for quantum phase transitions that allows to extract some universal parameters.

From a more practical point of view, as it was predicted by Feynman, the presence of entanglement makes difficult to deal with quantum many-body systems using a classical computer. For example, the Density Matrix Renormalization Group (DMRG) algorithm [25] works well in non critical one dimensional systems, but it becomes very inefficient when we approach a quantum critical point. In this case the growth of the entanglement originates long-range correlations that increase the complexity of simulating the system. Therefore, it is necessary to construct algorithms that implement the entanglement in a proper way. This is the case of the Multiscale Entanglement Renormalization Ansatz (MERA) [26] or the Projected Entangled Pair States (PEPS) method [27], designed with entanglement in mind. These methods are based on tensor network techniques [28] that try to capture the essential properties of the state's entanglement.

Those theoretical studies have been stimulated by a spectacular development of experiments with cold ion traps [29] or polar molecules [30] that reproduce these models in the laboratory (quantum simulators). For example, the group of Monroe has recently been able to trap and control a chain of 53 Yb^+ ions and simulate a quantum phase transition in a quantum Ising model with long-range interactions [31].

Ion traps are in fact one of the most promising physical supports for the design of a universal scalable quantum computer [32, 29]. From this perspective, one has to take into account that, at the end of the day, a quantum computer is no more than a quantum many-body system that can be controlled and manipulated. In particular, the ability of controlling parts or subsystems of a quantum system is crucial in the development of a quantum computer. Such ability presupposes the control of local operations on parts of the system and its effects due to the entanglement with the rest.

The above points make clear the necessity of a profound comprehension of the entanglement in quantum many-body systems. This task is far from being complete, in spite of the great effort done in the last two decades.

That is the main motivation for the research carried out in this thesis. To be precise, we shall study the entanglement in a particular kind of quantum many-body systems: translational invariant quadratic fermionic chains. The analysis of the entanglement in these systems has received a lot of attention in the last years. Nonetheless, as we shall see, there are still several issues that we do not understand. In spite of their apparent simplicity, in these solvable models the entanglement shows many non-trivial properties and leads to a very rich and sophisticated mathematical structure.

In order to characterize it we have to choose an appropriate quantity that gives the degree of entanglement between the different parts of the system. Any entanglement mea-

sure must be a real function of the state that vanishes when it is separable. Moreover, it should not grow on average under operations that do not increase the degree of entanglement (the so called LOCC, local unitary transformations and classical communications, e.g. to call by phone or to send a mail). There are many proposed measures, each one is adequate under different circumstances. A nice introduction to entanglement measures is Ref. [33].

In this thesis we shall consider a fermionic chain in a stationary state and divide it in two subsystems, i.e. a bipartite system in a pure state. For this situation, the canonical quantity that gives the degree of entanglement between the two subsystems is the Rényi entanglement entropy. We shall introduce it in the following section.

1.1 Rényi entanglement entropy

As we just said, in the following chapters we shall consider bipartite quantum systems. That is, quantum systems that can be divided into two parts X and Y such that the Hilbert space of states $\mathcal{H}$ of the full system is written as the tensor product of the two subsystems,

$$\mathcal{H} = \mathcal{H}_X \otimes \mathcal{H}_Y,$$

that we shall take finite dimensional.

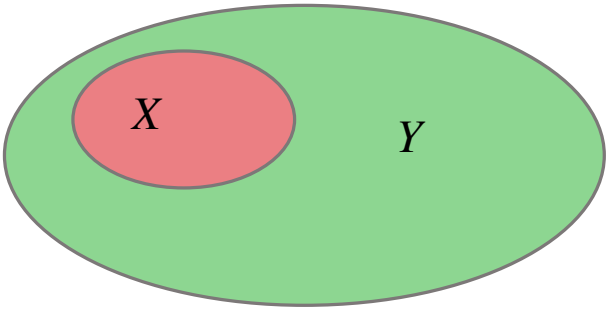

Figure 1.1: A bipartite quantum system can be divided into two parts X and Y such that the Hilbert space of states $\mathcal{H}$ of the full system $X \cup Y$ is factorized as $\mathcal{H} = \mathcal{H}_X \otimes \mathcal{H}_Y$.

When we consider this bipartition, every normalized vector $|\Psi\rangle \in \mathcal{H}$, that represents a pure state of the full system, can be written according to the Schmidt decomposition

$$|\Psi\rangle = \sum_{n=1}^{r} \sqrt{c_n}\, |n\rangle_X \otimes |n\rangle_Y \,, \tag{1.2}$$

where $\{|n\rangle_X\}$ and $\{|n\rangle_Y\}$ are respectively an orthonormal basis of $\mathcal{H}_X$ and $\mathcal{H}_Y$. The coefficients c_n are real numbers lying on the interval $(0, 1]$ and satisfy

$$\sum_{n=1}^{r} c_n = 1.$$

The upper limit r in the sum is called the Schmidt rank of $|\Psi\rangle$ and it satisfies $r \leq d \equiv \min\{\dim\mathcal{H}_X, \dim\mathcal{H}_Y\}$. The Schmidt decomposition of $|\Psi\rangle$ is unique except for the possible degeneracy of the coefficients.

We say that the state $|\Psi\rangle$ is *separable* if $r = 1$ and, therefore, it can be expressed as a product

$$|\Psi\rangle = |\varphi_X\rangle \otimes |\varphi_Y\rangle \,,$$

with $|\varphi_X\rangle$ and $|\varphi_Y\rangle$ two vectors in $\mathcal{H}_X$ and $\mathcal{H}_Y$ respectively. Otherwise, if $r > 1$, the state $|\Psi\rangle$ is *entangled* and

$$|\Psi\rangle \neq |\varphi_X\rangle \otimes |\varphi_Y\rangle \,.$$

Therefore, the Schmidt rank provides a first quantifier for the degree of entanglement of a pure state. The problem is that it is too rough. For example, suppose two states $|\Psi^{(1)}\rangle$ and $|\Psi^{(2)}\rangle$ with an equal Schmidt rank $r = 2$ but different decomposition. For $|\Psi^{(1)}\rangle$ we have $c_1^{(1)} = 0.99$ and $c_2^{(1)} = 0.01$ while for $|\Psi^{(2)}\rangle$, $c_1^{(2)} = 0.50$ and $c_2^{(2)} = 0.50$. It is clear that the state $|\Psi^{(1)}\rangle$ is closer to a separable state and, in a sense, less entangled than the state $|\Psi^{(2)}\rangle$, while both share the same Schmidt rank.

As we anticipated before, a more accurate way to quantify the degree of entanglement in this case is using the Rényi entanglement entropy. In order to define it, we should introduce the density matrix of the full state $\rho = |\Psi\rangle \langle\Psi|$.

In the bipartite system, the state of the subsystems X and Y is described respectively by the reduced density matrices

$$\rho_X = \mathrm{Tr}_{\mathcal{H}_Y}(\rho), \quad \rho_Y = \mathrm{Tr}_{\mathcal{H}_X}(\rho),$$

that are obtained by taking the partial trace of ρ in the corresponding complementary subsystem.

Employing the Schmidt decomposition (1.2) of $|\Psi\rangle$, the density matrix $\rho = |\Psi\rangle \langle\Psi|$ can be written as

$$\rho = \sum_{m,n=1}^{r} \sqrt{c_m c_n} (|m\rangle_X |m\rangle_Y)({}_X\langle n| \, {}_Y\langle n|). \tag{1.3}$$

If we take now the partial trace in the space $\mathcal{H}_Y$, we find

$$\rho_X = \mathrm{Tr}_{\mathcal{H}_Y}(\rho) = \sum_{n=1}^{r} c_n |n\rangle_X \langle n| \,. \tag{1.4}$$

Notice that when $r = 1$, $|\Psi\rangle$ is separable, and the reduced density matrix ρ_X corresponds to a pure state, $\rho_X = |\varphi_X\rangle \langle\varphi_X|$.

On the contrary, if $r > 1$, $|\Psi\rangle$ is entangled, and ρ_X corresponds to a mixed state, a statistical ensemble of the pure states $\{|n\rangle_X\}$ with probabilities $\{c_n\}$.

In Physics, the standard quantity that measures the lack of knowledge of a system in a mixed state is the entropy. Let us introduce the *Rényi entropy of* ρ_X

$$S_{\alpha,X} = \frac{1}{1-\alpha} \log \mathrm{Tr}(\rho_X^\alpha) \tag{1.5}$$

where $\alpha \geq 1$. The limit $\alpha \to 1$,

$$S_{1,X} = -\lim_{\alpha \to 1} \frac{\partial}{\partial \alpha} \log \mathrm{Tr}(\rho_X^\alpha),$$

gives the *von Neumann entropy of* ρ_X

$$S_{1,X} = -\operatorname{Tr}(\rho_X \log \rho_X). \tag{1.6}$$

If we now substitute ρ_X by (1.4) in the definition of the Rényi entropy (1.5), we find

$$S_{\alpha,X} = \frac{1}{1-\alpha} \log \left(\sum_{n=1}^{r} c_n^{\alpha} \right). \tag{1.7}$$

In information theory the latter corresponds to the entropy that Rényi introduced in [34] for a discrete probability distribution, defined in this case by the Schmidt coefficients $\{c_n\}$.

We can do the same for the von Neumann entropy (1.6), expressing ρ_X as in (1.4) we have

$$S_{1,X} = -\sum_{n=1}^{r} c_n \log c_n. \tag{1.8}$$

This is, in information theory, the Shannon entropy of the discrete probability distribution defined by the Schmidt coefficients $\{c_n\}$.

Notice that if we take in (1.3) the partial trace in $\mathcal{H}_X$, instead of $\mathcal{H}_Y$ as above, we obtain

$$\rho_Y = \operatorname{Tr}_{\mathcal{H}_X}(\rho) = \sum_{n=1}^{r} c_n \left|n\right\rangle_Y \left\langle n\right|.$$

If we compute the Rényi entropy of ρ_Y we arrive at

$$S_{\alpha,Y} = \frac{1}{1-\alpha} \log \operatorname{Tr}(\rho_Y^{\alpha}) = \frac{1}{1-\alpha} \log \left(\sum_{n=1}^{r} c_n^{\alpha} \right) = S_{\alpha,X}.$$

That is, $S_{\alpha,Y} = S_{\alpha,X}$ provided the full system is in a pure state $|\Psi\rangle$. The same happens with the von Neumann entropy. This is in general not true if the full system is in a mixed state, for example when it is at a certain temperature.

Observe now that from (1.7) and (1.8) one can conclude that, due to the properties of the Schmidt coefficients c_n, $S_{\alpha,X} = 0$ if an only if the state $|\Psi\rangle$ is separable, while $S_{\alpha,X} > 0$ if it is entangled. Notice that in any case the entropy of the full system is zero since it is in a pure state.

The highest value for $S_{\alpha,X}$ is attained when all the Schmidt coefficients are equal, $c_1 = c_2 = \cdots = c_d = 1/d$. In this situation, ρ_X corresponds to the most mixed state,

$$\rho_X = \frac{1}{d} I_d,$$

where I_d is the identity matrix of dimension d. In this case, the state $|\Psi\rangle$ is maximally entangled. Thus the entropy $S_{\alpha,X}$ satisfies the bounds

$$0 \leq S_{\alpha,X} \leq \log d,$$

and it only vanishes when the state is separable.

In conclusion, $S_{\alpha,X}$ provides an accurate measure for the entanglement of a bipartite system in a pure state. This was first noted by Bennett, Bernstein, Popescu and Schumacher in Ref. [35]. In the following, we shall denominate $S_{\alpha,X}$ the Rényi entanglement entropy or simply the entanglement entropy.

We could only consider the von Neumann entanglement entropy, but it is worth studying the Rényi entropy. If we know $S_{\alpha,X}$ for any α we can reconstruct the spectrum of the reduced density matrix ρ_X. This determines ρ_X up to a unitary transformation. The spectrum of ρ_X is known in the literature as *entanglement spectrum*, term coined by Li and Haldane in [36]. In recent times the entanglement spectrum has attracted much attention because it allows to extract more information about the system than the von Neumann entanglement entropy, see for instance Refs. [37, 38, 39, 40, 41, 42, 43, 44].

As we emphasized at the beginning, the notion of entanglement accounts for the fact that the knowledge of the parts may be non complete even if we perfectly know the state of the whole quantum system. Here we have seen this for a general bipartite system in a pure state. We have found that if it is entangled then the parts are described by a statistical mixture. Thus, since the entropy measures the degree of ignorance about a system, the presence of entanglement implies that the entropy of the parts is larger than the entropy of the full system (that it is actually zero since it is in a pure state),

$$S_{\alpha,X} \geq S_{\alpha,X\cup Y} = 0,$$

where the equality is satisfied when the state of the full system is separable.

Schrödinger claimed that entanglement is the characteristic trait of Quantum Mechanics. In fact, let us repeat the previous discussion but considering a classical statistical system made up of two parts $X \cup Y$. In this case, there is a lack of knowledge about the system because several microscopically different configurations may correspond to the same values for the macroscopic state variables. Therefore, if $\mathcal{P}_X$ and $\mathcal{P}_Y$ are respectively the space of configurations of the subsystems X and Y, the full system is characterized by the set

$$\{p_{i,j} \mid i \in \mathcal{P}_X,\ j \in \mathcal{P}_Y\},$$

where $p_{i,j}$ is the probability that X is in the configuration i and Y in the configuration j.

Then the probability for the subsystem X of being in the configuration $i \in \mathcal{P}_X$ is

$$p_i = \sum_{j\in\mathcal{P}_Y} p_{i,j}. \tag{1.9}$$

Now we can use the entropy to measure the degree of knowledge that we have about the system and its parts. The classical analogue of the von Neumann entropy is the Gibbs entropy. The Gibbs entropy of the full system $X \cup Y$ is

$$S^{\mathrm{G}}_{X\cup Y} = -\sum_{i,j} p_{i,j} \log p_{i,j},$$

and the Gibbs entropy of subsystem X is

$$S^{\mathrm{G}}_{X} = -\sum_{i\in\mathcal{P}_X} p_i \log p_i.$$

If in the latter entropy we replace p_i by (1.9), it is clear that we have

$$S_X^{\mathrm{G}} = -\sum_{i,j} p_{i,j} \log \left(\sum_{j'} p_{i,j'} \right) \leq -\sum_{i,j} p_{i,j} \log p_{i,j} = S_{X\cup Y}^{\mathrm{G}}$$

since the logarithm is a monotone increasing function and, therefore,

$$\log \sum_{j'\in\mathcal{P}_Y} p_{i,j'} \geq \log p_{i,j}.$$

In conclusion,

$$S_X^{\mathrm{G}} \leq S_{X\cup Y}^{\mathrm{G}}.$$

This implies that classically the knowledge of the subsystem X is always better (or equal) than the knowledge of the whole, $X \cup Y$. Just the contrary of what we have obtained above for a quantum system: while the entropy of the full quantum system in a pure state vanishes, the entropy of the parts is non-zero when there is entanglement.

1.2 Applications of the Rényi entanglement entropy

The Rényi entanglement entropy is a really powerful tool. It provides useful information about the state under consideration. Moreover, it establishes very suggestive and unexpected connections between ideas from different fields.

In order to calculate the entanglement entropy we need to divide the quantum system into two parts, X and Y. When we are dealing with a many-body system, such as the lattice of Fig. 1.2, a central question is to study how the entanglement entropy depends on the size of the chosen division. Indeed this will be one of the main objectives in our analysis of the entanglement entropy for fermionic chains.

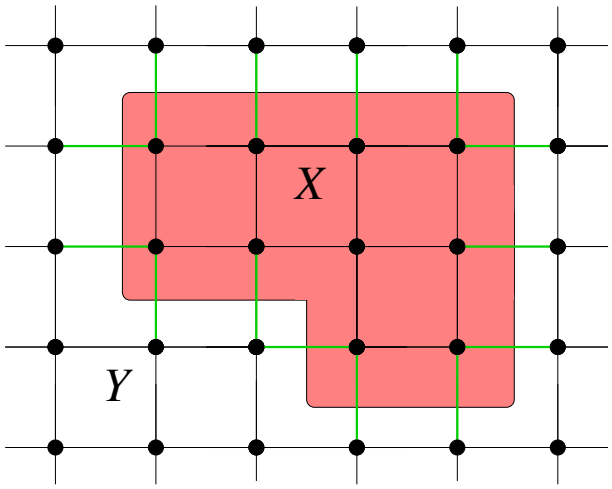

Figure 1.2: Quantum many-body system made of a bidimensional lattice. On each site n of the lattice we define a system (as a spin, a fermion or bosons) with a space of states $\mathcal{H}_n$. Then the Hilbert space of the full system is $\mathcal{H} = \bigotimes_n \mathcal{H}_n$. The links represent the interactions between the systems defined on the sites. In this case there are only nearest neighbour interactions. To compute the entanglement entropy we have to divide the lattice into two subsystems X (coloured) and Y such that $\mathcal{H} = \mathcal{H}_X \otimes \mathcal{H}_Y$. The entanglement entropy of the ground state often verifies an area law: it grows with the number of bonds broken (in green) when we separate X and Y.

In Thermodynamics we learn that the usual thermal entropy is an extensive quantity. It is proportional to the volume of the subsystem. Such a behaviour is commonly referred to as a *volume law*. However, it turns out that the entanglement entropy often follows an *area law*. That is, it is proportional to the border that separates the two subsystems X and Y, as it is illustrated in Fig. 1.2.

The first example of an entropy that satisfies an area law was the Bekenstein-Hawking entropy for a black hole. In 1973 Bekenstein suggested [45], and shortly later Hawking proved [46], that the entropy of a black hole is proportional to the area of its event horizon.

In 1986, trying to understand better the Bekenstein-Hawking entropy, Bombelli, Lee, Koul and Sorkin considered in [47] a real scalar field and computed the von Neumann entropy of the reduced density matrix obtained by tracing out a region of the space. They found that this entropy verifies an area law too. Their result not only revealed that entanglement may play a role in the black hole physics, but also showed that the area law does not restrict to the black hole entropy.

In fact, in 2007, Hastings established in [48] that, for the ground state of one dimensional Hamiltonians with mass gap and finite-range interactions, the entanglement entropy follows an area law. In a unidimensional system, like that in Fig. 1.3, the area law translates into the saturation of the entanglement entropy for large subsystems to a constant value that depends on the correlation length. Later it was set in [49, 50] that any state in one dimension with an exponential decay of the correlations, as the ground state of theories with mass gap and finite-range interactions, must satisfy an area law.

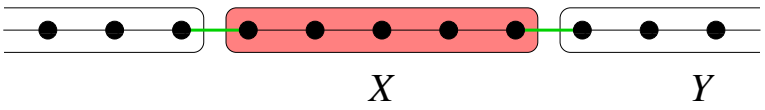

Figure 1.3: In this chain the boundary between the subsystems X and Y (green bonds) is independent from their sizes. This means that the entanglement entropy follows an area law if it tends to a constant value when the length of the intervals is large enough.

On the other hand, if the mass gap becomes zero, the correlation length diverges and the ground state correlation functions decay algebraically. A symmetry of these systems is conformal invariance. This symmetry has been extensively studied in the context of 1+1 dimensional quantum field theory since Belavin, Polyakov, and Zamalodchikov recognised it as a powerful tool to determine the correlation functions of non trivial massless theories [51]. The techniques of Conformal Field Theory (CFT) have been extensively applied to the study of the entanglement entropy. In particular, in the pioneer works of Holzhey, Larsen and Wilczek [52] and Calabrese and Cardy [53] it is found that, for the ground state of gapless local Hamiltonians in one dimension, the area law is corrected by a logarithmic term. In the thermodynamic limit they obtain

$$S_{\alpha,X} \sim \frac{\alpha+1}{6\alpha} \mathrm{c} \log |X|, \tag{1.10}$$

where $|X|$ is the length of the subsystem X, like that of Fig. 1.3, and c is the central charge of the underlying CFT. The central charge is a characteristic parameter of the theory related to the number of massless particles.

Observe that for the systems above the ground state entanglement entropy can be employed as an order parameter that detects the quantum critical points. Moreover, the central charge c can be used to characterise the different universality classes of critical theories. In this thesis we shall develop a systematic method to study when the area law is violated in fermionic chains and to determine the central charge in those cases in which the entanglement entropy satisfies the form predicted by CFT.

In our approach we shall also cover fermionic chains with long-range interactions. In spite of some attempts [54], there is not a general understanding about the behaviour of the entanglement entropy when there are long-range interactions. Their presence modifies the picture previously described for systems with only finite-range interactions [55, 56, 57]. As it is discussed in several recent works, the ground state correlations can display algebraic decay even with non-zero mass gap [58, 59]. This implies that the entanglement entropy may violate the area law while the system is non critical as we shall see for fermionic chains.

With respect to higher dimensions, to our knowledge, there are no rigorous and general proofs for the area law as it happens in one dimension. It is known that for non-critical, local systems of free fermions the entanglement entropy of the ground state fulfils an area law. The same occurs if we consider bosons instead of fermions. On the other hand, for critical fermions with a finite, non-zero Fermi surface, the entanglement entropy of the ground state presents logarithmic corrections to the area law. For a comprehensive review of area laws in entanglement entropy we recommend Ref. [60].

The knowledge of the dependence of the entanglement entropy on the size of the subsystem can also serve to design efficient numerical methods. As we have said before, the numerical simulation with a classical computer of a quantum system may become inefficient as the degree of entanglement of the state increases. The entanglement entropy can be interpreted as the minimum amount of information needed to describe the subsystem X. In this sense, the entanglement entropy gives the computational complexity of simulating the system. This can be used to interpret for instance the efficiency of the DMRG algorithm mentioned above. Outside criticality it works well because the entanglement entropy follows an area law that bounds the information needed to describe a subsystem. On the contrary, it fails at criticality because the area law is violated and the entanglement entropy diverges with the size of the subsystem.

The entanglement entropy has also revealed to be an attractive guide to unravel some aspects of quantum gravity by means of the Holographic Principle [61, 62]. Inspired by the black hole entropy, this principle claims that given a region of the space-time the number of degrees of freedom that it may contain is proportional to the area of its boundary. One realisation of the Holographic Principle is the AdS/CFT correspondence, that argues that a theory of quantum gravity in an Anti-de Sitter (AdS) space is equivalent to a CFT defined on the boundary of the former [63]. In this framework, Ryu and Takanayagi found the way to compute the entanglement entropy in the CFT from the holographic dual theory [64]. This leads to the connection of entanglement with space-time geometry and gravity [65].

In the rest of the thesis we will have the opportunity to investigate some of the properties of the entanglement entropy mentioned above, specially those concerning the area

law and the logarithmic correction predicted by CFT. Therefore, it will be important to bear in mind the general results stated here. But before entering fully into the study of the entanglement entropy we must introduce the kind of physical systems we will be dealing with. This will be the first goal of the next Chapter.

Chapter 2

Fermionic and Spin Chains

In the previous Chapter we have seen that there are very interesting reasons that motivate the study of the entanglement entropy in quantum many-body systems: to investigate their critical properties, to explore new phases of matter, to analyse the computational complexity of simulating the system, to advance in the development of quantum computers, or even to unravel the origin of space-time.

In this thesis we shall analyse the entanglement entropy in the stationary states of fermionic chains described by a quadratic, homogeneous Hamiltonian that may present long-range couplings. These systems are very appropriate to gain understanding about the entanglement entropy. They are solvable and, therefore, we completely know the state under investigation. They can be related to spin chains employing the Jordan-Wigner transformation. We can apply efficient numerical methods and analytical techniques and the entanglement entropy displays several non trivial properties.

In this Chapter we shall introduce and solve this kind of chains, obtaining the spectrum and the eigenstates of the Hamiltonian. We shall also review some general properties of these systems that will be relevant in the study of the entanglement entropy as well as their connection with spin chains.

Then we shall move on to the problem of computing the entanglement entropy of a subsystem of the chain. Following the works of Peschel [66] and Vidal, Latorre, Rico, and Kitaev [24], we shall find that, for the stationary states, the entanglement entropy can be expressed in terms of the two-point correlation functions. This relation happens to be incredibly powerful. It will actually be the basis of the research done in the rest of the thesis. On the one hand, it reduces exponentially the complexity of computing numerically the entanglement entropy. On the other hand, it opens the possibility of applying several analytical tools based on the properties of block Toeplitz determinants that we shall develop in the subsequent chapters. We shall finish the Chapter calculating and studying some properties of the two-point correlation matrix for the stationary states.

2.1 Homogeneous quadratic fermionic chains

A fermionic chain consists of a unidimensional lattice of N sites with spinless fermions. The space of states of each site is $\mathbb{C}^2$. Then the space of states for the whole chain is the tensor product

$$\mathcal{H} = \mathbb{C}^2 \otimes \mathbb{C}^2 \otimes \cdots \otimes \mathbb{C}^2 = (\mathbb{C}^2)^N.$$

We define in each site $n = 1, \ldots, N$ the fermionic creation and annihilation operators $a_n^\dagger$, a_n that respectively create and annihilate a spinless fermion. These operators follow the canonical anticommutation relations

$$\{a_n^\dagger, a_m\} = \delta_{nm}, \quad \{a_n^\dagger, a_m^\dagger\} = \{a_n, a_m\} = 0, \quad n, m = 1, \ldots, N, \tag{2.1}$$

where δ_{nm} denotes the Kronecker delta.

The dynamics of the fermionic chain is described by a quadratic, homogeneous (translational invariant) Hamiltonian with finite-range couplings ($L < N/2$),

$$H = \frac{1}{2} \sum_{n=1}^{N} \sum_{l=-L}^{L} \left(2A_l a_n^\dagger a_{n+l} + B_l a_n^\dagger a_{n+l}^\dagger - \overline{B_l} a_n a_{n+l} \right). \tag{2.2}$$

We shall assume along all the thesis periodic boundary conditions, i.e. $a_{n+N} = a_n$. The couplings A_l, B_l will be in general complex numbers. Observe that in order that the Hamiltonian H be Hermitian, the hopping couplings must satisfy $A_{-l} = \overline{A_l}$ while, without loss of generality, we may take $B_{-l} = -B_l$ for the pairing couplings.

We can express the Hamiltonian H in terms of uncoupled fermions. First, since it is translational invariant, let us introduce the Fourier modes

$$b_k = \frac{1}{\sqrt{N}} \sum_{n=1}^{N} \mathrm{e}^{-\mathrm{i}\theta_k n} a_n, \quad \theta_k = \frac{2\pi k}{N}, \quad k \in \mathbb{Z}. \tag{2.3}$$

Notice that, by construction, they also satisfy periodic boundary conditions, $b_{k+N} = b_k$. In terms of them the Hamiltonian H reads

$$H = \mathcal{E} + \frac{1}{2} \sum_{k=0}^{N-1} (b_k^\dagger, b_{-k}) R_k \begin{pmatrix} b_k \\ b_{-k}^\dagger \end{pmatrix}, \tag{2.4}$$

where $\mathcal{E}$ is a constant shift in the energy levels,

$$\mathcal{E} = \frac{1}{2} \sum_{k=0}^{N-1} F_k,$$

and

$$R_k = \begin{pmatrix} F_k & G_k \\ \overline{G_k} & -F_{-k} \end{pmatrix}, \tag{2.5}$$

with

$$F_k = \sum_{l=-L}^{L} A_l \mathrm{e}^{\mathrm{i}\theta_k l}, \quad G_k = \sum_{l=-L}^{L} B_l \mathrm{e}^{\mathrm{i}\theta_k l}. \tag{2.6}$$

Since $A_{-l} = \overline{A_l}$ and $B_{-l} = -B_l$, F_k is real while G_k is an odd function, i.e. $G_{-k} = -G_k$.

Observe that if we have pairing couplings B_l, the Hamiltonian is not diagonalised after the Fourier transformation because the k and $-k$ modes are still coupled. We can decouple them by performing a Bogoliubov transformation.

The matrix R_k is Hermitian and satisfies

$$R_{-k} = -\begin{pmatrix} 0 & 1 \\ 1 & 0 \end{pmatrix} \overline{R_k} \begin{pmatrix} 0 & 1 \\ 1 & 0 \end{pmatrix}, \tag{2.7}$$

where $\overline{R_k}$ is the complex conjugate matrix of R_k. Therefore, its diagonal form will be

$$U_k R_k U_k^\dagger = \begin{pmatrix} \omega_k & 0 \\ 0 & -\omega_{-k} \end{pmatrix}, \tag{2.8}$$

where U_k is a unitary matrix and ω_k will be the dispersion relation of the uncoupled modes. The latter satisfies periodic boundary conditions, i.e. $\omega_{k+N} = \omega_k$. The ambiguity in the order of the eigenvalues can be removed by imposing that $\omega_k^+ \equiv (\omega_k + \omega_{-k})/2 \geq 0$. Thus the dispersion relation is defined univocally.

The unitary transformation U_k corresponds to performing a Bogoliubov transformation from the Fourier modes b_k to the new set of modes

$$\begin{pmatrix} d_k \\ d_{-k}^\dagger \end{pmatrix} = U_k \begin{pmatrix} b_k \\ b_{-k}^\dagger \end{pmatrix}. \tag{2.9}$$

In terms of the Bogoliubov modes d_k the Hamiltonian H is diagonal,

$$H = \mathcal{E} + \sum_{k=0}^{N-1} \omega_k \left(d_k^\dagger d_k - \frac{1}{2} \right).$$

From (2.8) and using the invariance of the trace and the determinant of a matrix under a unitary transformation, we deduce that

$$\omega_k^- \equiv \frac{\omega_k - \omega_{-k}}{2} = \frac{F_k - F_{-k}}{2} \equiv F_k^-,$$

and

$$\omega_k^+ = \sqrt{(F_k^+)^2 + |G_k|^2} \geq 0,$$

with

$$F_k^+ \equiv \frac{F_k + F_{-k}}{2}.$$

Therefore, we get that the dispersion relation of the Bogoliubov modes is

$$\omega_k = \sqrt{(F_k^+)^2 + |G_k|^2} + F_k^-. \tag{2.10}$$

An eigenstate of H is determined by a subset of occupied Bogoliubov modes $\mathbf{K} \subset \{0, \ldots, N-1\}$. Let us denote by $|0\rangle$ the vacuum for these new modes. This is the

state that satisfies $d_k |0\rangle = 0$ for all k. Then to the configuration $\mathbf{K}$ it corresponds the stationary state

$$|\mathbf{K}\rangle = \prod_{k\in\mathbf{K}} d_k^\dagger |0\rangle ,$$

with energy

$$E_{\mathbf{K}} = \mathcal{E} + \frac{1}{2}\sum_{k\in\mathbf{K}} \omega_k - \frac{1}{2}\sum_{k\notin\mathbf{K}} \omega_k.$$

In particular, the ground state $|\hat{\mathbf{K}}\rangle$ is obtained by filling those modes with negative energy (the Dirac sea),

$$|\hat{\mathbf{K}}\rangle = \prod_{\omega_k<0} d_k^\dagger |0\rangle .$$

Its energy is

$$E_{\hat{\mathbf{K}}} = \mathcal{E} - \frac{1}{2}\sum_{k=0}^{N-1} |\omega_k|.$$

Notice that if

$$|F_k^-| < \sqrt{(F_k^+)^2 + |G_k|^2}$$

for all $k = 0, \ldots, N-1$, the dispersion relation (2.10) is always positive and the ground state of H is the vacuum $|0\rangle$. In this case, there is an energy (mass) gap between the ground state and the first excited state. Therefore, the correlation length of the system is finite and the theory is *non critical*. An example of this case is illustrated in Fig. 2.1 *a*.

On the other hand, if there are momenta for which

$$|F_k^-| > \sqrt{(F_k^+)^2 + |G_k|^2},$$

i.e. with negative energy, a Dirac sea develops and the ground state corresponds to the configuration in which all the modes with negative energy are occupied. This occurs in Fig. 2.1 *b*. In this situation the mass gap is zero, the correlation length diverges and, therefore, the system is *critical*. The modes at which the dispersion relation changes its sign are the Fermi points.

There is a third possibility, represented in Fig. 2.1 *c*, in which the ground state is the vacuum $|0\rangle$ but for certain modes the dispersion relation vanishes. Thus the mass gap is zero and the system is also critical.

2.1.1 Discrete symmetries

The discrete transformations of parity (P) and charge conjugation (C) will be relevant in our study of the entanglement entropy. These transformations preserve the Fock space vacuum $|0_a\rangle$ of the fermions in real space, i.e. $a_n |0_a\rangle = 0$ for all n,

$$P |0_a\rangle = |0_a\rangle , \quad C |0_a\rangle = |0_a\rangle ,$$

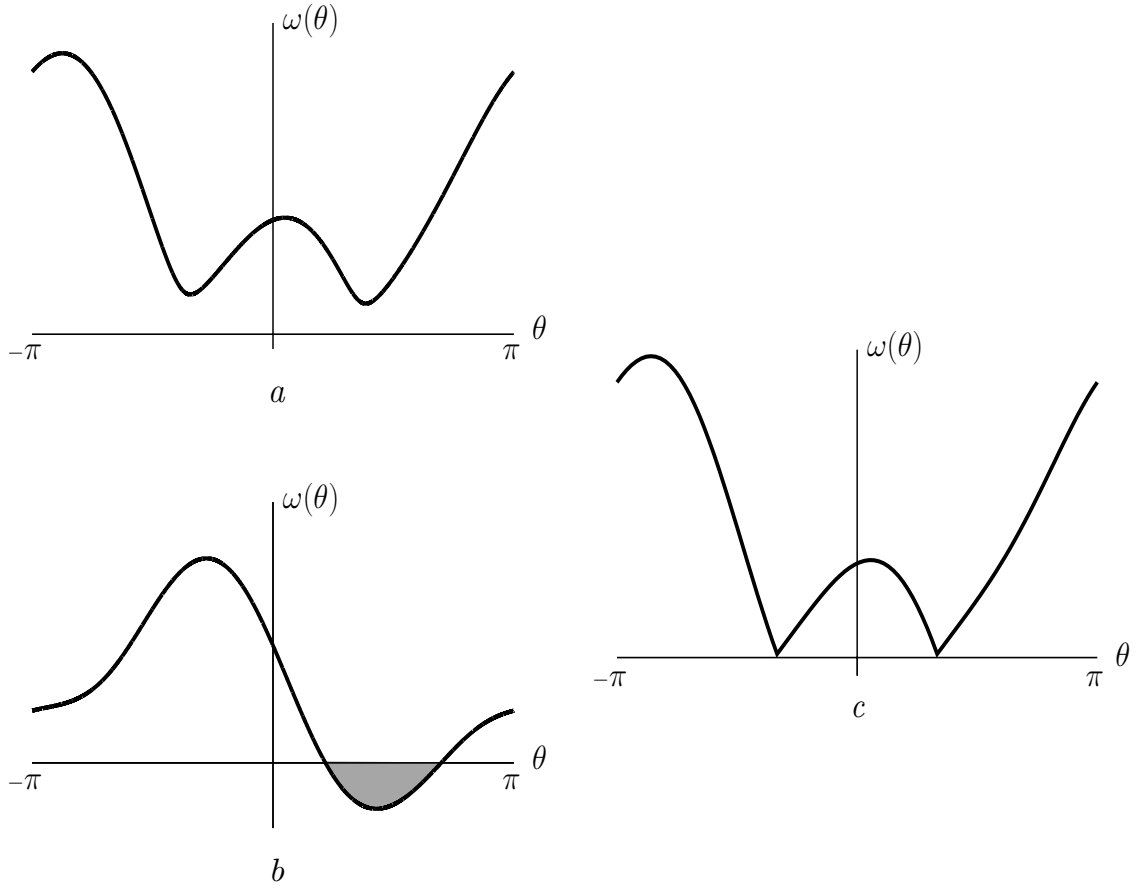

Figure 2.1: Dispersion relation $\omega(\theta)$ in the thermodynamic limit $N \to \infty$, $\theta_k \to \theta \in [-\pi, \pi)$, for three representative Hamiltonians of the form (2.2). The parity symmetry is broken in all of them. In the case a the theory has a mass gap, hence its ground state is $|0\rangle$, which preserves parity. The dispersion relation in b is negative for a set of modes (shadowed interval). Therefore, the theory is gapless and the ground state is obtained by filling these modes (Dirac sea). In this case the ground state breaks the parity symmetry. In the panel c, ω is non-negative but it has zeros. Then the model is gapless and the ground state is $|0\rangle$ that is invariant under parity.

and its action on the creation and annihilation operators is given by

$$P a_n P^{-1} = \mathrm{i} a_{N-n}, \quad C a_n C^{-1} = a_n^\dagger. \tag{2.11}$$

Applying this to the Fourier modes (2.3) we obtain

$$P b_k P^{-1} = \mathrm{i} b_{-k}, \quad C b_k C^{-1} = b_{-k}^\dagger.$$

Then the Hamiltonian (2.4) transformed under parity reads

$$PHP^{-1} = \mathcal{E} + \frac{1}{2} \sum_{k=0}^{N-1} (b_k^\dagger, -b_{-k}) R_{-k} \begin{pmatrix} b_k \\ -b_{-k}^\dagger \end{pmatrix}.$$

Therefore, the Hamiltonian is parity invariant ($PHP^{-1} = H$) when $F_{-k} = F_k$. That is, when the antisymmetric part F_k^- of F_k (2.6) vanishes. Given that $A_{-l} = \overline{A_l}$, this occurs if all the hopping couplings A_l are real.

Interestingly, if in the transformed Hamiltonian we apply the Bogoliubov transformation (2.9) given by the unitary matrix U_k, we obtain

$$U_k\sigma_z R_{-k}\sigma_z U_k^\dagger = \begin{pmatrix} \omega_{-k} & 0 \\ 0 & -\omega_k \end{pmatrix}. \tag{2.12}$$

Observe that there is actually an ambiguity in the Bogoliubov transformation,

$$\begin{pmatrix} \mathrm{e}^{\mathrm{i}\psi} & 0 \\ 0 & \mathrm{e}^{-\mathrm{i}\psi} \end{pmatrix}\begin{pmatrix} \omega_k & 0 \\ 0 & -\omega_{-k} \end{pmatrix}\begin{pmatrix} \mathrm{e}^{-\mathrm{i}\psi} & 0 \\ 0 & \mathrm{e}^{\mathrm{i}\psi} \end{pmatrix} = \begin{pmatrix} \omega_k & 0 \\ 0 & -\omega_{-k} \end{pmatrix},$$

that can be fixed by taking

$$U_{-k}\sigma_z = \sigma_z U_k. \tag{2.13}$$

Hence when we perform the P transformation on the Bogoliubov operators (2.9),

$$P\begin{pmatrix} d_k \\ d_{-k}^\dagger \end{pmatrix}P^{-1} = \mathrm{i}U_k\sigma_z\begin{pmatrix} b_{-k} \\ b_k^\dagger \end{pmatrix},$$

and apply (2.13), we have

$$P\begin{pmatrix} d_k \\ d_{-k}^\dagger \end{pmatrix}P^{-1} = \mathrm{i}\sigma_z U_{-k}\begin{pmatrix} b_{-k} \\ b_k^\dagger \end{pmatrix} = \begin{pmatrix} \mathrm{i}\, d_{-k} \\ -\mathrm{i}\, d_k^\dagger \end{pmatrix}. \tag{2.14}$$

On the other hand, under PC the Hamiltonian (2.4) transforms as

$$PCH(PC)^{-1} = \mathcal{E} + \frac{1}{2}\sum_{k=0}^{N-1}(b_{-k}, -b_k^\dagger)R_{-k}\begin{pmatrix} b_{-k}^\dagger \\ -b_k \end{pmatrix}. \tag{2.15}$$

Then PC is a symmetry of the theory provided $\overline{G_k} = -G_k$. That is, if G_k is purely imaginary. This is fulfilled when the pairing couplings B_l are real. Observe that in this case, PC takes $H - \mathcal{E}$ into $\mathcal{E} - H$.

Let

$$\begin{pmatrix} \overline{d}_{-k}^\dagger \\ \overline{d}_k \end{pmatrix} = \overline{U}_k\begin{pmatrix} b_{-k}^\dagger \\ -b_k \end{pmatrix} \tag{2.16}$$

be the Bogoliubov transformation that diagonalises the PC-transformed Hamiltonian (2.15),

$$\overline{U}_k R_{-k}\overline{U}_k^\dagger = \begin{pmatrix} \omega_{-k} & 0 \\ 0 & -\omega_k \end{pmatrix}.$$

Taking into account (2.12) we have that

$$\overline{U}_k = U_k\sigma_z. \tag{2.17}$$

The charge conjugation C acts on the Bogoliubov operators as

$$C\begin{pmatrix} d_k \\ d_{-k}^\dagger \end{pmatrix}C^{-1} = U_k C\begin{pmatrix} b_k \\ b_{-k}^\dagger \end{pmatrix}C^{-1} = U_k\begin{pmatrix} b_{-k}^\dagger \\ b_k \end{pmatrix}.$$

Applying now (2.16) and (2.17) we finally find

$$C\begin{pmatrix} d_k \\ d_{-k}^\dagger \end{pmatrix}C^{-1} = \begin{pmatrix} \overline{d}_{-k}^\dagger \\ \overline{d}_k \end{pmatrix}. \tag{2.18}$$

Summarising, the action of P and C on the Fourier and Bogoliubov modes is

$$P : b_k \mapsto \mathrm{i}b_{-k}, \quad C : b_k \mapsto b^\dagger_{-k},$$

$$P : d_k \mapsto \mathrm{i}d_{-k}, \quad C : d_k \mapsto \overline{d}^\dagger_{-k}.$$

Observe that the Bogoliubov modes transform covariantly under parity even if the Hamiltonian is not invariant, while they are covariant under charge conjugation only if the Hamiltonian is PC symmetric.

Notice that if the Hamiltonian violates parity this does not imply that its ground state breaks this symmetry too. As we have seen, the ground state, $|\hat{\mathbf{K}}\rangle = \prod_{\omega_k<0} d^\dagger_k |0\rangle$, is obtained by filling the Bogoliubov modes with negative energy. When the mass gap is non-zero, the dispersion relation ω_k is positive for all k. Then the ground state is the Bogoliubov vacuum $|0\rangle$. The latter is invariant under P, irrespective of the symmetries of the Hamiltonian. Therefore, if the Hamiltonian is non critical, the ground state is always P invariant, even if the Hamiltonian breaks this symmetry, as it happens in Fig. 2.1 *a*. This is just opposite to spontaneous symmetry breaking in which the ground state is not invariant under a symmetry of the Hamiltonian.

On the other hand, if the dispersion relation ω_k attains negative values, the mass gap is zero and the ground state is given by the occupation of the modes in the Dirac sea. Then this state is not parity invariant. This is the situation represented in Fig. 2.1 *b*.

Finally, if the dispersion relation is non negative and it vanishes for some k, as in Fig. 2.1 *c*, the theory is critical but the ground state is the Bogoliubov vacuum $|0\rangle$. Therefore, as it occurs in non critical theories, the ground state is parity invariant regardless the Hamiltonian breaks this symmetry.

These three scenarios will be relevant in the analysis of the entanglement entropy since this quantity will display different behaviour in each of these situations.

2.1.2 The Jordan-Wigner transformation: spin chains

The fermionic chain defined in the previous section can be related to a spin chain applying the Jordan-Wigner transformation.

A spin chain is again a unidimensional lattice in which the space of states for each site is $\mathbb{C}^2$ and the total Hilbert space $(\mathbb{C}^2)^N$. But instead of a spinless fermion as it happens in the fermionic chain, in each site n there is a spin 1/2 particle described by the Pauli operators σ^μ_n, with $\mu = x, y, z$.

The Pauli operators satisfy the commutation algebra

$$[\sigma^x_n, \sigma^y_m] = 2\mathrm{i}\delta_{nm}\sigma^z_n, \quad n, m = 1, \ldots, N,$$

and all the cyclic permutations in x, y, z. They also obey the anticommutation rules

$$\{\sigma^\mu_n, \sigma^\nu_n\} = \delta^{\mu\nu}, \quad \mu, \nu = x, y, z.$$

We can construct a transformation that relates the Pauli operators σ_n^μ to the fermionic creation and annihilation operators $a_n^\dagger$, a_n. For this purpose, consider the spin ladder operators

$$\sigma_n^\pm = \frac{1}{2}(\sigma_n^x \pm \mathrm{i}\sigma_n^y).$$

They fulfil the following anticommutation algebra

$$\{\sigma_n^+, \sigma_n^-\} = 1, \quad \{\sigma_n^+, \sigma_n^+\} = \{\sigma_n^-, \sigma_n^-\} = 0,$$

which is similar to that satisfied in (2.1) by the fermionic operators a_n, $a_n^\dagger$ in the same site n. However, the fermionic anticommutation rules (2.1) involve in general operators that act on different sites of the chain. For spin ladder operators in different sites n, m, we have

$$\{\sigma_n^+, \sigma_m^-\} = 2\sigma_n^+\sigma_m^-, \quad \{\sigma_n^\pm, \sigma_m^\pm\} = 2\sigma_n^\pm\sigma_m^\pm,$$

while the commutation relations,

$$[\sigma_n^+, \sigma_m^-] = [\sigma_n^\pm, \sigma_m^\pm] = 0,$$

are like those of bosonic creation and annihilation operators.

Hence we cannot directly identify the spin ladder operators σ_n^+, σ_n^- with the fermionic operators $a_n^\dagger$, a_n. However, if we introduce a non local factor we can define the set of operators

$$a_n \equiv \prod_{j=1}^{n-1}(-\sigma_j^z)\sigma_n^-, \quad a_n^\dagger \equiv \prod_{j=1}^{n-1}(-\sigma_j^z)\sigma_n^+, \tag{2.19}$$

that actually satisfy the rules (2.1).

This map between Pauli spin operators and fermionic operators is the so-called *Jordan-Wigner transformation* [67].

Note that taking into account $[\sigma_n^+, \sigma_n^-] = \sigma_n^z$, we have

$$\sigma_n^z = 2a_n^\dagger a_n - 1.$$

This implies

$$a_n^\dagger a_n = \sigma_n^+\sigma_n^-.$$

Therefore, the Jordan-Wigner transformation preserves locally the *number of excitations*: the number of fermions in the chain is equal to the number of spins whose z-component is $+1/2$.

The Jordan-Wigner transformation allows to map any spin chain into a chain of spinless fermions and viceversa. Then many properties of one of these systems may be extended to the other one.

If we apply the Jordan-Wigner transformation (2.19) to the Hamiltonian (2.2), the long-range terms give rise to non-local products of σ_n^z operators (cluster terms),

$$\sigma_n^\mu \prod_{j=n+1}^{n+l-1}(-\sigma_j^z)\sigma_{n+l}^\nu, \quad \mu, \nu = x, y,$$

in the corresponding spin chain. Spin chains with cluster terms have been attracted the attention because of their capabilities for quantum computation and in the study of quantum phase transitions [68, 69, 70].

When we apply the Jordan-Wigner transformation one should pay special attention to the boundary terms. Consider, for example, periodic (or antiperiodic) boundary conditions in the spin chain, that is

$$\sigma_0^{\pm} \left|\Psi\right\rangle = \delta \sigma_N^{\pm} \left|\Psi\right\rangle ,$$

for all $\left|\Psi\right\rangle \in (\mathbb{C}^2)^{N+1}$ and $\delta = 1$ (-1) for periodic (antiperiodic) boundary conditions. Then the corresponding relations for the fermionic operators are

$$a_0^{\dagger} \left|\Psi\right\rangle = -\delta a_N^{\dagger} \mathrm{e}^{\mathrm{i}\pi \sum_{n=1}^{N} a_n^{\dagger} a_n} \left|\Psi\right\rangle , \quad a_0 \left|\Psi\right\rangle = -\delta a_N \mathrm{e}^{\mathrm{i}\pi \sum_{n=1}^{N} a_n^{\dagger} a_n} \left|\Psi\right\rangle .$$

Hence we must separate the space of states into two independent sectors depending on the number of fermions that contain.

For the states with an even number of particles we have

$$a_0^{\dagger} = -\delta a_N^{\dagger}, \quad a_0 = -\delta a_N .$$

This means that the periodic (antiperiodic) boundary conditions for the spin operators translate into antiperiodic (periodic) boundary conditions for the fermionic operators.

On the contrary, for the sector with an odd number of particles,

$$a_0^{\dagger} = \delta a_N^{\dagger}, \quad a_0 = \delta a_N .$$

Therefore, in this case the periodic (antiperiodic) boundary conditions of the spin operators lead to periodic (antiperiodic) boundary conditions for the fermionic operators.

Nevertheless, in this thesis we shall be interested in the thermodynamic limit and the boundary effects play no role. Therefore, the previous considerations can be neglected. Quantities like the energy spectrum or the entanglement entropy of connected subsystems that we shall obtain for a fermionic chain will be the same for the corresponding spin chain.

2.2 Examples

Let us now discuss several relevant examples of theories of the form (2.2) that will be used in the next chapters.

2.2.1 Kitaev chain/XY spin chain

Among the systems described by a Hamiltonian of the form (2.2) the simplest one corresponds to the case with only nearest-neighbour couplings, i.e. $L = 1$,

$$H_{\mathrm{XY}} = \sum_{n=1}^{N} \left[t a_n^{\dagger} a_{n+1} + t a_n^{\dagger} a_{n-1} + \gamma (a_n^{\dagger} a_{n+1}^{\dagger} - a_n a_{n+1}) - h a_n^{\dagger} a_n \right] + \frac{Nh}{2}, \tag{2.20}$$

where the couplings t, γ, h are assumed to be real and non negative. Hence this Hamiltonian is invariant under the parity and charge conjugation transformations defined in (2.11).

This Hamiltonian can describe, for example, a quantum wire that lies on the surface of a superconductor. After the seminal work [71] where Kitaev showed that this theory may contain unpaired Majorana modes at the boundaries (if we take open boundary conditions), it is known by many authors as *Kitaev chain*.

The Jordan-Wigner transformation (2.19) allows to write this Hamiltonian in terms of 1/2-spin operators. The corresponding Hamiltonian is that of a *XY spin chain* with a transverse magnetic field,

$$H_{\mathrm{XY}} = \frac{1}{2}\sum_{n=1}^{N}\left[(t+\gamma)\sigma_n^x\sigma_{n+1}^x + (t-\gamma)\sigma_n^y\sigma_{n+1}^y - h\sigma_n^z\right]. \tag{2.21}$$

Here h is the intensity of the magnetic field in the z direction while t and γ give the coupling between the x and y components of contiguous spins. In particular, γ plays the role of an anisotropy parameter between the x and y directions.

The case $\gamma = 0$,

$$H_{\mathrm{XX}} = \sum_{n=1}^{N}[ta_n^\dagger(a_{n-1}+a_{n+1}) - ha_n^\dagger a_n] + \frac{Nh}{2},$$

corresponds to the *Tight Binding Model* or, in terms of the spin operators, to the *XX spin chain*,

$$H_{\mathrm{XX}} = \frac{1}{2}\sum_{n=1}^{N}\left[t\sigma_n^x\sigma_{n+1}^x + t\sigma_n^y\sigma_{n+1}^y - h\sigma_n^z\right],$$

for which the coupling in the x and y components of the spins is the same.

Notice that if we start from the XY spin chain (2.21) with periodic boundary conditions, the Jordan-Wigner transformation does not map it exactly into (2.20). In fact, if we write the spin operators in terms of fermionic operators using (2.19), we obtain

$$\begin{aligned} H_{\mathrm{XY}} \;=\; & \frac{Nh}{2} + \sum_{n=1}^{N-1}\left[\gamma\left(a_n^\dagger a_{n+1}^\dagger - a_n a_{n+1}\right) + t(a_n^\dagger a_{n+1} - a_n a_{n+1}^\dagger)\right] - \sum_{n=1}^{N} ha_n^\dagger a_n \\ & -\mathrm{e}^{\mathrm{i}\pi\sum_{n=1}^{N}a_n^\dagger a_n}\left[\gamma(a_N^\dagger a_1^\dagger - a_N a_1) + t(a_N^\dagger a_1 - a_N a_1^\dagger)\right]. \end{aligned} \tag{2.22}$$

Observe the last term of this Hamiltonian, it is the boundary term. The boundary conditions of the resulting fermionic chain are periodic or antiperiodic depending on the number of fermions that the state contains, as we already pointed out in Section 2.1.2. If we want to be careful, we should treat separately the states with an odd number of fermions (for which the fermionic chain is periodic) from those with an even number of fermions (for which we have to take antiperiodic boundary conditions). Nevertheless, the difference between considering periodic or antiperiodic boundary conditions are terms of the order of $1/N$ in the observables. They can be neglected for large N, as it will be

our case. Then we can assume periodic boundary conditions in both sectors. That is, consider the Hamiltonian (2.20) instead of (2.22).

The XY spin chain without an external magnetic field h was introduced and solved by Lieb, Mattis and Schultz in [72]. They precisely applied the Jordan-Wigner transformation (2.19) in order to map (2.21) into (2.22). Then they diagonalised the latter Hamiltonian by performing a Bogoliubov transformation just exactly as we have done here in the general case.

This system has been employed as a paradigmatic model to understand the properties of quantum many-body systems [72, 73, 74, 75]. In the last years the interest in the XY spin chain has been renewed due to its application in the study of quantum phase transitions and in quantum computation [18, 22, 24, 76]. In addition, it is possible to simulate it in the laboratory. Some experiments with cold ions traps have implemented successfully this Hamiltonian [29, 31, 77, 78, 79].

In this case, F_k and G_k (2.6) are

$$F_k = F_k^+ = -h + 2t\cos\theta_k, \quad G_k = 2\mathrm{i}\gamma\sin\theta_k.$$

Therefore, if we take the thermodynamic limit $N \to \infty$, $\theta_k \to \theta \in [-\pi, \pi)$, and the general dispersion relation (2.10) particularises to

$$\omega_{\mathrm{XY}}(\theta) = \sqrt{(h - 2t\cos\theta)^2 + 4\gamma^2\sin^2\theta}. \tag{2.23}$$

Observe that since the model has parity symmetry the antisymmetric parts F_k^- and $\omega_{\mathrm{XY}}^-(\theta)$ are absent.

In the following we shall fix the scale of the coupling constants by taking $t = 1$. For this choice, the case $\gamma = 1$ corresponds to the so called *quantum Ising chain*.

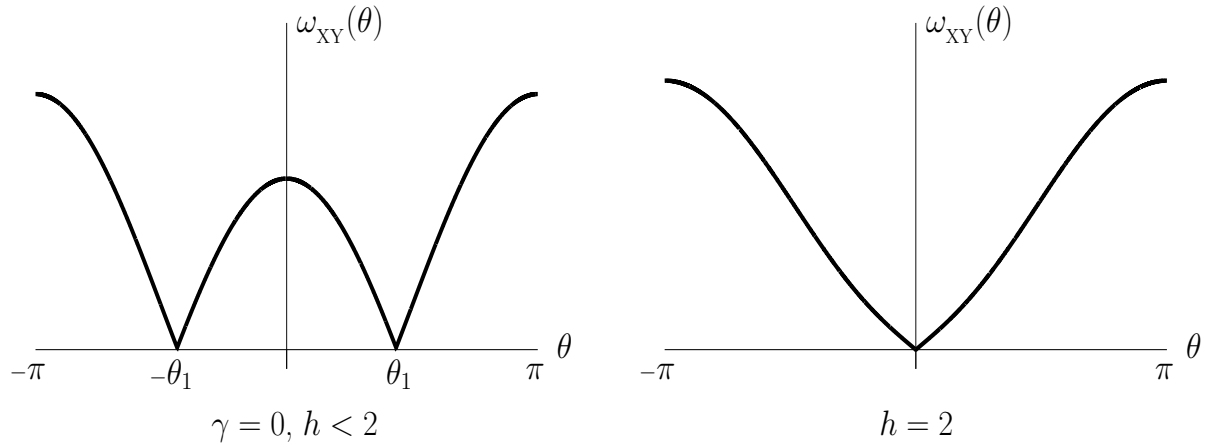

Figure 2.2: Dispersion relation (2.23) of the XY spin chain at two representative critical points. The dispersion relation on the left corresponds to a Hamiltonian with $\gamma = 0$ (XX spin chain) and $h < 2$. Then it vanishes at $\theta_1 = \arccos(h/2)$ and $-\theta_1$. The dispersion relation on the right corresponds to a theory with $h = 2$. Hence it is zero at $\theta = 0$.

Inspecting (2.23) one can deduce that the mass gap of H_{XY} is zero for $\gamma = 0$ and $h < 2$ or when $h = 2$. In fact, if $\gamma = 0$ the dispersion relation reduces to

$$\omega_{\mathrm{XX}}(\theta) = |h - 2\cos\theta|,$$

that vanishes for $h < 2$ at the modes $\theta_1 = \arccos(h/2)$ and $\theta_2 = -\theta_1$. This is represented in the left plot of Fig. 2.2. For the line $h = 2$, the dispersion relation only vanishes at the point $\theta = 0$. An example of this situation is depicted on the right-hand side of Fig. 2.2.

2.2.2 XY spin chain with a Dzyaloshinski-Moriya coupling

We can break parity symmetry in the previous model by adding an antisymmetric exchange term or Dzyaloshinski-Moriya (DM) coupling [80, 81] to the Hamiltonian of the XY spin chain (2.21),

$$H_{\mathrm{DM}} = \frac{1}{2}\sum_{n=1}^{N}\left[(1+\gamma)\sigma_n^x\sigma_{n+1}^x + (1-\gamma)\sigma_n^y\sigma_{n+1}^y + s(\sigma_n^x\sigma_{n+1}^y - \sigma_{n+1}^x\sigma_n^y) - h\sigma_n^z\right].$$

The new coupling constant s is taken real.

After the Jordan-Wigner transformation (2.19) we have

$$H_{\mathrm{DM}} = \sum_{n=1}^{N}\Big[(1+\mathrm{i}s)a_n^\dagger a_{n+1} + (1-\mathrm{i}s)a_n^\dagger a_{n-1} + \gamma(a_n^\dagger a_{n+1}^\dagger - a_n a_{n+1}) - h a_n^\dagger a_n\Big] + \frac{Nh}{2}.$$

This Hamiltonian is similar to that of a Kitaev chain (2.20) but with complex hopping couplings that violate parity symmetry.

Thus, according to (2.6), F_k has now a non-zero antisymmetric part, while its symmetric part F_k^+ and G_k remain unchanged with respect to those of the XY spin chain,

$$F_k^+ = -h + 2\cos\theta_k, \quad F_k^- = 2s\sin\theta_k,$$

$$G_k = 2\mathrm{i}\gamma\sin\theta_k.$$

Therefore, applying (2.10), the dispersion relation in the thermodynamic limit is

$$\omega_{\mathrm{DM}}(\theta) = \omega_{\mathrm{DM}}^+(\theta) + 2s\sin\theta, \tag{2.24}$$

with

$$\omega_{\mathrm{DM}}^+(\theta) = \omega_{\mathrm{XY}}(\theta) = \sqrt{(h - 2\cos\theta)^2 + 4\gamma^2\sin^2\theta}.$$

The DM coupling modifies the conditions under which the system is critical. Introducing $\Delta = s^2 - \gamma^2$, if $\Delta > 0$ and $(h/2)^2 - \Delta < 1$ the dispersion relation changes its sign at the Fermi momenta θ_j, $j = 1, 2$,

$$\cos\theta_j = \frac{-h/2 \pm \sqrt{(s^2-\gamma^2)(s^2-\gamma^2+1-(h/2)^2)}}{s^2-\gamma^2+1}, \tag{2.25}$$

with $\theta_j \in (-\pi, 0]$ for $s > 0$. In the ground state of these theories all the modes with negative energy, i.e. those between θ_1 and θ_2, are occupied. Since $\theta_j \in (-\pi, 0]$ the ground state has a negative total momentum, and it breaks parity symmetry. This is the case of the dispersion relation plotted on the left-hand side of Fig. 2.3.

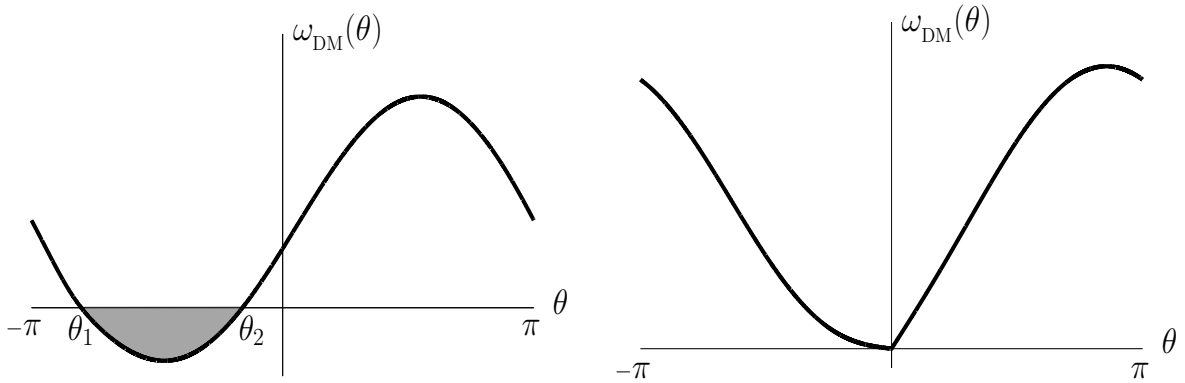

$\Delta > 0,\ (h/2)^2 - \Delta < 1$ $\qquad$ $\Delta < 0,\ h = 2$

Figure 2.3: Archetypical dispersion relations (2.24) of the XY spin chain with a DM coupling at the critical points. When $\Delta = s^2 - \gamma^2 > 0$ and $(h/2)^2 - \Delta < 1$, as in the case represented on the left, the dispersion relation is negative in the interval $\theta \in (\theta_1, \theta_2)$. The points θ_1 and θ_2 are the Fermi momenta. They can be obtained from (2.25). In these theories there is a Dirac sea (coloured). When $\Delta < 0$ and $h = 2$ the dispersion relation vanishes at $\theta = 0$, as it happens in the plot on the right. Here there is no Dirac sea.

The theories for which $\Delta < 0$ and $h = 2$ are also critical. Their dispersion relation vanishes at $\theta = 0$ but it does not change the sign. Hence the ground state in this case is the Bogoliubov vacuum $|0\rangle$. The dispersion relation at one of these critical points is represented in the right panel of Fig. 2.3.

2.2.3 The Long-Range Kitaev chain

We can also consider models in which the couplings extend throughout the whole chain. In particular we shall study the Long-Range Kitaev chain. It is a unidimensional homogeneous fermionic chain with nearest-neighbour hoppings and power-like decaying pairings,

$$H_{\rm LRK} = \sum_{n=1}^{N} \left(a_n^\dagger a_{n+1} + a_{n+1}^\dagger a_n + h a_n^\dagger a_n \right) + \sum_{n=1}^{N} \sum_{l=-N/2}^{N/2} |l|^{-\delta-1} \left(a_n^\dagger a_{n+l}^\dagger - a_n a_{n+l} \right) - \frac{Nh}{2}, \tag{2.26}$$

where the exponent $\delta > 0$ characterises the dumping of the pairing with distance. As we will see its value is crucial for the properties of the ground state entanglement.

This model was first considered by Ercolessi and collaborators in the 2014 paper [58]. Since then it has been the object of an intense study. It is very useful to analyse the effects of long-range interactions. Here we shall restrict to the entanglement entropy but

different authors have investigated the form of the correlations [58, 59, 82], the breaking of conformal symmetry [83], the propagation of information [84], the behaviour out of equilibrium [85] or the occurrence and structure of topological phases [86, 87, 88, 89, 90, 91].

In this case, after taking the thermodynamic limit, F_k and G_k in (2.6) become

$$F(\theta) = F^+(\theta) = h + 2\cos\theta,$$

$$G_\delta(\theta) = \sum_{l=1}^{\infty} \left(\mathrm{e}^{\mathrm{i}\theta l} - \mathrm{e}^{-\mathrm{i}\theta l}\right) l^{-\delta} = \mathrm{Li}_\delta(\mathrm{e}^{\mathrm{i}\theta}) - \mathrm{Li}_\delta(\mathrm{e}^{-\mathrm{i}\theta}),$$

where Li_δ stands for the polylogarithm of order δ [92],

$$\mathrm{Li}_\delta(z) = \sum_{l=1}^{\infty} \frac{z^l}{l^\delta}.$$

This is a multivalued function, analytic outside the real interval $[1, \infty)$. It has a finite limit at $z = 1$ for $\delta > 1$ while it diverges at this point for $\delta < 1$. For $\delta = 1$ the polylogarithm function reduces to the logarithm $\mathrm{Li}_1(z) = -\log(1 - z)$. We shall take as its branch cut the real interval $[1, \infty)$, thus $G_1(\theta)$ is discontinuous at $\theta = 0$.

Observe that the model has parity symmetry and, therefore, the antisymmetric part of F is zero. According to (2.10), the dispersion relation of this model reads

$$\omega_{\mathrm{LRK}}(\theta) = \sqrt{(h + 2\cos\theta)^2 + |G_\delta(\theta)|^2}.$$

It vanishes, and the system is critical, at $\theta = -\pi$ for $h = 2$, and at $\theta = 0$ for $h = -2$ and $\delta > 1$. Since the dispersion relation is non negative, the ground state of the chain is always the Bogoliubov vacuum $|0\rangle$.

2.3 Entanglement entropy and correlation matrix

The main purpose of this thesis is the analysis of the Rényi entanglement entropy for the eigenstates $|\mathbf{K}\rangle = \prod_{k\in\mathbf{K}} d_k^\dagger |0\rangle$ of the Hamiltonian (2.2), created by the action of certain Bogoliubov modes on the Fock space vacuum $|0\rangle$, as it is explained in Section 2.1.

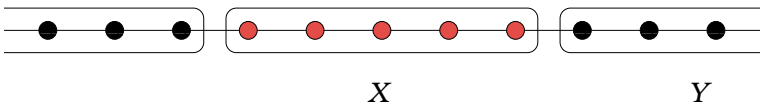

Figure 2.4: In order to compute the Rényi entanglement entropy we have to divide the fermionic chain into two subsystems X and Y. In this case X and Y are two intervals of contiguous sites.

In Section 1.1, we examined the main properties of the Rényi entanglement entropy. As we explained there, in order to calculate this quantity we have to divide the fermionic chain into two parts X and Y. For instance in Fig. 2.4 we have separated the chain into

two intervals of contiguous sites. Thus the total space of states of the chain $\mathcal{H} = (\mathbb{C}^2)^N$ factorises in the tensor product of the space of states for X and Y,

$$\mathcal{H} = \mathcal{H}_X \otimes \mathcal{H}_Y,$$

with

$$\mathcal{H}_X = (\mathbb{C}^2)^{|X|}, \quad \mathcal{H}_Y = (\mathbb{C}^2)^{N-|X|},$$

and $|X|$ the number of sites that the subsystem X contains.

We need now the reduced density matrix of X when the state of the chain is $|\mathbf{K}\rangle$,

$$\rho_X = \mathrm{Tr}_{\mathcal{H}_Y}(|\mathbf{K}\rangle \langle \mathbf{K}|),$$

that is obtained by computing the partial trace in the space $\mathcal{H}_Y$.

Finally the Rényi entanglement entropy is defined as

$$S_{\alpha,X} = \frac{1}{1-\alpha} \log \mathrm{Tr}(\rho_X^\alpha),$$

where $\alpha \geq 1$. Remember that the value $\alpha = 1$ corresponds to the von Neumann entanglement entropy

$$S_{1,X} = -\mathrm{Tr}(\rho_X \log \rho_X).$$

We shall be particularly interested in the behaviour of the entanglement entropy for large $|X|$. As we discussed in Section 1.2, this question is relevant for several reasons. The dependence of $S_{\alpha,X}$ on $|X|$ will be useful to study, for example, the properties of the critical chains.

The computation of $S_{\alpha,X}$ from the reduced density matrix ρ_X is a difficult task when $|X|$ is large enough, even numerically. Observe that the dimension of the space $\mathcal{H}_X$ is $2^{|X|}$. It grows exponentially with $|X|$. For instance if $|X| = 80$ the dimension of $\mathcal{H}_X$ is approximately twice the Avogadro number. We would need a Yottabyte of memory to store a vector of this space in a computer.

Fortunately, we can bypass this problem expressing the Rényi entanglement entropy in terms of the two-point correlation functions. Let us obtain this relation following the works of Peschel [66] and Vidal, Latorre, Rico, and Kitaev [24].

The crucial property is that the eigenstates $|\mathbf{K}\rangle$ of the general Hamiltonian (2.2) are Slater determinants and, therefore, they satisfy the Wick decomposition theorem. The Wick theorem implies that the correlation function of $2J$ points can be decomposed into the two-point correlation functions of the different pairings of points. More specifically, a state described by the density matrix ρ satisfies the Wick theorem if the correlation of an odd number of points is zero and for every J we have

$$\mathrm{Tr}(\rho \hat{a}_1 \dots \hat{a}_{2J}) = \frac{1}{J!} \sum_{\sigma \in \mathcal{S}'_{2J}} \prod_{j=1}^{J} (-1)^{|\sigma|} \mathrm{Tr}(\rho \hat{a}_{\sigma(2j-1)} \hat{a}_{\sigma(2j)}) \tag{2.27}$$

where

$$\hat{a}_j = \sum_{n=1}^{N} \varphi_j(n) a_n + \psi_j(n) a_n^\dagger$$

is any linear combination of the creation and annihilation operators in the real space,

$$\mathcal{S}'_{2J} = \{\sigma \in \mathcal{S}_{2J} \,|\, \sigma(2j-1) < \sigma(2j),\ j = 1, \ldots, J\}$$

is the set of permutations that preserve the order in every pair and $|\sigma|$ is the signature of the permutation σ. It is important to note that if the total density matrix ρ of the system satisfies this property, the reduced density matrix ρ_X also fulfils this decomposition.

First, let us determine the form of ρ assuming that it satisfies the Wick decomposition. In general, ρ will break the fermionic number conservation, hence we have to take into account both $C_{nm} = \mathrm{Tr}(\rho a_n^\dagger a_m)$ and $F_{nm} = \mathrm{Tr}(\rho a_n a_m)$. Observe that, if ρ preserves the fermionic number, $F_{nm} = 0$.

Therefore, consider the matrix W with entries

$$\begin{aligned} W_{nm} &= \mathrm{Tr}\left[\rho \begin{pmatrix} a_n \\ a_n^\dagger \end{pmatrix} (a_m^\dagger, a_m)\right] \\ &= \begin{pmatrix} \delta_{nm} - C_{mn} & F_{nm} \\ \overline{F_{nm}} & C_{nm} \end{pmatrix}, \quad n, m = 1, \ldots, N. \end{aligned} \tag{2.28}$$

This is a $2N \times 2N$ Hermitian matrix with eigenvalues lying on the real interval $[0, 1]$. Let us perform the Bogoliubov transformation

$$a_n = \sum_{l=1}^{N} (\varphi_{nl} c_l + \psi_{nl} c_l^\dagger), \quad n = 1, \ldots, N,$$

to the basis of fermionic modes c_l where W is diagonal. The coefficients φ_{nl}, ψ_{nl} are real, and they must satisfy the relations

$$\varphi^2 + \psi^2 = I, \quad \varphi\psi^t + \psi\varphi^t = 0,$$

where $\varphi = (\varphi_{nl})$ and $\psi = (\psi_{nl})$.

Expressing W_{nm} in terms of the new fermionic modes we have that

$$W_{nm} = \sum_{l=1}^{N} \Omega_l(n) \begin{pmatrix} \mu_l & 0 \\ 0 & 1 - \mu_l \end{pmatrix} \Omega_l(m),$$

where $\{\Omega_1, \ldots, \Omega_N\}$ is an orthonormal basis with elements

$$\Omega_l(n) = \begin{pmatrix} \varphi_{nl} & \psi_{nl} \\ \psi_{nl} & \varphi_{nl} \end{pmatrix},$$

and $\mu_l = \mathrm{Tr}(\rho c_l^\dagger c_l)$ while $\mathrm{Tr}(\rho c_l c_l) = \mathrm{Tr}(\rho c_l^\dagger c_l^\dagger) = 0$.

It is useful to distinguish three different subsets of c_l modes: E_1 that contains the modes with $\mu_l = 0$, E_2 that is made by the modes for which $\mu_l = 1$, and E_3 that denotes the subset of modes with eigenvalue $\mu_l \in (0, 1)$. For $l \in E_1$ we have that $\mathrm{Tr}(\rho c_l^\dagger c_l) = 0$ and, if P_l is the orthogonal projector into the image of c_l, we can factorize the density matrix as $\rho = QP_l$. Analogously, if $l \in E_2$ then $\mathrm{Tr}(\rho c_l^\dagger c_l) = 1$ and $\rho = Q'(I - P_l)$. The

operators Q and Q' account in each case for the rest of the eigenspaces. Finally, recalling that the Gaussian states satisfy the Wick decomposition, we may conjecture that the density matrix ρ should be of the form

$$\rho = K\mathrm{e}^{-h} \prod_{p\in E_1} P_p \prod_{q\in E_2} (I - P_q), \tag{2.29}$$

with

$$h = \sum_{l\in E_3} \epsilon_l c_l^\dagger c_l,$$

and K is the normalization constant. Observe that (2.29) satisfies the Wick decomposition and matches the eigenspaces of eigenvalues 0 and 1. We will show that with an adequate choice of h it also accounts for the rest of the eigenvalues.

Using the fact that $\mathrm{Tr}(\rho) = 1$ we can determine the normalization constant

$$K = \prod_{l\in E_3} \frac{1}{1+\mathrm{e}^{-\epsilon_l}}.$$

Computing

$$\mathrm{Tr}(\rho c_l^\dagger c_l) = \frac{1}{1+\mathrm{e}^{\epsilon_l}}, \quad \text{for } l \in E_3,$$

we can relate the eigenvalues of the correlation matrix W to those of h and, finally, we obtain the desired expression for the coefficients ϵ_l,

$$\epsilon_l = \log \frac{1-\mu_l}{\mu_l}, \quad \text{for } 0 < \mu_l < 1. \tag{2.30}$$

As it was noted by Peschel in [66], the above discussion gives a way to obtain the state ρ from the two-point correlation matrix W. Just a month earlier the same idea was also published by Vidal, Latorre, Rico, and Kitaev in [24] who applied it to the numerical computation of the entanglement entropy for the ground state of the XY spin chain.

In fact, we can express the Rényi entropy of ρ,

$$S_\alpha = \frac{1}{1-\alpha} \log \mathrm{Tr}(\rho^\alpha),$$

as a function of the correlation matrix W. Applying the relation (2.30) between the eigenvalues of ρ and W that belong to the subset E_3 we have

$$\mathrm{Tr}(\rho^\alpha) = \prod_{l\in E_3} \frac{1+\mathrm{e}^{-\alpha\epsilon_l}}{(1+\mathrm{e}^{-\epsilon_l})^\alpha} = \prod_{l=1}^{N} [(1-\mu_l)^\alpha + \mu_l^\alpha],$$

where in the last equality the product can be extended to all the eigenvalues of W without any change in the final expression. Therefore, we arrive at an expression for the Rényi entropy of ρ in terms of the spectrum of the two-point correlation matrix W,

$$S_\alpha = \frac{1}{1-\alpha} \sum_{l=1}^{N} \log[(1-\mu_l)^\alpha + \mu_l^\alpha].$$

In matrix form, the latter reads

$$S_\alpha = \frac{1}{2(1-\alpha)} \operatorname{Tr} \log[(I-W)^\alpha + W^\alpha]. \tag{2.31}$$

For the von Neumann entropy, that is the limit $\alpha \to 1$, the previous formulae lead to

$$S_1 = -\sum_{l=1}^{N} [(1-\mu_l)\log(1-\mu_l) + \mu_l \log \mu_l],$$

or

$$S_1 = -\frac{1}{2} \operatorname{Tr}[(I-W)\log(I-W) + W \log W].$$

Taking in the above expressions the restriction of the correlation matrix W to the sites of the chain that belong to the subsystem X, we obtain the entropy $S_{\alpha,X}$ of the reduced density matrix ρ_X.

Observe that the dimension of the density matrix ρ is 2^N while the correlation matrix W has dimension $2N$. The relation found between them implies a drastic reduction of the computational complexity, from an exponential to a polynomial dependence on the size of the system. We shall exploit this fact in the numerical calculations in order to go to larger sizes of X without exhausting the computational capabilities. Of course, this simplification of the problem is valid provided the density matrix satisfies the Wick decomposition and, therefore, all the information about the state is encoded in the two-point correlation functions.

For the stationary states $|\mathbf{K}\rangle$ of the Hamiltonian (2.2) E_1 corresponds to the set of occupied modes, $E_1 = \mathbf{K}$, while E_2 is the set of empty modes, $E_2 = \{0, \ldots, N-1\} \setminus \mathbf{K}$. Hence $E_3 = \emptyset$. Of course, according to our previous discussion, the reduced density matrix ρ_X obtained from $|\mathbf{K}\rangle$ has also the Wick property and the results of this section can be applied to the study of the entanglement entropy in these states.

In the theory of entanglement, the operator h corresponding to ρ_X is denominated entanglement Hamiltonian and its eigenvalues $\{\epsilon_l\}$ give the entanglement spectrum. The entanglement Hamiltonian has been the subject of several recent works [42, 93, 94, 95, 96, 97]. Observe that, in principle, if we know the expression of the Rényi entropy S_α for every α, we can compute all the momenta $\operatorname{Tr}(\rho^\alpha)$ of the Gaussian operator $K\mathrm{e}^{-h}$ and, therefore, determine all the spectral invariants of h.

It will be convenient to redefine the correlation matrix as $V = 2W - I$. In the rest of the thesis we shall always work with V instead of W. Therefore, in the following, the term correlation matrix will refer to V. Given the form of W, see (2.28), the entries of V are

$$V_{nm} = 2 \operatorname{Tr}\left[\rho \begin{pmatrix} a_n \\ a_n^\dagger \end{pmatrix} (a_m^\dagger, a_m)\right] - \delta_{nm} I, \quad n, m = 1, \ldots, N. \tag{2.32}$$

Replacing the matrix W by V in (2.31) we have

$$S_\alpha = \frac{1}{2(1-\alpha)} \operatorname{Tr} \log \left[\left(\frac{I+V}{2}\right)^\alpha + \left(\frac{I-V}{2}\right)^\alpha\right]. \tag{2.33}$$

Since the eigenvalues of W, μ_l, belong to the interval $[0,1]$, those of V, $v_l = 2\mu_l - 1$, lie on the real interval $[-1,1]$. Introducing the function

$$f_\alpha(\lambda) = \frac{1}{1-\alpha}\log\left[\left(\frac{1+\lambda}{2}\right)^\alpha + \left(\frac{1-\lambda}{2}\right)^\alpha\right], \tag{2.34}$$

the entropy can be written in terms of the eigenvalues of V as

$$S_\alpha = \sum_{l=1}^{N} f_\alpha(v_l). \tag{2.35}$$

If we now apply the Cauchy's residue theorem, we can express S_α as the contour integral

$$S_\alpha = \frac{1}{4\pi \mathrm{i}} \lim_{\varepsilon\to 1^+} \oint_{\mathscr{C}} f_\alpha(\lambda/\varepsilon)\frac{\mathrm{d}}{\mathrm{d}\lambda}\log D_N(\lambda)\mathrm{d}\lambda, \tag{2.36}$$

where $\mathscr{C}$ is a contour that surrounds the eigenvalues v_l and $D_N(\lambda)$ is the determinant of $\lambda I - V$,

$$D_N(\lambda) = \det(\lambda I - V) = \prod_{l=1}^{N}(\lambda^2 - v_l^2).$$

In Fig. 2.5 we depict the integration contour $\mathscr{C}$ and the poles and the branch cuts of the integrand.

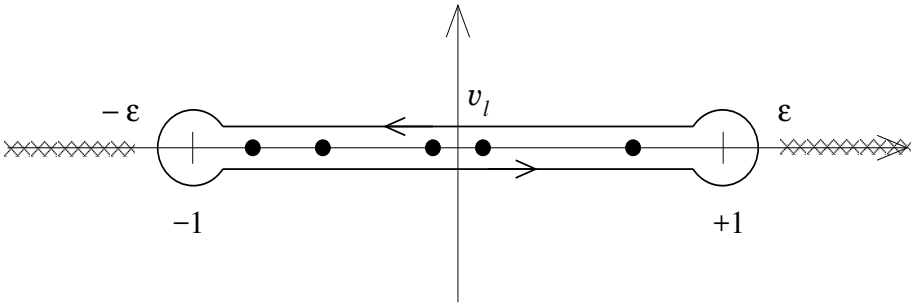

Figure 2.5: Contour of integration, cuts and poles for the computation of S_α in (2.36). The contour surrounds the eigenvalues v_l of V, all of them lying on the real interval $[-1,1]$. The branch cuts for the function f_α extend to $\pm\infty$.

The contour integral (2.36) was first obtained by Jin and Korepin in Ref. [98] for the ground state of the XX spin chain. As we have seen here, their result can be extended to any eigenstate $|\mathbf{K}\rangle$ of the Hamiltonian (2.2).

In this way, the entropy S_α is derived from the determinant of the resolvent $\lambda I - V$ of the two-point correlation matrix. Our problem, therefore, reduces to the computation of the latter. In the following section, we shall take the first step in this direction by computing the correlation matrix V for the stationary states $|\mathbf{K}\rangle$.

2.4 Correlation matrix for the stationary states

Notice that the entries (2.32) of the correlation matrix V for the states $|\mathbf{K}\rangle$ can be calculated from

$$V_{nm} = 2\left\langle \mathbf{K}\left|\begin{pmatrix} a_n \\ a_n^\dagger \end{pmatrix}(a_m^\dagger, a_m)\right|\mathbf{K}\right\rangle - \delta_{nm}I, \quad n,m=1,\ldots,N. \tag{2.37}$$

First, let us express them in the Fourier basis (2.3),

$$V_{nm} = \frac{1}{N}\sum_{k=0}^{N-1}\mathcal{G}_k \mathrm{e}^{\mathrm{i}\theta_k(n-m)}, \tag{2.38}$$

where $\mathcal{G}_k$ is the 2×2 matrix

$$\mathcal{G}_k = 2\left\langle \mathbf{K}\left|\begin{pmatrix} b_k \\ b_{-k}^\dagger \end{pmatrix}(b_k^\dagger, b_{-k})\right|\mathbf{K}\right\rangle - I.$$

In terms of the Bogoliubov modes (2.9), $\mathcal{G}_k$ is of the form

$$\mathcal{G}_k = 2U_k^\dagger\left\langle \mathbf{K}\left|\begin{pmatrix} d_k \\ d_{-k}^\dagger \end{pmatrix}(d_k^\dagger, d_{-k})\right|\mathbf{K}\right\rangle U_k - I.$$

Since $|\mathbf{K}\rangle = \prod_{k\in\mathbf{K}} d_k^\dagger|0\rangle$, the expectation values in the matrix above are

$$\left\langle \mathbf{K}\left|\begin{pmatrix} d_k \\ d_{-k}^\dagger \end{pmatrix}(d_k^\dagger, d_{-k})\right|\mathbf{K}\right\rangle = \begin{pmatrix} 1-\chi_{\mathbf{K}}(k) & 0 \\ 0 & \chi_{\mathbf{K}}(N-k) \end{pmatrix},$$

where $\chi_{\mathbf{K}}(k)$ is the characteristic function of the set of occupied Bogoliubov modes $\mathbf{K}$,

$$\chi_{\mathbf{K}}(k) = \begin{cases} 1, & k\in\mathbf{K}, \\ 0, & k\notin\mathbf{K}. \end{cases}$$

Therefore,

$$\mathcal{G}_k = U_k^\dagger\begin{pmatrix} 1-2\chi_{\mathbf{K}}(k) & 0 \\ 0 & -1+2\chi_{\mathbf{K}}(N-k) \end{pmatrix}U_k.$$

Considering the different possibilities we finally arrive at

$$\mathcal{G}_k = \begin{cases} -M_k, & \text{if } k\in\mathbf{K} \text{ and } N-k\in\mathbf{K}, \\ -I, & \text{if } k\in\mathbf{K} \text{ and } N-k\notin\mathbf{K}, \\ M_k, & \text{if } k\notin\mathbf{K} \text{ and } N-k\notin\mathbf{K}, \\ I, & \text{if } k\notin\mathbf{K} \text{ and } N-k\in\mathbf{K}, \end{cases} \tag{2.39}$$

where

$$M_k = U_k^\dagger\begin{pmatrix} 1 & 0 \\ 0 & -1 \end{pmatrix}U_k.$$

The matrix M_k depends on the couplings A_l, B_l of the Hamiltonian. In fact, if in the identity (2.8) we split the dispersion relation ω_k into its symmetric and antisymmetric parts, ω_k^+ and ω_k^-, we have

$$U_k R_k U_k^\dagger = \omega_k^+ \begin{pmatrix} 1 & 0 \\ 0 & -1 \end{pmatrix} + \omega_k^- I.$$

Therefore,

$$M_k = U_k^\dagger \begin{pmatrix} 1 & 0 \\ 0 & -1 \end{pmatrix} U_k = \frac{1}{\omega_k^+} \left(R_k - \omega_k^- I \right),$$

and, finally, using (2.5) we obtain

$$M_k = \frac{1}{\sqrt{(F_k^+)^2 + |G_k|^2}} \begin{pmatrix} F_k^+ & G_k \\ \overline{G_k} & -F_k^+ \end{pmatrix}.$$

Observe that the form of $\mathcal{G}_k$ at k not only depends on the occupation of this mode but also on that of the mode $N-k$.

We shall be particularly interested in computing the entanglement entropy for the ground state. This state corresponds to the configuration $\hat{\mathbf{K}} = \{k \,|\, \omega_k < 0\}$. Taking into account that $\omega_k = \omega_k^+ + F_k^-$ and $\omega_k^+ = \omega_{N-k}^+$, $F_k^- = -F_{N-k}^-$, the general expression of $\mathcal{G}_k$ in (2.39) particularises for the ground state $|\hat{\mathbf{K}}\rangle$ as

$$\hat{\mathcal{G}}_k = \begin{cases} -I, & \text{if} \quad -\omega_k^+ > F_k^-, \\ M_k, & \text{if} \quad -\omega_k^+ < F_k^- < \omega_k^+, \\ I, & \text{if} \quad F_k^- > \omega_k^+. \end{cases} \tag{2.40}$$

Since we imposed that $\omega_k^+ \geq 0$, ω_k and ω_{N-k} cannot be both negative. This implies that the first case in (2.39) never happens in the ground state.

Some transformation properties of the correlation matrix result in the invariance of the corresponding Rényi entropy (2.33):

1. Translational invariance in the real space (a-fermions). Due to the homogeneity of the Hamiltonian, the entries of V_{nm} only depend on the distance between sites $n-m$.

2. Translational invariance in the momentum space (d-fermions). Consider a particular configuration $\mathbf{K}$. Let $\mathbf{K}_\Delta$ be another one with the same number of occupied modes and their momentum displaced a constant Δ, i.e. $\mathbf{K}_\Delta = \{k + \Delta \,|\, k \in \mathbf{K}\}$. The correlation matrix of $\mathbf{K}_\Delta$ has entries

$$V_{nm}^\Delta = \frac{1}{N} \sum_{k'=0}^{N-1} \mathcal{G}_{k'}^\Delta \mathrm{e}^{i\theta_{k'}(n-m)},$$

where $\mathcal{G}_k^\Delta$ is given by (2.39) taking the displaced configuration $\mathbf{K}_\Delta$ instead of $\mathbf{K}$. Changing the variable of the sum, $k = k' - \Delta$, we find

$$V_{nm}^\Delta = \mathrm{e}^{\frac{2\pi \mathrm{i} \Delta n}{N}} V_{nm} \mathrm{e}^{-\frac{2\pi \mathrm{i} \Delta m}{N}}.$$

That is, V^Δ results from a unitary transformation of V. Therefore, they have the same spectrum and the corresponding entropies (2.33) are equal.

3. *PC* invariance. If we apply the *PC* transformation, (2.14) and (2.18), to a configuration $\mathbf{K}$ we obtain the complementary configuration $\mathbf{K}^{\complement}$, that is, $\mathbf{K} \cup \mathbf{K}^{\complement}$ is the configuration in which all the Bogoliubov modes are occupied. Given the form of the matrix $\mathcal{G}_k$ for $\mathbf{K}$, see (2.39), it is straightforward that for $\mathbf{K}^{\complement}$ this matrix is $\mathcal{G}_k^{\complement} = -\mathcal{G}_k$. Hence, under the *PC* transformation, the correlation matrix changes its sign,
$$V_{nm}^{\complement} = -V_{nm}.$$
The entropy (2.33) is invariant under the change of the sign of the correlation matrix. In conclusion, the entropies of $\mathbf{K}$ and $\mathbf{K}^{\complement}$ are equal.

In the thermodynamic limit $N \to \infty$, all the N-tuples that we have introduced, such as ω_k, F_k, G_k, M_k and the others, become 2π-periodic functions $\omega(\theta)$, $F(\theta)$, $G(\theta)$, $M(\theta)$... determined by the relation $\omega(\theta_k) = \omega_k$. Then the entries (2.38) of the correlation matrix V become
$$V_{nm} = \frac{1}{2\pi} \int_{-\pi}^{\pi} \mathcal{G}(\theta) \mathrm{e}^{\mathrm{i}\theta(n-m)} \mathrm{d}\theta, \quad n, m = 1, \dots, N, \tag{2.41}$$
with the matrix $\mathcal{G}(\theta)$ defined by
$$\frac{1}{2\pi} \int_{-\pi}^{\pi} \Psi(\theta) \mathcal{G}(\theta) \mathrm{d}\theta = \lim_{N\to\infty} \frac{1}{N} \sum_{k=0}^{N-1} \Psi(\theta_k) \mathcal{G}_k,$$
where the equality should be valid for any continuous scalar function Ψ.

A matrix with entries like those of (2.41) is a *block Toeplitz matrix* with symbol the 2×2 matrix $\mathcal{G}(\theta)$. That is, the entry V_{nm} is given by the $(n-m)$-Fourier coefficient of the entries in $\mathcal{G}(\theta)$. Therefore, V is a block matrix in which the elements V_{nm} of every subdiagonal parallel to the main one are equal. A sketch of this kind of matrices is represented in Fig. 2.6.

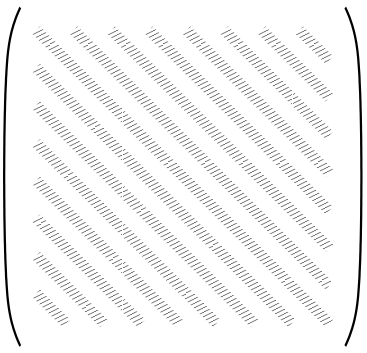

Figure 2.6: By the diagonal bars we represent the defining property of a block Toeplitz matrix: the entries along any subdiagonal parallel to the principal one are equal.

In order to compute the entanglement entropy $S_{\alpha,X}$ using (2.36) we have to take the restriction of the correlation matrix (2.41) to the sites that belong to X, that we denote V_X. In the following chapters we shall take advantage of the properties of block Toeplitz matrices to obtain the asymptotic behaviour for the determinant of $\lambda I - V_X$ and, employing (2.36), the dependence of the entanglement entropy on the size of the subsystem.

Chapter 3

Hopping chains

In this Chapter we shall study the asymptotic behaviour of the entanglement entropy for an interval of contiguous sites in the stationary states of a particular subset of the fermionic chains introduced previously.

We shall consider those models described by a Hamiltonian of the form (2.2) in which all the pairings B_l are zero. That is, it only has hopping terms,

$$H = \sum_{n=1}^{N} \sum_{l=-L}^{L} A_l a_n^\dagger a_{n+l}, \tag{3.1}$$

so it commutes with the number operator $\hat{N} = \sum_{n=1}^{N} a_n^\dagger a_n$.

This symmetry simplifies enormously the problem. In Section 2.3, generalising the work [98] of Jin and Korepin, we obtained that the Rényi entanglement entropy for the stationary states can be derived from the determinant of the resolvent of the two-point correlation matrix. We shall see here that for chains without pairing terms this matrix is a Toeplitz matrix.

Therefore, the problem of analysing the asymptotic behaviour of the entanglement entropy reduces to computing the determinant of a Toeplitz matrix. It turns out that there exist asymptotic formulas for these determinants. In particular, using the Fisher-Hartwig conjecture (actually a theorem as it has been proven in our case) we shall be able to obtain the asymptotic expansion of the entanglement entropy. We shall check numerically the validity of this expression for different states. Finally we shall give a physical interpretation of the results. For this purpose, we shall introduce local fermionic ladders as a generalisation of the fermionic chains.

3.1 Correlation matrix

In order to solve the Hamiltonian (3.1), observe that it is diagonalized by the Fourier modes

$$b_k = \frac{1}{\sqrt{N}} \sum_{n=1}^{N} \mathrm{e}^{-\mathrm{i}\theta_k n} a_n, \quad \theta_k = \frac{2\pi k}{N}, \quad k \in \mathbb{Z}.$$

Hence we do not have to perform a Bogoliubov transformation as in the general case. In fact, in terms of the operators above, the Hamiltonian (3.1) reads

$$H = \sum_{k=-N/2}^{N/2-1} \omega_k b_k^\dagger b_k,$$

with dispersion relation

$$\omega_k = F_k = \sum_{l=-L}^{L} A_l \mathrm{e}^{\mathrm{i}\theta_k l}. \tag{3.2}$$

For convenience, we have taken $k = -N/2, \ldots, N/2-1$. Remember that we are always considering periodic boundary conditions, $a_{n+N} = a_n$, and, therefore, $b_{k+N} = b_k$.

Thus the eigenstates of (3.1) are characterised by the subset of occupied Fourier modes $\mathbf{K} \subset \{-N/2, \ldots, N/2-1\}$,

$$|\mathbf{K}\rangle = \prod_{k \in \mathbf{K}} b_k^\dagger |0\rangle, \tag{3.3}$$

where $|0\rangle$ denotes the vacuum of the b-operators, that is $b_k |0\rangle = 0$ for all k. In particular, the ground state $|\hat{\mathbf{K}}\rangle$ is obtained by filling the Fourier modes with negative energy

$$|\hat{\mathbf{K}}\rangle = \prod_{\omega_k < 0} b_k^\dagger |0\rangle.$$

Remark: in the previous Chapter we demand that $(\omega_k + \omega_{-k})/2 \geq 0$ in order to remove the ambiguities. Here it will be more convenient to fix the Bogoliubov transformation to the identity. As a consequence of this choice the symmetric part of ω_k may take negative values.

For the eigenstates $|\mathbf{K}\rangle$, the entries of the correlation matrix V, introduced in Section 2.3, are

$$V_{nm} = 2 \left\langle \mathbf{K} \left| \begin{pmatrix} a_n \\ a_n^\dagger \end{pmatrix} (a_m^\dagger, a_m) \right| \mathbf{K} \right\rangle - \delta_{nm} I, \quad n, m = 1, \ldots, N. \tag{3.4}$$

In the Fourier basis, they can be expressed as

$$V_{nm} = \frac{1}{N} \sum_{k=-N/2}^{N/2-1} \mathcal{G}_k \mathrm{e}^{\mathrm{i}\theta_k (n-m)},$$

where

$$\mathcal{G}_k = 2 \left\langle \mathbf{K} \left| \begin{pmatrix} b_k \\ b_{-k}^\dagger \end{pmatrix} (b_k^\dagger, b_{-k}) \right| \mathbf{K} \right\rangle - I.$$

Taking into account that $|\mathbf{K}\rangle = \prod_{k \in \mathbf{K}} b_k^\dagger |0\rangle$, we compute the expectation values in $\mathcal{G}_k$ obtaining

$$\mathcal{G}_k = \begin{pmatrix} 1 - 2\chi_{\mathbf{K}}(k) & 0 \\ 0 & -1 + 2\chi_{\mathbf{K}}(N-k) \end{pmatrix},$$

where $\chi_{\mathbf{K}}(k)$ is the characteristic function of the set $\mathbf{K}$ of occupied Fourier modes, that it is 1 or 0 according to whether k belongs to $\mathbf{K}$ or not.

Therefore, we have

$$\mathcal{G}_k = \begin{cases} -\sigma_z, & \text{if } k \in \mathbf{K} \text{ and } N-k \in \mathbf{K}, \\ -I, & \text{if } k \in \mathbf{K} \text{ and } N-k \notin \mathbf{K}, \\ \sigma_z, & \text{if } k \notin \mathbf{K} \text{ and } N-k \notin \mathbf{K}, \\ I, & \text{if } k \notin \mathbf{K} \text{ and } N-k \in \mathbf{K}. \end{cases}$$

In this case the matrix $\mathcal{G}_k$ is diagonal. Then there is a similarity transformation that rearranges the rows and columns of V

$$TVT^{-1} = \begin{pmatrix} V^S & 0 \\ 0 & -(V^S)^t \end{pmatrix},$$

and maps the $2N \times 2N$ matrix V to the direct sum of a $N \times N$ matrix V^S and its opposite and transpose. The entries of V^S are

$$(V^S)_{nm} = \frac{1}{N}\left(\sum_{k\in\mathbf{K}} \mathrm{e}^{\mathrm{i}\theta_k(n-m)} - \sum_{k\notin\mathbf{K}} \mathrm{e}^{\mathrm{i}\theta_k(n-m)} \right), \quad n,m = 1,\dots,N. \tag{3.5}$$

Observe that the states (3.3) preserve the fermionic number. Hence the correlations $F_{nm} = \langle \mathbf{K}| \, a_n a_m \, |\mathbf{K}\rangle$ vanish, and we only have to consider those of the form $C_{nm} = \langle \mathbf{K}| \, a_n^\dagger a_m \, |\mathbf{K}\rangle$. If we express C_{nm} in the Fourier basis, we have

$$C_{nm} = \frac{1}{N} \sum_{k\in\mathbf{K}} \mathrm{e}^{\mathrm{i}\theta_k(n-m)}.$$

Comparing with (3.5) we conclude that $V^S = 2C - I$.

Consider now the relation found in (2.33) between the entropy and the correlation matrix. For the states $|\mathbf{K}\rangle$, the entropy of a subsystem X can be computed from the restriction of the correlation matrix (3.5) to the indices that belong to X, that we denote V_X^S. Hence, the entanglement entropy reads

$$S_{\alpha,X} = \frac{1}{1-\alpha} \operatorname{Tr} \log \left[\left(\frac{I+V_X^S}{2} \right)^\alpha + \left(\frac{I-V_X^S}{2} \right)^\alpha \right], \tag{3.6}$$

or, in terms of the contour integral (2.36),

$$S_{\alpha,X} = \frac{1}{2\pi\mathrm{i}} \lim_{\varepsilon\to 1^+} \oint_{\mathscr{C}} f_\alpha(\lambda/\varepsilon) \frac{\mathrm{d}}{\mathrm{d}\lambda} \log D_X^S(\lambda) \mathrm{d}\lambda, \tag{3.7}$$

where $D_X^S(\lambda) = \det(\lambda I - V_X^S)$. The integration contour $\mathscr{C}$ and the branch cuts of f_α are those depicted in Fig. 2.5.

In the thermodynamic limit $N \to \infty$, we can replace the sum in (3.5) by the integral

$$(V^S)_{nm} = \frac{1}{2\pi} \int_{-\pi}^{\pi} g(\theta) \mathrm{e}^{\mathrm{i}\theta(n-m)} \mathrm{d}\theta, \tag{3.8}$$

where $g(\theta)$ is a periodic function that takes values in the interval $[-1,1]$ and defined by

$$\frac{1}{2\pi}\int_{-\pi}^{\pi}\Psi(\theta)g(\theta)\mathrm{d}\theta=\lim_{N\to\infty}\frac{1}{N}\left[\sum_{k\in\mathbf{K}}\Psi(\theta_k)-\sum_{k\notin\mathbf{K}}\Psi(\theta_k)\right],$$

where the equality should be valid for any continuous function Ψ.

The function $g(\theta)$ represents the occupation density of the set of occupied Fourier modes in the configuration $\mathbf{K}$. Observe that $g(\theta)=1$ means that the modes with momenta around $N\theta/(2\pi)$ are all occupied while $g(\theta)=-1$ if all of them are empty. An intermediate value corresponds to the occupation of a fraction of the Fourier modes with momenta near $N\theta/(2\pi)$.

In order to determine $g(\theta)$ it is useful to describe the configuration $\mathbf{K}$ by a sequence of 1 and -1 where every digit represents the occupation (1) or not (-1) of the mode of the corresponding momentum k.

Let us illustrate this with several particular examples.

State 0: the Fock space vacuum $|\mathbf{K}^{(0)}\rangle=|0\rangle$. It corresponds to the configuration in which all the Fourier modes are empty, $\mathbf{K}^{(0)}=\emptyset$. This can be represented by the sequence (-1 -1 ... -1). Therefore, the density of occupied modes is

$$g^{(0)}(\theta)=-1.$$

State 1: half of the Fourier modes, corresponding to the lowest absolute value of the momenta, are occupied, while the others are empty. Therefore, the set of occupied modes is $\mathbf{K}^{(1)}=\{-N/4+1,\ldots,N/4-1\}$. This corresponds to the sequence (-1 ...-1 1 ... 1 1... 1 -1 ...-1). The occupation density is

$$g^{(1)}(\theta)=\begin{cases}-1, & \theta\in[-\pi,-\pi/2]\cup[\pi/2,\pi),\\ \\ 1, & \theta\in(-\pi/2,\pi/2).\end{cases}$$

State 2: the state

$$|\mathbf{K}^{(2)}\rangle=\prod_{n=1}^{N/2}\frac{1}{\sqrt{2}}\left(a_n^\dagger-a_{n+N/2}^\dagger\right)|0\rangle \tag{3.9}$$

corresponds to alternatively occupied and empty Fourier modes, $\mathbf{K}^{(2)}=\{-N/2+1,-N/2+3,-N/2+5,\ldots,1,3,5,\ldots,N/2-1\}$. That is, (-1 1 -1 1 ... 1 -1 1). Therefore,

$$g^{(2)}(\theta)=0.$$

State 3: as a mixture of the two previous cases, let us consider that the Fourier modes with momenta $|k|\geq N/4$ are empty while those with $|k|<N/4$ are occupied alternatively. That is, $\mathbf{K}^{(3)}=\{-N/4+1,-N/4+3,\ldots,1,3,5,\ldots,N/4-1\}$. This corresponds to the sequence (-1 -1 ... -1 1 -1 1 -1 ... -1 1 -1 -1 ... -1). Therefore, the occupation density is

$$g^{(3)}(\theta)=\begin{cases}-1, & \theta\in[-\pi,-\pi/2]\cup[\pi/2,\pi),\\ \\ 0, & \theta\in(-\pi/2,\pi/2).\end{cases}$$

State 4: all the Fourier modes with $|k| \geq N/4$ are empty, while for smaller momenta three out of four modes are occupied. That is, $\mathbf{K}^{(4)} = \{-N/4+1, -N/4+2, -N/4+3, -N/4+5, -N/4+6, -N/4+7, \ldots, 1, 2, 3, \ldots, N/4-3, N/4-2, N/4-1\}$. Hence we have the sequence (-1 -1 ...-1 -1 1 1 1 -1 1 1 1 ... -1 ... -1). Then the occupation density is

$$g^{(4)}(\theta) = \begin{cases} -1, & \theta \in [-\pi, \pi/2] \cup [\pi/2, \pi), \\ \\ 1/2, & \theta \in (-\pi/2, \pi/2). \end{cases}$$

In general, we shall be interested in piecewise constant occupation densities, such as the previous ones,

$$g(\theta) = t_{r-1}, \quad \theta_{r-1} \leq \theta < \theta_r, \tag{3.10}$$

where θ_1, θ_2, ..., θ_R are the discontinuity points and $\theta_0 = \theta_R - 2\pi$.

Observe that the entries (3.8) of V^S only depend on the difference $n - m$. This is a consequence of the translational invariance of the theory. If the subsystem X is a single interval of contiguous sites, all the entries in V_X^S of each subdiagonal parallel to the principal one are equal and correspond to one of the Fourier coefficients of the occupation density $g(\theta)$. A matrix with this property is called *Toeplitz*. In this case, we shall say that V_X^S is a Toeplitz matrix generated by the symbol $g(\theta)$. Therefore, using (3.7) the analysis of the entanglement entropy of an interval reduces to the study of the determinant of a Toeplitz matrix.

The asymptotic behaviour of Toeplitz determinants has been heavily investigated during the last century. This study was stimulated by the large variety of problems in Physics that can be formulated using this kind of determinants, from random walk to the description of the adsorption of dimeric molecules on a crystalline surface. In the 1949 paper [99] Kaufman and Onsager found that the spin-spin correlation functions for the classical Ising model in two dimensions may be expressed in terms of a Toeplitz determinant. This discovery led to an intense effort of physicists and mathematicians towards the understanding of these determinants. The whole story about the relevance of the Ising model in the development of the theory of Toeplitz determinants can be found in the nice review [100].

The study of the correlations in the Ising model gave rise to the two main results concerning the asymptotic behaviour of Toeplitz determinants: the Strong Szegő theorem [101] and the Fisher-Hartwig conjecture [102]. The first one gives the asymptotic behaviour for Toeplitz matrices with a continuous (smooth enough), non-zero symbol. The Fisher-Hartwig conjecture generalises the Strong Szegő theorem to piecewise symbols with discontinuities, as it is our case, and/or zeros. Of course, there is a plethora of other results on the properties of Toeplitz determinants. Many of them can be found, for example, in the mentioned review [100] or in the book by Böttcher and Silbermann [103].

In 2003 Jin and Korepin found another application of Toeplitz determinants in Physics: entanglement entropy. In Ref. [98] they arrived at the expression (3.7) for the ground state of the XX spin chain. Then they employed the Fisher-Hartwig conjecture to determine the asymptotic behaviour of the entanglement entropy of an interval. We shall generalise here their result to any stationary state of the Hamiltonian (3.1) with occupation density like (3.10). This will be the objective of the next section.

3.2 Asymptotic behaviour of the entanglement entropy

In this Section we shall obtain the asymptotic behaviour of the entanglement entropy of an interval X of length $|X|$ in the stationary states (3.3). As we have just seen, the correlation matrix of this subsystem, V_X^S, is a Toeplitz matrix of dimension $|X| \times |X|$ and symbol the density of occupied modes $g(\theta)$. Hence using the expression (3.7) we can determine the entropy of the interval from the determinant $D_X^S(\lambda)$ of the Toeplitz matrix $\lambda I - V_X^S$. The asymptotic behaviour of this determinant can be computed using the Fisher-Hartwig conjecture, that for symbols like (3.10) is actually a theorem proved by Basor in [104].

The Fisher-Hartwig conjecture states that if $g(\theta)$ is a piecewise constant function with jump discontinuities at $\theta_1, \ldots, \theta_R$, like (3.10), then the Toeplitz determinant $D_X^S(\lambda)$ generated by $\lambda - g(\theta)$ has the following asymptotic behaviour

$$\log D_X^S(\lambda) = s(\lambda)|X| - \sum_{r=1}^{R} \beta_r^2 \log |X| + \log E + o(1), \tag{3.11}$$

where

$$s(\lambda) = \frac{1}{2\pi} \int_{-\pi}^{\pi} \log[\lambda - g(\theta)] \mathrm{d}\theta,$$

the coefficient β_r accounts for the value of the symbol $\lambda - g(\theta)$ at each side of the discontinuity point θ_r,

$$\beta_r \equiv \beta_r(\lambda) = \frac{1}{2\pi i} \log \left(\frac{\lambda - t_r}{\lambda - t_{r-1}} \right),$$

with t_{r-1} and t_r given by (3.10). The constant term reads

$$E \equiv E[\{\beta_r\}, \{\theta_r\}] = \prod_{r=1}^{R} G(1+\beta_r) G(1-\beta_r) \prod_{1 \le r \ne r' \le R} (1 - \mathrm{e}^{\mathrm{i}(\theta_r - \theta_{r'})})^{\beta_r \beta_{r'}}.$$

Here $G(z)$ denotes the Barnes G-function [92]. Observe that the factor $s(\lambda)$, the zero mode of $\log[\lambda - g(\theta)]$, contributes to $\log D_X^S(\lambda)$ with a term proportional to the size of the interval $|X|$. On the other hand, the discontinuities give rise to a term that grows with $\log |X|$ as well as to a constant term independent from $|X|$. When the symbol is continuous ($R = 0$) the expansion (3.11) reduces to that predicted by the Strong Szegő theorem [101]. In particular, if the occupation density is constant, $g(\theta) = t$ for $-\pi \le \theta < \pi$, the determinant $D_X(\lambda)$ behaves as

$$\log D_X(\lambda) = |X| \log(\lambda - t) + o(1).$$

In the next Chapter we shall enunciate the Strong Szegő theorem and the Fisher-Hartwig conjecture for more general symbols, not only piecewise constant functions.

If we now insert the expression (3.11) given by the Fisher-Hartwig conjecture into the contour integral (3.7) for $S_{\alpha,X}$, we conclude that the Rényi entanglement entropy behaves like

$$S_{\alpha,X} = \mathcal{A}_\alpha |X| + \mathcal{B}_\alpha \log |X| + \mathcal{C}_\alpha + o(1). \tag{3.12}$$

Let us compute now the coefficients of this expansion.

The coefficient $\mathcal{A}_\alpha$ of the linear term reads

$$\mathcal{A}_\alpha = \frac{1}{2\pi \mathrm{i}} \lim_{\varepsilon \to 1^+} \oint_{\mathscr{C}} f_\alpha(\lambda/\varepsilon) \frac{\mathrm{d}}{\mathrm{d}\lambda} s(\lambda) \mathrm{d}\lambda. \tag{3.13}$$

Taking into account the form (3.10) of $g(\theta)$,

$$s(\lambda) = \frac{1}{2\pi} \sum_{r=1}^{R} \int_{\theta_{r-1}}^{\theta_r} \log(\lambda - t_{r-1}) \mathrm{d}\theta = \log \prod_{r=1}^{R} (\lambda - t_{r-1})^{\frac{\theta_r - \theta_{r-1}}{2\pi}}.$$

Then if we compute the derivative of $s(\lambda)$ in (3.13),

$$\mathcal{A}_\alpha = \frac{1}{4\pi^2 \mathrm{i}} \lim_{\varepsilon \to 1^+} \oint_{\mathscr{C}} f_\alpha(\lambda/\varepsilon) \sum_{r=1}^{R} \frac{\theta_r - \theta_{r-1}}{\lambda - t_{r-1}} \mathrm{d}\lambda.$$

Employing now the Cauchy's residue theorem and taking the limit, we finally find

$$\mathcal{A}_\alpha = \frac{1}{2\pi} \sum_{r=1}^{R} (\theta_r - \theta_{r-1}) f_\alpha(t_{r-1}). \tag{3.14}$$

In the case $R = 0$, that is when the occupation density is continuous and $g(\theta) = t$ for $-\pi \leq \theta < \pi$, the coefficient of the linear term is

$$\mathcal{A}_\alpha = f_\alpha(t). \tag{3.15}$$

For the coefficient $\mathcal{B}_\alpha$, we have

$$\mathcal{B}_\alpha = -\frac{1}{2\pi \mathrm{i}} \sum_{r=1}^{R} \lim_{\varepsilon \to 1^+} \oint_{\mathscr{C}} f_\alpha(\lambda/\varepsilon) \frac{\mathrm{d}\beta_r^2}{\mathrm{d}\lambda} \mathrm{d}\lambda.$$

In Fig. 3.1 we represent the branch points and cuts for the integrand of the r-term of the above sum.

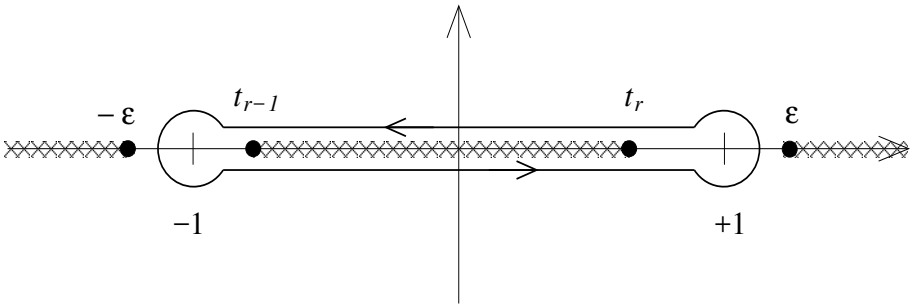

Figure 3.1: Contour of integration, branch points and cuts for the computation of $\mathcal{B}_\alpha$

There are different ways of dealing with this integral. One strategy, employed for example in [98], is to decompose the contour $\mathscr{C}$ into different pieces where the integrals diverge. After a tedious computation, one can see that the divergences cancel and the

final result is finite. An alternative strategy that leads directly to the finite result is to perform an integration by parts

$$\mathcal{B}_\alpha = \frac{1}{2\pi \mathrm{i}} \sum_{r=1}^{R} \lim_{\varepsilon \to 1^+} \oint_{\mathscr{C}} \frac{\mathrm{d}f_\alpha(\lambda/\varepsilon)}{\mathrm{d}\lambda} \beta_r^2 \mathrm{d}\lambda. \tag{3.16}$$

For each r-term, we can deform the integration contour $\mathscr{C}$ into a curve that only encloses the cut between the points t_{r-1} and t_r. Taking now into account the change in the branch of β_r when we go around t_{r-1} and t_r,

$$\mathcal{B}_\alpha = \frac{1}{8\pi^3 \mathrm{i}} \sum_{r=1}^{R} \int_{t_{r-1}}^{t_r} \frac{\mathrm{d}f_\alpha(\lambda)}{\mathrm{d}\lambda} \left[\left(\log \left| \frac{\lambda - t_r}{\lambda - t_{r-1}} \right| + \mathrm{i}\pi \right)^2 - \left(\log \left| \frac{\lambda - t_r}{\lambda - t_{r-1}} \right| - \mathrm{i}\pi \right)^2 \right] \mathrm{d}\lambda.$$

After simplifying we arrive at

$$\mathcal{B}_\alpha = \frac{1}{2\pi^2} \sum_{r=1}^{R} \int_{t_{r-1}}^{t_r} \frac{\mathrm{d}f_\alpha(\lambda)}{\mathrm{d}\lambda} \log \left| \frac{\lambda - t_r}{\lambda - t_{r-1}} \right| \mathrm{d}\lambda. \tag{3.17}$$

In the next sections, we shall consider some particular cases in which $\mathcal{B}_\alpha$ can be obtained analytically. In general, however, for non integer α this integral can only be computed numerically.

For integer $\alpha > 1$, we can give an explicit expression for $\mathcal{B}_\alpha$. In order to find it, we should come back to (3.16), after integrating by parts. Let us take the r-term

$$\mathcal{B}_{\alpha,r} = \frac{1}{2\pi \mathrm{i}} \lim_{\varepsilon \to 1^+} \oint_{\mathscr{C}} \frac{\mathrm{d}f_\alpha(\lambda/\varepsilon)}{\mathrm{d}\lambda} \beta_r^2 \mathrm{d}\lambda.$$

The derivative

$$\frac{\mathrm{d}f_\alpha(\lambda)}{\mathrm{d}\lambda} = \frac{\alpha}{1-\alpha} \frac{(1+\lambda)^{\alpha-1} - (1-\lambda)^{\alpha-1}}{(1+\lambda)^\alpha + (1-\lambda)^\alpha},$$

is a meromorphic function for integer $\alpha > 1$ with poles along the imaginary axis located at

$$\lambda_l = \mathrm{i} \tan \frac{(2l-1)\pi}{2\alpha}, \quad l = 1, \cdots, \alpha, \quad l \neq \frac{\alpha+1}{2}.$$

Since β_r^2 is holomorphic outside the integration contour $\mathscr{C}$ we can send this curve to infinity and reduce the integral in $\mathcal{B}_{\alpha,r}$ to the computation of the corresponding residues of the integrand at λ_l,

$$\mathcal{B}_{\alpha,r} = - \sum_{\substack{l=1 \\ l \neq \frac{\alpha+1}{2}}}^{\alpha} \mathrm{Res} \left(\frac{\mathrm{d}f_\alpha}{\mathrm{d}\lambda} \beta_r^2, \lambda_l \right).$$

The residues of the poles of $\mathrm{d}f_\alpha/\mathrm{d}\lambda$ are

$$\mathrm{Res} \left(\frac{\mathrm{d}f_\alpha}{\mathrm{d}\lambda} \beta_r^2, \lambda_l \right) = \frac{1}{4\pi^2(\alpha-1)} \left(\log \frac{\lambda_l - t_r}{\lambda_l - t_{r-1}} \right)^2.$$

After some simplifications we arrive at

$$\mathcal{B}_{\alpha,r} = \frac{1}{4\pi^2(1-\alpha)} \sum_{l=1}^{\alpha} \left[\frac{1}{4} \left(\log \frac{(t_r^2-1)\cos^2 \frac{(2l-1)\pi}{2\alpha} + 1}{(t_{r-1}^2-1)\cos^2 \frac{(2l-1)\pi}{2\alpha} + 1} \right)^2 - \varphi_l^2 \right], \tag{3.18}$$

where

$$\varphi_l = \arctan \frac{(t_r - t_{r-1}) \tan \frac{(2l-1)\pi}{2\alpha}}{t_r t_{r-1} + \tan^2 \frac{(2l-1)\pi}{2\alpha}}, \quad \varphi_l \in (-\pi/2, \pi/2).$$

Hence the coefficient $\mathcal{B}_\alpha$ will be the sum of all these terms,

$$\mathcal{B}_\alpha = \sum_{r=1}^{R} \mathcal{B}_{\alpha,r}, \tag{3.19}$$

provided $\alpha > 1$ is an integer.

Finally, the constant term $\mathcal{C}_\alpha$,

$$\mathcal{C}_\alpha = \frac{1}{2\pi \mathrm{i}} \lim_{\varepsilon \to 1^+} \oint_{\mathscr{C}} f_\alpha(\lambda/\varepsilon) \left[\sum_{r=1}^{R} \frac{\mathrm{d}}{\mathrm{d}\lambda} \log[G(1+\beta_r)G(1-\beta_r)] + \right.$$
$$\left. + \sum_{1 \le r \ne r' \le R} \log(1 - \mathrm{e}^{\mathrm{i}(\theta_r - \theta_{r'})}) \frac{\mathrm{d}}{\mathrm{d}\lambda}(\beta_r \beta_{r'}) \right] \mathrm{d}\lambda,$$

has two integrals that can be treated as the previous one. Let us take the first one

$$I_\alpha(r) = \frac{1}{2\pi \mathrm{i}} \lim_{\varepsilon \to 1^+} \oint_{\mathscr{C}} f_\alpha(\lambda/\varepsilon) \frac{\mathrm{d}}{\mathrm{d}\lambda} \log[G(1+\beta_r)G(1-\beta_r)] \mathrm{d}\lambda,$$

and perform an integration by parts,

$$I_\alpha(r) = -\frac{1}{2\pi \mathrm{i}} \lim_{\varepsilon \to 1^+} \oint_{\mathscr{C}} \frac{\mathrm{d} f_\alpha(\lambda/\varepsilon)}{\mathrm{d}\lambda} \log[G(1+\beta_r)G(1-\beta_r)] \mathrm{d}\lambda.$$

The branch points and cuts of the integrand are again those of Fig. 3.1. Analogously to what we have done for the r-terms of $\mathcal{B}_\alpha$, the integration over $\mathscr{C}$ reduces to integrate along the cut between t_{r-1} and t_r taking into account the change in the branch of β_r. Hence

$$I_\alpha(r) = \frac{1}{2\pi \mathrm{i}} \int_{t_{r-1}}^{t_r} \frac{\mathrm{d} f_\alpha(\lambda)}{\mathrm{d}\lambda} \log \left[\frac{G(1+\beta_r^-)G(1-\beta_r^-)}{G(1+\beta_r^+)G(1-\beta_r^+)} \right] \mathrm{d}\lambda,$$

where $\beta_r^\pm$ are the two different branches of β_r involved in the integration,

$$\beta_r^\pm = \mathrm{i}\varpi_r(\lambda) \pm \frac{1}{2}, \quad \varpi_r(\lambda) = \frac{1}{2\pi} \log \left| \frac{\lambda - t_r}{\lambda - t_{r-1}} \right|.$$

Observe that $\beta_r^+ = \beta_r^- + 1$. Therefore, applying the property of the Barnes G-function $G(z+1) = \Gamma(z)G(z)$, where Γ is the Gamma function, we finally arrive at

$$I_\alpha(r) = \frac{1}{2\pi \mathrm{i}} \int_{t_{r-1}}^{t_r} \frac{\mathrm{d} f_\alpha(\lambda)}{\mathrm{d}\lambda} \log \left[\frac{\Gamma(1/2 - \mathrm{i}\varpi_r(\lambda))}{\Gamma(1/2 + \mathrm{i}\varpi_r(\lambda))} \right] \mathrm{d}\lambda. \tag{3.20}$$

We proceed as before with the second integral,

$$J_\alpha(r, r') = -\frac{1}{2\pi \mathrm{i}} \lim_{\varepsilon \to 1^+} \oint_{\mathscr{C}} f_\alpha(\lambda/\varepsilon) \frac{\mathrm{d}(\beta_r \beta_{r'})}{\mathrm{d}\lambda} \mathrm{d}\lambda.$$

We integrate by parts,

$$J_\alpha(r,r') = \frac{1}{2\pi \mathrm{i}} \lim_{\varepsilon\to 1^+} \oint_{\mathscr{C}} \frac{\mathrm{d}f_\alpha(\lambda/\varepsilon)}{\mathrm{d}\lambda} \beta_r \beta_{r'} \mathrm{d}\lambda,$$

avoiding the divergences that directly cancel with this strategy, There are now two different cuts inside the integration contour. One from t_{r-1} to t_r and another one from $t_{r'-1}$ to $t_{r'}$. We can decompose the integral in the following way,

$$J_\alpha(r,r') = \frac{1}{2\pi \mathrm{i}} \lim_{\varepsilon\to 1^+} \oint_{\mathscr{C}_r} \frac{\mathrm{d}f_\alpha(\lambda/\varepsilon)}{\mathrm{d}\lambda} \beta_r \beta_{r'} \mathrm{d}\lambda + \frac{1}{2\pi \mathrm{i}} \lim_{\varepsilon\to 1^+} \oint_{\mathscr{C}_{r'}} \frac{\mathrm{d}f_\alpha(\lambda/\varepsilon)}{\mathrm{d}\lambda} \beta_r \beta_{r'} \mathrm{d}\lambda,$$

where $\mathscr{C}_r$ ($\mathscr{C}_{r'}$) is a contour that only encloses the cut with endpoints t_{r-1} ($t_{r'-1}$) and t_r ($t_{r'}$). Since we will only meet logarithmic singularities, we integrate each term along the corresponding cut taking into account the change in the branch of β_r or $\beta_{r'}$ when we go around their branch points. Then we arrive at

$$J_\alpha(r,r') = K_\alpha(r,r') + K_\alpha(r',r),$$

with

$$K_\alpha(r,r') = \frac{1}{4\pi^2} \int_{t_{r-1}}^{t_r} \frac{\mathrm{d}f_\alpha(\lambda)}{\mathrm{d}\lambda} \log \left| \frac{\lambda - t_{r'}}{\lambda - t_{r'-1}} \right| \mathrm{d}\lambda. \tag{3.21}$$

Finally, putting all together we have

$$\mathcal{C}_\alpha = \sum_{r=1}^{R} I_\alpha(r) - \sum_{1\le r\neq r'\le R} \log\left[2 - 2\cos(\theta_r - \theta_{r'})\right] K_\alpha(r,r'). \tag{3.22}$$

To our knowledge, such an explicit expression of the asymptotic behaviour of the Rényi entanglement entropy was obtained for the first time by the author jointly with Esteve, Falceto and Sánchez-Burillo in [105]. Keating and Mezzadri generalised in [106, 107] the original result of Jin and Korepin to any state with occupation density $g(\theta) = \pm 1$ and a finite number of discontinuities. In [108], Alba, Fagotti and Calabrese already studied some aspects of the entanglement entropy for the states with $g(\theta) \neq \pm 1$ applying the Fisher-Hartwig conjecture too. Several authors have employed this approach to study the entanglement entropy in different fermionic chains, see for instance [109, 110, 111, 112, 113]. In [114] Calabrese and Essler proposed a generalisation of the Fisher-Hartwig expansion (3.11) that accounts for the $o(1)$ terms in the Rényi entanglement entropy for the ground state of the XX spin chain. They found that these corrections oscillate with $|X|$.

Note that, by its definition (2.34), $f_\alpha(\pm 1) = 0$. Hence if $g(\theta) = \pm 1$ the coefficient of the linear term $\mathcal{A}_\alpha$ vanishes. The logarithmic and the finite terms arise from the discontinuities of $g(\theta)$. In fact, if $g(\theta)$ is continuous then $\mathcal{B}_\alpha$ and $\mathcal{C}_\alpha$ are zero. Therefore, if the state has $g(\theta) = \pm 1$ with a finite number of discontinuities, the entropy of the interval grows with $\log|X|$. On the other hand, if there are intervals with $g(\theta) \neq \pm 1$ the entropy exhibits both linear and logarithmic contributions.

3.2.1 Examples

Using the previous results, let us compute the entanglement entropy (3.12) for the particular states considered in Section 3.1

State 0: since $g^{(0)}(\theta) = -1$, we do not have linear term. The symbol does not present discontinuities and, therefore, the coefficients of the logarithmic and constant terms, $\mathcal{B}_\alpha^{(0)}$ and $\mathcal{C}_\alpha^{(0)}$, vanish too. Hence the entanglement entropy is zero. This result can be obtained directly by noticing that the vacuum of the Fourier modes $|0\rangle$ is separable.

State 1: the coefficient of the linear term, $\mathcal{A}_\alpha^{(1)}$, is zero because $g^{(1)}(\theta) = \pm 1$. Since $g^{(1)}$ is discontinuous, the entanglement entropy grows with $\log|X|$. We can compute the coefficient of this term applying (3.17). In this case it reads

$$\mathcal{B}_\alpha^{(1)} = \frac{1}{\pi^2}\int_{-1}^{1} \frac{\mathrm{d}f_\alpha(\lambda)}{\mathrm{d}\lambda} \log\frac{1-\lambda}{1+\lambda}\mathrm{d}\lambda.$$

Here we have taken into account that $g^{(1)}$ has two jumps ($R = 2$) from -1 to 1. Therefore, they give an equal contribution to $\mathcal{B}_\alpha^{(1)}$.

The integral above can be computed analytically for any α. In fact, after integrating by parts and changing the variable to $t = (1+\lambda)/(1-\lambda)$ we have

$$\mathcal{B}_\alpha^{(1)} = \frac{1}{\pi^2(1-\alpha)}\left[\int_0^\infty \log(t^\alpha+1)\frac{\mathrm{d}t}{t} - \alpha\int_0^\infty \log(t+1)\frac{\mathrm{d}t}{t}\right].$$

Performing now the change of variable $t^\alpha = \mathrm{e}^u$ in the first integral and $t = \mathrm{e}^u$ in the second one, we arrive at

$$\mathcal{B}_\alpha^{(1)} = \frac{2(1+\alpha)}{\pi^2\alpha}\int_0^\infty \log(\mathrm{e}^{-u}+1)\mathrm{d}u = \frac{\alpha+1}{6\alpha}. \tag{3.23}$$

There is also a constant $\mathcal{C}_\alpha^{(1)}$ in the entropy. We can use (3.22) to compute it. Notice that this term not only depends on the value of $g^{(1)}(\theta)$ at each side of the discontinuities but also on their location. In this case they are located at $\theta_1 = -\pi/2$ and $\theta_2 = \pi/2$. Then the expression in (3.22) particularises to

$$\mathcal{C}_\alpha^{(1)} = I_\alpha^{(1)}(1) + I_\alpha^{(1)}(2) - \left[K_\alpha^{(1)}(1,2) + K_\alpha^{(1)}(2,1)\right]2\log 2.$$

According to (3.20), since the value of $g^{(1)}(\theta)$ changes from -1 to 1 at both discontinuity points, $I_\alpha^{(1)}(1) = I_\alpha^{(1)}(2) = \Upsilon_\alpha$, with

$$\Upsilon_\alpha = \frac{1}{2\pi\mathrm{i}}\int_{-1}^{1}\frac{\mathrm{d}f_\alpha(\lambda)}{\mathrm{d}\lambda}\log\left[\frac{\Gamma(1/2-\mathrm{i}\beta(\lambda))}{\Gamma(1/2+\mathrm{i}\beta(\lambda))}\right]\mathrm{d}\lambda, \quad \beta(\lambda) = \frac{1}{2\pi}\log\frac{1-\lambda}{1+\lambda}. \tag{3.24}$$

Taking into account (3.21) we have

$$K_\alpha^{(1)}(1,2) = K_\alpha^{(1)}(2,1) = -\frac{\mathcal{B}_\alpha^{(1)}}{4} = -\frac{\alpha+1}{24\alpha}.$$

Therefore, the constant term is

$$\mathcal{C}_\alpha^{(1)} = 2\Upsilon_\alpha + \frac{\alpha+1}{6\alpha}\log 2.$$

In conclusion, the entanglement entropy of an interval in this state is

$$S_{\alpha,X}^{(1)} = \frac{\alpha+1}{6\alpha}\log|X| + \mathcal{C}_\alpha^{(1)} + o(1). \tag{3.25}$$

State 2: since $g^{(2)}(\theta) = 0$ for all θ, the entanglement entropy grows linearly with $|X|$. The proportionality constant can be obtained from (3.15),

$$\mathcal{A}_\alpha^{(2)} = f_\alpha(0) = \log 2.$$

The coefficients $\mathcal{B}_\alpha^{(2)}$, $\mathcal{C}_\alpha^{(2)}$ of the logarithmic and the constant terms are zero because the symbol is continuous. Therefore,

$$S_{\alpha,X}^{(2)} = |X| \log 2 + o(1). \tag{3.26}$$

The entanglement entropy for this state can be exactly computed by taking the partial trace of

$$|\mathbf{K}^{(2)}\rangle = \prod_{n=1}^{N/2} \frac{1}{\sqrt{2}} \left(a_n^\dagger - a_{n+N/2}^\dagger\right) |0\rangle .$$

In particular, for any interval of length $|X| < N/2$, the reduced density matrix is

$$\rho_X = 2^{-|X|} I,$$

which leads to the same result (3.26) that we have obtained employing the Fisher-Hartwig expansion, which is exact for $|X| < N/2$. Observe that $S_{\alpha,X}^{(2)}$ is independent from the Rényi parameter α and it is the largest possible entropy of a mixed state in a Hilbert space of dimension $2^{|X|}$.

State 3: the entanglement entropy for this state combines the features of the two previous ones. It presents a linear term since $g^{(3)}(\theta)$ is zero in the interval between $\theta_1 = -\pi/2$ and $\theta_2 = \pi/2$. We calculate the coefficient of this term using (3.14)

$$\mathcal{A}_\alpha^{(3)} = \frac{\theta_2 - \theta_1}{2\pi} f_\alpha(0) = \frac{\log 2}{2}. \tag{3.27}$$

This symbol is discontinuous and, therefore, the entropy has also logarithmic and constant terms. Since it has two jumps from -1 to 0, the coefficient of the logarithmic term obtained applying (3.17) is

$$\mathcal{B}_1^{(3)} = \frac{1}{2\pi^2} \int_{-1}^{0} \log \frac{1-\lambda}{1+\lambda} \log \frac{-\lambda}{\lambda+1} \mathrm{d}\lambda = \frac{1}{8} - \frac{1}{2} \left(\frac{\log 2}{\pi}\right)^2, \tag{3.28}$$

for $\alpha = 1$.

For integer $\alpha \geq 2$ we can use (3.18). In this case it gives

$$\mathcal{B}_\alpha^{(3)} = \frac{\alpha+1}{24\alpha} - \frac{1}{2\pi^2(\alpha-1)} \sum_{l=1}^{\alpha} \left(\log \sin \frac{(2l-1)\pi}{2\alpha}\right)^2. \tag{3.29}$$

When α is not an integer this coefficient and the constant term $\mathcal{C}_\alpha^{(3)}$ (for any α) have to be computed numerically from the expressions (3.17) and (3.22) respectively.

Hence the entropy of an interval for this state is

$$S_{\alpha,X}^{(3)} = \frac{\log 2}{2} |X| + \mathcal{B}_\alpha^{(3)} \log |X| + \mathcal{C}_\alpha^{(3)} + o(1). \tag{3.30}$$

State 4: as in the previous state, the entanglement entropy presents the three terms. The coefficient of the linear term is non-zero because $g^{(4)}(\theta) = 1/2$ in the interval between $\theta_1 = -\pi/2$ and $\theta_2 = \pi/2$. Hence employing (3.14) we find

$$\mathcal{A}_\alpha^{(4)} = \frac{\theta_2 - \theta_1}{2\pi} f_\alpha(1/2) = \frac{f_\alpha(1/2)}{2}.$$

For $\alpha = 1$, the latter particularises to

$$\mathcal{A}_1^{(4)} = \frac{1}{2} \log \frac{4}{3^{3/4}}, \tag{3.31}$$

while for any $\alpha > 1$,

$$\mathcal{A}_\alpha^{(4)} = \frac{1}{2(1-\alpha)} \log \frac{3^\alpha + 1}{4^\alpha}. \tag{3.32}$$

The occupation density $g^{(4)}$ has two discontinuities with lateral limits -1 and $1/2$. Thus, considering (3.17), the coefficient of the logarithmic term for $\alpha = 1$ is

$$\mathcal{B}_1^{(4)} = \frac{1}{2\pi^2} \int_{-1}^{1/2} \log \frac{1-\lambda}{1+\lambda} \log \frac{1/2-\lambda}{\lambda+1} \mathrm{d}\lambda = \frac{1}{8} - \frac{1}{2} \left(\frac{\log 2}{\pi} \right)^2 + \frac{3}{4\pi^2} \mathrm{Li}_2 \left(\frac{3}{4} \right), \tag{3.33}$$

where $\mathrm{Li}_2(z)$ stands for the dilogarithm function [92].

We can obtain an explicit expression of $\mathcal{B}_\alpha^{(4)}$ for integer $\alpha > 1$ using (3.18). For this state we have

$$\mathcal{B}_\alpha^{(4)} = \frac{1}{2\pi^2(\alpha-1)} \sum_{l=1}^{\alpha} \left(\arctan^2 \frac{3 \tan \frac{(2l-1)\pi}{2\alpha}}{2 \tan^2 \frac{(2l-1)\pi}{2\alpha} - 1} - \frac{1}{4} \log^2 \frac{3 \sin^2 \frac{(2l-1)\pi}{2\alpha} + 1}{4} \right). \tag{3.34}$$

In conclusion the entropy of an interval for this configuration behaves as

$$S_{\alpha,X}^{(4)} = \frac{f_\alpha(1/2)}{2} |X| + \mathcal{B}_\alpha^{(4)} \log |X| + \mathcal{C}_\alpha^{(4)} + o(1).$$

The coefficient $\mathcal{B}_\alpha^{(4)}$, for non-integer α, and the constant $\mathcal{C}_\alpha^{(4)}$ should be calculated numerically using respectively (3.17) and (3.22).

Let us check these results numerically. For this purpose we can employ the expression (3.6) of the entanglement entropy in terms of the correlation matrix V_X^S. This formula has the advantage that reduces the complexity of the numerical computation of the entropy with respect to the definition of $S_{\alpha,X}$ through the reduced density matrix ρ_X. In fact, while the dimension of ρ_X is $2^{|X|}$, the size of V_X^S is $|X|$. Hence we can go to large enough values of $|X|$, for which the Fisher-Hartwig expansion is a good approximation, without the necessity of special numerical techniques or high performance computing resources. Since we are interested in the thermodynamic limit, we only have to compute the entries of the correlation matrix V_X^S using (3.8), diagonalise it and calculate the entanglement entropy employing (3.6). Here we have performed the numerical diagonalisation employing the corresponding routine for Hermitian matrices included in the *GNU Scientific Library* for *C* [115]. We refer the interested reader to Appendix A where we discuss the details about the numerical calculations that we have performed in the thesis.

In Figs. 3.2, 3.3 and 3.4 we plot the numerical entanglement entropy obtained for the states 1, 3, and 4 varying the size $|X|$ of the interval from 10 to 1000. The solid lines represent the analytical expansion that we have just obtained for these states using the Fisher-Hartwig conjecture. The analytical prediction is a very good approximation even for the smaller sizes of the interval.

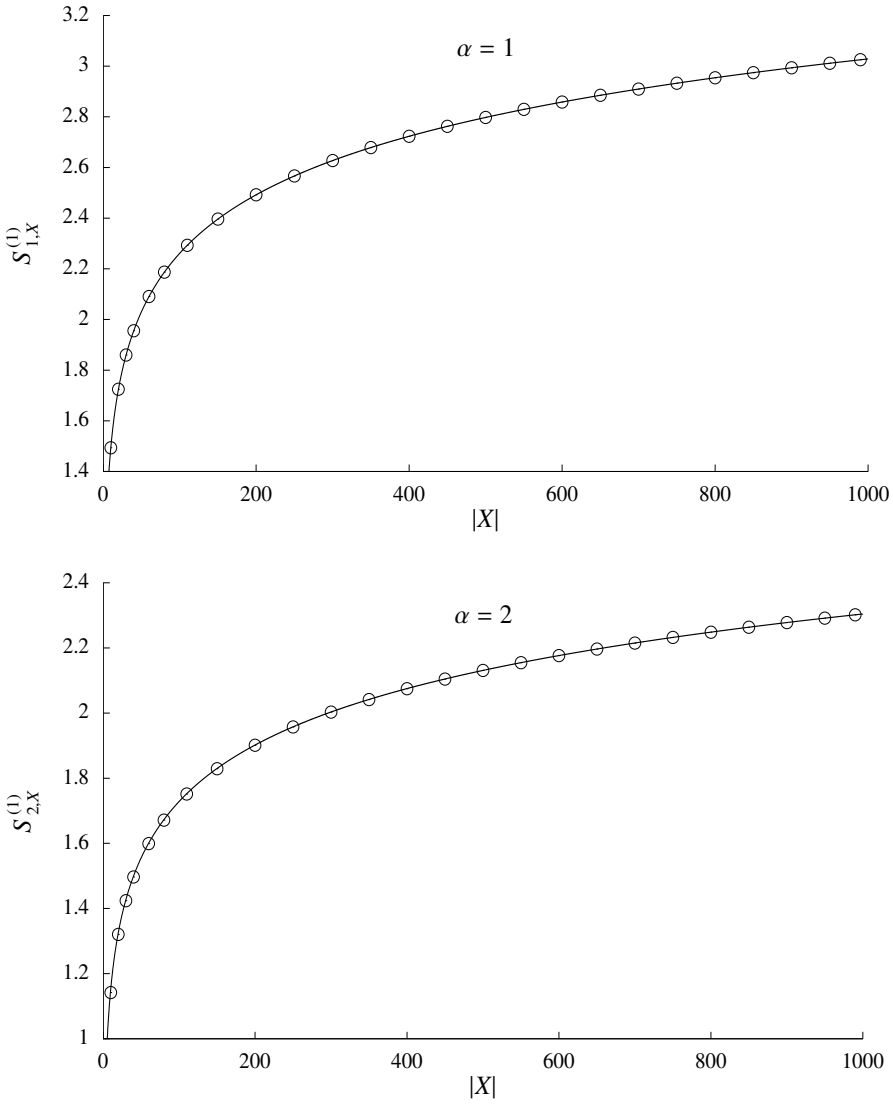

Figure 3.2: Entanglement entropy with $\alpha = 1$ (upper panel) and $\alpha = 2$ (lower panel) for a single interval of length $|X|$ when we take the **state 1**. The dots are the numerical values and the continuous line represents the asymptotic expansion (3.25) predicted by the Fisher-Hartwig conjecture for this state.

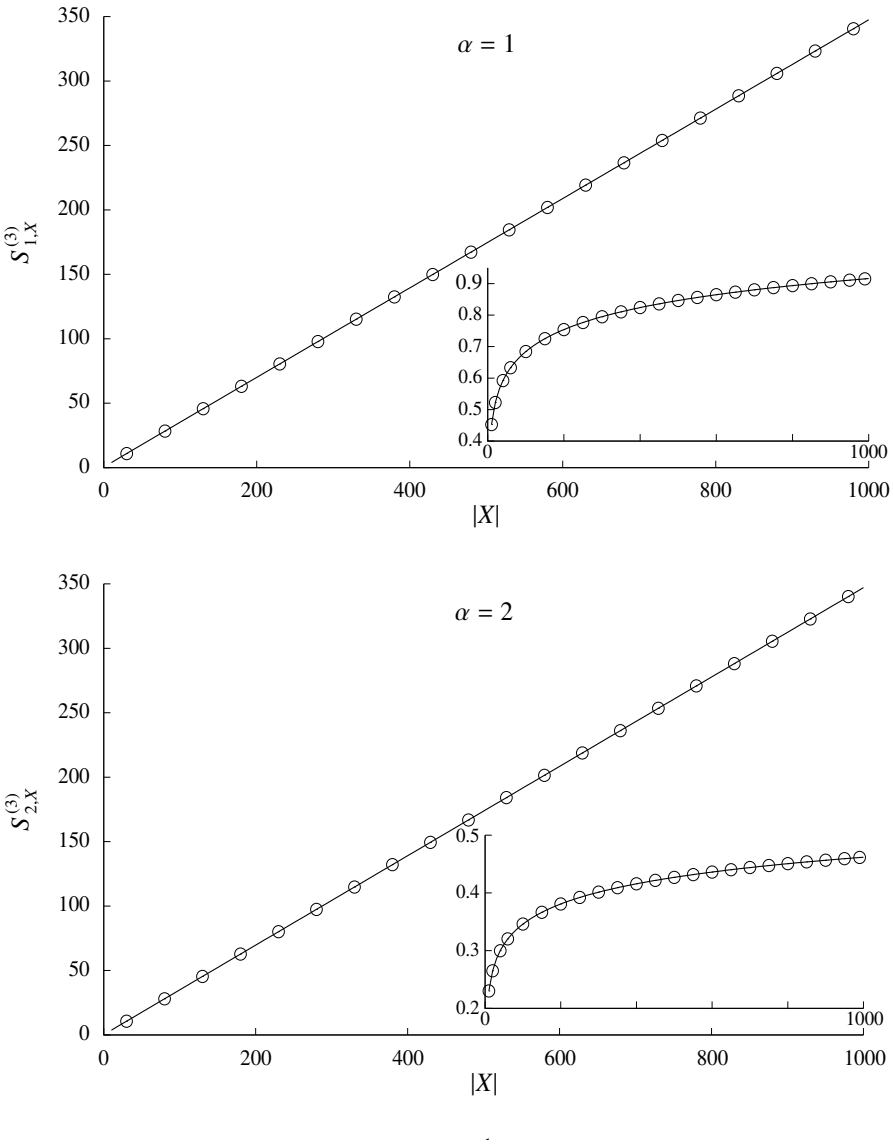

Figure 3.3: Entanglement entropy with $\alpha = 1$ (upper panel) and $\alpha = 2$ (lower panel) for a single interval of length $|X|$ when we take the **state 3**. The dots are the numerical values and the continuous line represents the asymptotic expansion (3.12) with the coefficient $\mathcal{A}_\alpha^{(3)}$ that we have obtained in (3.27), while $\mathcal{B}_\alpha^{(3)}$ is (3.28) for $\alpha = 1$ and that given by (3.29) for $\alpha = 2$. The constant term $\mathcal{C}_\alpha^{(3)}$ is computed numerically using (3.22). In the insets we plot the entropy subtracting the linear contribution to reveal the logarithmic term.

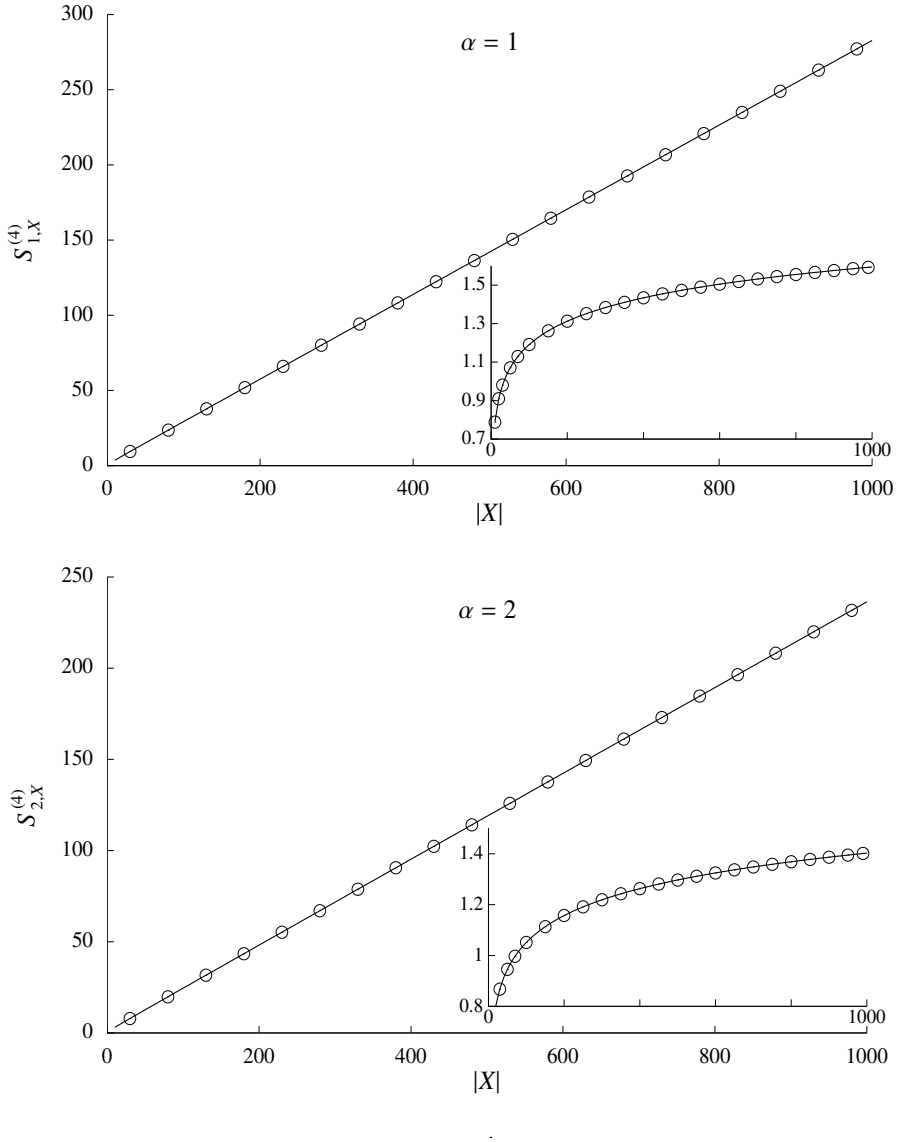

Figure 3.4: Entanglement entropy with $\alpha = 1$ (upper panel) and $\alpha = 2$ (lower panel) for a single interval of length $|X|$ when we take the **state 4**. The dots are the numerical values and the continuous line corresponds to the asymptotic expansion (3.12) obtained applying the Fisher-Hartwig conjecture. The coefficient of the expansion $\mathcal{A}_\alpha^{(4)}$ is (3.31) for $\alpha = 1$ while for $\alpha = 2$ is given by (3.32). The coefficient $\mathcal{B}_\alpha^{(4)}$ is (3.33) for $\alpha = 1$ and that obtained from (3.34) for $\alpha = 2$. The constant term $\mathcal{C}_\alpha^{(4)}$ has been computed numerically using (3.22). In the insets we plot the entropy subtracting the linear contribution to reveal the logarithmic term.

Discussion of the results

In Ref. [108] Alba, Fagotti and Calabrese showed that the configurations for which the density of occupied states is $g(\theta) = \pm 1$, whose entanglement entropy grows logarithmically or it is zero, are the ground state of a Hamiltonian with finite-range couplings. On the other hand, as we have seen, if $g(\theta) \neq \pm 1$ the leading term of the entropy is linear in $|X|$. They proposed that these configurations correspond to the ground state of a Hamiltonian with long-range couplings. This can be shown to hold in the particular states studied above. The general discussion will be postponed to the next section.

State 1: is the ground state of the Tight Binding Model described by the critical Hamiltonian

$$H = -\sum_{n=1}^{N} a_n^\dagger (a_{n-1} + a_{n+1}). \tag{3.35}$$

Its dispersion relation (3.2) is

$$\omega_k = -2\cos\theta_k.$$

In this case ω_k is negative for $|k| < N/4$. In the upper plot of Fig. 3.5 we represent this dispersion relation in the thermodynamic limit $\theta_k \to \theta \in [-\pi, \pi)$. In the ground state all the modes with negative energy are occupied. The plot in the lower half of Fig. 3.5 corresponds to the density of occupied modes in this configuration. It is precisely that of the state 1.

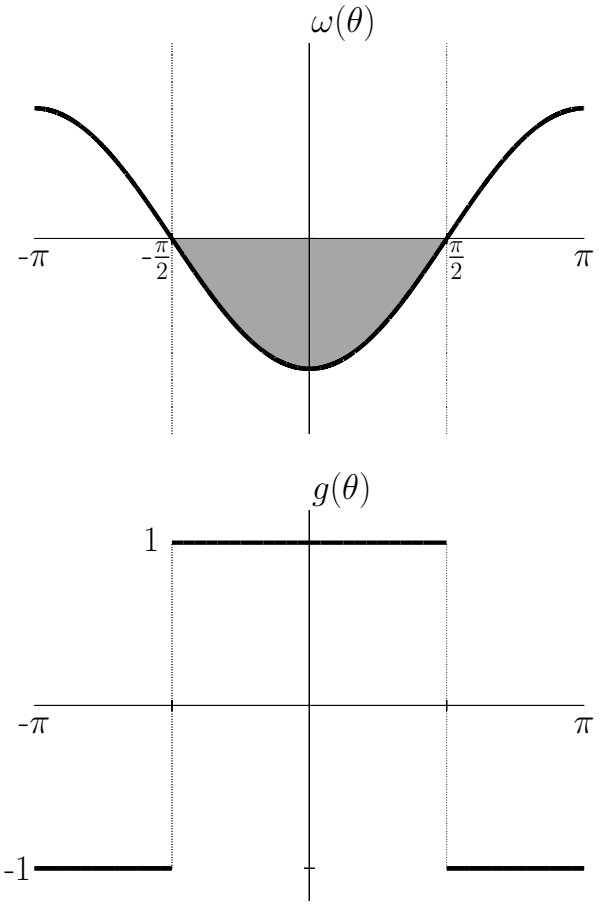

Figure 3.5: At the top, dispersion relation of the Hamiltonian (3.35) in the thermodynamic limit. The mass gap is zero and the theory is critical. In the ground state all the modes with negative energy are occupied. At the bottom, the density of occupied modes in the ground state.

State 2: is the ground state of the long-range Hamiltonian

$$H = \sum_{n=1}^{N} (A_0 a_n^\dagger a_n + A_1 a_n^\dagger a_{n+1} + A_{N/2} a_n^\dagger a_{n+N/2}) + \text{h.c.} \tag{3.36}$$

with the adequate choice of coupling constants.

The dispersion relation (3.2) is in this case

$$\omega_k = A_0 + 2A_1 \cos\left(\frac{2\pi k}{N}\right) + 2A_{N/2} \cos\left(\frac{2\pi k}{N} \cdot \frac{N}{2}\right). \tag{3.37}$$

Observe that it splits into two bands for even and odd k. If $k = 0 \,(\mathrm{mod}\, 2)$ we have

$$\omega_k = A_0 + 2A_{N/2} + 2A_1 \cos\theta_k,$$

while if $k = 1 \,(\mathrm{mod}\, 2)$,

$$\omega_k = A_0 - 2A_{N/2} + 2A_1 \cos\theta_k.$$

Hence when

$$A_0, A_{N/2} > 0, \quad A_1 < 0, \quad A_0 - 2A_1 < 2A_{N/2}$$

all the modes with even momentum have positive energy, while it is negative for those with odd momentum. In the upper plot of Fig. 3.6 we represent the two bands in the thermodynamic limit. Therefore, in the ground state all the modes with odd k are occupied while those with even k are empty. Thus the occupation density is $g^{(2)}(\theta) = 0$.

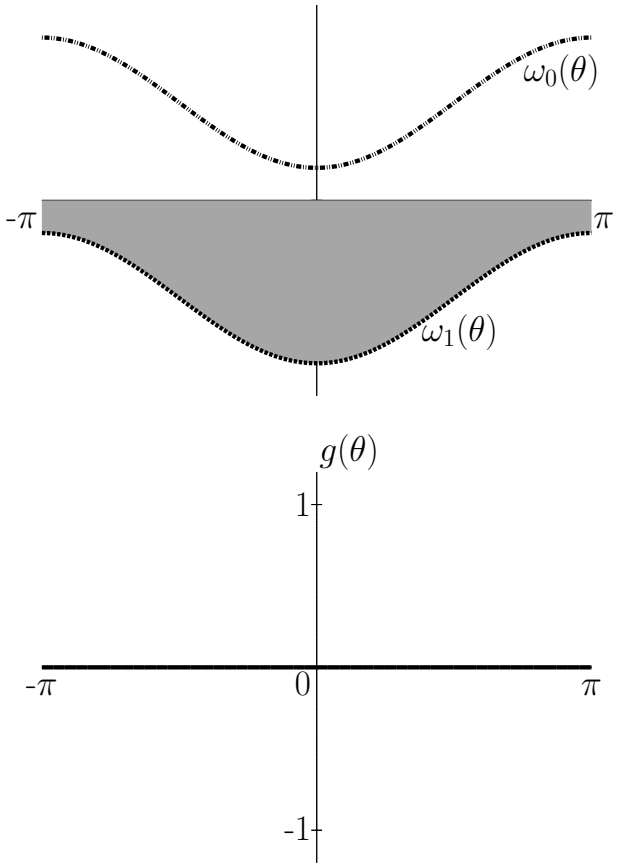

Figure 3.6: In the upper panel, bands of the dispersion relation of the long-range Hamiltonian (3.36) when the couplings satisfy the condition $A_0, A_{N/2} > 0$, $A_1 < 0$, and $A_0 - 2A_1 < 2A_{N/2}$. Then the band for even modes, $\omega_0(\theta)$, is positive while that for odd modes, $\omega_1(\theta)$, is negative. Therefore, in the ground state only the odd modes are occupied, and the occupation density, depicted in the lower panel, is 0.

State 3: is the ground state of the previous long-range Hamiltonian (3.36) when

$$A_0 = 2A_{N/2} > 0, \quad A_1 < 0, \quad 2A_{N/2} > -A_1.$$

For these couplings, the two bands of the dispersion relation (3.37) are

$$\omega_k = 4A_{N/2} + 2A_1 \cos\theta_k, \quad \text{if} \quad k = 0 \,(\mathrm{mod}\, 2),$$

and

$$\omega_k = 2A_1 \cos\theta_k, \quad \text{if} \quad k = 1 \,(\mathrm{mod}\, 2).$$

The modes with even momentum have positive energy. The band of the modes with odd momentum is negative for $|k| < N/4$. In the upper half of Fig. 3.7 we represent them in the thermodynamic limit. Therefore, in the ground state the modes with odd k and $|k| < N/4$ are occupied. This is is the state 3 studied before. In the lower half of Fig. 3.7 we plot the corresponding occupation density.

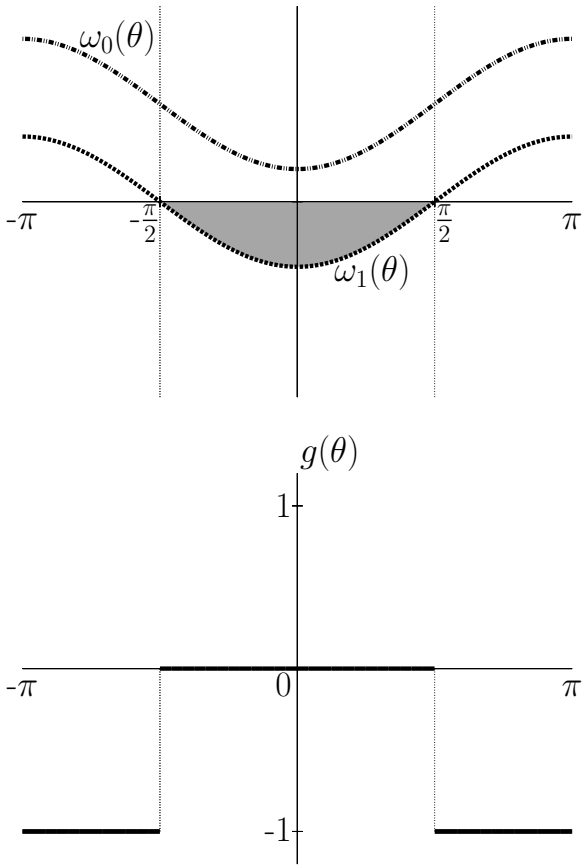

Figure 3.7: The upper plot represents the bands of the dispersion relation of the long-range Hamiltonian (3.36) when $A_0 = 2A_{N/2} > 0$, $A_1 < 0$, and $2A_{N/2} > -A_1$. The band $\omega_0(\theta)$, corresponding to the modes with even momentum, is positive, while that for the odd modes, $\omega_1(\theta)$, is negative in the interval $\theta \in (-\pi/2, \pi/2)$. Hence all the modes with odd momentum lying in this interval are occupied in the ground state. In the plot of the lower half we represent the occupation density in this configuration.

State 4: is the ground state of the long-range Hamiltonian

$$H = \sum_{n=1}^{N} \left(A_0 a_n^\dagger a_n + A_1 a_n^\dagger a_{n+1} + A_{N/4} a_n^\dagger a_{n+N/4} + A_{N/2} a_n^\dagger a_{n+N/2} \right) + \text{h.c.} \tag{3.38}$$

provided

$$2A_{N/2} = A_0 > 0, \quad A_{N/4} = A_0, \quad \text{and} \quad 2A_0 > -A_1.$$

For this system, the dispersion relation (3.2) reads

$$\omega_k = A_0 + 2A_1 \cos\left(\frac{2\pi k}{N}\right) + 2A_{N/2} \cos\left(\frac{2\pi k}{N} \cdot \frac{N}{2}\right) + 2A_{N/4} \cos\left(\frac{2\pi k}{N} \cdot \frac{N}{4}\right).$$

Simplifying

$$\omega_k = A_0 + 2A_1 \cos\left(\frac{2\pi k}{N}\right) + 2A_{N/2} \cos\left(\pi k\right) + 2A_{N/4} \cos\left(\frac{\pi k}{2}\right).$$

Therefore, taking into account the conditions for the couplings, it splits into

$$\omega_k = \begin{cases} 4A_{N/4} + 2A_1 \cos\theta_k, & k = 0 \,(\mathrm{mod}\, 4), \\ \\ 2A_1 \cos\theta_k, & k \neq 0 \,(\mathrm{mod}\, 4) \end{cases} .$$

In Fig. 3.8 (top) we represent these bands in the thermodynamic limit. Note that three of the bands coincide, $\omega_1 = \omega_2 = \omega_3 = \omega^*$. In this case the modes with $k \neq 0 \,(\mathrm{mod}\, 4)$ have negative energy when $|k| < N/4$. In the ground state they are occupied. Since three out of four modes with momentum $|k| < N/4$ are occupied, the occupation density is $1/2$ in the interval $\theta \in (-\pi/2, \pi/2)$. We have plotted it in Fig. 3.8 (bottom).

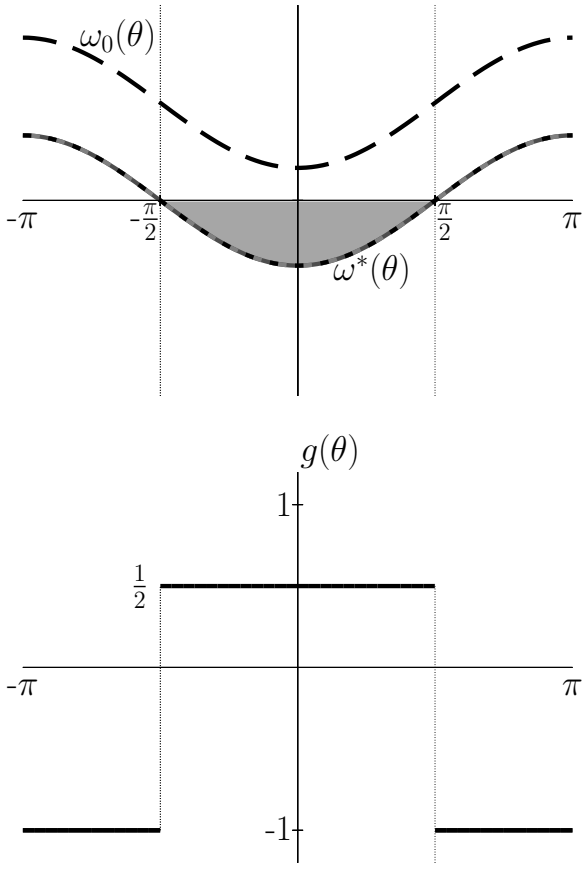

Figure 3.8: In the upper plot, we depict the bands of the dispersion relation of the long-range Hamiltonian (3.38) for the set of couplings $2A_{N/2} = A_0 > 0$, $A_{N/4} = A_0$ and $2A_0 > -A_1$. We call $\omega_0(\theta)$ the band corresponding to the modes with $k = 0 \,(\mathrm{mod}\, 4)$. The bands for the modes with $k \neq 0 \,(\mathrm{mod}\, 4)$ coincide and are denoted by $\omega^*(\theta)$. They are negative for $\theta \in (-\pi/2, \pi/2)$. Thus in the ground state three out of four modes lying in this interval are occupied. In the lower plot we represent the occupation density in this state.

As a further matter, in Section 1.2 we discussed that the entanglement entropy of the ground state often satisfies an area law: it grows with the area of the boundary between the two subsystems in which we have divided the system. In the case of the chains that we are studying the boundary between the interval X and the rest of the chain is independent from the number of sites $|X|$ in the interval. Therefore, if the entropy satisfies an area law, it should be a constant in the large $|X|$ limit. However, the entropies for the states investigated above seem to violate the area law.

In the state 1 we have obtained that the entropy presents a logarithmic term (3.25). Nevertheless, we have seen that it is the ground state of a critical theory with only nearest-neighbour couplings (3.35). As we mentioned in Section 1.2, when a system with finite-range interactions is critical the area law is corrected by a logarithmic term if the model can be described by a conformal field theory. In fact, the logarithmic term in the entropy of the state 1 (3.25) is of the form predicted by CFT (1.10),

$$S^{(1)}_{\alpha,X} = \frac{\alpha+1}{6\alpha} \mathrm{c} \log |X| + \mathcal{C}^{(1)}_{\alpha} + o(1)$$

with central charge $\mathrm{c} = 1$. The logarithmic term actually arises from the discontinuities of the occupation density that have their origin in the absence of mass gap, see Fig. 3.5.

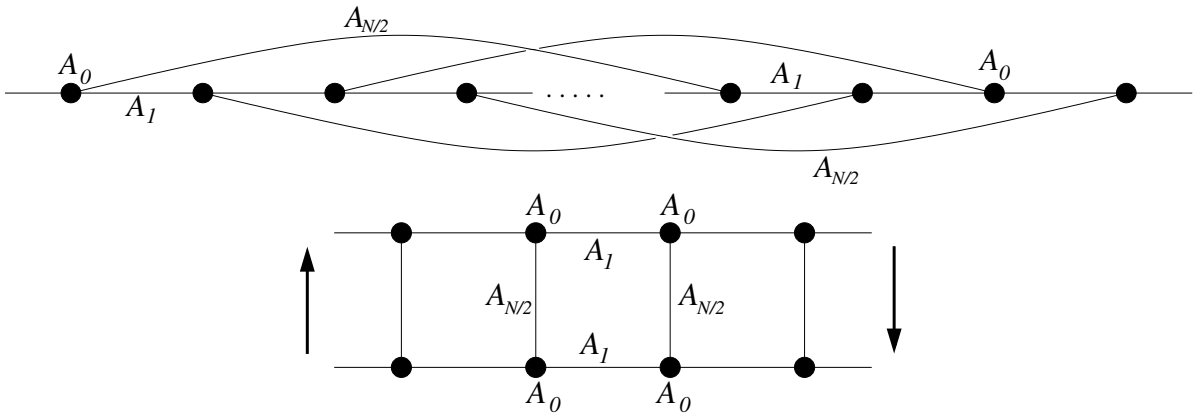

Figure 3.9: Representation of the fermionic chain described by the long-range Hamiltonian of (3.36), upper half, as a ladder, lower half. The upper row of the ladder contains the sites from 1 to $N/2$ and the lower one those from $N/2+1$ to N, both from left to right. The ends of the ladder are joined with an inversion as it is indicated by the arrows, forming, therefore, a Möbius strip.

On the other hand, in the states 2, 3 and 4, the entanglement entropy presents a linear term with the length of the interval. Then one may conclude that in these states the entanglement entropy follows a volume law, since the dominant term is extensive, proportional to the size of the subsystem. However, these configurations are the ground state of chains with long-range couplings like that depicted in the upper plot of Fig. 3.9. As it is described in the figure, this chain can also be seen as the ladder of the lower half. From the perspective of the ladder, it is clear that these entropies satisfy an area law.

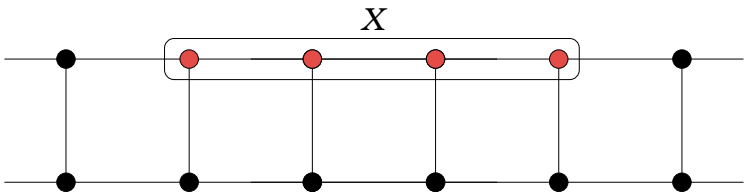

Figure 3.10: In the ladder of Fig. 3.9 the interval of contiguous sites X that we are considering to compute the entropy is located at one of the rails. Then the area of the border that separates X from the rest of the ladder grows with the number of sites in X. Therefore, the linear growth of the entanglement entropy in the ground state of this ladder can be interpreted as an area law.

In fact, as we can see in Fig. 3.10, in the ladder the area of the boundary between an interval X and the rest of the system is the number of bonds that we break when we isolate the interval. Observe that the number of bonds broken depends linearly on the size of the interval. This explains the presence of a linear term in the expansion of the entanglement entropy, and gives the correct interpretation of the area law for these states.

3.3 Local chains and ladders

In this section we shall try to gain physical insights from the previous results and extend them to more general states, connecting with the idea of Alba, Fagotti and Calabrese [108]. We shall discuss two kinds of Hamiltonians that correspond to local chains and local ladders.

A local chain is characterized by interactions of finite range, i.e.

$$A_l = 0, \quad \forall\, l > L.$$

Therefore, in the thermodynamic limit $N \to \infty$ the dispersion relation,

$$\omega(\theta) = \sum_{l=-L}^{L} A_l \mathrm{e}^{\mathrm{i}l\theta},$$

is a smooth function that generically has a finite (even) number R of zeros where $\omega(\theta)$ changes its sign. A typical example with $R = 4$ is depicted in the upper half of Fig. 3.11.

In the ground state all the modes with negative energy, i.e. $\omega(\theta) < 0$, are occupied. Therefore, its occupation density will be given by

$$g(\theta) = \begin{cases} 1, & \text{if} \quad \omega(\theta) < 0, \\ -1, & \text{if} \quad \omega(\theta) > 0. \end{cases} \tag{3.39}$$

We represent in the lower half of Fig. 3.11 the occupation density for the particular dispersion relation plotted above it. Notice that, as Alba, Fagotti and Calabrese showed in [108], any configuration described by an occupation density like (3.39) with a finite number of discontinuities is the ground state of a local chain whose dispersion relation changes its sign at the discontinuity points.

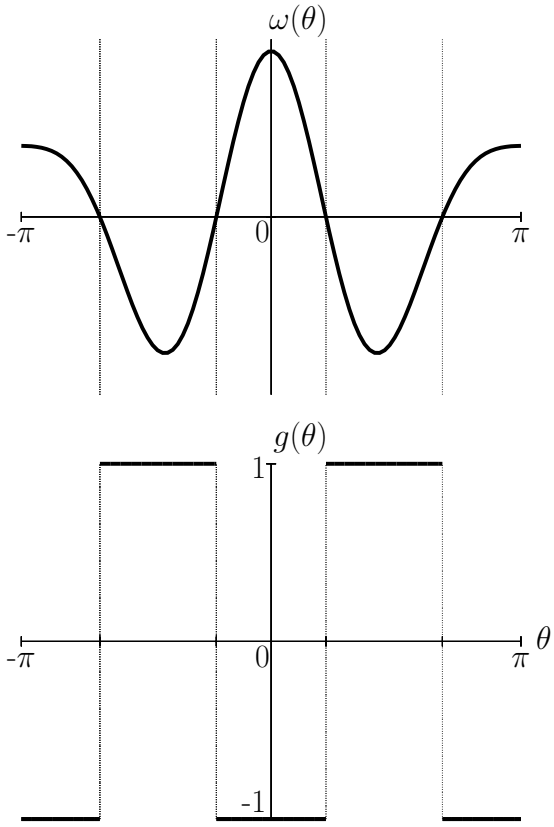

Figure 3.11: The upper plot represents the dispersion relation for a local chain, while the occupation density for its ground state is plotted below.

Another example with an occupation density of this type is the state 1 studied in the previous section, see Fig. 3.5. Generalising the result (3.25) obtained for it, we have that the entanglement entropy of an interval in the ground state with the occupation density (3.39) behaves like

$$S_{\alpha,X} = \frac{\alpha+1}{\alpha}\frac{R}{12}\log|X| + \mathcal{C}_\alpha + o(1), \tag{3.40}$$

where the constant term $\mathcal{C}_\alpha$, that it is given by (3.22), depends on the precise location θ_1,..., θ_R of the discontinuities of $g(\theta)$,

$$\mathcal{C}_\alpha = R\Upsilon_\alpha + \frac{\alpha+1}{12\alpha}\sum_{1\leq r\neq r'\leq R}\log[2-2\cos(\theta_r-\theta_{r'})], \tag{3.41}$$

with Υ_α the integral that has already appeared at (3.24).

Observe that the coefficient of the logarithmic term is universal in the sense that, in general, it is invariant under small modifications of the couplings. It only depends on the number of changes of sign of $\omega(\theta)$ and not on their position. However, the constant term $\mathcal{C}_\alpha$ is not universal as it varies under small changes of the couplings.

In particular, the coefficient of the logarithmic term counts the number of massless excitations in the thermodynamic limit of the Hamiltonian, i.e. the zeros of the dispersion relation $\omega(\theta)$. This result is consistent with the CFT interpretation, where the central charge of a free field theory also counts the number of massless particles. On the other

hand, if the Hamiltonian has a mass gap then $\omega(\theta)$ does not change its sign, the occupation density of the ground state (3.39) does not have jumps (is -1 for all θ), and the entanglement entropy exactly vanishes (in fact, the ground state is the Fock space vacuum $|0\rangle$ which is separable).

As we have seen, the states 2, 3, and 4 of the previous section can be viewed as the ground state of a second type of Hamiltonians. They describe prismatic ladders with q rails and local interactions,

$$H = \sum_{n=1}^{N} \sum_{p=0}^{q-1} \sum_{l=0}^{L} A_{p,l} a_n^\dagger a_{n+pN/q+l} + \text{h.c.}, \quad L < \frac{N}{2q}. \tag{3.42}$$

An example with $q = 3$ and $L = 1$ is represented in Fig. 3.12.

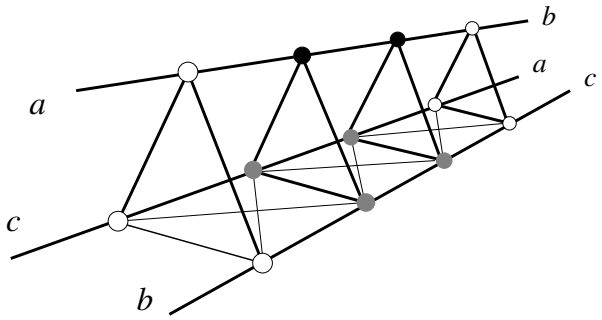

Figure 3.12: Representation of a triangular ladder described by the Hamiltonian of (3.42). The rails are joined at the end after a twist, forming therefore a twisted ring. For the sake of clarity, next to nearest neighbours interactions are represented (with thin lines) only in the lower lateral face of the ladder, but they are present in all three faces. Subsystems are represented by dark sites: the black ones represent the interval while black and grey ones represent the fragment.

The dispersion relation of (3.42) is

$$\omega_k = \sum_{p=0}^{q-1} \sum_{l=0}^{L} A_{p,l} \mathrm{e}^{\mathrm{i}\theta_k(pN/q+l)} + \text{c.c.},$$

that splits into q bands. In fact, taking $k = s \pmod q$, we have

$$\omega_k = \sum_{p=0}^{q-1} \mathrm{e}^{2\pi \mathrm{i} sp/q} \sum_{l=0}^{L} A_{p,l} \mathrm{e}^{2\pi \mathrm{i} kl/N} + \text{c.c.}$$

In the thermodynamic limit we can replace $2\pi k/N$ by the continuous variable θ, obtaining a different dispersion relation (band)

$$\omega_s(\theta) = \sum_{l=0}^{L} \left(\sum_{p=0}^{q-1} A_{p,l} \mathrm{e}^{2\pi \mathrm{i} sp/q} \right) \mathrm{e}^{\mathrm{i}\theta l} + \text{c.c.}$$

for each value of $s = 0, \ldots, q-1$. Given the conditions for the couplings $A_{p,l}$, every band is a continuous, smooth, periodic function. A generic case for $q = 3$ is depicted in the upper half of Fig. 3.13. If none of the bands vanishes, the ladder has a mass gap and

it is non critical. On the contrary, if one or more bands change of sign, the mass gap is zero and the ladder is critical. As we did for local chains, to every change of sign we associate a massless excitation. For example, the dispersion relation depicted in the Fig. 3.13 corresponds to a critical ladder with four massless excitations.

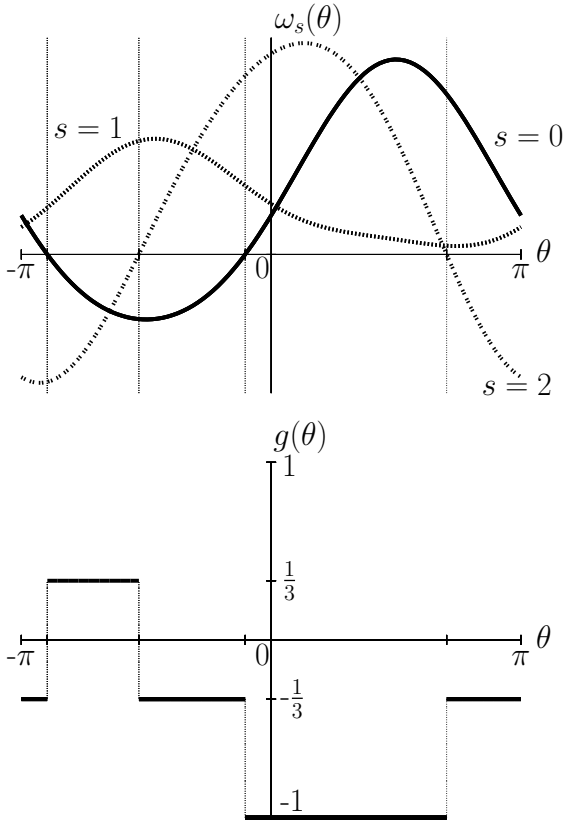

Figure 3.13: In the upper half, the bands for the dispersion relation of a local ladder with 3 rails and below the occupation density of its ground state.

The ground state of the ladder is obtained by filling all the modes with negative energy. We can define an occupation density for each band

$$g_s(\theta) = \begin{cases} 1, & \omega_s(\theta) < 0, \\ -1, & \omega_s(\theta) > 0. \end{cases} \tag{3.43}$$

Then the occupation density of the ground state of the ladder is

$$g(\theta) = \frac{1}{q} \sum_{s=0}^{q-1} g_s(\theta), \tag{3.44}$$

that represents the excess of bands with negative energy over those with positive energy for momentum θ divided by the number of bands q. The plot in the lower panel of Fig. 3.13 is the occupation density of the ground state for the dispersion relation represented over it. The occupation density (3.44) will be a piecewise constant function like (3.10) with t_{r-1} acquiring rational values. Note that every occupation density with these characteristics represents the ground state of certain local ladder Hamiltonian, as Alba, Fagotti and Calabrese proposed in [108].

Since (3.44) is in general different from ± 1, the entanglement entropy of the ground state described by it will present a linear term in $|X|$. The presence of this term is understood by the correct interpretation of the area law for ladders that we stated in the previous section. In the ladder, the area of the boundary between an interval of contiguous sites X and the rest of the system is proportional to the number of bonds connecting the subsystems, that grows with the number of sites $|X|$ in the interval.

Since the logarithmic term is due to the discontinuities of $g(\theta)$, it is zero if none of the bands have a change of sign and, therefore, the ladder has a mass gap. On the other hand, when one or more bands cross the zero value, the occupation density is in general discontinuous and the coefficient of the logarithmic term is non-vanishing (an exception occurs in the case in which two bands cross the zero value at the same point in opposite directions). The discontinuities of the occupation density also give rise to the constant term.

The logarithmic term is always universal since it only depends on the value of the occupation density at the sides of each discontinuity and this is not affected by small variations in the Hamiltonian. The linear term is not universal if the ladder is critical. In this situation, it depends on the location of the discontinuities of $g(\theta)$ and, consequently, on the zeros of the dispersion relation. On the contrary, if the theory has a mass gap, since $g(\theta)$ is constant, it is not affected by small changes in the Hamiltonian, and the linear term is universal.

The physical interpretation of the coefficient of the logarithmic term is more involved now than for local chains, where it is proportional to the number of massless excitations of the theory. For ladders, the logarithmic coefficient depends not only on the number of discontinuities (massless particles) but also on the value of $g(\theta)$ at both sides of each discontinuity. They are now rational values instead of ± 1, and the relation between such values and the contribution to the logarithmic term (3.17) is highly non trivial and hard to interpret.

However, the origin of these difficulties is the same that in the interpretation of the linear term: the choice of the subsystem X as an interval of contiguous sites in one of the rails of the ladder (the black dots in Fig. 3.12). Somehow, it is more natural to take as subsystem a fragment of the ladder: q intervals, one in every rail and placed opposite to each other as it is represented in Fig. 3.12 by black and grey sites. More formally, calling $X_p = \{1 + pN/q, \ldots, |X| + pN/q\}$ a single interval of $|X|$ contiguous sites on the rail $p = 0, \ldots, q-1$, a fragment X of length $|X|$ is the subsystem

$$X = \bigcup_{p=0}^{q-1} X_p.$$

Observe that interpreting the ladder as a chain with non-local interactions the fragment X corresponds to q disjoint intervals of size $|X|$ separated by a distance $N/q - |X|$.

Let us see that for the fragment X the entanglement entropy has a clear physical meaning, compatible with the interpretation of the logarithmic contribution in terms of massless excitations.

Let us proceed by introducing a correlation matrix for each band of the dispersion

relation

$$(V_s)_{nm} = \frac{q}{N}\left(\sum_{\substack{k\in\mathbf{K}\\ k=s \,(\mathrm{mod}\, q)}} \mathrm{e}^{\mathrm{i}\theta_k(n-m)} - \sum_{\substack{k\notin\mathbf{K}\\ k=s \,(\mathrm{mod}\, q)}} \mathrm{e}^{\mathrm{i}\theta_k(n-m)}\right), \quad s=0,\dots,q-1, \quad n,m\in X.$$

Then the correlation matrix V_X^S can be written as a sum of them,

$$V_X^S = \frac{1}{q}\sum_{s=0}^{q-1} V_s.$$

The correlation matrices of the bands are quasiperiodic (actually following a quasiperiodicity very similar to that of Bloch functions in a periodic crystal lattice)

$$(V_s)_{n+pN/q,m+p'N/q} = \mathrm{e}^{2\pi\mathrm{i}s(p-p')/q}(V_s)_{nm}.$$

This implies that if we introduce the matrices

$$(T_s)_{pp'} = \mathrm{e}^{2\pi\mathrm{i}(p-p')/q}, \quad p,p'=0,\dots,q-1,$$

we have

$$V_X^S = \frac{1}{q}\sum_{s=0}^{q-1}(V_s)_{X_0}\otimes T_s,$$

where $(V_s)_{X_0}$ denotes the restriction of V_s to one of the intervals that compose X.

The matrices T_s commute and are diagonalised simultaneously by

$$U_{pp'} = \frac{1}{\sqrt{q}}\mathrm{e}^{2\pi\mathrm{i}pp'/q}$$

such that

$$(UT_sU^{-1})_{pp'} = q\delta_{s,p}\delta_{s,p'}.$$

Finally, taking all together we arrive at

$$(I\otimes U)V_X^S(I\otimes U^{-1}) = \begin{pmatrix} (V_0)_{X_0} & 0 & \cdots & 0\\ 0 & (V_1)_{X_0} & \cdots & 0\\ \cdots & \cdots & \cdots & \cdots\\ \cdots & \cdots & \cdots & \cdots\\ 0 & 0 & \cdots & (V_{q-1})_{X_0}\end{pmatrix}.$$

From this result, the entanglement entropy of the whole fragment X of the ladder is

$$S_{\alpha,X} = \sum_{s=0}^{q-1} S_{\alpha,X_0,s},$$

where $S_{\alpha,X_0,s}$ is the Rényi entanglement entropy for the single interval X_0 in the state with correlation matrix V_s. In the thermodynamic limit,

$$(V_s)_{nm} = \frac{1}{2\pi}\int_{-\pi}^{\pi} g_s(\theta)\mathrm{e}^{\mathrm{i}\theta(n-m)}\mathrm{d}\theta,$$

with g_s the occupation density (3.43) for the band $\omega_s(\theta)$.

Now we can calculate $S_{\alpha,X}$ using the results obtained for the local chains. Taking into account (3.40), if R_s represents the number of discontinuities in $g_s(\theta)$, i.e. the number of changes of sign in the band $\omega_s(\theta)$, we have

$$S_{\alpha,X_0,s} = \frac{\alpha+1}{\alpha}\frac{R_s}{12}\log|X| + \mathcal{C}_{\alpha,s} + o(1),$$

where the expression for the finite term $\mathcal{C}_{\alpha,s}$ is the same as in (3.41) particularised to the occupation density g_s.

In consequence, the asymptotic behaviour of the entropy of the fragment is

$$S_{\alpha,X} = \frac{\alpha+1}{12\alpha}\left(\sum_{s=0}^{q-1} R_s\right)\log|X| + \sum_{s=0}^{q-1}\mathcal{C}_{\alpha,s} + o(1). \tag{3.45}$$

Since $g_s(\theta) = \pm 1$, the linear term cancels in agreement with the prediction of the area law. Observe that the coefficient of the logarithmic term coincides with that obtained from CFT (1.10) and it is proportional to the number of massless excitations of the theory which is equal to the total number of changes of sign of the q bands for the dispersion relation.

In order to illustrate the previous discussion, let us compute the ground state entropy of the fragment $X = X_0 \cup X_1$ in the ladder of Fig. 3.14. It is described by the Hamiltonian

$$H = \sum_{n=1}^{N}(A_0 a_n^\dagger a_n + A_1 a_n^\dagger a_{n+1} + A_{N/2} a_n^\dagger a_{n+N/2}) + \text{h.c.}, \tag{3.46}$$

with

$$A_0 = 2A_{N/2} > 0, \quad A_1 < 0, \quad 2A_{N/2} > -A_1.$$

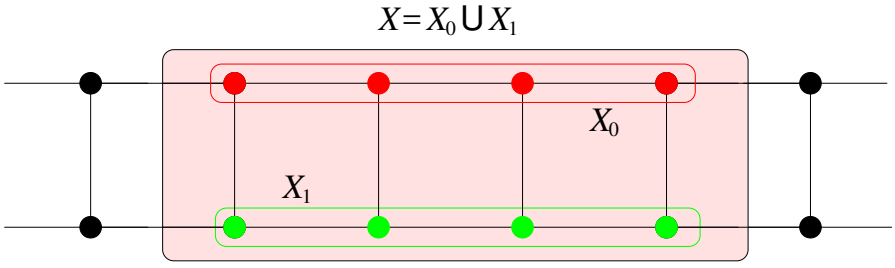

Figure 3.14: Fragment X of the ladder described by the Hamiltonian (3.46). The fragment is the union of two intervals of contiguous sites, X_0 and X_1, placed in front of each other in different rails.

Remember that in Section 3.2.1 we already studied the ground state of this ladder and computed the entanglement entropy for an interval (see state 3).

Since the ladder has two rails, $q = 2$, and the dispersion relation,

$$\omega_k = A_0 + 2A_1\cos\left(\frac{2\pi k}{N}\right) + 2A_{N/2}\cos\left(\frac{2\pi k}{N}\cdot\frac{N}{2}\right), \tag{3.47}$$

splits into two bands corresponding to modes with even and odd k, as we already noted in Section 3.2.1. In the thermodynamic limit, they read

$$\omega_0(\theta) = 4A_{N/2} + 2A_1 \cos\theta,$$

and

$$\omega_1(\theta) = 2A_1 \cos\theta,$$

for the set of couplings considered. We plotted these bands in the upper half of Fig. 3.7.

The occupation density (3.43) associated to each band is

$$g_0(\theta) = -1, \quad \theta \in [-\pi, \pi),$$

for $\omega_0(\theta)$ since it is positive, and

$$g_1(\theta) = \begin{cases} 1, & \theta \in (-\pi/2, \pi/2), \\ -1, & \theta \in [-\pi, \pi/2] \cup [\pi/2, \pi), \end{cases}$$

for $\omega_1(\theta)$, that is negative for $\theta \in (-\pi/2, \pi/2)$.

Now according to (3.45) the entropy of the fragment X is

$$S_{\alpha,X} = \frac{\alpha+1}{12\alpha}(R_0 + R_1)\log|X| + \mathcal{C}_{\alpha,0} + \mathcal{C}_{\alpha,1} + o(1),$$

where R_0 and R_1 are respectively the number of discontinuities of g_0 and g_1. Hence $R_0 = 0$ and $R_1 = 2$.

The constant $\mathcal{C}_{\alpha,0}$ vanishes since g_0 is continuous and $\mathcal{C}_{\alpha,1}$ is given by (3.41), that particularises for the occupation density g_1 to

$$\mathcal{C}_{\alpha,1} = 2\Upsilon_\alpha + \frac{\alpha+1}{6\alpha}\log 2.$$

In conclusion, the entropy of a fragment of this ladder in the ground state is

$$S_{\alpha,X} = \frac{\alpha+1}{6\alpha}\log|X| + \mathcal{C}_{\alpha,1} + o(1).$$

The coefficient of the logarithmic term coincides with the prediction of CFT (1.10) for central charge c = 1, half of the total number of change of signs (massless excitations) in the two bands.

Chapter 4

Chains with pairing terms

In the previous Chapter we obtained the asymptotic behaviour of the entanglement entropy for a single interval in the stationary states of a chain with only hopping couplings A_l. Now we shall move to the general case (2.2) where we have both hopping A_l and pairing B_l couplings. We shall focus on the ground state. As it happened for the hopping chains, its entanglement entropy will contain valuable information about the system.

The ground state of a chain that has only hopping couplings has the particularity that the correlation matrix V_X can be reduced to a Toeplitz matrix since the symbol $\hat{\mathcal{G}}$, see (2.40), becomes diagonal. This has simplified the problem because we can apply the Fisher-Hartwig conjecture that allowed us to derive the asymptotic expansion of the entanglement entropy of an interval. Unfortunately, in the general case, when there are pairing couplings B_l different from zero, the symbol $\hat{\mathcal{G}}$ is not diagonal anymore, the correlation matrix cannot be reduced to a Toeplitz one, and one is forced to consider full-fledged block Toeplitz determinants.

In this Chapter we shall accomplish this goal. Since our symbol $\hat{\mathcal{G}}$ can be discontinuous we shall be particularly interested in calculating the contribution of the discontinuities to the determinant. For block Toeplitz matrices there is not a result like the Fisher-Hartwig conjecture that gives the asymptotic expansion of the determinant when the symbol is discontinuous. We shall try to solve here this issue. Later we shall apply the obtained results to study the ground state entanglement entropy.

4.1 Asymptotic behaviour of block Toeplitz determinants

Let us consider an arbitrary $d \times d$ dimensional matrix valued function J defined on the unit circle S^1 and with entries in $L^1(S^1)$. We shall denote by $T_X[J]$ the corresponding $|X| \cdot d$ block Toeplitz matrix with entries

$$(T_X[J])_{nm} = J_{n-m} = \frac{1}{2\pi} \int_{-\pi}^{\pi} J(\theta) \mathrm{e}^{\mathrm{i}\theta(n-m)} \mathrm{d}\theta, \quad n, m = 1, \ldots, |X|.$$

In this section we want to study the asymptotic behaviour of its determinant that we shall call $D_X[J]$, so that $D_X[J] = \det T_X[J]$.

For this purpose, it will be useful to recap some results for Toeplitz determinants, i.e. when $d = 1$. If g is a real and positive scalar symbol that generates a $|X| \times |X|$ Toeplitz matrix $T_X[g] = (g_{n-m})$, the **(First) Szegő theorem** [116] establishes that the dominant term of its determinant $D_X[g]$ should be

$$\log D_X[g] = \frac{|X|}{2\pi} \int_{-\pi}^{\pi} \log g(\theta) \mathrm{d}\theta + o(|X|). \tag{4.1}$$

If the symbol g is *smooth enough* [1] such that

$$\sum_{k=-\infty}^{\infty} |g_k| + \sum_{k=-\infty}^{\infty} |k||g_k|^2 < \infty,$$

the **Strong Szegő Theorem** [101, 117] states that the next term in (4.1) is finite in the limit $|X| \to \infty$,

$$\log D_X[g] = \frac{|X|}{2\pi} \int_{-\pi}^{\pi} \log g(\theta) \mathrm{d}\theta + E[g] + o(1), \tag{4.2}$$

where the constant term reads

$$E[g] = \sum_{k=1}^{\infty} k s_k s_{-k}$$

and the s_k's are the Fourier modes of $\log g(\theta)$,

$$s_k = \frac{1}{2\pi} \int_{-\pi}^{\pi} \log g(\theta) \mathrm{e}^{\mathrm{i}\theta k} \mathrm{d}\theta.$$

The above series diverges when, for example, the symbol g has a jump discontinuity. In this case the **Fisher-Hartwig conjecture** [102, 104], that we applied in Section 3.2, precisely gives the next terms in $o(|X|)$. If the symbol g presents discontinuities at $\theta_1, \ldots, \theta_R$, the next term in the expansion (4.1) is logarithmic,

$$\log D_X[g] = \frac{|X|}{2\pi} \int_{-\pi}^{\pi} \log g(\theta) \mathrm{d}\theta + \frac{\log |X|}{4\pi^2} \sum_{\sigma=1}^{R} \left(\log \frac{g_\sigma^-}{g_\sigma^+} \right)^2 + O(1), \tag{4.3}$$

where $g_\sigma^\pm$ are the lateral limits of g at the discontinuity point θ_σ,

$$g_\sigma^+ = \lim_{\theta \to \theta_\sigma^+} g(\theta) \quad \text{and} \quad g_\sigma^- = \lim_{\theta \to \theta_\sigma^-} g(\theta).$$

Gyires [118] found a generalisation of the Szegő theorem (4.1) for the determinant of block Toeplitz matrices that later Hirschman [119] and Widom [120] extended to a wider variety of symbols. According to them, the leading term in the asymptotic expansion of $\log D_X[J]$ should be also linear

$$\log D_X[J] = \frac{|X|}{2\pi} \int_{-\pi}^{\pi} \log \det J(\theta) \mathrm{d}\theta + o(|X|), \tag{4.4}$$

[1] This is the case if the symbol is $C^{1+\epsilon}$, i.e. its derivative is Hölder continuous with exponent $\epsilon > 0$.

provided $\det J(\theta) \neq 0$ and the argument of $\det J(\theta)$ is continuous and periodic for $\theta \in [-\pi, \pi]$ (zero winding number).

We can apply this result to compute the entanglement entropy using (2.36),

$$S_{\alpha,X} = \frac{1}{4\pi \mathrm{i}} \lim_{\varepsilon \to 1^+} \oint_{\mathscr{C}} f_\alpha(\lambda/\varepsilon) \frac{\mathrm{d}}{\mathrm{d}\lambda} \log D_X[\hat{\mathcal{G}}_\lambda] \mathrm{d}\lambda,$$

where the contour $\mathscr{C}$ is represented in Fig. 2.5, and $\hat{\mathcal{G}}_\lambda = \lambda I - \hat{\mathcal{G}}$. The symbol $\hat{\mathcal{G}}$ of the correlation matrix for the ground state was obtained in (2.40). In the thermodynamic limit it is of the form

$$\hat{\mathcal{G}}(\theta) = \begin{cases} -I, & \text{if} \quad -\omega^+(\theta) > F^-(\theta), \\ M(\theta), & \text{if} \quad -\omega^+(\theta) < F^-(\theta) < \omega^+(\theta), \\ I, & \text{if} \quad F^-(\theta) > \omega^+(\theta). \end{cases} \tag{4.5}$$

Then we have

$$\det \hat{\mathcal{G}}_\lambda(\theta) = \begin{cases} (\lambda+1)^2, & \text{if} \quad -\omega^+(\theta) > F^-(\theta), \\ \lambda^2 - 1, & \text{if} \quad -\omega^+(\theta) < F^-(\theta) < \omega^+(\theta), \\ (\lambda-1)^2, & \text{if} \quad F^-(\theta) > \omega^+(\theta). \end{cases}$$

We now insert this into (4.4) and then into the previous contour integral. Applying the Cauchy residue theorem and taking into account that, by its definition (2.34), $f_\alpha(\pm 1) = 0$, one can immediately see that the linear, dominant contribution to the entanglement entropy vanishes in this case. Therefore, in order to determine its asymptotic behaviour one is forced to compute the subdominant terms that are hidden in $o(|X|)$.

Analogously to the scalar case, if the symbol $J(\theta)$ is smooth enough such that

$$\sum_{k=-\infty}^{\infty} \|J_k\| + \sum_{k=-\infty}^{\infty} |k| \, \|J_k\|^2 < \infty,$$

where $\|\cdot\|$ is the Hilbert-Schmidt norm of the $d \times d$ matrices, the **Widom theorem** [120, 121, 122] states that the next contribution in the expansion (4.4) should be finite when $|X| \to \infty$,

$$\log D_X[J] = \frac{|X|}{2\pi} \int_{-\pi}^{\pi} \log \det J(\theta) \mathrm{d}\theta + E[J] + o(1). \tag{4.6}$$

If we call $T[J]$ the semi-infinite matrix obtained from $T_X[J]$ when $|X| \to \infty$, the constant term $E[J]$ reads

$$E[J] = \log \det T[J] T[J^{-1}]. \tag{4.7}$$

The Widom theorem reduces to the Strong Szegő theorem (4.2) when the symbol is a scalar function, i.e. $d = 1$.

In spite of its simplicity, it is hard to apply the expression (4.7) for the constant $E[J]$ in particular cases. A more practical way to determine it is the following.

Suppose that the symbol depends on a parameter λ, J_λ, as it is our case. Let $\mathcal{J}_\lambda(z)$ be the analytical continuation of $J_\lambda(\theta)$ from the unit circle $\gamma = \{z : |z| = 1\}$ to the Riemann sphere $\overline{\mathbb{C}} = \mathbb{C} \cup \{\infty\}$.

Consider now that there exist two pairs of $d \times d$ matrices $u_\pm(z)$ and $v_\pm(z)$ that solve the following **Wiener-Hopf factorisation** problem:

1. $\mathcal{J}_\lambda(z) = u_+(z)u_-(z) = v_-(z)v_+(z)$,
2. $u_-^{\pm 1}(z)$, $v_-^{\pm 1}(z)$ are analytic outside the unit disk and $u_+^{\pm 1}(z)$, $v_+^{\pm 1}(z)$ are analytic inside it.

The Wiener-Hopf factorisation is one particular example of a Riemann-Hilbert problem [123].

If the previous factorisation problem can be solved then the constant term $E[J_\lambda]$ in the Widom theorem (4.6) verifies

$$\frac{\mathrm{d}E[J_\lambda]}{\mathrm{d}\lambda} = \frac{1}{2\pi \mathrm{i}} \oint_\gamma \mathrm{Tr} \left[(u_+'(z)u_+^{-1}(z) + v_+^{-1}(z)v_+'(z))\mathcal{J}_\lambda(z)^{-1} \frac{\mathrm{d}\mathcal{J}_\lambda(z)}{\mathrm{d}\lambda} \right] \mathrm{d}z. \tag{4.8}$$

This result was first obtained by Widom in [120] as an intermediate step in the search of the general expression (4.7) for $E[J]$. It was rediscovered in [124] employing the connection between the determinants of Toeplitz and Fredholm operators by Its, Jin and Korepin, who applied it to obtain the ground state entanglement entropy of the non critical XY spin chain. As we shall see in the next section, this result can be employed to derive the entanglement entropy in the ground state of non critical fermionic chains with finite range couplings.

On the contrary, if the chain is critical the symbol $\hat{\mathcal{G}}$ is discontinuous, as it is clear from (4.5), and the Widom theorem does not apply. To our knowledge, the case of a symbol with discontinuities has not been considered in the literature. In the papers [125] and [126] by the author and Esteve, Falceto and de Queiroz, we have tried to fill this gap.

4.1.1 Discontinuous symbols

Observe that, in the scalar case, the Fisher-Hartwig conjecture (4.3) states that the discontinuities of the symbol contribute with a logarithmic term $\log |X|$. The contribution of each discontinuity to the coefficient is independent from the rest and it only depends on the value of the lateral limits $g_\sigma^\pm$.

This can be explained as a consequence of the **localisation theorem** found by Basor in [104]. If we consider two $d \times d$ symbols $J_1(\theta)$, $J_2(\theta)$ such that their block Toeplitz matrices $T_X[J_1]$ and $T_X[J_2]$ are invertible for $|X|$ large enough and the semi-infinite matrices $T[J_1J_2] - T[J_1]T[J_2]$, $T[J_2J_1] - T[J_2]T[J_1]$ are trace-class then

$$\lim_{|X|\to\infty} \frac{D_X[J_1J_2]}{D_X[J_1]D_X[J_2]} < \infty. \tag{4.9}$$

The operator $T[J_1J_2] - T[J_1]T[J_2]$ is trace-class if there exists a smooth partition of the unit $\{f_1(\theta), f_2(\theta)\}$ such that the derivatives of J_1f_1 and J_2f_2 are Hölder continuous with an exponent greater than $1/2$. Or, in more informally words, the operator $T[J_1J_2] - T[J_1]T[J_2]$ is trace-class provided J_1 and J_2 are not *bad* (non smooth) at the same point.

The localisation theorem implies that if the symbol $J(\theta)$ has several discontinuities at $\theta_1, \ldots, \theta_R$, the divergent contribution in the large $|X|$ limit of each one to $D_X[J]$ is

independent from the rest and they can be studied separately. In addition, the divergent contribution of the discontinuity at θ_σ will only depend on the lateral limits

$$J_\sigma^- = \lim_{\theta\to\theta_\sigma^-} J(\theta), \quad \text{and} \quad J_\sigma^+ = \lim_{\theta\to\theta_\sigma^+} J(\theta).$$

First, let us suppose that these lateral limits commute and are diagonalisable. Hence they are diagonal in the same basis. Let us call $\mu_{\sigma,j}^\pm$, with $j = 1, \ldots, d$, the eigenvalues of $J_\sigma^\pm$.

Observe that, in this case, we can always construct a $d \times d$ smooth enough, periodic matrix valued symbol $U(\theta)$ that diagonalises all the lateral limits, i.e.

$$U(\theta_\sigma) J_\sigma^\pm U(\theta_\sigma)^{-1} = \begin{pmatrix} \mu_{\sigma,1}^\pm & 0 & \cdots & 0 \\ 0 & \mu_{\sigma,2}^\pm & \cdots & 0 \\ \cdots & \cdots & \cdots & \cdots \\ 0 & 0 & \cdots & \mu_{\sigma,d}^\pm \end{pmatrix}, \quad \sigma = 1, \ldots, R. \tag{4.10}$$

Let us consider the block Toeplitz determinant with symbol the product UJU^{-1}. Since U is smooth we can apply the localisation theorem (4.9). In this case, it leads to

$$\lim_{|X|\to\infty} \frac{D_X[UJU^{-1}]}{D_X[U]D_X[J]D_X[U^{-1}]} < \infty.$$

That is,

$$\log D_X[J] = \log D_X[UJU^{-1}] - \log D_X[U] - \log D_X[U^{-1}] + O(1). \tag{4.11}$$

Given the properties of U and U^{-1}, we can apply the Widom theorem (4.6) to determine $\log D_X[U]$ and $\log D_X[U^{-1}]$. According to this theorem, their linear terms in $|X|$ have opposite sign and, therefore, they cancel in (4.11). The rest of terms in $\log D_X[U]$ and $\log D_X[U^{-1}]$ are finite in the limit $|X| \to \infty$. Thus the expression (4.11) implies that the divergent contribution of the discontinuities of J is the same as those of UJU^{-1}.

Notice that J and UJU^{-1} are discontinuous at the same θ_σ, $\sigma = 1, \ldots, R$. The lateral limits of UJU^{-1} at the discontinuity points are (4.10). Since they are diagonal we can study the jump in each entry separately from the rest. This means that the discontinuity of an eigenvalue of $J(\theta)$ at θ_σ can be treated as that of a scalar symbol with lateral limits $\mu_{\sigma,j}^+$, $\mu_{\sigma,j}^-$. We can now make use of the Fisher-Hartwig conjecture (4.3) to determine the divergent contribution of the discontinuity of each eigenvalue. It is logarithmic,

$$\frac{1}{4\pi^2} \left(\log \frac{\mu_{\sigma,j}^-}{\mu_{\sigma,j}^+} \right)^2 \log |X|, \quad j = 1, \ldots, d.$$

Therefore, the divergent contribution to $\log D_X[UJU^{-1}]$ of the discontinuity in $UJU^{-1}(\theta)$ at θ_σ is

$$\beta_\sigma \log |X|$$

with

$$\beta_\sigma = \frac{1}{4\pi^2} \sum_{j=1}^{d} \left(\log \frac{\mu_{\sigma,j}^-}{\mu_{\sigma,j}^+} \right)^2. \tag{4.12}$$

According to (4.11), this is also the divergent contribution to $\log D_X[J]$ in the large $|X|$ limit of the discontinuity at θ_σ, provided the lateral limits $J_\sigma^\pm$ commute.

The expression of the coefficient β_σ can be written in a more compact and meaningful form as

$$\beta_\sigma = \frac{1}{4\pi^2}\,\mathrm{Tr}[\log J_\sigma^-(J_\sigma^+)^{-1}]^2. \tag{4.13}$$

Let us show that the same expression is also valid when the two lateral limits $J_\sigma^\pm$ do not commute. In this case, there is not a basis in which $J_\sigma^\pm$ are both diagonal.

Nevertheless, we can invoke a useful result by Widom [122] that, in the particular case that concerns us, can be stated in the following form: for any $d \times d$ constant matrix C and any symbol $J(\theta)$ as before we have

$$T_X[JC] = T_X[J]T_X[C].$$

Actually $T_X[C] = I_{|X|} \otimes C$ from which the previous relation immediately follows. In terms of the determinant,

$$\log D_X[JC] = \log D_X[J] + \log D_X[C].$$

Since C is constant we can apply the Widom theorem (4.6) to determine $\log D_X[C]$. Then we obtain

$$\log D_X[JC] = \log D_X[J] + |X| \log\det C. \tag{4.14}$$

If we now apply this identity choosing the constant matrix $C = (J_\sigma^+)^{-1}$, we have

$$\log D_X[J] = \log D_X[J(J_\sigma^+)^{-1}] + |X| \log\det J_\sigma^+. \tag{4.15}$$

Observe that the symbol $J(J_\sigma^+)^{-1}$ has also a discontinuity at θ_σ but with lateral limits $J_\sigma^-(J_\sigma^+)^{-1}$ and I which, of course, always commute. Therefore, we can apply the result that we have just obtained for commuting lateral limits. Combining it with (4.15), we can conclude that the discontinuity of J at θ_σ contributes to $\log D_X[J]$ with a term $\beta_\sigma \log|X|$ being the coefficient β_σ equal to (4.13).

Finally, in virtue of the localisation theorem, the total divergent contribution of the discontinuities of $J(\theta)$ will be the sum of the divergent contribution $\beta_\sigma \log|X|$ of each discontinuity considered separately. Then, taking into account (4.4), the previous reasoning leads to formulate the following result.

Conjecture: let J be a piecewise $d \times d$ matrix valued symbol such that $\det J(\theta) \neq 0$, and zero winding number. If J has discontinuities at $\theta_1, \ldots, \theta_R$, the determinant $D_X[J]$ of its block Toeplitz matrix behaves as

$$\log D_X[J] = \frac{|X|}{2\pi}\int_{-\pi}^{\pi} \log\det J(\theta)\mathrm{d}\theta + \frac{\log|X|}{4\pi^2}\sum_{\sigma=1}^{R}\mathrm{Tr}[\log J_\sigma^-(J_\sigma^+)^{-1}]^2 + O(1), \tag{4.16}$$

where $J_\sigma^\pm$ are the lateral limits of $J(\theta)$ at θ_σ.

Observe that this result is a generalisation for matrix symbols of that in (4.3) predicted by the Fisher-Hartwig conjecture for scalar ones.

Notice the apparent non unicity of the coefficient that we have obtained for the logarithmic term. In fact, when we have expressed the coefficient β_σ in (4.12) in the matrix form (4.13), we can also consider for instance $\log[(J_\sigma^+)^{-1}J_\sigma^-]$, $\log[(J_\sigma^-)^{-1}J_\sigma^+]$ or even

$\log[(J_\sigma^+)^{-1/2} J_\sigma^- (J_\sigma^+)^{-1/2}]$, and they can be generalised to non commutative lateral limits applying the identity (4.14). Nevertheless, one can show that, at the end of the day, all the possibilities give the same value for the coefficient.

In the following sections of this chapter we shall apply the above general results to compute the asymptotic behaviour of the ground state entanglement entropy of an interval in any quadratic fermionic chain described by (2.2).

4.2 Non critical chains

We start by considering the case of non critical fermionic chains with finite range couplings A_l and B_l, where $l = -L, -L+1, \ldots, L$ and $L < N/2$. For these systems, the mass gap is non-zero, and the dispersion relation (2.10),

$$\omega(\theta) = \sqrt{F^+(\theta)^2 + |G(\theta)|^2} + F^-(\theta), \tag{4.17}$$

is positive. Therefore, the symbol of the ground state correlation matrix (2.40) can be written

$$\hat{\mathcal{G}}(\theta) = M(\theta) = \frac{1}{\omega^+(\theta)} \begin{pmatrix} F^+(\theta) & G(\theta) \\ \overline{G(\theta)} & -F^+(\theta) \end{pmatrix}, \tag{4.18}$$

since the existence of a mass gap implies

$$|F^-(\theta)| < \omega^+(\theta) = \sqrt{F^+(\theta)^2 + |G(\theta)|^2}$$

for all θ.

In this case $M(\theta)$ is smooth. Therefore, according to the discussion of the previous section, the determinant $D_X(\lambda)$, or $D_X[\hat{\mathcal{G}}_\lambda]$ in the notation employed therein, with symbol $\hat{\mathcal{G}}_\lambda = \lambda I - M$ satisfies the asymptotic expansion (4.6) and the constant term $E[\hat{\mathcal{G}}_\lambda]$ verifies (4.8).

Thus we have to solve the Wiener-Hopf factorisation of the analytical continuation of $\hat{\mathcal{G}}_\lambda$ in order to obtain $E[\hat{\mathcal{G}}_\lambda]$. In general, this is a difficult problem. There is not a general method to obtain the Wiener-Hopf factorisation of a given symbol. It may require applying different sophisticated techniques depending on its particular form. In [124] Its, Jin and Korepin found the solution for the symbol of the non critical XY spin chain ($L = 1$) inspired by methods of algebraic geometry previously applied to deal with asymptotic problems of random matrices and integrable statistical models [127]. In [128] Its, Mezzadri and Mo extended the solution to arbitrary range $L < N/2$ provided the couplings A_l and B_l take real values, that is for theories with parity and charge conjugation symmetries. Let us present here their results recasting them in a very convenient way. In Appendix B we describe in detail the Wiener-Hopf factorisation of these symbols.

In order to define the analytical continuation of (4.18), let us introduce the Laurent polynomials

$$\Phi(z) = \sum_{l=-L}^{L} A_l z^l, \quad \Xi(z) = \sum_{l=-L}^{L} B_l z^l, \tag{4.19}$$

that map meromorphically the Riemann sphere $\overline{\mathbb{C}}$ into itself. Due to the properties of the coupling constants, $A_{-l} = \overline{A_l}$ and $B_{-l} = -B_l$, we have that

$$\overline{\Phi(\overline{z})} = \Phi(z^{-1}), \quad \Xi(z^{-1}) = -\Xi(z).$$

Notice also that $F(\theta) \equiv \Phi(\mathrm{e}^{\mathrm{i}\theta})$ and $G(\theta) \equiv \Xi(\mathrm{e}^{\mathrm{i}\theta})$.

Then, if A_l and B_l take complex values, the analytical continuation of $M(\theta)$ to the Riemann sphere reads

$$\mathcal{M}(z) = \frac{1}{\sqrt{\Phi^+(z)^2 - \Xi(z)\overline{\Xi(\overline{z})}}} \begin{pmatrix} \Phi^+(z) & \Xi(z) \\ -\overline{\Xi(\overline{z})} & -\Phi^+(z) \end{pmatrix}, \tag{4.20}$$

where

$$\Phi^{\pm}(z) = \frac{\Phi(z) \pm \Phi(z^{-1})}{2}.$$

As we show in Appendix B, the crucial point to solve the Wiener-Hopf problem is to understand the analytical structure of $\mathcal{M}(z)$. Observe that $\mathcal{M}(z)$ is bivalued in the Riemann sphere $\overline{\mathbb{C}}$, but it is a single valued meromorphic function in the compact Riemann surface determined by the complex curve

$$w^2 = P(z) \equiv z^{2L}(\Phi^+(z)^2 - \Xi(z)\overline{\Xi(\overline{z})}). \tag{4.21}$$

By its definition $P(z)$ is a polynomial of degree $4L$ on $\overline{\mathbb{C}}$. Hence $w^2 = P(z)$ describes a hyperelliptic curve. It defines a double covering of the Riemann sphere with branch points at the roots of $P(z)$. Its genus g is given by the range L of the couplings of the Hamiltonian such that $\mathrm{g} = 2L - 1$. The properties of Φ and Ξ imply that $P(z)$ has real coefficients and verifies $z^{4L}P(z^{-1}) = P(z)$. Therefore, the roots of $P(z)$ come in quartets related by inversion and complex conjugation, except for the real ones that come in pairs related by inversion.

The criticality of the theory can be characterised in terms of the roots of $P(z)$. In fact, consider the relation

$$(\omega(\theta) + \omega(-\theta))^2 = 4|P(\mathrm{e}^{\mathrm{i}\theta})|. \tag{4.22}$$

If the theory is non critical, $\omega(\theta) > 0$ for all θ. Then, according to (4.22), $P(\mathrm{e}^{\mathrm{i}\theta}) \neq 0$ and there are no roots lying on the unit circle. On the other hand, if $P(z)$ has roots at the unit circle, they necessarily have multiplicity different from one, and the dispersion relation vanishes at some points. Observe that using (4.22) the dispersion relation (4.17) can be expressed as

$$\omega(\theta) = \sqrt{|P(\mathrm{e}^{\mathrm{i}\theta})|} + F^-(\theta).$$

Consider now that $z_1 = \mathrm{e}^{\mathrm{i}\theta_1}$, with $\theta_1 \neq 0, -\pi$, is a root of $P(z)$. Then $\omega(\theta_1) = F^-(\theta_1)$. Since the roots of $P(z)$ are related by inversion, $z_1^{-1} = \mathrm{e}^{-\mathrm{i}\theta_1}$ is also root, $P(\mathrm{e}^{-\mathrm{i}\theta_1}) = 0$. Thus $\omega(-\theta_1) = F^-(-\theta_1) = -F^-(\theta_1)$, due to the antisymmetry of F^-. Hence we conclude that $\omega(\theta_1) = -\omega(-\theta_1)$. Therefore, $\omega(\theta)$ is zero at θ_1 or, since it is a continuous function, there is at least a point in the interval $(-\theta_1, \theta_1)$ where $\omega(\theta)$ changes its sign. In the case $\theta_1 = 0$, that is when $z_1 = 1$ is a root of P, we have $\omega(0) = 0$ since $F^-(0) = 0$ (the case

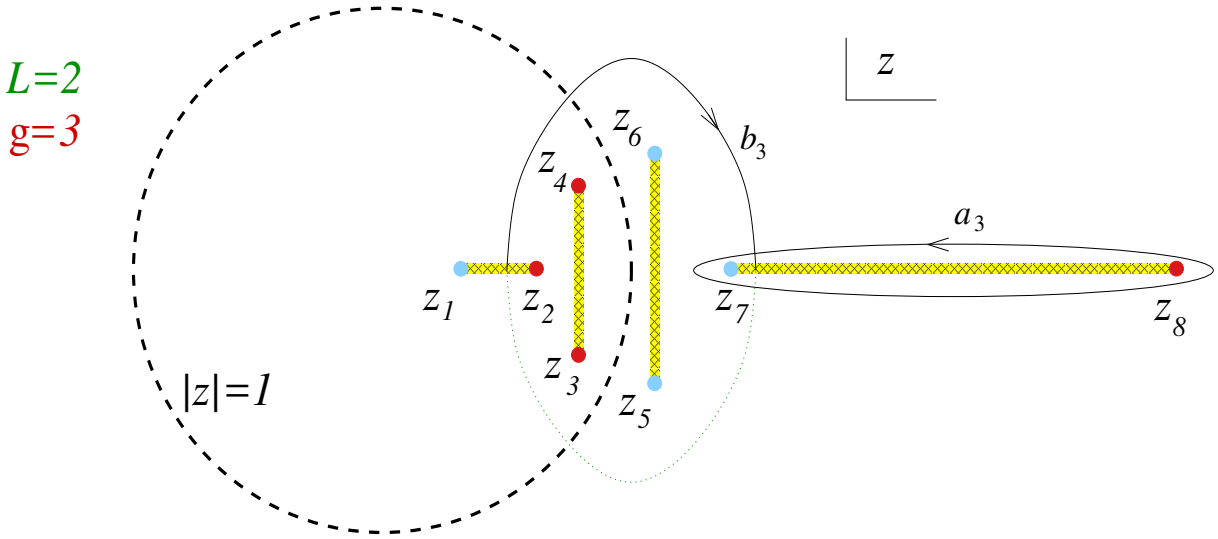

Figure 4.1: Possible arrangement of the branch points and cuts of $w = \sqrt{P(z)}$ for genus g = 3 ($L = 2$). Note that we must have $z_1 = z_8^{-1}$, $z_2 = z_7^{-1}$, $z_3 = \overline{z}_4 = \overline{z}_5^{-1} = z_6^{-1}$. The blue branch points • are zeros of $\mathfrak{g}(z)$ ($\epsilon_j = 1$) while those in red • are poles ($\epsilon_j = -1$). The oriented curves a_3 and b_3 are two of the basic cycles.

$\theta_1 = -\pi$ is analogous). In all these situations, since the dispersion relation vanishes at some points, the mass gap is zero and the theory is critical.

Let us restrict from this point to Hamiltonians that are PC invariant (the couplings B_l are real). For them, $\overline{\Xi(\overline{z})} = \Xi(z)$, and the analytical continuation $\mathcal{M}(z)$ can be expressed in the antidiagonal form

$$\mathcal{M}(z) = \mathfrak{U} \begin{pmatrix} 0 & \sqrt{\mathfrak{g}(z)} \\ \sqrt{\mathfrak{g}(z)^{-1}} & 0 \end{pmatrix} \mathfrak{U}^{-1},$$

where $\mathfrak{U}$ is the unitary matrix

$$\mathfrak{U} = \frac{1}{\sqrt{2}} \begin{pmatrix} 1 & 1 \\ -1 & 1 \end{pmatrix} \tag{4.23}$$

and

$$\mathfrak{g}(z) = \frac{\Phi^+(z) + \Xi(z)}{\Phi^+(z) - \Xi(z)}.$$

In this case the polynomial $P(z)$ factorises such that

$$w^2 = P(z) = z^{2L}(\Phi^+(z) + \Xi(z))(\Phi^+(z) - \Xi(z)).$$

Then the roots of $P(z)$, z_j, are either zeros or poles of the rational function $\mathfrak{g}(z)$. According to this we assign an index ϵ_j to every root, which is $+1$ if z_j is a zero of $\mathfrak{g}(z)$ and -1 if it is a pole. Moreover, since $\mathfrak{g}(z) = \overline{\mathfrak{g}(\overline{z})} = 1/\mathfrak{g}(z^{-1})$, if z_j is a zero (pole) of $\mathfrak{g}(z)$, its complex conjugate $\overline{z_j}$ is also a zero (pole) while its inverse z_j^{-1} is a pole (zero). Note that the indices must satisfy $\epsilon_j = -\epsilon_{j'}$ whenever $z_j = z_{j'}^{-1}$ and $\epsilon_j = \epsilon_{j'}$ if $z_j = \overline{z_{j'}}$.

We must fix an order in the roots with the only requirement that the first half of them is inside the unit disk and the other half outside it, i.e. $|z_j| < 1$, $j = 1, \ldots, 2L$ and $|z_j| > 1$, $2L+1, \ldots, 4L$. Let us consider that all roots are simple. The branch cuts of

$w = \sqrt{P(z)}$ are chosen to be the $2L$ non-intersecting curves Σ_ρ, $\rho = 0, \ldots, \mathrm{g}$ that join $z_{2\rho+1}$ and $z_{2\rho+2}$. Notice that it is always possible to choose them such that they do not cross the unit circle.

Associated to these cuts we have a canonical homology basis of cycles in the Riemann surface: a_r, b_r, $r = 1, \ldots, \mathrm{g}$. The cycle a_r surrounds Σ_r anticlockwise in the upper Riemann sheet. The dual cycle b_r encloses the branch points $z_2, z_3, \ldots, z_{2r+1}$ clockwise. In Fig. 4.1 we depict a possible arrangement of the branch points and cuts for $\mathrm{g} = 3$ ($L = 2$) as well as the cycles a_3 and b_3.

The canonical basis of holomorphic forms

$$\mathrm{d}\eta_r = \frac{\phi_r(z)}{\sqrt{P(z)}}\mathrm{d}z, \quad r = 1, \ldots, \mathrm{g},$$

with $\phi_r(z)$ a polynomial of degree smaller than g, is chosen such that

$$\oint_{a_r} \mathrm{d}\eta_{r'} = \delta_{rr'}, \quad r, r' = 1, \ldots, \mathrm{g}.$$

The integration of the elements of the basis of holomorphic forms along the dual cycles b_r,

$$\Pi_{rr'} = \oint_{b_r} \mathrm{d}\eta_{r'},$$

gives the entries of the $\mathrm{g} \times \mathrm{g}$ symmetric matrix of periods $\Pi = (\Pi_{rr'})$.

Associated with this matrix of periods we can now introduce the Riemann theta function with characteristics $\vec{p}$, $\vec{q} \in \mathbb{R}^{\mathrm{g}}$,

$$\vartheta\left[\begin{smallmatrix}\vec{p}\\ \vec{q}\end{smallmatrix}\right] : \mathbb{C}^{\mathrm{g}} \to \mathbb{C},$$

defined by

$$\vartheta\left[\begin{smallmatrix}\vec{p}\\ \vec{q}\end{smallmatrix}\right](\vec{s}) \equiv \vartheta\left[\begin{smallmatrix}\vec{p}\\ \vec{q}\end{smallmatrix}\right](\vec{s}\,|\Pi) = \sum_{\vec{n}\in\mathbb{Z}^{\mathrm{g}}} \mathrm{e}^{\pi\mathrm{i}(\vec{n}+\vec{p})\Pi\cdot(\vec{n}+\vec{p})+2\pi\mathrm{i}(\vec{s}+\vec{q})\cdot(\vec{n}+\vec{p})}. \tag{4.24}$$

It will be useful to introduce its *normalized* version

$$\widehat{\vartheta}\left[\begin{smallmatrix}\vec{p}\\ \vec{q}\end{smallmatrix}\right](\vec{s}) \equiv \widehat{\vartheta}\left[\begin{smallmatrix}\vec{p}\\ \vec{q}\end{smallmatrix}\right](\vec{s}\,|\Pi) = \frac{\vartheta\left[\begin{smallmatrix}\vec{p}\\ \vec{q}\end{smallmatrix}\right](\vec{s}\,|\Pi)}{\vartheta\left[\begin{smallmatrix}\vec{p}\\ \vec{q}\end{smallmatrix}\right](0|\Pi)}.$$

Finally, after solving the Wiener-Hopf problem for $\lambda I - \mathcal{M}$ (see Appendix B) and applying (4.6) and (4.8), one has the following expression for the asymptotic expansion of the determinant

$$\log D_X(\lambda) = |X| \log(\lambda^2 - 1) + \log\left(\widehat{\vartheta}\left[\begin{smallmatrix}\vec{\mu}\\ \vec{\nu}\end{smallmatrix}\right](\beta(\lambda)\vec{e})\widehat{\vartheta}\left[\begin{smallmatrix}\vec{\mu}\\ \vec{\nu}\end{smallmatrix}\right](-\beta(\lambda)\vec{e})\right) + o(1). \tag{4.25}$$

In the argument of the theta function we have

$$\beta(\lambda) = \frac{1}{2\pi\mathrm{i}} \log\frac{\lambda+1}{\lambda-1},$$

and $\vec{e} \in \mathbb{Z}^{\mathrm{g}}$ whose first $L-1$ entries are 0 and the last L are 1. The characteristics of the theta function are half integer vectors $\vec{\mu}$, $\vec{\nu} \in (\mathbb{Z}/2)^{\mathrm{g}}$ that depend on the branch points of $w = \sqrt{P(z)}$ as zeros or poles of $\mathfrak{g}(z)$,

$$\begin{aligned} \mu_r &= \frac{1}{4}(\epsilon_{2r+1} + \epsilon_{2r+2}), \\ \nu_r &= \frac{1}{4}\sum_{j=2}^{2r+1} \epsilon_j, \quad r = 1, \ldots, \mathrm{g}. \end{aligned} \tag{4.26}$$

In order to write an explicit expression of the determinant $D_X(\lambda)$ we have used the rule that we previously established for choosing the order of the roots of $P(z)$. Of course, for consistency, (4.25) should not depend on the chosen order. In Appendix C we show that the expansion of the determinant (in the thermodynamic limit) is in fact invariant under the transposition of two roots provided they sit at the same side of the unit circle. As we discuss in Appendix C, a transposition in the order of the roots corresponds to performing a modular transformation in the homology basis of the Riemann surface.

When the theory breaks the PC symmetry the symbol $M(\theta)$ does not become anti-diagonal after a global unitary transformation as in the symmetric case. Now the branch points are not the zeros or poles of a rational function like $\mathfrak{g}(z)$. This makes difficult to find the asymptotic expansion of $D_X(\lambda)$. Actually, for this case, the Wiener-Hopf factorisation problem has not been solved yet and we do not have a general expression for the constant term of the entanglement entropy.

However, the asymptotic expansion (4.25) for systems with PC symmetry can be straightforwardly extended to theories with complex pairings provided

$$\overline{G(\theta)} = -\mathrm{e}^{\mathrm{i}\psi} G(\theta),$$

where ψ is a global phase. This, together with $\Xi(z^{-1}) = -\Xi(z)$, implies

$$\overline{\Xi(z)} = \mathrm{e}^{\mathrm{i}\psi}\Xi(\overline{z}).$$

Therefore, the corresponding compact Riemann surface is described by

$$w^2 = P(z) \equiv z^{2L}[\Phi^+(z) + \mathrm{e}^{\mathrm{i}\psi/2}\Xi(z)][\Phi^+(z) - \mathrm{e}^{\mathrm{i}\psi/2}\Xi(z)].$$

Of course, we can get ride of the global phase ψ by performing a redefinition of the annihilation and creation operators a_n, $a_n^\dagger$. In fact, by introducing $a'_n = \mathrm{e}^{\mathrm{i}\psi/4} a_n$, the new meromorphic functions are $\Phi' = \Phi$ and $\Xi' = \mathrm{e}^{\mathrm{i}\psi/2}\Xi$. Hence

$$\overline{\Xi'(\overline{z})} = \Xi'(z),$$

and the global phase is absent. Then the expression (4.25) is also valid in these particular theories that break the PC symmetry.

Once we have obtained $D_X(\lambda)$ we can determine the entanglement entropy. We must introduce the asymptotic expansion (4.25) for $D_X(\lambda)$ into the contour integral (2.36),

$$S_{\alpha,X} = \frac{1}{4\pi\mathrm{i}} \lim_{\varepsilon \to 1^+} \oint_{\mathscr{C}} f_\alpha(\lambda/\varepsilon) \frac{\mathrm{d}}{\mathrm{d}\lambda} \log D_X(\lambda) \mathrm{d}\lambda,$$

where the curve $\mathscr{C}$ is that depicted in Fig. 2.5.

As we have seen in Section 4.1, the contribution of the linear term to $D_X(\lambda)$ vanishes when we insert it in this contour integral. This is in agreement with the general discussion of Section 1.2: in the ground state of a non critical theory with finite range coupling the entanglement entropy should satisfy an area law and it tends to a constant value in the limit $|X| \to \infty$. In this case, this constant is precisely

$$S_{\alpha,X} = \lim_{\varepsilon \to 1^+} \frac{1}{4\pi \mathrm{i}} \oint_{\mathscr{C}} f_\alpha(\lambda/\varepsilon) \frac{\mathrm{d}E[\hat{\mathcal{G}}_\lambda]}{\mathrm{d}\lambda} \mathrm{d}\lambda + o(1), \tag{4.27}$$

where

$$E[\hat{\mathcal{G}}_\lambda] = \log \left(\widehat{\vartheta}\big[\begin{smallmatrix} \vec{\mu} \\ \vec{\nu} \end{smallmatrix}\big](\beta(\lambda)\vec{e}) \widehat{\vartheta}\big[\begin{smallmatrix} \vec{\mu} \\ \vec{\nu} \end{smallmatrix}\big](-\beta(\lambda)\vec{e}) \right).$$

We can express (4.27) in a simpler form. As we did in Section 3.2, if we integrate by parts,

$$S_{\alpha,X} = - \lim_{\varepsilon \to 1^+} \frac{1}{4\pi \mathrm{i}} \oint_{\mathscr{C}} \frac{\mathrm{d}f_\alpha(\lambda/\varepsilon)}{\mathrm{d}\lambda} E[\hat{\mathcal{G}}_\lambda] \mathrm{d}\lambda + o(1), \tag{4.28}$$

we can circumvent the presence of divergences that finally cancel out. This renders the integrals finite and makes the computations simpler.

Let us evaluate the latter integral for $\alpha = 1$ and integer $\alpha > 1$. For $\alpha = 1$, notice that

$$\frac{\mathrm{d}f_1(\lambda/\varepsilon)}{\mathrm{d}\lambda} = \frac{1}{2} \log \frac{1 - \lambda/\varepsilon}{1 + \lambda/\varepsilon}$$

has branch points at $\lambda = \pm\varepsilon$, with $\varepsilon > 1$. We take as the branch cuts the intervals in the real line $(-\infty, -\varepsilon]$ and $[\varepsilon, \infty)$. The rest of the integrand $E[\hat{\mathcal{G}}_\lambda]$, which contains the theta functions, is analytic outside the interval $[-1, 1]$.

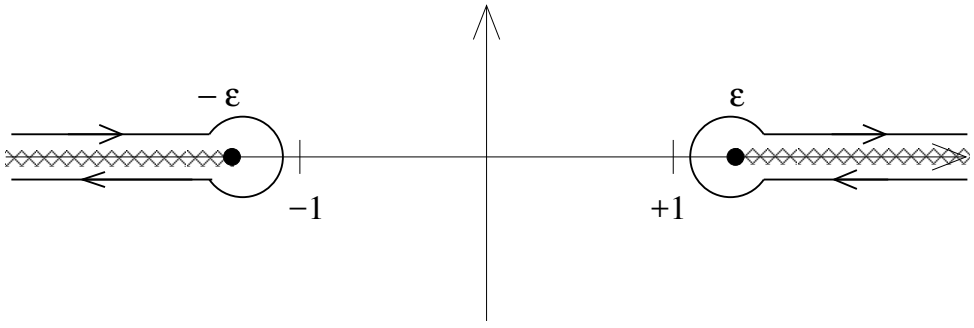

Figure 4.2: Contour of integration $\mathscr{C}'$ for the computation of the von Neumann entanglement entropy in (4.29). The contour extends to infinity and surrounds the branch cuts of the function $\mathrm{d}f_1(\lambda/\varepsilon)/\mathrm{d}\lambda$ that correspond to the intervals $(-\infty, -\varepsilon]$ and $[\varepsilon, \infty)$.

Then, using the Cauchy integral theorem we can deform the integration contour from $\mathscr{C}$ to $\mathscr{C}'$, that tends to infinity as we illustrate in Fig. 4.2,

$$S_{1,X} = - \lim_{\varepsilon \to 1^+} \frac{1}{4\pi \mathrm{i}} \oint_{\mathscr{C}'} \frac{\mathrm{d}f_1(\lambda/\varepsilon)}{\mathrm{d}\lambda} E[\hat{\mathcal{G}}_\lambda] \mathrm{d}\lambda + o(1). \tag{4.29}$$

The only non-vanishing contributions to the integral above come from the change in the phase of $\mathrm{d}f_1(\lambda/\varepsilon)/\mathrm{d}\lambda$ when we are integrating along its branch cuts and we go around the branch points $\pm\varepsilon$. Thus, after taking the limit in ε,

$$\begin{aligned} S_{1,X} &= \frac{1}{8\pi\mathrm{i}}\left[\int_{-\infty}^{-1}\left(\log\frac{\lambda+1}{\lambda-1}+\mathrm{i}\pi\right)E[\hat{\mathcal{G}}_\lambda]\mathrm{d}\lambda-\int_{-\infty}^{-1}\left(\log\frac{\lambda+1}{\lambda-1}-\mathrm{i}\pi\right)E[\hat{\mathcal{G}}_\lambda]\mathrm{d}\lambda\right. \\ &\quad \left.-\int_{1}^{\infty}\left(\log\frac{\lambda+1}{\lambda-1}-\mathrm{i}\pi\right)E[\hat{\mathcal{G}}_\lambda]\mathrm{d}\lambda+\int_{1}^{\infty}\left(\log\frac{\lambda+1}{\lambda-1}+\mathrm{i}\pi\right)E[\hat{\mathcal{G}}_\lambda]\mathrm{d}\lambda\right]+o(1). \end{aligned}$$

Simplifying this expression, and taking into account that $f_\alpha(\lambda)$ and $E[\hat{\mathcal{G}}_\lambda]$ are even functions, we arrive at the integral

$$S_{1,X}=\frac{1}{2}\int_1^\infty \log\left(\widehat{\vartheta}\left[\begin{smallmatrix}\vec{\mu}\\ \vec{\nu}\end{smallmatrix}\right](\beta(\lambda)\vec{e})\widehat{\vartheta}\left[\begin{smallmatrix}\vec{\mu}\\ \vec{\nu}\end{smallmatrix}\right](-\beta(\lambda)\vec{e})\right)\mathrm{d}\lambda+o(1), \tag{4.30}$$

which can be evaluated numerically.

For integer $\alpha>1$, we can follow similar steps than those performed in Section 3.2 in order to compute, in the hopping chains, the coefficient of the logarithmic term when α takes these values. In fact, $E[\hat{\mathcal{G}}_\lambda]$ is analytic outside the region enclosed by $\mathscr{C}$ and

$$\frac{\mathrm{d}f_\alpha(\lambda)}{\mathrm{d}\lambda}=\frac{\alpha}{1-\alpha}\frac{(1+\lambda)^{\alpha-1}-(1-\lambda)^{\alpha-1}}{(1+\lambda)^\alpha+(1-\lambda)^\alpha}$$

is a meromorphic function with poles along the imaginary axis located at

$$\lambda_l=\mathrm{i}\tan\frac{\pi(2l-1)}{2\alpha},\quad l=1,2,\ldots,\alpha,\quad \text{with}\quad l\neq\frac{\alpha+1}{2}.$$

Then we can send the integration contour $\mathscr{C}$ in (4.28) to infinity and reduce the integral to the computation of the corresponding residues of the integrand at the poles λ_l. In this way we get an integrated expression of $S_{\alpha,X}$ for integer $\alpha>1$,

$$S_{\alpha,X}=\frac{1}{2(1-\alpha)}\sum_{l=1}^{\alpha}\log\left(\widehat{\vartheta}\left[\begin{smallmatrix}\vec{\mu}\\ \vec{\nu}\end{smallmatrix}\right](\beta(\lambda_l)\vec{e})\widehat{\vartheta}\left[\begin{smallmatrix}\vec{\mu}\\ \vec{\nu}\end{smallmatrix}\right](-\beta(\lambda_l)\vec{e})\right)+o(1). \tag{4.31}$$

In particular, for $\alpha=2,3$ the sum in the previous expression reduces to

$$S_{2,X}=-\log\left[\widehat{\vartheta}\left[\begin{smallmatrix}\vec{\mu}\\ \vec{\nu}\end{smallmatrix}\right]\left(\frac{\vec{e}}{4}\right)\widehat{\vartheta}\left[\begin{smallmatrix}\vec{\mu}\\ \vec{\nu}\end{smallmatrix}\right]\left(-\frac{\vec{e}}{4}\right)\right]+o(1),$$

$$S_{3,X}=-\frac{1}{2}\log\left[\widehat{\vartheta}\left[\begin{smallmatrix}\vec{\mu}\\ \vec{\nu}\end{smallmatrix}\right]\left(\frac{\vec{e}}{6}\right)\widehat{\vartheta}\left[\begin{smallmatrix}\vec{\mu}\\ \vec{\nu}\end{smallmatrix}\right]\left(-\frac{\vec{e}}{6}\right)\right]+o(1).$$

In Section 4.4 we shall apply these results to the non critical XY spin chain in which there are only nearest-neighbour couplings, i.e. $L=1$, and the corresponding compact Riemann surface is a torus.

4.2.1 Degeneration of branch points

At the beginning of this section, we have seen that the theory is critical when there are roots of $P(z)$ lying on the unit circle. Since the roots are related by inversion and complex conjugation, this happens when pairs of simple roots degenerate in a single double root at the unit circle. Let us analyse the asymptotic expansion (4.25) for $D_X(\lambda)$ when pairs of single roots approach each other. The degeneration of a pair of roots produces a pinching of the complex curve $w^2 = P(z)$ and the divergence of some of the entries of the period matrix Π. We shall show that the resulting entanglement entropy is finite when the roots degenerate in a point that does not belong to the unit circle so the theory is not critical. On the contrary, if the degeneration takes place at the unit circle the entropy diverges logarithmically at the critical point. Let us treat these two situations separately.

Degeneration outside the unit circle

The study of a pinching of the hyperelliptic curve $w^2 = P(z)$ requires the choice of a homology basis (a, b) that allows to extract easily the divergent entries of the period matrix Π. This will be conveniently chosen such that each pair of colliding branch points is surrounded by one of the a cycles. An example is the basis given previously for writing the asymptotic expansion (4.25) of $D_X(\lambda)$. It is determined by fixing an order in the branch points such that the first half of them are inside the unit disk and the rest outside it. Let us focus on the situation in which two branch points lying in the same side of the unit circle, let say z_j and z_{j+1}, with $j = 2\hat{r} + 1$, approach each other. In this case, the cycle $a_{\hat{r}}$ is enclosing them. Notice that this cannot be done if the two branch points were in opposite sides of the unit circle.

When $z_j \to z_{j+1}$ the only entry of the period matrix that diverges is

$$\Pi_{\hat{r}\hat{r}} \sim -\frac{\mathrm{i}}{\pi} \log |z_j - z_{j+1}|.$$

The rest of the entries of the matrix, Π_{lm} with $l, m \neq \hat{r}$, remain finite in this limit. They define a new $(\mathrm{g}-1)\times(\mathrm{g}-1)$ period matrix that we denote by $\Pi_\circ$. This new period matrix is associated to the Riemann surface resulting from the removal of the two merging branch points. Let us also define with the entries $\Pi_{l\hat{r}}$, with $l \neq \hat{r}$, a $\mathrm{g}-1$ dimensional vector $\vec{\Delta}_\circ$. Then we can rewrite the theta function (4.24) in the following form

$$\vartheta\left[\begin{smallmatrix}\vec{\mu}\\ \vec{\nu}\end{smallmatrix}\right](\vec{s}) = \sum_{n_{\hat{r}}\in\mathbb{Z}} \mathrm{e}^{\mathrm{i}\pi(n_{\hat{r}}+\mu_{\hat{r}})^2\Pi_{\hat{r}\hat{r}}+2\pi\mathrm{i}(n_{\hat{r}}+p_{\hat{r}})(s_{\hat{r}}+\nu_{\hat{r}})} \times \sum_{\vec{n}_\circ\in\mathbb{Z}^{\mathrm{g}-1}} \mathrm{e}^{\pi\mathrm{i}(\vec{n}_\circ+\vec{\mu}_\circ)\Pi_\circ\cdot(\vec{n}_\circ+\vec{\mu}_\circ)+2\pi\mathrm{i}(\vec{n}_\circ+\vec{\mu}_\circ)\cdot[(\vec{s}_\circ+\vec{\nu}_\circ)+(n_{\hat{r}}+\mu_{\hat{r}})\vec{\Delta}_\circ]} \quad (4.32)$$

where $\vec{n}_\circ$, $\vec{\mu}_\circ$, $\vec{\nu}_\circ$ and $\vec{s}_\circ$ stand for the $\mathrm{g}-1$ dimensional vectors obtained by removing the $\hat{r}$-entry from $\vec{n}$, $\vec{\mu}$, $\vec{\nu}$ and $\vec{s}$ respectively.

We find two different cases for the resulting theta function after the coalescence limit. One of them is when the indices of z_j and z_{j+1} are different, i.e. $\epsilon_j \neq \epsilon_{j+1}$. This means

that one is a zero and the other is a pole of $\mathfrak{g}(z)$. This implies that the corresponding $\hat{r}$-entry in the characteristics $\vec{\mu}$ is

$$\mu_{\hat{r}} = \frac{1}{4}(\epsilon_{2\hat{r}+1} + \epsilon_{2\hat{r}+2}) = 0.$$

Taking into account this and the divergent behaviour of $\Pi_{\hat{r}\hat{r}}$, after the limit $z_j \to z_{j+1}$ the only surviving terms in the theta function (4.32) are those with $n_{\hat{r}} = 0$. Hence we have

$$\lim_{z_j \to z_{j+1}} \vartheta\left[\begin{smallmatrix}\vec{\mu}\\ \vec{\nu}\end{smallmatrix}\right](\vec{s}\,|\Pi) = \vartheta\left[\begin{smallmatrix}\vec{\mu}_\circ\\ \vec{\nu}_\circ\end{smallmatrix}\right](\vec{s}_\circ\,|\Pi_\circ), \tag{4.33}$$

that is, a theta function associated to the Riemann surface of genus $\mathrm{g}-1$ obtained after the removal of the two merging branch points z_j, z_{j+1}.

It is important to bear in mind that the branch points of $w^2 = P(z)$ are related by inversion and complex conjugation. This means that if a pair of real branch points degenerates there will be another merging pair related by inversion to the former. In the complex case there will be three other merging pairs, related by inversion and complex conjugation. In both situations, the pairs are composed of branch points of different index. Therefore, by successive application of the degeneration limit (4.33), the resulting theta function corresponds to a Riemann surface of genus either $\mathrm{g}-2$ for real branch points or $\mathrm{g}-4$ for complex ones, obtained by the removal of all the pairs of branch points that degenerate.

The limit (4.33) implies that the resulting entanglement entropy after the coalescence of the branch points is equal to that of a theory with range of couplings either $L-1$ for the real case or $L-2$ for the complex one, obtained by removing all the pairs of degenerating branch points. It is important to remark that although these theories with different range of couplings have the same ground state entanglement spectrum their respective Hamiltonians are not related by any unitary transformation.

The other possibility that we can find is that the two merging branch points z_j and z_{j+1} have the same index, i.e. $\epsilon_j = \epsilon_{j+1}$. Therefore, $\mu_{\hat{r}} = \pm 1/2$. Thus, the divergence of $\Pi_{\hat{r}\hat{r}}$ kills now all the terms in (4.32) and in the coalescence limit $\vartheta\left[\begin{smallmatrix}\vec{\mu}\\ \vec{\nu}\end{smallmatrix}\right]$ vanishes. However, for the study of the entanglement entropy we are interested in the normalised theta function $\widehat{\vartheta}\left[\begin{smallmatrix}\vec{\mu}\\ \vec{\nu}\end{smallmatrix}\right]$ which does not vanish in this limit. We can compute its limit from

$$\begin{aligned}\lim_{z_j \to z_{j+1}} \vartheta\left[\begin{smallmatrix}\vec{\mu}\\ \vec{\nu}\end{smallmatrix}\right](\vec{s}\,|\,\Pi)\,\mathrm{e}^{-\pi \mathrm{i}\Pi_{\hat{r}\hat{r}}/4} &= \mathrm{e}^{\pi \mathrm{i}(s_{\hat{r}}+\nu_{\hat{r}})}\,\vartheta\left[\begin{smallmatrix}\vec{\mu}_\circ\\ \vec{\nu}_\circ\end{smallmatrix}\right](\vec{s}_\circ + \vec{\Delta}_\circ/2|\Pi_\circ)\\ &+ \mathrm{e}^{-\pi \mathrm{i}(s_{\hat{r}}+\nu_{\hat{r}})}\,\vartheta\left[\begin{smallmatrix}\vec{\mu}_\circ\\ \vec{\nu}_\circ\end{smallmatrix}\right](\vec{s}_\circ - \vec{\Delta}_\circ/2|\Pi_\circ),\end{aligned} \tag{4.34}$$

that results from the non vanishing terms in (4.32), i.e. those corresponding to $n_{\hat{r}} = 0, -2\mu_{\hat{r}}$.

Again when we apply this scenario to the curve $w^2 = P(z)$ either two pairs of branch points, when they are real, or four, if they are complex, merge simultaneously. The resulting theta functions after the successive application of (4.34) correspond to Riemann surfaces of genus $\mathrm{g}-2$, for the real case, and $\mathrm{g}-4$, for the complex one. However, in contrast to the case of merging roots with opposite index, now the resulting entanglement, as it is clear from the form of (4.34), is no longer equal to that of a theory with a smaller range of couplings.

Degeneration at the unit circle: approaching criticality

Equipped with the previous results, let us study now the behaviour of the entanglement entropy when the pairs of branch points come together at the unit circle and the system approaches a critical theory. In this case the degenerating points have different indices. Therefore, according to the previous analysis, the entanglement entropy would coincide with that of a theory of smaller range in which the merging branch points have been removed.

However, there is a problem because the limiting procedure was carried out assuming that one of the a cycles encircles the pair of merging points. On the other hand, the asymptotic expansion (4.25) for $D_X(\lambda)$ is valid provided no a cycle intersects the unit circle. In the case of branch points degenerating at the unit circle, these two prescriptions are not compatible.

The way to overcome this difficulty is by performing a modular transformation from one basis where (4.25) is true to a new one (a', b') where some a cycles cross the unit circle and enclose the pairs of degenerating branch points. We shall initially order the branch points so that z_{2L} degenerates with $z_{2L+2} = \overline{z}_{2L}^{-1}$ at the unit circle. If these branch points are real we do not have to impose other conditions to the ordering. If they are not real we shall take $z_{2L-1} = \overline{z}_{2L}$ and $z_{2L+1} = \overline{z}_{2L+2}$ that also degenerate at the unit circle. In this ordering, where the first branch points are inside the unit disk and the last ones outside, the transposition of z_{2L} and z_{2L+1} induces the desired transformation of the basic cycles, as we illustrate in Fig. 4.3.

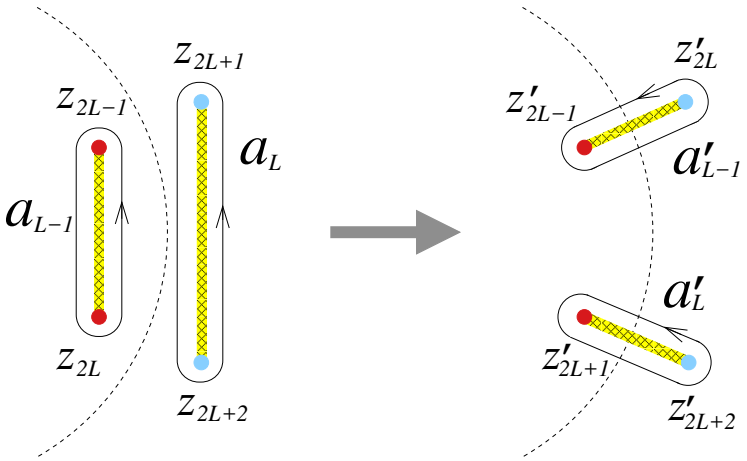

Figure 4.3: Representation of the change of homology basis used to extract the divergent behaviour under a pinching. On the left, the usual homology basis taken to compute the determinant $D_X(\lambda)$, in which the a cycles do not cross the unit circle, is depicted. On the right, we represent the alternative homology basis in which a' cycles enclose pairs of approaching branch points. This modular transformation is equivalent to a permutation in the labelling of the branch points: $z_{2L} = z'_{2L+1}$ and $z_{2L+1} = z'_{2L}$.

In Appendix C, we describe in detail how Riemann theta functions transform under a modular transformation. For our particular modular transformation we have the following relation between the original $\hat{\vartheta}$ function and the new one

$$\widehat{\vartheta}\big[\tfrac{\vec{\mu}}{\vec{\nu}}\big](\beta(\lambda)\vec{e}\,|\Pi) = \mathrm{e}^{\pi \mathrm{i}\beta(\lambda)^2(\Pi'_{L-1,L-1}+\Pi'_{L,L}-2\Pi'_{L,L-1}-1)}\widehat{\vartheta}\big[\tfrac{\vec{\mu}'}{\vec{\nu}}\big](\beta(\lambda)\vec{e'}\,|\Pi'), \tag{4.35}$$

where Π' is the period matrix for the new basic cycles, $e'_r = e_r - (\Pi'_{L,r} - \Pi'_{L-1,r})$ and $\vec{\mu'}$ differs from $\vec{\mu}$ only in the $L-1$ and L entries:

$$\mu'_{L-1} = \mu_{L-1} + \nu_L - \nu_{L-1} + 1/2, \quad \mu'_L = \mu_L - \nu_L + \nu_{L-1} + 1/2. \tag{4.36}$$

The advantage of using this basis of cycles is that the divergences of Π' are very simple to analyse. In fact, for the real pinching (when z_{2L} and z_{2L+2} degenerate) only $\Pi'_{L,L}$ diverges, so that

$$\Pi'_{L,L} \sim \frac{\mathrm{i}}{\pi} \log |z_{2L+2} - z_{2L}|, \tag{4.37}$$

while the rest of the entries of Π' have a finite limit. In the complex pinching (when also $z_{2L-1} = \overline{z}_{2L}$ and $z_{2L+1} = \overline{z}_{2L+2}$ degenerate) both $\Pi'_{L-1,L-1}$ and $\Pi'_{L,L}$ have divergent behaviour,

$$\Pi'_{L-1,L-1} + \Pi'_{L,L} \sim -\frac{2\mathrm{i}}{\pi} \log |z_{2L+2} - z_{2L}|. \tag{4.38}$$

The study of the coalescence limit of $\widehat{\vartheta}\left[\begin{smallmatrix}\vec{\mu}'\\ \vec{\nu}\end{smallmatrix}\right](\beta(\lambda)\vec{e}'\,|\Pi')$ in (4.35) follows similar lines than in the case of merging points outside the unit circle that have different index. Since $z_{2L+2} = \overline{z}_{2L}^{-1}$, $\epsilon_{2L} = -\epsilon_{2L+2}$. This implies that $\mu'_L = 0$. In the complex case we also have to regard that $z_{2L-1} = \overline{z}_{2L+1}^{-1}$ and $\epsilon_{2L-1} = -\epsilon_{2L+1}$, so that $\mu'_{L-1} = \mu'_L = 0$. Therefore, adapting the limit (4.33), we have

$$\widehat{\vartheta}\left[\begin{smallmatrix}\vec{\mu}'\\ \vec{\nu}\end{smallmatrix}\right](\beta(\lambda)\vec{e}'\,|\Pi') \longrightarrow \widehat{\vartheta}\left[\begin{smallmatrix}\vec{\mu}'_\circ\\ \vec{\nu}_\circ\end{smallmatrix}\right](\beta(\lambda)\vec{e}'_\circ\,|\Pi'_\circ). \tag{4.39}$$

Again the resulting $\hat{\vartheta}$ function is associated to a genus $\mathrm{g}-1$ Riemann surface in the real pinching or $\mathrm{g}-2$ in the complex one. The period matrix $\Pi'_\circ$ is obtained in the real case by removing from Π' the L row and column. For the complex case, we remove the $L-1$ and L rows and columns. Likewise, $\vec{\mu}'_\circ$, $\vec{\nu}_\circ$ and $\vec{e}'_\circ$ stand for the vectors resulting after the removal of the L component for the real case or both the $L-1$ and L ones in the complex pinching.

Since $\widehat{\vartheta}\left[\begin{smallmatrix}\vec{\mu}'\\ \vec{\nu}\end{smallmatrix}\right](\beta(\lambda)\vec{e}'\,|\Pi')$ gives a finite value and Π'_{LL}, and eventually Π'_{L-1L-1}, diverges logarithmically like (4.37) the asymptotic behaviour of (4.35) in the limit $z_{2L} \to z_{2L+2}$ is

$$\log \widehat{\vartheta}\left[\begin{smallmatrix}\vec{\mu}\\ \vec{\nu}\end{smallmatrix}\right](\beta(\lambda)\vec{e}\,|\Pi) = -\frac{c}{2\pi^2}\left(\log\frac{\lambda+1}{\lambda-1}\right)^2 \log |z_{2L} - z_{2L+2}| + \cdots, \tag{4.40}$$

where $c = 1/2$ for the real pinching, $c = 1$ for the complex one, and the dots refer to the contributions which are finite in this limit.

Plugging now this result into (4.27) and employing the integral identity

$$\lim_{\varepsilon\to 1^+} \frac{1}{4\pi\mathrm{i}} \oint_{\mathscr{C}} f_\alpha(\lambda/\varepsilon) \frac{\mathrm{d}}{\mathrm{d}\lambda}\left(\log\frac{\lambda+1}{\lambda-1}\right)^2 \mathrm{d}\lambda = \frac{\pi^2}{6}\frac{\alpha+1}{\alpha}, \tag{4.41}$$

that we found in the previous chapter, see (3.23), we conclude that when the system approaches criticality the entanglement entropy behaves like

$$S_{\alpha,X} \sim -c\frac{\alpha+1}{6\alpha} \log |z_{2L} - z_{2L+2}|.$$

The previous reasoning can be straightforwardly extended to situations where different couples of branch points degenerate at the unit circle. For instance $z_{j_\upsilon}, \overline{z}_{j_\upsilon}^{-1} \to u_\upsilon = \mathrm{e}^{\mathrm{i}\theta_\upsilon}$ with $u_\upsilon \neq u_{\upsilon'}$ for $\upsilon \neq \upsilon'$. In this case,

$$S_{\alpha,X} = -\frac{\alpha+1}{12\alpha} \sum_{\upsilon=1}^{R} \log |z_{j_\upsilon} - \overline{z}_{j_\upsilon}^{-1}| + \cdots , \tag{4.42}$$

where the dots represent the contributions that remain finite in the limit $z_{j_\upsilon} \to u_\upsilon$, $\upsilon = 1, \ldots, R$. According to this expression, the entropy should diverge at the critical point, i.e. when $z_{j_\upsilon} = \overline{z}_{j_\upsilon}^{-1}$. The reason for this is that we have taken the asymptotic limit $|X| \to \infty$. The entanglement entropy follows an area law when the theory is non critical. Hence the large size limit renders a finite entropy. However, as we shall see in the next section, this is no longer true when the chain is critical. The area law will be corrected by a term that grows logarithmically with the length $|X|$. Therefore, we may have a finite entropy in the critical theory by restoring the finite size of the interval X.

4.3 Critical chains

Now, let us move on to discuss the case of critical theories. In the generic situation, the mass gap is zero when for some open intervals of $\theta \in [-\pi, \pi)$

$$|F^-(\theta)| > \omega^+(\theta) = \sqrt{F^+(\theta)^2 + |G(\theta)|^2},$$

and the dispersion relation (2.10) becomes negative. The symbol of the ground state correlation matrix (2.40) is now discontinuous at the boundaries of these intervals, i.e. at the Fermi points,

$$\hat{\mathcal{G}}(\theta) = \begin{cases} -I, & \text{if } F^-(\theta) < -\omega^+(\theta), \\ M(\theta), & \text{if } |F^-(\theta)| < \omega^+(\theta), \\ I, & \text{if } F^-(\theta) > \omega^+(\theta). \end{cases} \tag{4.43}$$

Observe that if $\hat{\mathcal{G}}(\theta)$ has a discontinuity at θ it has also another at $-\theta$. Therefore, the discontinuities come in pairs θ, $-\theta$ except those at $\theta = 0$ or $-\pi$.

Employing the general result (4.16) that we have obtained in Section 4.1 for discontinuous symbols, we shall now analyse the different types of discontinuities that we can find when the mass gap is zero and their contribution to the logarithmic term of the entanglement entropy.

The first possibility is when the two lateral limits are $M(\theta)$ and $\pm I$. Obviously, the two limits commute and we can study its contribution analysing the discontinuity in the eigenvalues of the lateral limits. Since $\det M(\theta) = -1$ and $\operatorname{Tr} M(\theta) = 0$, the eigenvalues of $M(\theta)$ are $\mu_1^+ = -1$, and $\mu_2^+ = 1$. Hence only one of the eigenvalues of $M(\theta)$ is different from those of $\pm I$, $\mu_1^- = \mu_2^- = \pm 1$. Employing (4.12), this discontinuity in the symbol $\hat{\mathcal{G}}_\lambda = \lambda I - \hat{\mathcal{G}}$ contributes to the coefficient of the logarithmic term of $\log D_X(\lambda)$ with

$$\begin{aligned} \beta_{MI}(\lambda) &= \frac{1}{4\pi^2} \sum_{j=1}^{2} \left(\log \frac{\lambda - \mu_j^-}{\lambda - \mu_j^+} \right)^2 \\ &= \frac{1}{4\pi^2} \left(\log \frac{\lambda - 1}{\lambda + 1} \right)^2 . \end{aligned}$$

The second kind of discontinuity that we can have is when the lateral limits are I and $-I$. In this case both eigenvalues are different at each side, $\mu_1^{\pm} = \mu_2^{\pm} = \pm 1$, and we get twice the contribution of the previous kind of discontinuity,

$$\beta_{II} = 2\beta_{MI}.$$

Finally, it is also possible that the matrix $M(\theta)$ itself is discontinuous. This may happen when $F^+(\theta)$ and $G(\theta)$ vanish for some values of θ and at least one of them goes linearly to zero. In this case the two lateral limits have opposite sign and the contribution to the coefficient of the logarithmic term is also

$$\beta_{MM} = 2\beta_{MI}.$$

With all these ingredients we can compute the asymptotic behaviour of the determinant for the four archetypical situations sketched in Fig. 4.4.

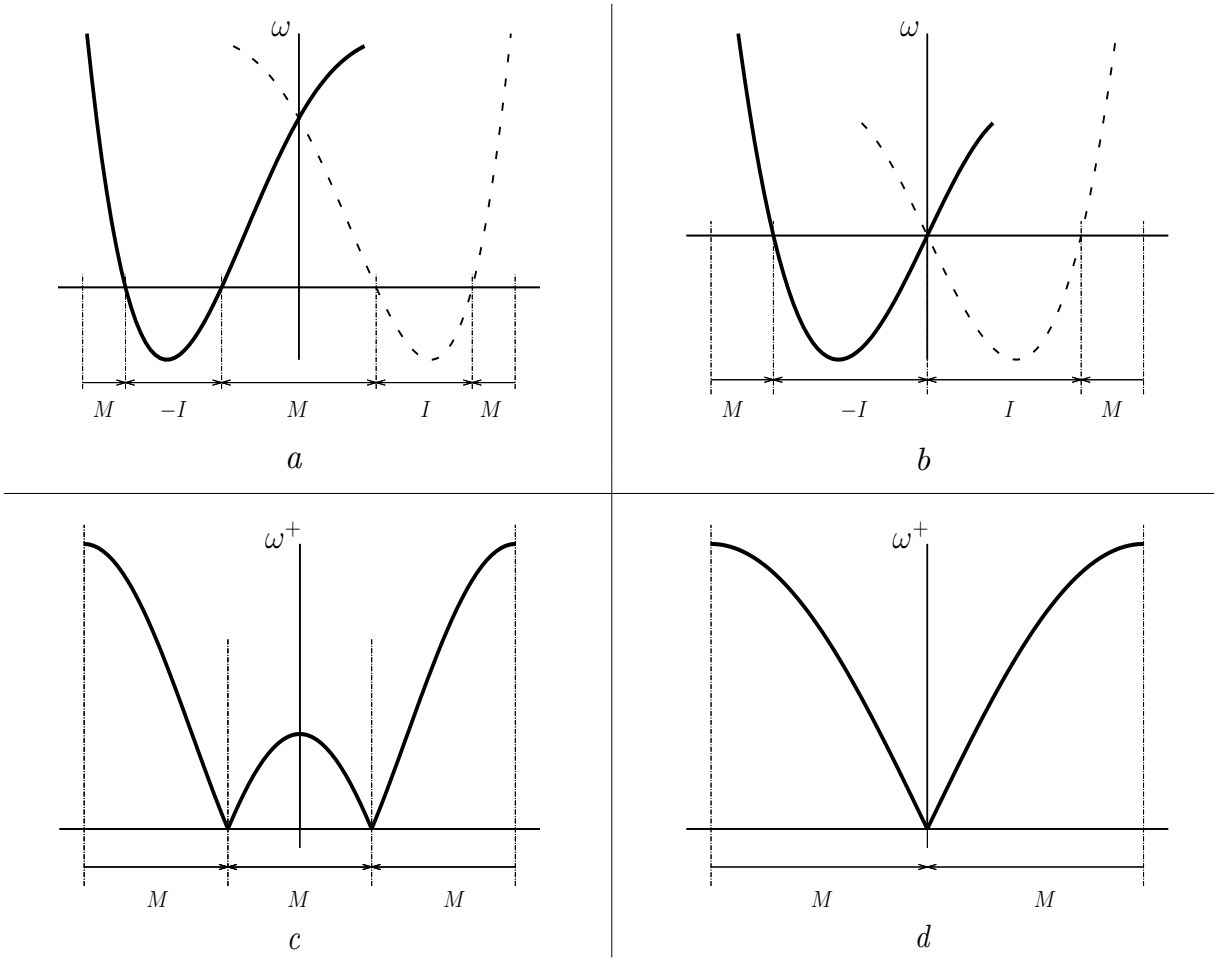

Figure 4.4: Four archetypical discontinuities for the symbol $\hat{\mathcal{G}}(\theta)$ of the ground state correlation matrix. In a and b the dispersion relation $\omega(\theta)$ is represented by the solid curve while the dashed curve depicts $\omega(-\theta)$. In the plots c and d the solid curve stands for $\omega^+(\theta)$. The lines with arrows, right below the plots, mark the angle θ where the discontinuities happen.

In panel a of Fig. 4.4 we represent a double change of sign of the dispersion relation for negative values of θ. From the form (4.43) of the symbol $\hat{\mathcal{G}}$ one can deduce that in

this case it presents four discontinuities of the kind MI, as it is indicated by the arrows below the plot. In this case the coefficient of the logarithmic term in $\log D_X(\lambda)$ is

$$\beta_a = 4\beta_{MI}.$$

In Fig. 4.4 *b* we consider the case in which $\omega(\theta)$ changes its sign at $\theta = 0$ (the case $\theta = -\pi$ is analogous). The symbol has now two discontinuities of the type MI and one II. They give a total contribution

$$\beta_b = 2\beta_{MI} + \beta_{II} = 4\beta_{MI}.$$

In the case *c* of Fig. 4.4 we exemplify the situation in which the symmetric part of the dispersion relation $\omega^+(\theta)$ vanishes at two symmetric modes (different from 0 or $-\pi$). This produces two discontinuities of the type MM that give rise to a logarithmic term in $\log D_X(\lambda)$ with coefficient

$$\beta_c = 2\beta_{MM} = 4\beta_{MI}.$$

It may also happen as in Fig. 4.4 *d* that $\omega^+(\theta)$ vanishes at $\theta = 0$ or $-\pi$. Here we have only a discontinuity of the type MM that contributes to $\log D_X(\lambda)$ with a logarithmic term with coefficient

$$\beta_d = 2\beta_{MI}.$$

Considering simultaneously all the above situations, we conclude that the asymptotic expansion (4.16) of $\log D_X(\lambda)$ is of the form

$$\log D_X(\lambda) = |X| \log(\lambda^2 - 1) + \beta_T \log |X| + O(1),$$

with

$$\beta_T = 2(2n_a + 2n_b + 2n_c + n_d)\beta_{MI} \equiv N_T \beta_{MI}$$

where n_i, $i = a, \ldots, d$, is the number of discontinuities of i-type (see Fig. 4.4).

Introducing this result into the contour integral (2.36) for $S_{\alpha,X}$ and applying the identity (4.41) we finally find that the asymptotic behaviour of the ground state Rényi entanglement entropy is

$$S_{\alpha,X} = N_T \frac{\alpha + 1}{24\alpha} \log |X| + O(1). \tag{4.44}$$

The coefficient of the logarithmic term is similar to that predicted by Conformal Field Theory (1.10) with a central charge $\mathrm{c} = N_T/4$. Notice that the appearance of these discontinuities in the symbol is actually a consequence of the vanishing of the mass gap.

It is interesting to discuss how the discrete symmetries of parity P and charge conjugation C affect the behaviour of the ground state entanglement entropy from the results that we have obtained. Recall that PC is a symmetry when the couplings B_l are real and, therefore, $G(\theta)$ is purely imaginary, something that does not play any role in the analysis of the discontinuities. Therefore, while the PC symmetry is crucial for the computation of the entanglement entropy when there is a mass gap (we do not actually have the solution of the Wiener-Hopf factorisation when PC is broken), it is irrelevant in the critical case.

With the symmetry under parity the situation is reversed. If the theory has a mass gap the vacuum is always parity invariant and this symmetry is irrelevant in the analysis of the entanglement entropy. On the contrary, it is crucial in the case of critical chains.

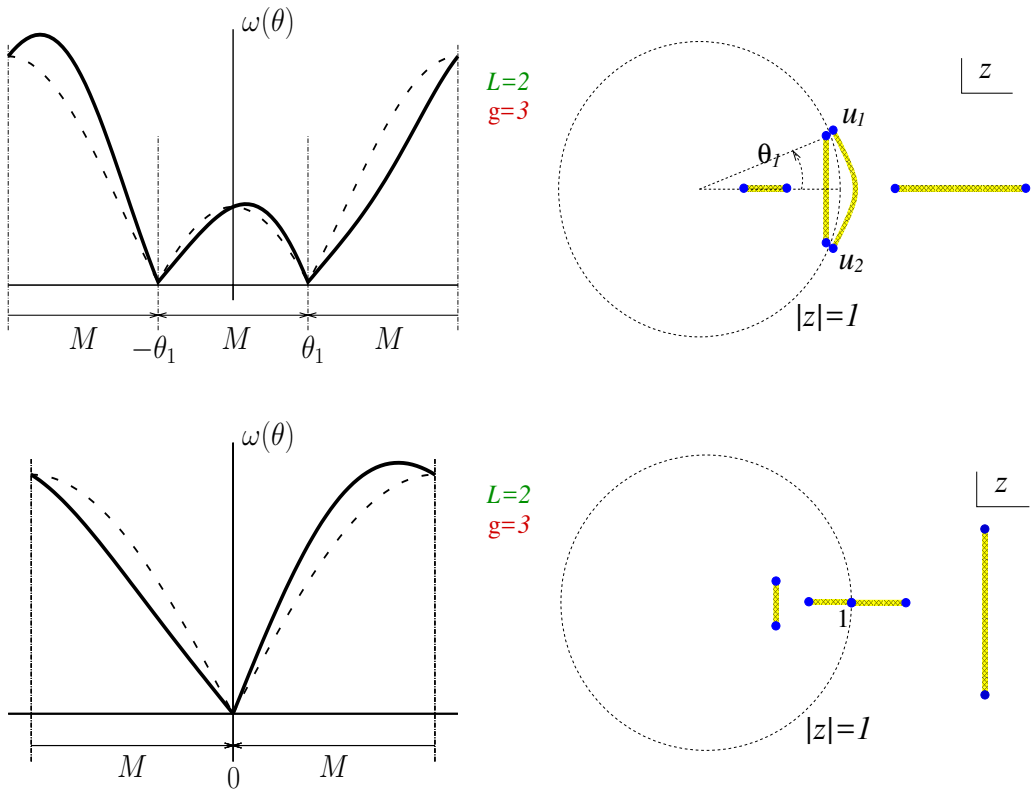

Figure 4.5: In the left panels we represent the dispersion relation (solid line) and its symmetric part (dashed line) of two critical theories whose ground state is the Fock space vacuum $|0\rangle$. As we indicate by the arrows, at the zeros of the dispersion relation the symbol $M(\theta)$ is discontinuous. These critical theories can be reached as the limit of a non critical one. On the right, we represent the disposition of the branch points of the curve $w^2 = P(z)$ in each case. The upper dispersion relation corresponds to a complex pinching of two pairs of branch points related by inversion and complex conjugation. The lower dispersion relation can be reached from a non critical ones by merging two real branch points related by inversion. Notice that the discontinuities of $M(\theta)$ are located at the angles θ_υ in which the pinchings sit at the unit circle, $u_\upsilon = \mathrm{e}^{\mathrm{i}\theta_\upsilon}$.

If the Hamiltonian is P invariant then the antisymmetric part of $\omega(\theta)$ vanishes, and we are restricted to the situations described in Figs. 4.4 *c* and *d*.

In Section 4.2.1, we studied the behaviour of the entanglement entropy of a non critical chain as we approach a critical point. Let us connect the result obtained there with the analysis of the discontinuities performed here.

We investigated the limit to the critical point in terms of the compact Riemann surface described by the curve $w^2 = P(z)$ introduced in Section 4.2. We saw that the theory becomes critical when one or more pairs of roots of $P(z)$, z_{j_υ}, $\overline{z}_{j_\upsilon}^{-1}$, $\upsilon = 1, \ldots, R$, merge at the unit circle, $z_{j_\upsilon} \to u_\upsilon = \mathrm{e}^{\mathrm{i}\theta_\upsilon}$ with $u_\upsilon \neq u_{\upsilon'}$ for $\upsilon \neq \upsilon'$. We found that in this limit the entropy diverges logarithmically as (4.42),

$$S_{\alpha,X} = -\frac{\alpha+1}{12\alpha} \sum_{\upsilon=1}^{R} \log |z_{j_\upsilon} - \overline{z}_{j_\upsilon}^{-1}| + \cdots , \tag{4.45}$$

We arrived at this formula considering $|X| \to \infty$. When the theory is non critical, the symbol of the correlation matrix is smooth and, therefore, the entropy tends to a

constant when $|X|$ is large enough. However, we have seen in this section that the symbol is discontinuous at the critical point, when $z_{j_v} = \overline{z}_{j_v}^{-1}$, and the discontinuities give rise to a logarithmic growth of the entropy with $|X|$. This explains the divergence of (4.45) at the critical point.

In fact, taking the expression (4.22), we have

$$\omega^+(\theta)^2 = F^+(\theta)^2 + |G(\theta)|^2 = |P(\mathrm{e}^{\mathrm{i}\theta})|.$$

Since $u_v = \mathrm{e}^{\mathrm{i}\theta_v}$ is a root of $P(z)$, then $F^+(\theta)$ and $G(\theta)$ vanish at the pinching angles θ_v. Therefore, given the form (4.18) of $M(\theta)$, there is a global change of sign in this matrix at the points θ_v. This means that to each pinching u_v of the Riemann surface it corresponds a discontinuity of the type MM in the symbol $M(\theta)$ at θ_v, as it is illustrated in Fig. 4.5.

According to our previous analysis, a discontinuity of the type MM contributes to the entanglement entropy with a logarithmic term

$$\frac{\alpha+1}{12\alpha}\log|X|.$$

Therefore, if R pairs of roots of $P(z)$ degenerate at the unit circle then $M(\theta)$ has R discontinuities MM. In this case, the entanglement entropy behaves as

$$S_{\alpha,X} = R\frac{\alpha+1}{12\alpha}\log|X| + O(1). \tag{4.46}$$

It is very suggestive the correspondence between this behaviour and that in (4.45). One sees that, up to constant terms, (4.46) is obtained from (4.45) by simply replacing $|z_{j_v} - \overline{z}_{j_v}^{-1}|$ with $|X|^{-1}$.

In the following sections we shall apply the previous general results to several particular fermionic chains.

4.4 Kitaev chain/XY spin chain

We first consider the simplest case of range $L = 1$ with P and C invariance; that corresponds to the Kitaev chain or XY spin chain for spin systems. Therefore, we only have nearest-neighbour real couplings: $A_0 = -h$, $A_1 = 1$ and $B_1 = \gamma$, with h and γ non negative. We already introduced this model in Section 2.2.1. The dispersion relation is

$$\omega_{\mathrm{XY}}(\theta) = \sqrt{(h - 2\cos\theta)^2 + 4\gamma^2\sin^2\theta}.$$

Then the ground state is the Fock space vacuum, $|\hat{\mathbf{K}}\rangle = |0\rangle$. The symbol of its correlation matrix is

$$\hat{\mathcal{G}}(\theta) = M(\theta) = \frac{1}{\omega_{\mathrm{XY}}(\theta)}\begin{pmatrix} -h + 2\cos(\theta) & 2\mathrm{i}\gamma\sin\theta \\ -2\mathrm{i}\gamma\sin\theta & h - 2\cos\theta \end{pmatrix}. \tag{4.47}$$

We obtained that the theory is critical when

$$\gamma = 0 \quad \text{and} \quad h < 2, \tag{4.48}$$

or

$$h = 2. \tag{4.49}$$

Observe that in the case (4.48) the dispersion relation is zero at

$$\theta_1 = \arccos \frac{h}{2} \quad \text{and} \quad \theta_2 = -\theta_1. \tag{4.50}$$

The symbol $\hat{\mathcal{G}}(\theta)$ has two discontinuities of the kind MM at these points like in Fig. 4.4*c*. Therefore, according to (4.44), the entanglement entropy of the ground state behaves with $|X|$ as

$$S^{\mathrm{XX}}_{\alpha,X} = \frac{\alpha+1}{6\alpha} \log |X| + O(1). \tag{4.51}$$

On the other hand, in the line $h = 2$ the dispersion relation vanishes at $\theta = 0$ and the symbol has a single discontinuity at this mode of the type MM similar to that plotted in Fig. 4.4*d*. Therefore, the entanglement entropy is

$$S^{\mathrm{Ising}}_{\alpha,X} = \frac{\alpha+1}{12\alpha} \log |X| + O(1).$$

Comparing these results with the expression for the entanglement entropy given by CFT (1.10) we conclude that the critical line in $\gamma = 0$ corresponds to central charge $\mathrm{c} = 1$ while in the line $h = 2$ the central charge is $\mathrm{c} = 1/2$. It is usual to say that a critical theory with central charge $\mathrm{c} = 1$ belongs to the XX universality class while a theory where $\mathrm{c} = 1/2$ is in the quantum Ising universality class. This agrees with the numerical studies performed by Vidal, Latorre, Rico and Kitaev in [24, 129].

The line $\gamma = 0$ corresponds to the XX spin chain/Tight Binding Model for which the correlation matrix (4.47) is a scalar Toeplitz matrix and we can apply the formulae of the previous Chapter. In particular, since it is a local chain, we can compute its entanglement entropy using the expression in (3.40). In this case the correlation matrix has two discontinuities at the points determined in (4.50). Then (3.40) reduces to

$$S^{\mathrm{XX}}_{\alpha,X} = \frac{\alpha+1}{6\alpha} \log |X| + 2\Upsilon_\alpha + \frac{\alpha+1}{12\alpha} \log[2 - 2\cos(\theta_1 - \theta_2)] + o(1).$$

Taking into account (4.50), we have $2 - 2\cos(\theta_1 - \theta_2) = 4 - h^2$, and

$$S^{\mathrm{XX}}_{\alpha,X} = \frac{\alpha+1}{6\alpha} \log |X| + 2\Upsilon_\alpha + \frac{\alpha+1}{12\alpha} \log(4 - h^2) + o(1), \tag{4.52}$$

where Υ_α is the integral that we introduced in (3.24). This is the result that Jin and Korepin found in their pioneer work [98]. Observe that we obtain the same logarithmic term as in (4.51) as well as the constant term hidden in $O(1)$.

In the line $h = 2$ an interesting point is $\gamma = 1$. For these couplings the Hamiltonian of the XY spin chain (2.21) is Kramers-Wannier self-dual [130]. The Kramers-Wannier transformation maps the 1/2 spin operators σ^ϵ_n ($\epsilon = x, y, z$) to the new set of 1/2 spin operators (see e.g. [131])

$$\hat{\sigma}^x_n = \prod_{l=1}^{n} \sigma^z_l, \quad \hat{\sigma}^z_n = \sigma^x_n \sigma^x_{n+1}, \quad \text{and} \quad \hat{\sigma}^y_n = \mathrm{i}\hat{\sigma}^x_n \hat{\sigma}^z_n.$$

If the Hamiltonian of the spin chain is invariant under this transformation it is said to be Kramers-Wannier self-dual. As it was noted in Ref. [109] by Kádar and Zimborás, the ground state correlation matrix reduces to a scalar Toeplitz matrix when the chain is self-dual. Hence employing the Fisher-Hartwig conjecture one can obtain not only the logarithmic contribution but also the constant term. Kádar and Zimborás applied this fact in the self-dual point $\gamma = 1$, $h = 2$. Adapting their result for any α, the entanglement entropy at this point reads

$$S_{\alpha,X} = \frac{\alpha+1}{12\alpha}\log(4|X|) + \Upsilon_\alpha + o(1).$$

The same result was obtained by Cardy, Castro-Alvaredo and Doyon using field theory methods in [132]. In Section 5.3 of the next Chapter we shall arrive at the same result establishing a relation between the entanglement entropy at this point and that at $\gamma = 0$, $h = 0$. Observe that the logarithmic term matches the one obtained by applying our general method.

With respect to the points (γ, h) outside the critical lines the dispersion relation is strictly positive for any θ. Therefore, the symbol (4.47) is smooth and we are in the case described in Section 4.2. Since the pairing γ is real, we can apply the expression (4.25) for $D_X(\lambda)$ that was actually obtained for this system by Its, Jin and Korepin in [124].

The meromorphic functions $\Phi(z)$ and $\Xi(z)$, see (4.19), are in this case

$$\Phi(z) = \Phi^+(z) = z - h + z^{-1}, \quad \Xi(z) = \gamma(z - z^{-1}). \tag{4.53}$$

Hence the associated compact Riemann surface is described by the elliptic curve

$$w^2 = P(z) = \left[(1+\gamma)z^2 - hz + 1 - \gamma\right]\left[(1-\gamma)z^2 - hz + 1 + \gamma\right]$$

that defines a torus of genus $\mathrm{g} = 1$. The branch points of $w^2 = P(z)$ are

$$z_\pm = \frac{h/2 \pm \sqrt{(h/2)^2 + \gamma^2 - 1}}{1+\gamma} \tag{4.54}$$

and their inverses $z_\pm^{-1}$. The branch points $z_\pm$ are the zeros of the rational function $\mathfrak{g}(z) = (\Phi(z) + \Xi(z))/(\Phi(z) - \Xi(z))$ while $z_\pm^{-1}$ are their poles.

In this case the Riemann theta function in g complex variables reduces to the Jacobi theta function with characteristics in one variable $\vartheta[{}^{\mu}_{\nu}](s|\tau)$ and with the matrix of periods Π replaced by the modulus τ,

$$\tau = \oint_b \mathrm{d}\eta.$$

The holomorphic form $\mathrm{d}\eta$ is in this case

$$\mathrm{d}\eta = \frac{\phi_0 \mathrm{d}z}{\sqrt{P(z)}}$$

where ϕ_0 is a constant that can be fixed using the normalisation condition

$$\oint_a \mathrm{d}\eta = 1.$$

Following the prescription described in Section 4.2, we should take an appropriate order z_1, z_2, z_3, z_4 for the branch points, with z_1 and z_2 lying inside the unit disk and z_3 and z_4 outside it. Then the a cycle is chosen to surround anticlockwise the branch points z_3 and z_4 in the upper Riemann sheet while the b cycle encloses z_2 and z_3 clockwise. According to these considerations,

$$\oint_a \mathrm{d}\eta = 1 \Leftrightarrow 2\int_{z_3}^{z_4} \frac{\phi_0 \mathrm{d}z}{\sqrt{P(z)}} = -1,$$

and the modulus τ can be expressed as the quotient

$$\tau = -\frac{\int_{z_2}^{z_3} \frac{\mathrm{d}z}{\sqrt{P(z)}}}{\int_{z_3}^{z_4} \frac{\mathrm{d}z}{\sqrt{P(z)}}}. \tag{4.55}$$

Legendre showed that the above integrals, with the square root of a quartic polynomial in the denominator, can be reduced to the complete elliptic integral of the first kind

$$I(\kappa) = \int_0^1 \frac{\mathrm{d}t}{\sqrt{(1-t^2)(1-\kappa^2 t^2)}}.$$

In fact, performing the change of variables

$$T(z) = \frac{az+b}{cz+d}, \quad ad - bc = 1, \tag{4.56}$$

that maps the branch points of $w^2 = P(z)$ to

$$T(z_1) = -1/\kappa, \quad T(z_2) = -1, \quad T(z_3) = 1, \quad T(z_4) = 1/\kappa,$$

the integral in the numerator of (4.55) is reduced to

$$\int_{z_2}^{z_3} \frac{\mathrm{d}z}{\sqrt{P(z)}} = \int_{-1}^{1} \frac{\kappa^2 \mathrm{d}t}{\sqrt{(1-t^2)(1-\kappa^2 t^2)}} = 2\kappa^2 I(\kappa).$$

On the other hand, for the integral in the denominator we obtain

$$\int_{z_3}^{z_4} \frac{\mathrm{d}z}{\sqrt{P(z)}} = \int_1^{1/\kappa} \frac{\kappa^2 \mathrm{d}t}{\sqrt{(1-t^2)(1-\kappa^2 t^2)}}.$$

Doing in the latter integral the change of variables $t = [1-(1-\kappa^2)u^2]^{-1/2}$ we arrive at

$$\int_{z_3}^{z_4} \frac{\mathrm{d}z}{\sqrt{P(z)}} = \mathrm{i}\kappa^2 \int_0^1 \frac{\mathrm{d}u}{\sqrt{(1-u^2)(1-(1-\kappa^2)u^2)}} = \mathrm{i}\kappa^2 I(\sqrt{1-\kappa^2}).$$

Then the modulus of the torus is the quotient of the complete elliptic integrals of the first kind

$$\tau = \mathrm{i}\frac{2I(\kappa)}{I(\sqrt{1-\kappa^2})}.$$

The relation between κ and the couplings γ and h can be obtained using the invariance of the cross-ratio of the four branch points under the transformation (4.56). We define the cross-ratio of four points $(z_1, z_2; z_3, z_4)$ as

$$(z_1, z_2; z_3, z_4) = \frac{(z_1 - z_3)(z_2 - z_4)}{(z_1 - z_4)(z_2 - z_3)}. \tag{4.57}$$

Then

$$\frac{1}{\chi^2} \equiv (z_1, z_2; z_3, z_4) = (-1/\kappa, -1; 1, 1/\kappa). \tag{4.58}$$

Therefore,

$$\kappa = \frac{1-\sqrt{1-\chi^2}}{1+\sqrt{1-\chi^2}}.$$

Applying the Landen transformations of the elliptic integrals [92],

$$I\left(\frac{2\sqrt{y}}{1+y}\right) = (1+y)I(y), \quad \text{and} \quad I\left(\frac{1-y}{1+y}\right) = \frac{1+y}{2}I(\sqrt{1-y^2}),$$

we have

$$\tau = \mathrm{i}\frac{2I\left(\frac{1-\sqrt{1-\chi^2}}{1+\sqrt{1-\chi^2}}\right)}{I\left(\frac{2(1-\chi^2)^{1/4}}{1+\sqrt{1-\chi^2}}\right)} = \mathrm{i}\frac{I(\chi)}{I(\sqrt{1-\chi^2})}.$$

Let us introduce the particular cross-ratio

$$x = (z_+, z_-; z_+^{-1}, z_-^{-1}) = \frac{1-(h/2)^2}{\gamma^2}. \tag{4.59}$$

We can distinguish three non-critical regions in the (γ, h) plane depending on the position of the branch points with respect to the unit circle and on their real or complex character. In regions 1a, $0 < x < 1$, and 1b, $x > 1$, the branch points that are the zeros of $\mathfrak{g}(z)$, $z_\pm$, are inside the unit disk while the poles are outside it. In region 1a all the branch points are real while in region 1b all of them are complex. In region 2, $x < 0$, we have one of the poles, z_+^{-1}, and one of the zeros, z_-, inside the unit disk and both are real. In Fig. 4.6 we summarise the disposition of the branch points in each of these regions. Let us take the branch points in the order

$$z_{a-}, z_{a+}, z_{a+}^{-1}, z_{a-}^{-1}, \quad \text{for region 1a,}$$

$$z_{b+}, z_{b-}, z_{b+}^{-1}, z_{b-}^{-1}, \quad \text{for region 1b,}$$

$$z_{2-}, z_{2+}^{-1}, z_{2+}, z_{2-}^{-1}, \quad \text{for region 2.}$$

Observe that the chosen order fulfils in all cases the requirement that the first two branch points are inside the unit disk and the last two outside. Consequently, the assignment of indices ϵ_j is $(+1, +1, -1, -1)$ for the regions 1a, 1b and $(+1, -1, +1, -1)$ for the region 2. Hence the characteristics are $\mu_a = \mu_b = -1/2$, $\nu_a = \nu_b = 0$ for the regions 1a and 1b and $\mu_2 = 0$, $\nu_2 = 0$ in the region 2.

Since the order of the branch points is different, according to (4.58), χ will be different in each region:

- Region 1a

$$(z_1, z_2; z_3, z_4) = (z_-, z_+; z_+^{-1}, z_-^{-1}) = x^{-1}. \tag{4.60}$$

- Region 1b

$$(z_1, z_2; z_3, z_4) = (z_+, z_-; z_+^{-1}, z_-^{-1}) = x.$$

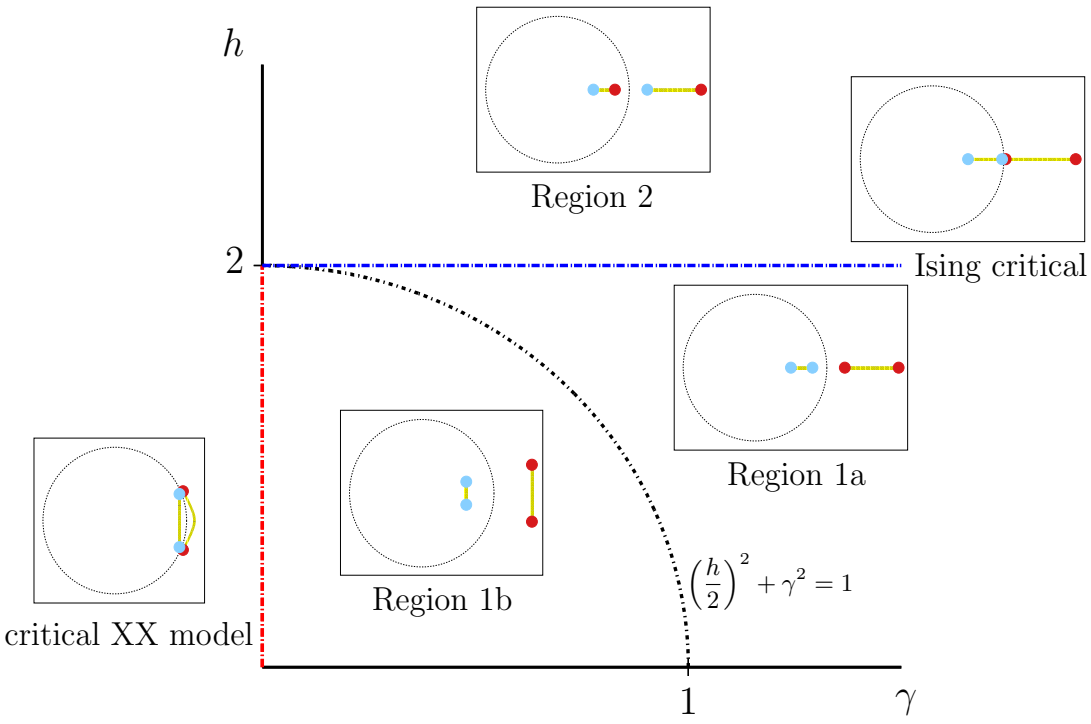

Figure 4.6: Disposition of the branch points of the curve $w^2 = P(z)$ for the XY spin chain in the (γ, h) plane. In the regions 1a, 1b and 2, the model is non-critical and the branch points are not degenerated. In regions 1a and 1b, the branch points • that are the zeros of the rational function $\mathfrak{g}(z)$ are inside the unit disk while their poles • are outside. In region 1a the branch points are real while in region 1b are complex. In region 2 one zero and one pole of $\mathfrak{g}(z)$ are inside the unit disk and they are real. In the critical lines the branch points degenerate at the unit circle producing the discontinuities in the symbol of the correlation matrix. In the critical XX spin chain (that corresponds to central charge c = 1), the two pairs of complex branch points degenerate (complex pinching). In the critical Ising line (for which c = 1/2) only one pair of real roots merges (real pinching).

- Region 2

$$(z_1, z_2; z_3, z_4) = (z_-, z_+^{-1}; z_+, z_-^{-1}) = 1 - x^{-1}.$$

In conclusion, the modulus τ is

$$\tau = \mathrm{i}\frac{I(\chi)}{I(\sqrt{1-\chi^2})}$$

where

$$\chi = \begin{cases} \sqrt{x}, & 0 < x < 1, \quad \text{region 1a}, \\ \sqrt{x^{-1}}, & x > 1, \quad \text{region 1b}, \\ \frac{1}{\sqrt{1-x^{-1}}}, & x < 0, \quad \text{region 2}. \end{cases}$$

Using the above results one can compute the entanglement entropy for the non critical regions employing the expression (4.30) for the von Neumann entropy or (4.31) for integer $\alpha > 1$.

We can explicitly express the entanglement entropy in terms of the cross-ratio x. Let

us start from the contour integral (4.27). Particularising it for genus one, we have

$$\begin{aligned} S_{\alpha,X} &= \lim_{\varepsilon\to 1^+} \frac{1}{4\pi \mathrm{i}} \oint_{\mathscr{C}} f_\alpha(\lambda/\varepsilon) \frac{\mathrm{d}}{\mathrm{d}\lambda} \log\left(\widehat{\vartheta}[\,{}^{\mu}_{\nu}\,](\beta(\lambda))\widehat{\vartheta}[\,{}^{\mu}_{\nu}\,](-\beta(\lambda))\right) \mathrm{d}\lambda + o(1) \\ &= \lim_{\varepsilon\to 1^+} \frac{1}{2\pi \mathrm{i}} \oint_{\mathscr{C}} f_\alpha(\lambda/\varepsilon) \frac{\vartheta'[\,{}^{\mu}_{\nu}\,](\beta(\lambda))}{\vartheta[\,{}^{\mu}_{\nu}\,](\beta(\lambda))} \beta'(\lambda) \mathrm{d}\lambda + o(1), \end{aligned}$$

where the prime denotes derivative. The Jacobi theta function with characteristics has simple zeros at the points of the complex plane $(\nu+1/2+m)+(\mu+1/2+n)\tau$, $m,n\in\mathbb{Z}$. Therefore the integrand of the latter contour integral has poles at the points

$$\lambda_n = \tanh\left[\left(n+\mu+\frac{1}{2}\right)\pi|\tau|\right], \quad n\in\mathbb{Z}.$$

All of them lie on the real interval between ± 1. Therefore, they are enclosed by the contour $\mathscr{C}$. Since the residue of the poles of the logarithmic derivative of $\vartheta[\,{}^{\mu}_{\nu}\,](z)$ is the unity, we have

$$S_{\alpha,X} = \sum_{n\in\mathbb{Z}} f_\alpha(\lambda_n) + o(1). \tag{4.61}$$

Comparing this expression with (2.35), one may deduce that the λ_n's are precisely the eigenvalues of the correlation matrix in the large $|X|$ limit.

In [133] Peschel obtained this series for $\alpha=1$ and was able to sum it in regions 1a and 2. He arrived at (4.61) by realising that the von Neumann entanglement entropy of the XY spin chain is connected with the corner transfer matrices of the triangular Ising model. In [124] Its, Jin and Korepin extended the result for the region 1b and, with Franchini [134], they summed the series for any α. In particular for the von Neumann entropy, $\alpha=1$, it is found that

- Region 1a:

$$S_{1,X} = \frac{1}{6}\left[\log\left(\frac{1-x}{16\sqrt{x}}\right) + \frac{2(1+x)}{\pi} I(\sqrt{1-x}) I(\sqrt{x})\right] + \log 2. \tag{4.62}$$

- Region 1b:

$$S_{1,X} = \frac{1}{6}\left[\log\left(\frac{1-x^{-1}}{16\sqrt{x^{-1}}}\right) + \frac{2(1+x^{-1})}{\pi} I(\sqrt{1-x^{-1}}) I(\sqrt{x^{-1}})\right] + \log 2. \tag{4.63}$$

- Region 2:

$$S_{1,X} = \frac{1}{12}\left[\log\left(16(2-x-x^{-1})\right) + \frac{4(x-x^{-1})}{\pi(2-x-x^{-1})} I\left(\frac{1}{\sqrt{1-x}}\right) I\left(\frac{1}{\sqrt{1-x^{-1}}}\right)\right]. \tag{4.64}$$

Observe that the entanglement entropy only depends on x. This fact was firstly noticed in Ref. [135]. Therefore, the ground states of two theories with the same x have identical entanglement entropy in the large $|X|$ limit. Since

$$x = \frac{1-(h/2)^2}{\gamma^2}$$

the curves of constant x in the (γ, h)-plane are ellipses in the regions 1a and 1b ($x > 0$) and hyperbolas in the region 2 ($x < 0$). In Fig. 4.7 we represent some of them. All these conics intersect at the critical point $\gamma = 0$, $h = 2$, where the entanglement entropy does not have a well-defined limit. For this reason it is called *essential critical point* in Ref. [135]. In the next chapter we shall find the origin of these conics of constant entanglement entropy and we shall study them in more detail and generality.

The curve $x = 1$ corresponds to the Barouch-McCoy circle [74], $(h/2)^2 + \gamma^2 = 1$, that separates regions 1a and 1b. The branch points of the elliptic curve $w^2 = P(z)$ are complex inside this circle (region 1b) and real outside it (region 1a). As it is shown in [75], at the Barouch-McCoy circle the ground state of the XY spin chain is doubly degenerated in two product states. As we know, the entanglement entropy of a product state always vanishes. But according to the above formulae, the von Neumman entanglement entropy along this curve is $\log 2$. The same happens with the Rényi entanglement entropy for any α [134]. The reason is that the ground state of the Kitaev fermionic chain for which we are computing the entanglement entropy is a linear superposition of the two ground states of the XY spin chain. Then $\log 2$ comes from the degeneration. This could also explain the $\log 2$ additive term that appears in the expressions for the von Neumann (and Rényi) entanglement entropy of these regions. The ground state of the XY spin chain is actually doubly degenerated when $h < 2$; that is, in regions 1a and 1b. On the other hand, it is unique for $h > 2$, in region 2, for which the $\log 2$ term does not appear in the expression of the entanglement entropy.

Finally, let us analyse how the entropy behaves when we approach the critical lines, which in the language of the associated Riemann surface means that the torus is pinched, see Fig. 4.6. The XX critical line is reached from the region 1b, where the branch points are complex, when $z_1 - z_4 \to 0$, $z_2 - z_3 \to 0$ (that is a complex pinching). In this limit $x \to \infty$. The Ising critical line can be reached from either region 1a or 2 when $z_2 - z_3 \to 0$. In both regions the branch points are real, so it is a real pinching, and $x \to 0$. In both limiting situations the cross-ratio χ tends to zero, $\chi \to 0$.

Remember that we have taken the a cycle surrounding z_3 and z_4 while the b cycle encircles z_2 and z_3. As we did in Section 4.2.1, it is convenient to study the pinching choosing a homology basis (a', b') in which a' surrounds one of the pairs of merging branch points. This can be achieved by exchanging the a and b cycles, i.e. $(a', b') = (b, -a)$, where the $-$ sign means reversing the orientation of the cycle. Under this modular transformation the modulus changes to, see Appendix C,

$$\tau' = -\tau^{-1},$$

and the normalised Jacobi theta function to

$$\widehat{\vartheta}\left[\begin{smallmatrix}\mu\\ \nu\end{smallmatrix}\right](\beta(\lambda)|\tau) = \mathrm{e}^{\mathrm{i}\pi\beta(\lambda)^2\tau'}\widehat{\vartheta}\left[\begin{smallmatrix}-\nu\\ \mu\end{smallmatrix}\right](-\beta(\lambda)\tau'|\tau'). \tag{4.65}$$

Since [92]

$$I(0) = \frac{\pi}{2}, \quad I(\sqrt{1-\chi^2}) \sim \log\frac{4}{\chi}, \quad \text{when} \quad \chi \to 0,$$

the modulus τ' of the torus diverges as

$$\tau' \sim -\frac{\mathrm{i}}{\pi}\log\frac{\chi^2}{16}.$$

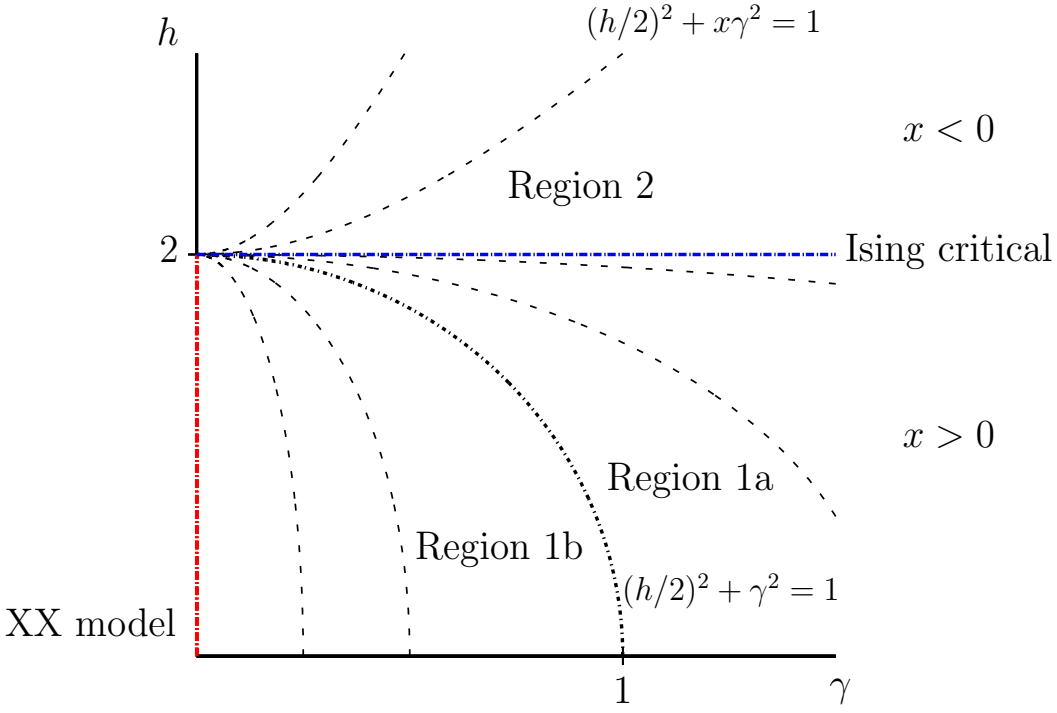

Figure 4.7: Phase diagram of the XY spin chain in the (γ, h) plane. The model is critical when $\gamma = 0$ and $h < 2$ (critical XX model) and when $h = 2$ (critical Ising line). In these lines the entanglement entropy grows logarithmically with the length of the interval X. The central charge in the critical XX chain is $c = 1$ while in the Ising line is $c = 1/2$. In regions 1a, 1b and 2, the system is non critical and in the large $|X|$ limit the entanglement entropy saturates to a constant value. The dashed curves in these regions represent some of the conics $(h/2)^2 + x\gamma^2 = 1$ of constant entanglement entropy. All of them intersect, as well as the critical lines, at $\gamma = 0$, $h = 2$ (essential critical point). The curve for $x = 1$ is the Barouch-McCoy circle that separates regions 1a and 1b.

Putting this together with (4.65) in the contour integral (4.27) of $S_{\alpha,X}$ and applying the identity (4.41) we have that the asymptotic entanglement entropy in the non-critical regions can be expressed in the convenient form

$$S_{\alpha,X} = \frac{\alpha+1}{12\alpha} \log \frac{4^{1/3}|z_1 - z_3||z_2 - z_4|}{|z_1 - z_4||z_2 - z_3|} + \cdots \tag{4.66}$$

where the dots represent terms that vanish when $(z_1 - z_4)(z_2 - z_3) \to 0$.

In the XX critical line, $z_1 = z_4 = u_1 = \mathrm{e}^{\mathrm{i}\theta_1}$ and $z_2 = z_3 = u_2 = \mathrm{e}^{-\mathrm{i}\theta_1}$ where θ_1 is the zero of the dispersion relation, $\theta_1 = \arccos(h/2)$. Then replacing in the above expression $|z_1 - z_3||z_2 - z_4|$ by $|u_1 - u_2|^2 = 4 - h^2$, we have

$$S_{\alpha,X} = -\frac{\alpha+1}{12\alpha} \log |z_1 - z_4||z_2 - z_3| + \frac{\alpha+1}{18\alpha} \log 2 + \frac{\alpha+1}{12\alpha} \log(4 - h^2).$$

If we now substitute in this expression the divergent terms $-\log|z_1 - z_4|$ and $-\log|z_2 - z_3|$ by

$$\log|X| + \frac{12\alpha}{\alpha+1} \Upsilon_\alpha - \frac{1}{3} \log 2, \tag{4.67}$$

we precisely obtain (4.52), the asymptotic entanglement entropy of the critical XX spin chain, including the finite term. The above replacement is universal in the sense that it

is independent from the coupling constants of the theory encoded in the pinchings u_1 and u_2.

Something similar happens for the Ising critical line. In the limit $h = 2$ we have that

$$z_1 = z_4^{-1} = \frac{1-\gamma}{1+\gamma}. \tag{4.68}$$

Replacing this into (4.66) we obtain

$$S_{\alpha,X} = -\frac{\alpha+1}{12\alpha}\log|z_2 - z_3| + \frac{\alpha+1}{12\alpha}\log 4^{\frac{1}{3}}\gamma + \cdots . \tag{4.69}$$

With the tools developed in this chapter we can only deduce the logarithmic term of the entanglement in the line $h = 2$. In the next chapter we shall be able to obtain the finite term too. Anticipating the result, we shall find that

$$S_{\alpha,X} = \frac{\alpha+1}{12\alpha}\log|X| + \Upsilon_\alpha + \frac{\alpha+1}{12\alpha}\log(4\gamma) + o(1),$$

that can be obtained from (4.69) replacing $-\log|z_2 - z_3|$ by

$$\log|X| + \frac{12\alpha}{\alpha+1}\Upsilon_\alpha + \frac{4}{3}\log 2, \tag{4.70}$$

which is also universal but differs by a constant from the replacement for the XX chain.

4.5 XY spin chain with a Dzyaloshinski-Moriya coupling

The XY spin chain has parity symmetry. As we discussed in section 2.2.2, this symmetry is broken by adding a Dzyaloshinski-Moriya (DM) coupling. In the corresponding fermionic chain this introduces an imaginary part s in the hopping term, $A_1 = 1 + \mathrm{i}s$, while the pairing, $B_1 = \gamma$, and the chemical potential, $A_0 = -h$, do not change. Hence in the dispersion relation there is now an antisymmetric part,

$$\omega_{\mathrm{DM}} = \omega^+_{\mathrm{DM}}(\theta) + 2s\sin\theta, \tag{4.71}$$

while the symmetric part ω^+_{DM} coincides with the dispersion relation of the XY/Kitaev spin chain,

$$\omega^+_{\mathrm{DM}}(\theta) = \sqrt{(h - 2\cos\theta)^2 + 4\gamma^2\sin^2\theta}.$$

Since the system breaks parity, the symbol of the ground state correlation matrix,

$$\hat{\mathcal{G}}(\theta) = \begin{cases} -I, & \text{if} \quad 2s\sin\theta < -\omega^+_{\mathrm{DM}}(\theta), \\ M(\theta), & \text{if} \quad |2s\sin\theta| < \omega^+_{\mathrm{DM}}(\theta), \\ I, & \text{if} \quad 2s\sin\theta > \omega^+_{\mathrm{DM}}(\theta), \end{cases}$$

with

$$M(\theta) = \frac{1}{\omega^+_{\mathrm{DM}}(\theta)}\begin{pmatrix} -h + 2\cos\theta & 2\mathrm{i}\gamma\sin\theta \\ -2\mathrm{i}\gamma\sin\theta & h - 2\cos\theta \end{pmatrix},$$

may also present discontinuities like those depicted in the panels a and b of Fig. 4.4.

Introducing $\Delta = s^2 - \gamma^2$, one can show that this model is gapless when

$$\Delta > 0, \quad (h/2)^2 - \Delta < 1, \quad \text{Region A}$$

or when

$$\Delta < 0, \quad h = 2, \quad \text{Region B},$$

In Fig. 4.8 we represent the Regions A and B (actually a line) in the (γ, h) plane for a fixed s.

In Region A the dispersion relation becomes negative in some interval. Hence the energy minimises when all these modes are occupied giving rise to a Dirac sea. In this situation, if $h \neq 2$, the symbol has four discontinuities of the type MI at the Fermi points $\theta_1, \theta_2 \in (-\pi, 0)$ where the dispersion relation changes the sign, as well as at their opposites modes $-\theta_1$, and $-\theta_2$. This corresponds to the situation considered in Fig. 4.4 a. For $h = 2$ one of the Fermi points is at $\theta = 0$. Hence we have two discontinuities of the type MI and one of the type II like in the case represented in the panel b of Fig. 4.4. In both cases, we obtain applying (4.44) that the entanglement entropy of the ground state grows with the length of the interval X as

$$S^{\mathrm{A}}_{\alpha,X} = \frac{\alpha+1}{6\alpha} \log |X| + O(1). \tag{4.72}$$

In the points of Region B the dispersion relation is positive except at $\theta = 0$ where it vanishes. Therefore, along this line the symbol is of the form $\hat{\mathcal{G}}(\theta) = M(\theta)$ and presents a single discontinuity of the type MM at $\theta = 0$. This corresponds to the case considered in Fig. 4.4 d. Then, according to (4.44), the entropy in this region is

$$S^{\mathrm{B}}_{\alpha,X} = \frac{\alpha+1}{12\alpha} \log |X| + O(1). \tag{4.73}$$

In Fig. 4.9 we check numerically the validity of these results for $\alpha = 1$. Observe that, comparing with the expression obtained from CFT (1.10), in Region A the central charge is $\mathrm{c} = 1$ and it lies in the XX universality class, while $\mathrm{c} = 1/2$ in Region B and it belongs to the quantum Ising universality class.

In [109] Kádar and Zimborás noted that the spin Hamiltonian of this model is Kramers-Wannier self-dual at the point $\gamma = 1$, $h = 2$. Hence, as we mentioned before, the correlation matrix can be reduced to a Toeplitz one. Then they obtained the complete asymptotic behaviour of the entropy at this point applying the Fisher-Hartwig conjecture. Adapting their result to our notation, we have

$$S_{\alpha,X} = \begin{cases} \frac{\alpha+1}{6\alpha} \log(2|X|) + \frac{\alpha+1}{24\alpha} \log(1 - s^{-2}) + 2\Upsilon_\alpha, & s > 1, \\ \\ \frac{\alpha+1}{12\alpha} \log(4|X|) + \Upsilon_\alpha, & s \leq 1. \end{cases} \tag{4.74}$$

Outside criticality the dispersion relation is strictly positive. Therefore, the symbol is $\hat{\mathcal{G}}(\theta) = M(\theta)$ and it is always continuous. Observe that $M(\theta)$ does not depend on the

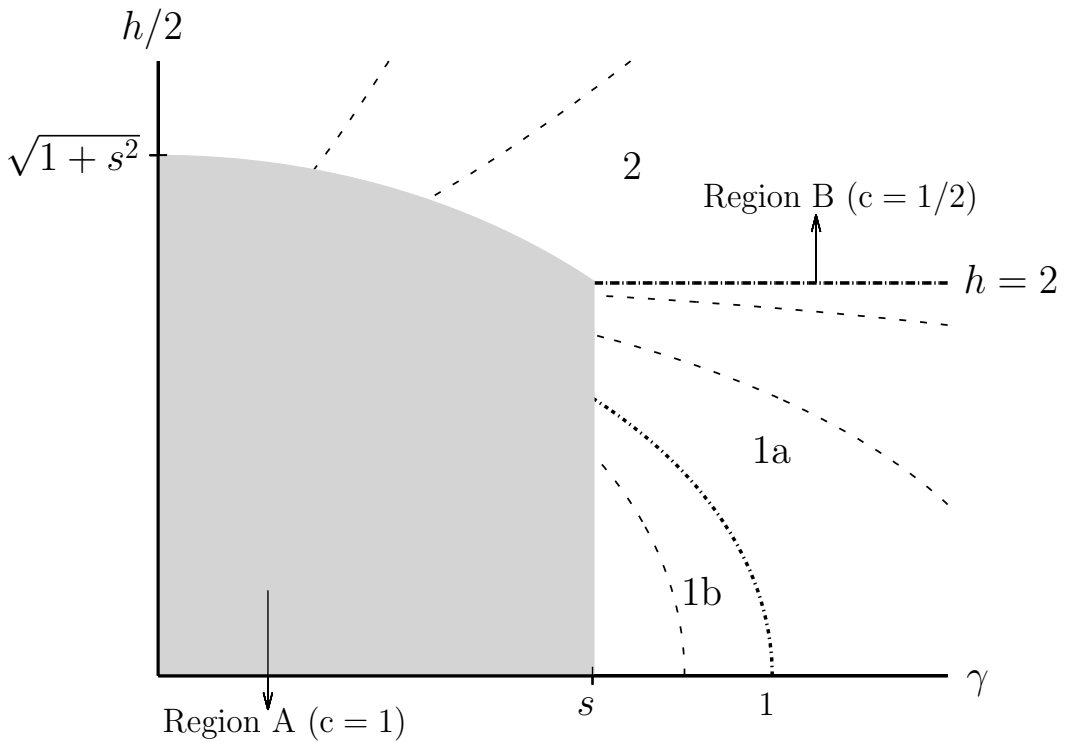

Figure 4.8: Phase diagram for the XY spin chain with a DM coupling in the (γ, h) plane for a fixed s. The shaded Region A is gapless and the central charge is c = 1 (XX universality class) while the dashed line Region B has central charge c = 1/2 (Ising universality class). In the unshaded area, the Hamiltonian has a gap and there are conical curves with the same entropy. The dashed ellipses and hyperbolas depict some of them.

coupling s and it is equal to that of the XY spin chain. Therefore, the formulae obtained for the entanglement entropy in the non critical regions of the XY spin chain apply.

As it happens in the Ising critical line of the XY spin chain, the value of the entanglement entropy diverges logarithmically in the large $|X|$ limit as we approach the critical Region B from 1a and 2, see Fig. 4.8. With respect to Region A its boundary can be reached from inside the critical region or from outside. These two limits are completely different. Inside the critical region the entropy grows logarithmically with $|X|$ and the coefficient of this term is constant throughout all the region. On the contrary, the next term in the asymptotic expansion of entropy, which is finite in the large $|X|$ limit, does change inside the Region A and, as we have numerically seen, it indeed diverges with negative values when reaching the boundary of the region. On the other hand, if we approach Region A from any of the non-critical ones (1a, 1b or 2) we find that the entanglement entropy saturates at a finite value in the limit of large $|X|$, which is different at any point of the boundary but independent of the path (always inside the non-critical region) that we follow to reach the boundary. Recall that in the non-critical regions 1a, 1b and 2 the ground state is the Fock space vacuum $|0\rangle$ of the Bogoliubov modes; the same occurs in the critical Region B where the dispersion relation has a zero but does not change the sign. On the contrary, in Region A the dispersion relation changes its sign and the ground state has the Bogoliubov modes with negative energy occupied (the Dirac sea). The above anomalous behaviour of the entropy near the transition could be a sign of this

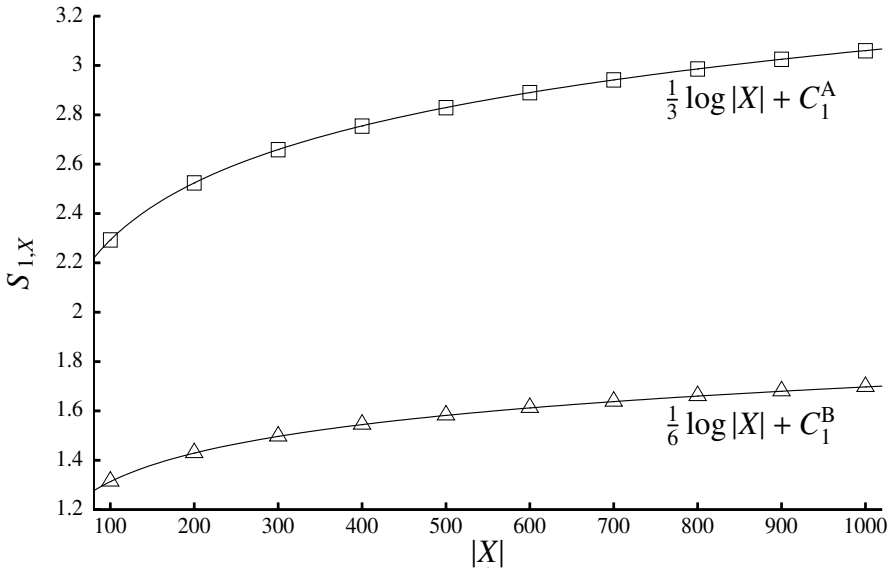

Figure 4.9: Numerical von Neumann entanglement entropy ($\alpha = 1$) for the ground state of the XY spin chain with a DM coupling. The points $\square$ correspond to the theory with $s = 0.75$, $\gamma = 0.5$ and $h = 0.5$, that belongs to Region A. The points $\triangle$ represent the numerical entropy for $s = 0.75$, $\gamma = 1.5$ and $h = 2$, and it is in Region B. The solid lines depict our predictions (4.72) and (4.73) for the logarithmic term of the entanglement entropy in each critical region. The constant term $C_1^{\mathrm{A,B}}$ in each solid curve is obtained by subtracting to the numerical value of the entropy at $|X| = 100$ the expected value of the logarithmic term at this length, i.e. $C_1^{\mathrm{A,B}} = S_{1,100}^{\mathrm{A,B}} - \mathrm{c}/3 \log 100$ with $\mathrm{c} = 1$ for region A and $1/2$ for region B.

discontinuity in the ground state.

From a global point of view, the behaviour of the entanglement entropy in the border of Region A can be interpreted as a blow up of the essential critical point $\gamma = 0$, $h = 2$ of the XY spin chain. The different possible values for the limit of the entropy at that point (for $s = 0$) are obtained at different points of the boundary of Region A for $s \neq 0$ and the essential singularity at $\gamma = 0$, $h = 2$ disappears in this case.

4.6 Long-Range Kitaev chain

In the previous examples there are only nearest-neighbour couplings, and the discontinuities in the symbol are due to the zeros of the dispersion relation, i.e. they have their origin in the absence of mass gap. Their logarithmic contribution to the entanglement entropy can be actually cast in terms of an effective central charge. The presence of long-range interactions may introduce other discontinuities in the symbol that are not related to the mass gap. This implies that the entanglement entropy may grow logarithmically even when the system is non-critical, with a coefficient that may be different from that predicted by CFT.

We shall illustrate this behaviour with the Long-Range Kitaev Chain. As it was defined in Section 2.2.3, it only presents first-neighbour hoppings $A_1 = 1$ while the pairings decay with the distance $B_l = l|l|^{-\delta-1}$ with a dumping exponent $\delta > 0$. It also includes a chemical potential term $A_0 = h$. We showed there that in the thermodynamic limit the dispersion

relation can be expressed in terms of the polylogarithm function Li_δ,

$$\omega_{\mathrm{LRK}}(\theta) = \sqrt{(h + 2\cos\theta)^2 + |G_\delta(\theta)|^2},$$

where $G_\delta(\theta) = \Xi_\delta(\mathrm{e}^{\mathrm{i}\theta})$ and

$$\Xi_\delta(z) = \sum_{l=1}^{\infty}(z^l - z^{-l})l^{-\delta} = \mathrm{Li}_\delta(z) - \mathrm{Li}_\delta(z^{-1}).$$

Since ω_{LRK} has not antisymmetric part, it is non-negative, and the symbol of the ground state correlation matrix is of the form

$$\hat{\mathcal{G}}(\theta) = M(\theta) = \frac{1}{\omega_{\mathrm{LRK}}(\theta)} \begin{pmatrix} h + 2\cos\theta & G_\delta(\theta) \\ -G_\delta(\theta) & -h - 2\cos\theta \end{pmatrix}.$$

As we have done several times in this dissertation, in order to discuss the asymptotic behaviour of the entanglement entropy we should analyse the discontinuities of the symbol. Of course, one source of discontinuities are the zeros of the dispersion relation. In this model the latter only vanishes at $\theta = 0$ for $h = -2$ and at $\theta = -\pi$ for $h = 2$. The lateral limits of $M(\theta)$ at these discontinuities are $\pm\sigma_y$. Both discontinuities are of the type MM and match with the situation represented by the panel d of Fig. 4.4. Therefore, according to (4.44) both contribute to the logarithmic term of the entropy with

$$\frac{\alpha + 1}{12\alpha} \log |X|.$$

Note that this contribution has its origin in the absence of mass gap.

The other possible source of discontinuities are the divergences and the discontinuities of $G_\delta(\theta)$, which encodes the long-range pairings. Taking into account that $\mathrm{Li}_\delta(z)$ diverges for $\delta < 1$ at $z = 1$, $G_\delta(\theta)$ also diverges at $\theta = 0$ for $\delta < 1$ and any value of h. Then the symbol $M(\theta)$ is discontinuous at this point. Since the lateral limits are $\pm\sigma_y$, this discontinuity also contributes to the logarithmic term of the entropy with

$$\frac{\alpha + 1}{12\alpha} \log |X|.$$

If $h = 2$ this contribution must be added to the one coming from the zero of the dispersion relation at $\theta = -\pi$. When $h = -2$ such an addition does not happen as the two discontinuities are actually the same.

When $\delta > 1$ the polylogarithm function converges in the whole unit circle, and the symbol is continuous for any h except at the critical lines $h = \pm 2$.

Summing up all these considerations, we have that for $\delta \neq 1$, the ground state entanglement entropy behaves as

$$S_{\alpha,X} = \frac{\alpha + 1}{6\alpha} \mathrm{c} \log |X| + O(1),$$

with an effective central charge c,

$$\mathrm{c} = \begin{cases} 0, & \delta > 1 \text{ and } h \neq \pm 2, \\ 1/2, & \delta > 1 \text{ and } h = \pm 2 \text{ or } \delta < 1 \text{ and } h \neq 2, \\ 1, & \delta < 1 \text{ and } h = 2. \end{cases}$$

These results are very much compatible with the numerical study performed in Ref. [58] by Ercolessi and collaborators, where the regions with different effective central charge that we determine here appear smeared somehow. We interpret this fact as the consequence of the finite-size corrections to the thermodynamic limit that we are considering here.

A more intriguing behaviour for the entropy is observed when $\delta = 1$. In spite of its physical interest, as it may be experimentally implemented with chains of magnetic impurities on an s-wave superconductor [136], this case had not been considered in the literature until our work [126].

For $\delta = 1$, $\mathrm{Li}_1(z) = -\log(1-z)$. If we take as the branch cut of the logarithm the real interval $[1, \infty)$ then $\Xi_{\delta=1}(z)$ has a branch cut along $[0, \infty)$ and, for any h,

$$G_{\delta=1}(\theta) = \mathrm{i}(\pi - \theta), \quad \theta \in [0, 2\pi)$$

has a discontinuity at $\theta = 0$. Then the symbol $\hat{\mathcal{G}}_\lambda(\theta) = \lambda I - \hat{\mathcal{G}}(\theta)$ has a discontinuity at the same point with lateral limits

$$\hat{\mathcal{G}}^{\pm}_{\lambda,0} = \lambda I - \cos\xi\ \sigma_z \pm \sin\xi\ \sigma_y,$$

where

$$\cos\xi = \frac{h+2}{\sqrt{(h+2)^2+\pi^2}}, \quad \sin\xi = \frac{\pi}{\sqrt{(h+2)^2+\pi^2}}.$$

For $\xi \neq \pi/2$ the lateral limits do not commute. Now we must employ the expression (4.13). According to it, the discontinuity contributes to the coefficient of the logarithmic term of $\log D_X(\lambda)$ with

$$\beta_0(\lambda) = \frac{1}{4\pi^2}\,\mathrm{Tr}[\log \hat{\mathcal{G}}^{-}_{\lambda,0}(\hat{\mathcal{G}}^{+}_{\lambda,0})^{-1}]^2.$$

We have that

$$\hat{\mathcal{G}}^{-}_{\lambda,0}(\hat{\mathcal{G}}^{+}_{\lambda,0})^{-1} = \frac{1}{\lambda^2-1}\left((\lambda^2 - \cos 2\xi)I - 2\lambda\sin\xi\ \sigma_y - \mathrm{i}\sin\xi\ \sigma_x\right).$$

The eigenvalues $\mu_0^{\pm}(\lambda)$ of this matrix can be written in the form

$$\mu_0^{\pm}(\lambda) = \left(\frac{\sqrt{\lambda^2 - \cos^2\xi} \pm \sin\xi}{\sqrt{\lambda^2-1}}\right)^2. \tag{4.75}$$

Notice also that we have

$$\mu_0^{+}(\lambda) = \mu_0^{-}(\lambda)^{-1}. \tag{4.76}$$

Therefore,

$$\begin{aligned}\beta_0(\lambda) &= \frac{1}{4\pi^2}\left[(\log\mu_0^{+}(\lambda))^2 + (\log\mu_0^{-}(\lambda))^2\right] \\ &= \frac{2}{\pi^2}\left(\log\frac{\sqrt{\lambda^2-\cos^2\xi}+\sin\xi}{\sqrt{\lambda^2-1}}\right)^2.\end{aligned}$$

From this we compute the coefficient $\mathcal{B}_{\alpha,0}$ of the contribution of this discontinuity to the logarithmic term of the entanglement entropy. For this purpose we plug $\beta_0(\lambda)$ into the

contour integral (2.36) of $S_{\alpha,X}$,

$$\begin{aligned}\mathcal{B}_{\alpha,0} &= \lim_{\varepsilon\to 1^+}\frac{1}{4\pi\mathrm{i}}\oint_{\mathscr{C}} f_\alpha(\lambda/\varepsilon)\frac{\mathrm{d}\beta_0(\lambda)}{\mathrm{d}\lambda}\mathrm{d}\lambda \\ &= -\lim_{\varepsilon\to 1^+}\frac{1}{2\pi^3\mathrm{i}}\oint_{\mathscr{C}}\frac{\mathrm{d}f_\alpha(\lambda/\varepsilon)}{\mathrm{d}\lambda}\left(\log\frac{\sqrt{\lambda^2-\cos^2\xi}+\sin\xi}{\sqrt{\lambda^2-1}}\right)^2\mathrm{d}\lambda. \qquad (4.77)\end{aligned}$$

Here, as usual, we have performed an integration by parts. The branch cuts of the different multivalued functions involved in the latter integral are depicted in Fig. 4.10.

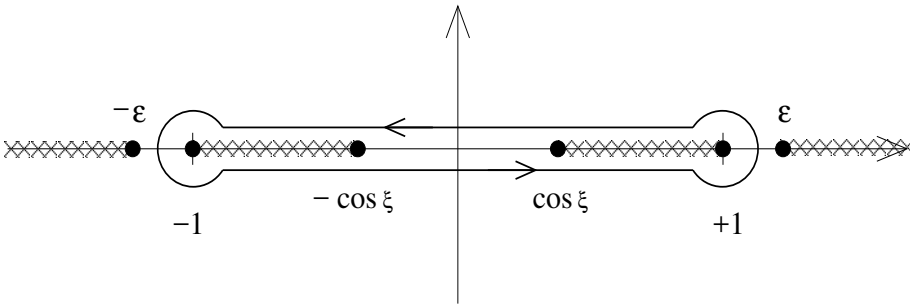

Figure 4.10: Contour of integration and cuts of the integrand in (4.77) for the computation of $\mathcal{B}_{\alpha,0}$. The cuts from $\pm\varepsilon$ to the infinity correspond to $\mathrm{d}f_\alpha(\lambda/\varepsilon)/\mathrm{d}\lambda$ while the cuts inside the contour, $[-1,-\cos\xi]$ and $[\cos\xi,1]$, are due to the other factor of the integrand.

Observe that the integral over the contour $\mathscr{C}$ can be divided into two integrals along curves enclosing respectively the cuts $[-1,-\cos\xi]$ and $[\cos\xi,1]$. Now, we perform the integration along the cuts taking into account the change in the phase of the logarithm of the integrand when we go around the branch points $\pm\cos\xi$ and ±1. Since f_α is an even function, the complex integral can be reduced to the following real one

$$\mathcal{B}_{\alpha,0}=\frac{2}{\pi^2}\int_{\cos\xi}^1\frac{\mathrm{d}f_\alpha(\lambda)}{\mathrm{d}\lambda}\log\frac{\sqrt{1-\lambda^2}}{\sqrt{\lambda^2-\cos^2\xi}+\sin\xi}\mathrm{d}\lambda \qquad (4.78)$$

where we take positive square roots.

Note that for integer $\alpha>1$ we can get an integrated expression for $\mathcal{B}_{\alpha,0}$ following the same strategy as for other integrals that have appeared before (see Sections 3.2 and 4.2). Exploiting again the fact that, for integer $\alpha>1$, $\mathrm{d}f_\alpha/\mathrm{d}\lambda$ is a meromorphic function with poles located at the points of the imaginary axis

$$\lambda_l=\mathrm{i}\tan\frac{(2l-1)\pi}{2\alpha},\quad l=1,\dots,\alpha,\quad l\neq\frac{\alpha+1}{2}, \qquad (4.79)$$

and that the another factor of the integrand is analytic in the whole region outside the contour $\mathscr{C}$, we can send this contour to infinity and reduce the calculation of $\mathcal{B}_{\alpha,0}$ to the computation of the corresponding residues. In this way, we obtain the explicit expression (valid only for integer $\alpha>1$)

$$\mathcal{B}_{\alpha,0}=\frac{1}{\pi^2(\alpha-1)}\sum_{l=1}^{\alpha}\left(\arctan\frac{\sin\xi}{\sqrt{\cos^2\xi+|\lambda_l|^2}}\right)^2.$$

In particular, for $\alpha = 2, 3$, the above expression simplifies to

$$\mathcal{B}_{2,0} = \frac{2}{\pi^2}\left(\arctan\frac{\sin\xi}{\sqrt{\cos^2\xi+1}}\right)^2, \tag{4.80}$$

$$\mathcal{B}_{3,0} = \frac{1}{\pi^2}\left(\arctan\frac{\sin\xi}{\sqrt{\cos^2\xi+1/3}}\right)^2. \tag{4.81}$$

For $h \neq 2$ this is the only discontinuity of $M(\theta)$ in the line $\delta = 1$ and the entanglement entropy is

$$S_{\alpha,X} = \mathcal{B}_{\alpha,0}\log|X| + O(1).$$

However, at $h = 2$ we have to add the contribution of the discontinuity due to the zero of the dispersion relation at $\theta = -\pi$. Hence for $\delta = 1$ and $h = 2$ we have

$$S_{\alpha,X} = \left(\mathcal{B}_{\alpha,0} + \frac{\alpha+1}{12\alpha}\right)\log|X| + O(1).$$

In Fig. 4.11 we check numerically these results for different values of h, including $h = 2$. There is a remarkable agreement between the numerical points and our analytical prediction.

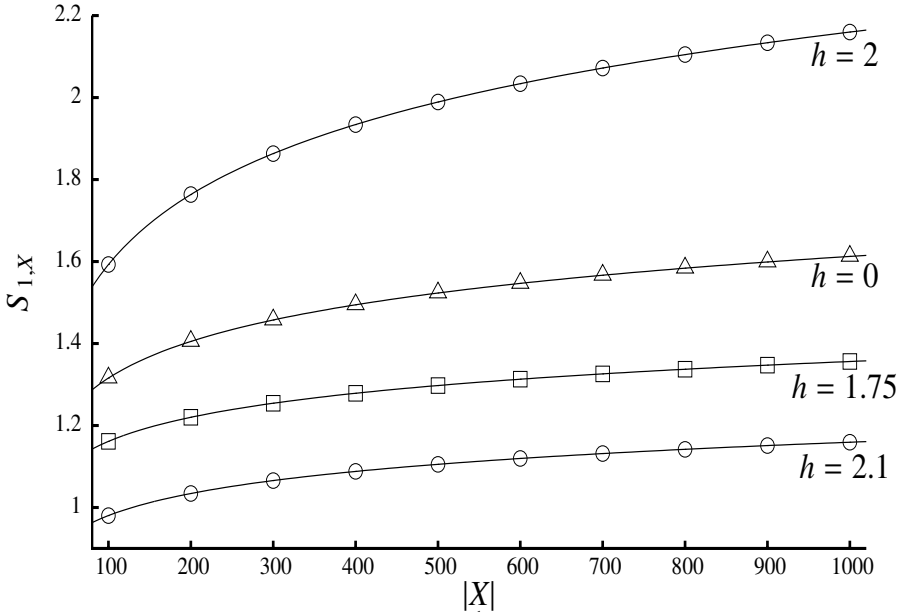

Figure 4.11: Numerical check of the asymptotic scaling of the von Neumann entanglement entropy ($\alpha = 1$) with the length of the interval $|X|$ in the ground state of the Long-Range Kitaev chain (2.26) for $\delta = 1$ and different values of h. The dots represent the numerical computation while the solid lines correspond to the curve $\mathcal{B}_1 \log|X| + \text{constant}$ where $\mathcal{B}_1 = \mathcal{B}_{1,0}$ for $h \neq 2$ and $\mathcal{B}_1 = \mathcal{B}_{1,0} + 1/6$ if $h = 2$, with $\mathcal{B}_{1,0}$ given by (4.78). The constant is determined by subtracting to the numerical value of the entropy for $|X| = 100$ the expected value for the logarithmic term at this length, $\mathcal{B}_1 \log 100$.

In Fig. 4.12 we summarize our results for the coefficient $\mathcal{B}_\alpha$ of the logarithmic term of the entanglement entropy. We have coloured the parameter space (h, δ) according to the value of $\mathcal{B}_\alpha$. The model is critical only in the lines $h = \pm 2$. However, we have found that the entanglement entropy grows logarithmically with $|X|$ for $\delta \leq 1$ and any h, even outside criticality.

As it is discussed in Refs. [58, 59], in the non-critical regions where the entropy grows logarithmically the correlation functions may actually show an algebraic decay with the distance similar to that of the critical ones. This radically differs from systems with finite-range interactions where, outside criticality, the correlation functions decay exponentially and the entanglement satisfies an area law.

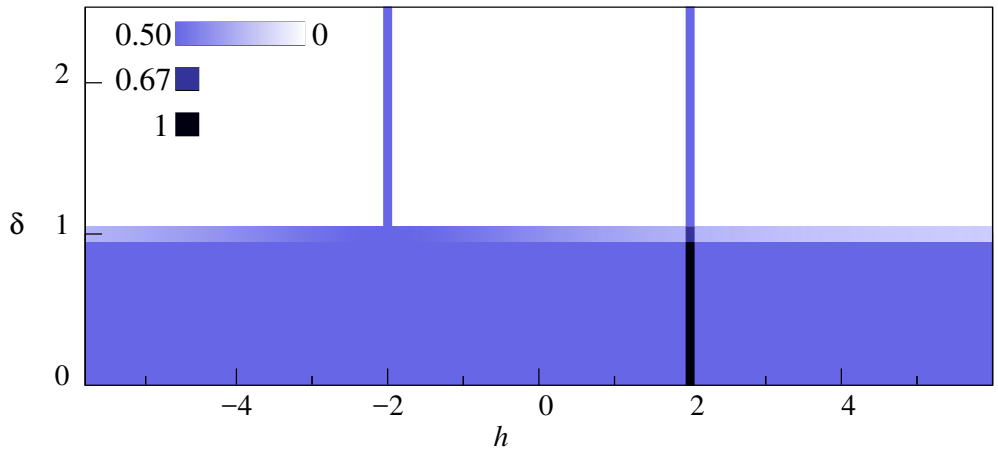

Figure 4.12: Plot of the different regions in the (h, δ) plane of the Long-Range Kitaev chain (2.26) according to the coefficient $\mathcal{B}_2$ of the logarithmic term in the entanglement entropy. The colouring stands for the value of $4\mathcal{B}_2$: from white for $\mathcal{B}_2 = 0$ to black when $4\mathcal{B}_2 = 1$. The intermediate dark blue that corresponds to the point $h = 2$, $\delta = 1$ represents $4\mathcal{B}_2 = \frac{8}{\pi^2} \arctan^2 \frac{\pi}{\sqrt{32+\pi^2}} + \frac{1}{2} \approx 0.67$.

Another striking feature is that in the line $\delta = 1$, the logarithmic term originated by the non commutative discontinuity shows a different dependence on the Rényi exponent α from that given by CFT,

$$\mathcal{B}_\alpha = \frac{\alpha+1}{6\alpha} \mathrm{c}, \tag{4.82}$$

and we cannot associate to it an effective central charge c as it happens with the commutative discontinuities. In fact, observe that (4.82) implies

$$\mathcal{B}_2 = \frac{9}{8} \mathcal{B}_3. \tag{4.83}$$

As it is clear from (4.80) and (4.81) this relation is violated by $\mathcal{B}_{\alpha,0}$, except at the point $h = -2$, where $\xi = \pi/2$ and we have

$$\mathcal{B}_{2,0} = \frac{1}{8}, \quad \mathcal{B}_{3,0} = \frac{1}{9}, \tag{4.84}$$

which fulfil (4.82) with $\mathrm{c} = 1/2$. The reason for this disagreement could be that the couplings of the theory have infinite range and therefore it cannot be related to any local field theory. However, as we have seen, outside $\delta = 1$ all the discontinuities of the symbol are commutative and the relation (4.82) holds, although the theory is still non local.

As a further check of the results that we have obtained, let us consider a variant of the Long-Range Kitaev chain where the discontinuity due to long-range pairings at $\theta = 0$ splits into two, located at $\theta = \pm\phi$. The new discontinuities in the symbol can be obtained

by adding to the Long-Range Kitaev chain (2.26) an oscillatory factor in the pairing,

$$H'_{\rm LRK} = \sum_{n=1}^{N} \left(a_n^\dagger a_{n+1} + a_{n+1}^\dagger a_n + h a_n^\dagger a_n + \sum_{|l|<N/2} \frac{l\cos(l\phi)}{|l|^{\delta+1}} (a_n^\dagger a_{n+l}^\dagger - a_n a_{n+l}) \right) - \frac{Nh}{2} \tag{4.85}$$

with $\phi \in [0, \pi)$.

In the thermodynamic limit the dispersion relation of this model is

$$\omega'_{\rm LRK}(\theta) = \sqrt{(h + 2\cos\theta)^2 + |G_{\delta,\phi}(\theta)|^2},$$

where

$$\begin{aligned} G_{\delta,\phi}(\theta) &= \sum_{l=1}^{\infty} \frac{\cos(l\phi)}{l^\delta} (\mathrm{e}^{\mathrm{i}\theta l} - \mathrm{e}^{-\mathrm{i}\theta l}) \\ &= \frac{1}{2} \left[\mathrm{Li}_\delta(\mathrm{e}^{\mathrm{i}(\phi+\theta)}) - \mathrm{Li}_\delta(\mathrm{e}^{\mathrm{i}(\phi-\theta)}) + \mathrm{Li}_\delta(\mathrm{e}^{-\mathrm{i}(\phi-\theta)}) - \mathrm{Li}_\delta(\mathrm{e}^{-\mathrm{i}(\phi+\theta)}) \right]. \end{aligned}$$

This function vanishes at $\theta = 0$ and $-\pi$. Taking into account the properties of the polylogarithm, it is smooth for $\delta > 1$, diverges at $\theta = \pm\phi$ for $\delta < 1$, and for $\delta = 1$ it reads

$$G_{1,\phi}(\theta) = \begin{cases} -\mathrm{i}(\pi + \theta), & -\pi \le \theta \le -\phi, \\ -\mathrm{i}\theta, & -\phi \le \theta < \phi, \\ \mathrm{i}(\pi - \theta), & \phi \le \theta < \pi. \end{cases}$$

The Hamiltonian $H'_{\rm LRK}$ is gapless for $h = \pm 2$. When $h = -2$ the dispersion relation vanishes at $\theta = 0$ while if $h = 2$ it has a zero at $\theta = -\pi$.

The symbol of the ground state correlation matrix is

$$\hat{\mathcal{G}}'(\theta) = \frac{1}{\omega'_{\rm LRK}(\theta)} \begin{pmatrix} h + 2\cos\theta & G_{\delta,\phi}(\theta) \\ -G_{\delta,\phi}(\theta) & -h - 2\cos\theta \end{pmatrix}.$$

For the lines $h = \pm 2$ the zeros of $\omega'_{\rm LRK}$ produce discontinuities in the symbol at $\theta = 0$ for $h = -2$ and at $\theta = -\pi$ when $h = 2$. The lateral limits of both discontinuities are $\pm\sigma_y$. They are similar to the ones obtained at these lines for $\phi = 0$. Therefore, they contribute to the logarithmic term of the entropy with

$$\frac{\alpha + 1}{12\alpha} \log |X|.$$

For $\delta < 1$ the discontinuities due to the divergences in $G_{\delta,\phi}(\theta)$ are located at $\theta = \pm\phi$. Both discontinuities have lateral limits $\pm\sigma_y$. Therefore, their total contribution to the logarithmic term of the entropy is

$$\frac{\alpha + 1}{6\alpha} \log |X|.$$

If $h \neq \pm 2$ this is the only contribution to the logarithmic term when $\delta < 1$. In the lines $h = \pm 2$ we must also take into account the discontinuity produced by the zero of the dispersion relation.

In conclusion, for $\delta \neq 1$, the ground state entanglement entropy of the modified Long-Range Kitaev chain behaves as

$$S'_{\alpha,X} = \frac{\alpha+1}{6\alpha} \mathrm{c} \log |X| + O(1),$$

with and effective central charge c

$$\mathrm{c} = \begin{cases} 0, & \text{for } \delta > 1 \text{ and } h \neq \pm 2, \\ 1/2, & \text{for } \delta > 1 \text{ and } h = \pm 2, \\ 1, & \text{for } \delta < 1 \text{ and } h \neq \pm 2, \\ 3/2, & \text{for } \delta < 1 \text{ and } h = \pm 2. \end{cases}$$

For $\delta = 1$ the discontinuities of $G_{1,\phi}$ give rise to discontinuities in the symbol $\hat{\mathcal{G}}'_\lambda = \lambda I - \hat{\mathcal{G}}'$ at $\theta = \phi$ with lateral limits

$$\hat{\mathcal{G}}'^{\pm}_{\lambda,\phi} = \lambda I - \cos \xi^{\pm}\, \sigma_z - \sin \xi^{\pm}\, \sigma_y,$$

and at $\theta = -\phi$ with lateral limits

$$\hat{\mathcal{G}}'^{\pm}_{\lambda,-\phi} = \lambda I - \cos \xi^{\mp}\, \sigma_z + \sin \xi^{\mp}\, \sigma_y,$$

where

$$\cos \xi^+ = \frac{h + 2\cos\phi}{\sqrt{(h+2\cos\phi)^2 + (\phi-\pi)^2}}, \quad \sin \xi^+ = \frac{\phi - \pi}{\sqrt{(h+2\cos\phi)^2 + (\phi-\pi)^2}}, \tag{4.86}$$

and

$$\cos \xi^- = \frac{h + 2\cos\phi}{\sqrt{(h+2\cos\phi)^2 + \phi^2}}, \quad \sin \xi^- = \frac{\phi}{\sqrt{(h+2\cos\phi)^2 + \phi^2}}. \tag{4.87}$$

We shall compute separately the contribution of each discontinuity to the coefficient of the logarithmic term of the entanglement entropy. Since the lateral limits do not commute we are bound to apply (4.13). The discontinuity at $\theta = \phi$ contributes to the coefficient of the logarithmic term of $\log D_X(\lambda)$ with

$$\beta_\phi(\lambda) = \frac{1}{4\pi^2} \operatorname{Tr}[\log \hat{\mathcal{G}}'^{-}_{\lambda,\phi} (\hat{\mathcal{G}}'^{+}_{\lambda,\phi})^{-1}]^2.$$

The eigenvalues of $\hat{\mathcal{G}}'^{-}_{\lambda,\phi} (\hat{\mathcal{G}}'^{+}_{\lambda,\phi})^{-1}$ are

$$\mu^{\pm}_\phi(\lambda) = \left(\frac{\sqrt{\lambda^2 - \cos^2(\Delta\xi/2)} \pm \sin(\Delta\xi/2)}{\sqrt{\lambda^2 - 1}} \right)^2,$$

where $\Delta\xi = \xi^+ - \xi^-$. Note that the expression for the eigenvalues is exactly that for the case $\phi = 0$, see (4.75), with the only change of ξ by $\Delta\xi/2$. Therefore, the contribution $\mathcal{B}_{\alpha,\phi}$ of this discontinuity to the coefficient of the logarithmic term in the entanglement entropy can be written as

$$\mathcal{B}_{\alpha,\phi} = \frac{2}{\pi^2} \int_{\cos\frac{\Delta\xi}{2}}^1 \frac{\mathrm{d}f_\alpha(\lambda)}{\mathrm{d}\lambda} \log \frac{\sqrt{1-\lambda^2}}{\sqrt{\lambda^2 - \cos^2(\Delta\xi/2)} + \sin(\Delta\xi/2)} \mathrm{d}\lambda. \tag{4.88}$$

The corresponding integrated expression for integer $\alpha > 1$ reads

$$\mathcal{B}_{\alpha,\phi} = \frac{1}{\pi^2(\alpha-1)} \sum_{l=1}^{\alpha} \left(\arctan \frac{\sin(\Delta\xi/2)}{\sqrt{\cos^2(\Delta\xi/2) + |\lambda_l|^2}} \right)^2 .$$

The contribution of the other discontinuity point, $\theta = -\phi$, can be computed along the same lines. In fact, the only difference with respect to the previous case is that we have to replace ξ^+ and ξ^- by $-\xi^-$ and $-\xi^+$ respectively. Hence $\Delta\xi$ is unchanged and

$$\mathcal{B}_{\alpha,-\phi} = \mathcal{B}_{\alpha,\phi}.$$

Therefore, for $\delta = 1$ and $h \neq \pm 2$, the entanglement entropy behaves as

$$S'_{\alpha,X} = 2\mathcal{B}_{\alpha,\phi} \log|X| + O(1),$$

with $\mathcal{B}_{\alpha,\phi}$ given by (4.88). For $\delta = 1$ and $h = \pm 2$ we have to take into account the discontinuity due to the absence of mass gap that adds an extra term to the logarithmic coefficient,

$$S'_{\alpha,X} = \left(2\mathcal{B}_{\alpha,\phi} + \frac{\alpha+1}{12\alpha} \right) \log|X| + O(1).$$

In Fig. 4.13 we study numerically the behaviour of the entanglement entropy in terms of the length $|X|$ of the interval for different values of h, including the critical point $h = 2$, along the line $\delta = 1$ with $\alpha = 2$ and $\phi = \pi/4$. We find again a full agreement with the analytical result.

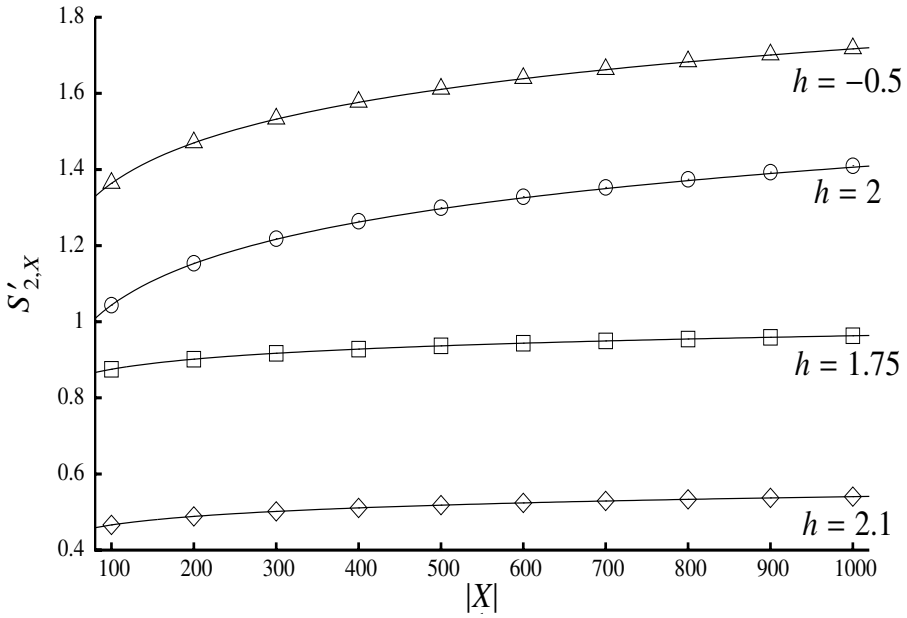

Figure 4.13: Rényi entanglement entropy with $\alpha = 2$ as a function of the length $|X|$ of the interval in the ground state of H'_{LRK}, (4.85), for $\phi = \pi/4$, $\delta = 1$ and different values of h. The dots correspond to the numerical entropy while the solid lines are our analytical prediction $\mathcal{B}'_2 \log|X| + \text{constant}$ with $\mathcal{B}'_2$ that obtained in the text: $\mathcal{B}'_2 = 2\mathcal{B}_{2,\pi/4} + 1/8$ for $h = \pm 2$ and $\mathcal{B}'_2 = 2\mathcal{B}_{2,\pi/4}$ otherwise, with $\mathcal{B}_{2,\pi/4}$ given by (4.88). The constant is the difference between the numerical value of the entropy for $|X| = 100$ and the corresponding value of the logarithmic term at this length, $\mathcal{B}'_2 \log 100$.

Chapter 5

Symmetries of the entanglement entropy

In the previous Chapter we saw that in the space of couplings of the XY spin chain there are ellipses and hyperbolas along which the entanglement entropy of the ground state is constant. This invariance is not only valid for the von Neumann entropy but also for the Rényi entanglement entropy. This fact implies something deeper: the full spectrum of the two-point correlation matrix remains invariant on these curves.

In the works [137] and [138], we noticed that this invariance occurs in more general systems and we traced back its origin. We realised that the group of symmetries of the entanglement entropy in homogeneous quadratic fermionic chains includes a realisation of the Möbius group that acts on the coupling constants of the theory. From this point of view, the conics of constant entropy found for the non critical XY spin chain correspond to the flow of the Möbius group in the space of couplings.

This Chapter is devoted to the study of this new symmetry. We shall consider separately critical and non critical theories. For non critical theories, whether they break or not parity and/or charge conjugation symmetries, we shall show that the spectrum of the ground state two-point correlation matrix is asymptotically invariant under Möbius transformations. Therefore, there are families of non critical theories related by a subgroup of these transformations with the same ground state entanglement spectrum. In critical theories, the entanglement entropy is no longer invariant under Möbius transformations. We shall find that the transformation law of the exponentiated entropy is analogous to that of a product of homogeneous fields inserted at the discontinuities of the correlation matrix. The scaling dimension under the transformation is different depending on whether the ground state is invariant or not under parity.

After the general discussion we shall exploit the Möbius symmetry to find some interesting dualities and results for the ground state entanglement entropy of the XY spin chain with a DM coupling. We shall also apply the results to the Long-Range Kitaev chain.

5.1 Möbius transformations in non critical chains

In this Section we consider the case of a non critical Hamiltonian with finite range of coupling L, for which the dispersion relation (2.10),

$$\omega(\theta) = \sqrt{F^+(\theta)^2 + |G(\theta)|^2} + F^-(\theta), \tag{5.1}$$

is positive for any θ. The ground state is the Fock space vacuum $|0\rangle$, and the two-point correlation matrix (2.41) is

$$V_{nm} = \frac{1}{2\pi}\int_{-\pi}^{\pi} M(\theta)\mathrm{e}^{\mathrm{i}\theta(n-m)}\mathrm{d}\theta, \tag{5.2}$$

with $M(\theta)$ the continuous matrix valued symbol

$$M(\theta) = \frac{1}{\sqrt{F^+(\theta)^2 + |G(\theta)|^2}} \begin{pmatrix} F^+(\theta) & G(\theta) \\ \overline{G(\theta)} & -F^+(\theta) \end{pmatrix}.$$

The first signal of the Möbius invariance in non critical theories comes from the fact that, if PC is a symmetry of the Hamiltonian, the ground state entanglement entropy is expressed in terms of a theta function, as we saw in Section 4.2. The theta function is defined by means of the matrix of periods of a compact Riemann surface described by a hyperelliptic curve that only depends on the couplings A_l, B_l of the theory.

It is a mathematical fact that the only holomorphic one-to-one transformations of the Riemann sphere into itself are the Möbius transformations,

$$z' = \frac{az+b}{cz+d}, \quad \begin{pmatrix} a & b \\ c & d \end{pmatrix} \in SL(2,\mathbb{C}). \tag{5.3}$$

If we perform a Möbius transformation in the Riemann sphere, we move the branch points and the cuts of the hyperelliptic curve, modifying the holomorphic forms. The couplings of the theory must also change since they determine the branch points. However, the matrix of periods is unchanged. Therefore, the theta function does not change and the Rényi entanglement entropy is left invariant.

We can deduce this invariance using a more general and deeper approach based on the existence of a similarity transformation of the correlation matrix when the length of the interval $|X| \to \infty$.

For this purpose, it will be useful to consider the *partition function*,

$$Z_{\alpha,X} = \mathrm{Tr}(\rho_X^\alpha),$$

instead of the entanglement entropy,

$$S_{\alpha,X} = \frac{1}{1-\alpha}\log Z_{\alpha,X}.$$

Consider the relation (2.33) between the entanglement entropy and the restriction of the two-point correlation matrix to the interval, V_X,

$$S_{\alpha,X} = \frac{1}{2(1-\alpha)}\,\mathrm{Tr}\log F_\alpha(V_X),$$

where

$$F_\alpha(\lambda) = \left(\frac{1+\lambda}{2}\right)^\alpha + \left(\frac{1-\lambda}{2}\right)^\alpha. \tag{5.4}$$

Then, applying the identity $\operatorname{Tr}\log F_\alpha(V_X) = \log\det F_\alpha(V_X)$, the partition function can be expressed in terms of the correlation matrix as

$$Z_{\alpha,X} = \det F_\alpha(V_X).$$

Let us also consider the analytic continuation $\mathcal{M}(z)$ of $M(\theta)$ from the unit circle $\boldsymbol{\gamma}$ to the Riemann sphere $\overline{\mathbb{C}}$,

$$\mathcal{M}(z) = \frac{1}{\sqrt{\Phi^+(z)^2 - \Xi(z)\overline{\Xi(\overline{z})}}} \begin{pmatrix} \Phi^+(z) & \Xi(z) \\ -\overline{\Xi(\overline{z})} & -\Phi^+(z) \end{pmatrix}$$

where

$$\Phi(z) = \sum_{l=-L}^{L} A_l z^l, \quad \Xi(z) = \sum_{l=-L}^{L} B_l z^l. \tag{5.5}$$

The matrix $\mathcal{M}(z)$ is meromorphic in the compact Riemann surface determined by the hyperelliptic curve of genus $\mathrm{g} = 2L-1$

$$w^2 = P(z) \equiv z^{2L}(\Phi^+(z)^2 - \Xi(z)\overline{\Xi(\overline{z})}). \tag{5.6}$$

Following the work [124] by Its, Jin and Korepin, we introduce the integral operator

$$K_X\mathbf{v}(z) = \mathbf{v}(z) - \frac{1}{2\pi\mathrm{i}}\oint_{\boldsymbol{\gamma}} \frac{(z/y)^{|X|}-1}{z-y}(I - \mathcal{M}(y))\mathbf{v}(y)\mathrm{d}y, \quad \mathbf{v} \in L^2(\boldsymbol{\gamma})\otimes\mathbb{C}^2,$$

defined on the Hilbert space $L^2(\boldsymbol{\gamma})\otimes\mathbb{C}^2$ with scalar product

$$(\mathbf{v}_1, \mathbf{v}_2) = \frac{1}{2\pi\mathrm{i}}\oint_{\boldsymbol{\gamma}} \mathbf{v}_1(y)^\dagger \mathbf{v}_2(y)\frac{\mathrm{d}y}{y}.$$

In the topology induced by this inner product, K_X is a continuous operator for any $\mathcal{M}$ bounded in $\boldsymbol{\gamma}$ and it fulfils the property

$$\det F_\alpha(V_X) = \det F_\alpha(K_X). \tag{5.7}$$

In the following, we shall prove this fact.

Consider an orthonormal basis in $L^2(\boldsymbol{\gamma})\otimes\mathbb{C}^2$ of the form $\{z^n\mathbf{e}_\nu | n\in\mathbb{Z}, \nu = 1,2\}$, where the vectors $\mathbf{e}_\nu$ are the canonical basis in $\mathbb{C}^2$. Taking into account that the entries of the two-point correlation matrix (5.2) can be expressed in terms of the analytic continuation $\mathcal{M}(z)$ in the form

$$V_{nm} = \frac{1}{2\pi\mathrm{i}}\oint_{\boldsymbol{\gamma}} z^{n-m}\mathcal{M}(z)\frac{\mathrm{d}z}{z},$$

the matrix representation of K_X in this basis is

$$(K_X) = \left(\begin{array}{c|c|c} I & 0 & 0 \\ \hline (V_{na}) & (V_{nm}) & (V_{nb}) \\ \hline 0 & 0 & I \end{array}\right).$$

The different indices are meant to run through the following ranges: $a \leq 0$, $n, m = 1, \ldots, |X|$ and $b > |X|$. Now due to the block form of K_X one has

$$\det F_\alpha(K_X) = \det F_\alpha(I)^2 \cdot \det F_\alpha(V_X).$$

According to the definition (5.4) of F_α, we have $F_\alpha(I) = I$, and we finally obtain the identity (5.7).

The relation between K_X and V_X can be extended to the limit $|X| \to \infty$. We may define the operator

$$K\mathbf{v}(z) = \mathbf{v}(z) + \lim_{\mu \to 1^-} \frac{1}{2\pi \mathrm{i}} \oint_\gamma \frac{I - \mathcal{M}(y)}{\mu z - y} \mathbf{v}(y) \mathrm{d}y, \tag{5.8}$$

where we take the lateral limit for real values of μ smaller than 1. The matrix representation of K in the basis introduced before is

$$(K) = \left(\begin{array}{c|c} I & 0 \\ \hline (V_{na}) & (V_{nm}) \end{array} \right),$$

with $a \leq 0$ and $n, m > 0$.

If we call V the semi-infinite matrix obtained from V_X when $|X| \to \infty$, we can immediately extend the relation (5.7) to this limit and thus we have

$$\det F_\alpha(V) = \det F_\alpha(K).$$

We shall denote by Z_α and S_α the partition function and the entanglement entropy in this limit, $|X| \to \infty$,

$$Z_\alpha = \det F_\alpha(K),$$

$$S_\alpha = \frac{1}{1-\alpha} \log Z_\alpha.$$

We shall proceed now in two steps. First we shall consider general Möbius transformations and check under which circumstances the determinant $Z_\alpha = \det F_\alpha(K)$ is left invariant. In the next step, we shall ask which of these transformations are physical. By physical we mean those transformations that can be implemented as a change in the coupling constants A_l, B_l of the theory.

An arbitrary Möbius transformation (5.3) acts on the Laurent polynomial Φ in (5.5) by

$$\Phi'(z') = (az + b)^{-L} (dz^{-1} + c)^{-L} \Phi(z), \tag{5.9}$$

which is again a Laurent polynomial with monomials of degree between $-L$ and L. Hence, the Möbius transformation can be seen as a change of the couplings from A_l to A'_l. In exactly the same way the Laurent polynomial Ξ with coefficients B_l is transformed to a new Ξ' with coefficients B'_l.

If we use the new Laurent polynomials Φ', Ξ' to get the transformed symbol $\mathcal{M}'$ we obtain

$$\mathcal{M}'(z') = \mathcal{M}(z).$$

Consequently this induces a transformation on the operator K, see (5.8), so that

$$K'\mathbf{v}(z') = \mathbf{v}(z') + \lim_{\mu\to 1^-} \frac{1}{2\pi \mathrm{i}} \oint_\gamma \frac{I - \mathcal{M}'(y')}{\mu z' - y'} \mathbf{v}(y') \mathrm{d}y',$$

where for convenience we use primed integration variable. Let us perform the change of variables $y'(y)$ induced by (5.3),

$$K'\mathbf{v}(z') = \mathbf{v}(z') + \lim_{\mu\to 1^-} \frac{1}{2\pi \mathrm{i}} \oint_{\gamma'} \frac{I - \mathcal{M}(y)}{\mu z' - y'(y)} \mathbf{v}(y'(y)) \frac{\partial y'}{\partial y} \mathrm{d}y, \tag{5.10}$$

where the relation $\mathcal{M}'(y'(y)) = \mathcal{M}(y)$ is used and $\gamma' = \{y : |y'(y)| = 1\}$. The crucial point is to notice that for any Möbius transformation

$$z'(z) - y'(y) = \left(\frac{\partial z'}{\partial z}\right)^{1/2} \left(\frac{\partial y'}{\partial y}\right)^{1/2} (z - y).$$

Plugging this into (5.10) we have

$$K'\mathbf{v}(z'(z)) = \mathbf{v}(z'(z)) + \left(\frac{\partial z'}{\partial z}\right)^{-1/2} \lim_{\mu\to 1^-} \frac{1}{2\pi \mathrm{i}} \oint_\gamma \frac{I - \mathcal{M}(y)}{\mu z - y} \left(\frac{\partial y'}{\partial y}\right)^{1/2} \mathbf{v}(y'(y)) \mathrm{d}y.$$

Here we have assumed that we can safely apply the Cauchy's integral theorem in order to deform γ' into γ, which in particular demands that $\mathcal{M}(y)$ is analytical in a region in which both curves are homotopic as it is illustrated in Fig. 5.1.

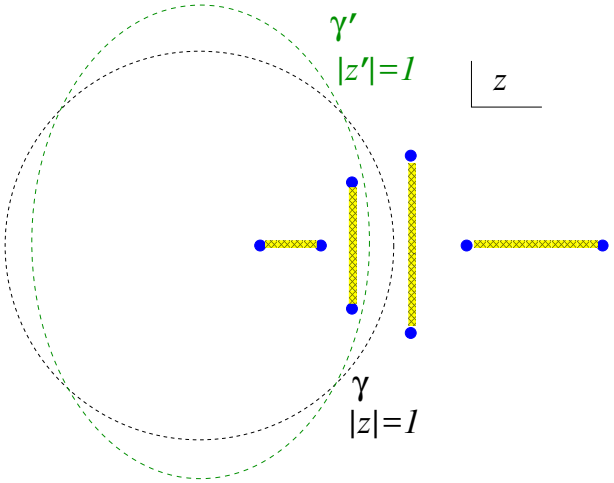

Figure 5.1: The curve γ is the unit circle in the z-plane, $\gamma = \{z : |z| = 1\}$, while γ' is the curve of all the points in the z-plane that are mapped into the unit circle after a Möbius transformation (5.3), $\gamma' = \{z : |z'(z)| = 1\}$. We can deform γ' into γ provided $\mathcal{M}(z)$ is analytic in the region in which γ' and γ are homotopic. This implies that, since $\mathcal{M}(z)$ is meromorphic in the Riemann surface determined by the curve $w^2 = P(z)$, the roots of $P(z)$ cannot sit in the region between γ and γ'.

Finally, defining the transformation

$$T\mathbf{v}(z) = \left(\frac{\partial z'}{\partial z}\right)^{1/2} \mathbf{v}(z'(z)),$$

we obtain

$$TK'\mathbf{v} = KT\mathbf{v}.$$

Therefore, K and K' are related by a similarity transformation and all their spectral invariants coincide. In particular,

$$Z'_\alpha = \det F_\alpha(K') = \det F_\alpha(K) = Z_\alpha.$$

It is important to remark that in order to be able to apply the Cauchy's integral theorem it is necessary not only that $\mathcal{M}(y)$ is analytic but also $\mathbf{v}(y'(y))$ should have this property. On the other hand, in the definition of T we implicitly use analytic continuation for determining $T\mathbf{v}(z)$ for $z \in \gamma$. This implies that we should restrict ourselves to situations in which $\mathbf{v}$ and $K'\mathbf{v}$ are analytic in a region such that γ and its Möbius transformed γ' are homotopic.

Since $\mathcal{M}(z)$ is meromorphic in the Riemann surface represented by the complex curve $w^2 = P(z)$, see (5.6), and $P(z)$ is a polynomial with $4L$ simple roots, the analyticity condition in $\mathcal{M}(z)$ can be satisfied by asking that for any root z_j of $P(z)$ inside (outside) the unit disk its Möbius transformed z'_j has to be also inside (outside).

The previous difficulties do not arise if the Möbius transformation preserves the unit circle γ. In this case, it is of the form

$$z' = \frac{az+b}{\overline{b}z+\overline{a}}, \quad |a|^2 - |b|^2 = 1. \tag{5.11}$$

Then T is a bounded operator and the similarity relation between K and K' holds for any $\mathbf{v} \in L^2(\gamma) \otimes \mathbb{C}^2$.

This is also the case of physical interest. As we shall show now the Möbius transformations associated with changes of the coupling constants of the theory do preserve the unit circle.

In fact, the roots of $P(z)$ satisfy certain properties. In particular, they come in quartets related by inversion and complex conjugation. Therefore, the roots of the transformed polynomial

$$P'(z') = (cz+d)^{-4L} P(z)$$

should come also in quartets: if z'_j is a root of P' then $1/z'_j$ and $\overline{z}'_j$ should be also roots. A way of guaranteeing this is by restricting to those Möbius transformations that commute with inversion and complex conjugation.

The commutation with conjugation restricts $SL(2,\mathbb{C})$ to the transformations that preserve the real line, $SL(2,\mathbb{R}) \rtimes \{I, \mathrm{i}\sigma_x\}$. The first factor in this semidirect product contains the transformations that map the upper half-plane into itself while the second factor is related to the inversion $z' = 1/z$ and maps the upper half-plane into the lower one.

If we further impose that the admissible transformations must commute with the inversion, we are finally left with the group generated by the discrete transformations

$$z' = -z, \quad z' = 1/z,$$

and the 1+1 Lorentz group $SO(1,1)$ whose elements act on the Riemann sphere by

$$z' = \frac{z\cosh\zeta + \sinh\zeta}{z\sinh\zeta + \cosh\zeta}, \quad \zeta \in \mathbb{R}. \tag{5.12}$$

This is precisely the subgroup of Möbius transformations that preserve the unit circle γ and the real line. The connected component of the subgroup, $SO(1,1)$, maps the upper half plane and the unit disk into themselves as it is clear in Fig. 5.2, where we represent the flow of $SO(1,1)$ in the complex plane.

The action of $SO(1,1)$ in $\overline{\mathbb{C}}$ has two fixed points in $z = \pm 1$. Since $z = -1$ is unstable and $z = 1$ is stable, all the flow lines of the transformation depart from the first one and they join in the second one as we sketch in Fig 5.2.

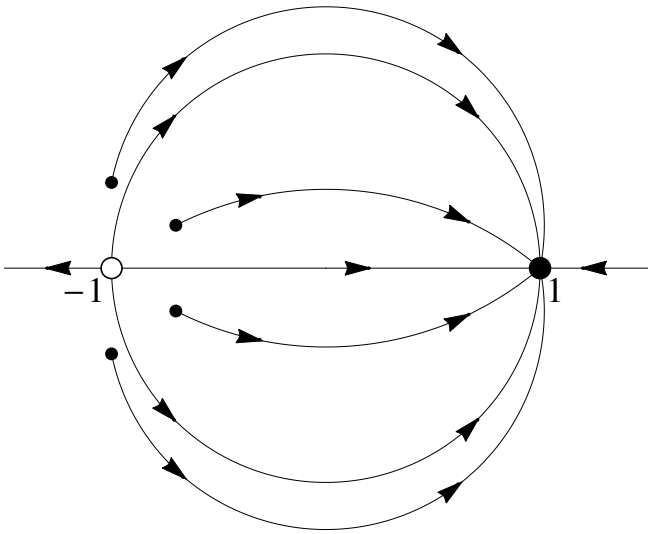

Figure 5.2: Flow of $SO(1,1)$ in $\mathbb{C}$. Note that it preserves the unit circle and the real line and maps the unit disk and the upper/lower half plane into themselves. The points $z = \pm 1$ are the fixed points of the transformation; 1 is stable and -1 unstable.

The induced flow in the space of Hamiltonians leads to a richer picture. There exist $2L + 1$ fixed points whose associated complex curves are

$$w^2 = P(z) \equiv (z-1)^{4L-2j}(z+1)^{2j}, \quad j = 0, \ldots, 2L. \tag{5.13}$$

The only stable one corresponds to $j = 0$. The rest of fixed points have a j-dimensional unstable manifold. Since the roots are degenerated at the unit circle, all these Hamiltonians describe critical theories as we showed in Section 4.2.

The Möbius transformations (5.3) act on the couplings $\mathbf{A} = (A_{-L}, \ldots, A_0, \cdots, A_L)$ and $\mathbf{B} = (B_{-L}, \ldots, B_0, \cdots, B_L)$ like the spin L representation of $SL(2,\mathbb{C})$. We show this in detail in Appendix D. The subset of Möbius transformations that preserve the unit circle and the real line is the only one that maps $\mathbf{A}$, $\mathbf{B}$ to another set $\mathbf{A}'$, $\mathbf{B}'$ that fulfils the hermiticity conditions of the Hamiltonian and the antisymmetry of Ξ': i.e. $A'_{-l} = \overline{A'_l}$ and $B'_{-l} = -B'_l$. In particular, $z' = -z$ corresponds to a change in the sign of the couplings $A'_l = -A_l$, $B'_l = -B_l$. The inversion $z' = 1/z$ acts on the couplings reversing the orientation in the chain $n \leftrightarrow N - n$ and, therefore, $A'_l = \overline{A_l}$, $B'_l = -B_l$.

With respect to the dynamical aspects of these transformations, we may say that they are not a symmetry of the Hamiltonian. In the thermodynamic limit, they act as a

rescaling of the spectrum. Actually, as the admissible Möbius transformations map the unit circle into itself, we may view the transformation as a change in the momentum of the modes together with a rescaling of its energy. More concretely, under $SO(1,1)$ we have that the dispersion relation (5.1) changes as

$$\omega'(\theta') = \left(\frac{\partial\theta'}{\partial\theta}\right)^{L} \omega(\theta), \tag{5.14}$$

where θ' is the image of θ under the transformation

$$\mathrm{e}^{\mathrm{i}\theta'} = \frac{\mathrm{e}^{\mathrm{i}\theta}\cosh\zeta + \sinh\zeta}{\mathrm{e}^{\mathrm{i}\theta}\sinh\zeta + \cosh\zeta},$$

and, therefore,

$$\frac{\partial\theta'}{\partial\theta} = \frac{1}{\sinh 2\zeta\cos\theta + \cosh 2\zeta}.$$

Notice that under the above transformation the dispersion relation $\omega(\theta)$ behaves as a homogeneous field of dimension L, that is, the range of the coupling. We emphasize again that such a transformation can be viewed as a change of the coupling constants of the theory.

Summarising, for a non critical theory the spectral properties of the ground state two-point correlation matrix are asymptotically invariant under the action of the Möbius group. As a by-product of this invariance, the asymptotic behaviour of the Rényi entanglement entropy is unchanged, whenever it is finite. This transformation induces a change in the coupling constants of the fermionic chain. The Möbius transformation is physically admissible if it preserves the unit circle and the real line in the z plane. This includes the 1+1 Lorentz group (5.12). Therefore, there are families of non-critical chains related by this group with the same ground state Rényi entanglement entropy for an interval in the infinite size limit.

5.2 Möbius transformations in critical chains

Our next goal is to extend these results to the case of critical theories. To obtain in the previous section the Möbius invariance we needed to take the limit $|X| \to \infty$. When the system is non critical there is no problem because in this limit the entanglement entropy is finite. However, when the mass gap is zero the symbol of the correlation matrix is discontinuous. As we showed in Section 4.3, these discontinuities give rise to a term in the entropy that grows logarithmically with $|X|$. Therefore, the entropy is divergent in the limit $|X| \to \infty$ and the results obtained above do not apply. The spectrum of the ground state correlation matrix will not be actually invariant under Möbius transformations.

It will be convenient to study separately the critical theories whose ground state is invariant under parity and those with a ground state that breaks this symmetry.

Parity invariant Ground States

Let us start by critical theories whose ground state is invariant under parity. In this case the dispersion relation $\omega(\theta)$ is positive except at some points where it vanishes, like that represented in Fig. 5.3. Therefore, the symbol of the correlation matrix is $\hat{\mathcal{G}}(\theta) = M(\theta)$ with $M(\theta)$ discontinuous at the values of θ for which $\omega(\theta)$ is zero. As we saw in Section 4.3, this kind of critical theories can be reached as the limit of a non critical one when pairs of branch points of the associated hyperelliptic curve $w^2 = P(z)$ merge at the unit circle. We obtained in (4.46) that at the critical point the entanglement entropy has a logarithmic term with a coefficient proportional to the number of pinchings.

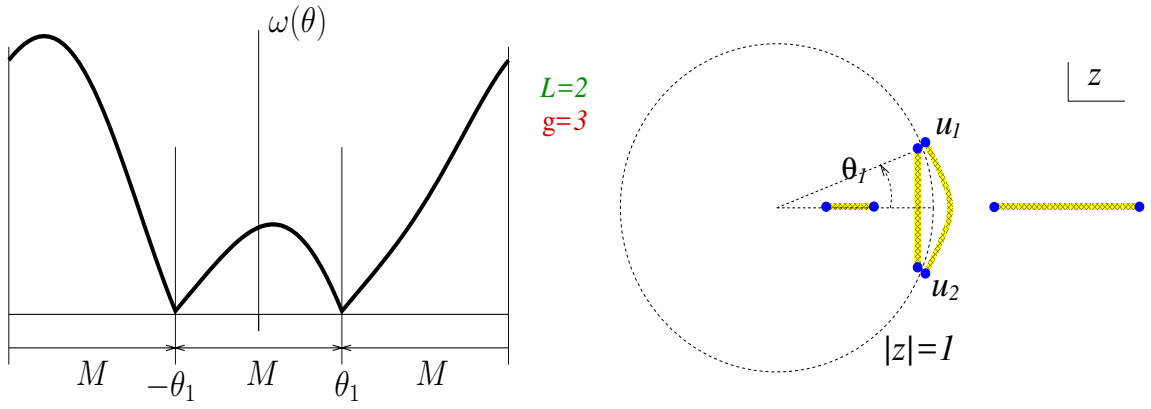

Figure 5.3: On the left, dispersion relation of a critical theory with a parity invariant ground state. It is positive except at the modes $\pm\theta_1$ where it vanishes. As we illustrate on the right, in terms of the compact Riemann surface $w^2 = P(z)$ this theory can be understood as the limit of a non critical one when two pairs of complex roots of $P(z)$ degenerate at the points of the unit circle $u_1 = \mathrm{e}^{\mathrm{i}\theta_1}$ and $u_2 = \overline{u_1} = \mathrm{e}^{-\mathrm{i}\theta_1}$. Then the Riemann surface is pinched.

The difficulty in this case is the following. The logarithmic term of the entropy is well-known and it does not change under Möbius transformations. However, we do not know in general how to compute the finite term that it is non-universal and depends on the values of the coupling constants A_l, B_l. We shall bypass this problem and determine how the entropy behaves under Möbius transformations following two different strategies. On the one hand, we shall consider special cases in which we know the finite term. Then we can easily deduce the behaviour of the entropy under Möbius transformations in these situations. The second strategy is to study the limit to criticality starting from a non-critical theory, for which the Möbius transformations leave the entropy invariant. From the results obtained using these two strategies we will be able to conjecture a transformation law for the entanglement entropy. We cannot prove this conjecture in general but the numerical check will leave no doubt that it is correct.

As we have mentioned, in some special situations we have the complete expression for the asymptotic behaviour of the ground state entanglement entropy. This is the case when $A_l \in \mathbb{R}$ and $B_l = 0$. We studied it in detail in Chapter 3. Since all the pairings B_l are zero, the function $G(\theta)$ vanishes and the matrix $M(\theta)$ is $\pm\sigma_z$. Therefore, the correlation matrix can be reduced to a Toeplitz matrix and we obtained the full asymptotic behaviour of the entropy applying the Fisher-Hartwig conjecture.

For these systems the dispersion relation is $\omega(\theta) = |\Phi(\mathrm{e}^{\mathrm{i}\theta})|$. Therefore the discontinuities of $M(\theta)$ correspond to the roots of $z^L\Phi(z)$ at the unit circle. We shall denote them by $u_\kappa = \mathrm{e}^{\mathrm{i}\theta_\kappa}$, $\kappa = 1, \ldots, R$, in anticlockwise order. Observe that due to the parity invariance, $\Phi(z^{-1}) = \Phi(z)$, and the roots u_κ come in pairs related by inversion. Let us assume that all of them are simple roots. This implies that they are different from ± 1 which are precisely the fixed points of the Möbius transformations in $SO(1,1)$.

In Section 3.3 we obtained that the asymptotic entanglement entropy for that particular symbol is given by the expression (3.40). We can rewrite it in the following convenient way

$$S_{\alpha,X}(\underline{u}) = \frac{(\alpha+1)R}{12\alpha}\log|X| - \frac{\alpha+1}{12\alpha}\sum_{1\le\kappa\neq\upsilon\le R}(-1)^{\kappa+\upsilon}\log|u_\kappa - u_\upsilon| + R\Upsilon_\alpha + o(1). \quad (5.15)$$

Notice that in this case the entanglement entropy and, therefore, the partition function $Z_{\alpha,X}$ depends solely on the set of roots $\underline{u} = (u_1, \ldots, u_R)$.

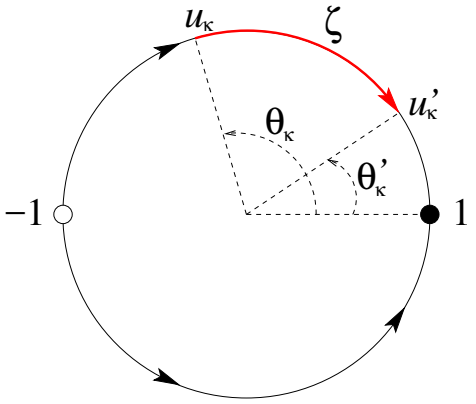

Figure 5.4: Flow of $SO(1,1)$ in the unit circle. The pinchings $u_\kappa = \mathrm{e}^{\mathrm{i}\theta_\kappa}$ of the compact Riemann surface and the corresponding discontinuities θ_κ of the symbol $M(\theta)$ move under a Lorentz transformation following the trajectory indicated by the arrows.

The group $SO(1,1)$ acts on the roots u_κ by

$$u'_\kappa = \frac{u_\kappa\cosh\zeta + \sinh\zeta}{u_\kappa\sinh\zeta + \cosh\zeta}.$$

In Fig. 5.4 we represent the trajectory that the root u_κ follows along the unit circle under the action of $SO(1,1)$.

Now applying any Möbius transformation in $SO(1,1)$

$$u'_\kappa - u'_\upsilon = \left(\frac{\partial u'_\kappa}{\partial u_\kappa}\frac{\partial u'_\upsilon}{\partial u_\upsilon}\right)^{1/2}(u_\kappa - u_\upsilon), \quad (5.16)$$

to the entropy (5.15), we obtain in the asymptotic limit that

$$S'_{\alpha,X}(\underline{u}') = S_{\alpha,X}(\underline{u}) + \frac{\alpha+1}{12\alpha}\sum_{\kappa=1}^{R}\log\frac{\partial u'_\kappa}{\partial u_\kappa}. \quad (5.17)$$

We conjecture that this transformation applies for any finite-range critical Hamiltonian with a ground state invariant under parity. To further motivate the conjecture and gain better understanding of its origin, we shall study the limit to criticality of a symmetric theory.

Let us consider a general finite-range non-critical Hamiltonian with PC symmetry, i.e. $B_l \in \mathbb{R}$ for all l. Criticality in this case is achieved when pairs of branch points of the associated complex curve $w^2 = P(z)$, say z_{j_κ} and $\overline{z}_{j_\kappa}^{-1}$, approach the point u_κ at the unit circle. This corresponds to the pinching of some cycles in the corresponding Riemann surface. We studied this limit in detail in Section 4.2.1. There, we obtained that when the branch points approach a limit point in the unit circle the asymptotic entanglement entropy diverges logarithmically. The result that we found in (4.42) can be expressed as

$$S_\alpha = -\frac{\alpha+1}{12\alpha}\sum_{\kappa=1}^{R}\log|z_{j_\kappa} - \overline{z}_{j_\kappa}^{-1}| + K_\alpha(\underline{u}) + \cdots , \tag{5.18}$$

where we have explicitly included the term $K_\alpha(\underline{u})$ that is finite in the limit $z_{j_\kappa} \to u_\kappa$, $\kappa = 1, \ldots, R$. Here the dots stand for contributions that vanish in the coalescence limit. We have also assumed that $u_\kappa \neq u_\upsilon$ for $\kappa \neq \upsilon$, and we have omitted the explicit dependence on the non degenerated branch points.

Now let us study the behaviour of K_α under an admissible Möbius transformation. We can use the invariance of S_α when the theory is non critical. After performing the transformation

$$S'_\alpha = -\frac{\alpha+1}{12\alpha}\sum_{\kappa=1}^{R}\log|z'_{j_\kappa} - \overline{z}'^{-1}_{j_\kappa}| + K'_\alpha(\underline{u}') + \cdots .$$

Employing now the fact that the transformations in $SO(1,1)$ commute with complex conjugation we have

$$z'_{j_\kappa} - \overline{z}'^{-1}_{j_\kappa} = \frac{\overline{z}'_{j_\kappa}}{\overline{z}_{j_\kappa}}\left|\frac{\partial z'_{j_\kappa}}{\partial z_{j_\kappa}}\right|(z_{j_\kappa} - \overline{z}_{j_\kappa}^{-1}).$$

Since $SO(1,1)$ also commutes with inversion and the points u_κ lie in the unit circle,

$$S'_\alpha = -\frac{\alpha+1}{12\alpha}\sum_{\kappa=1}^{R}\left(\log|z_{j_\kappa} - \overline{z}_{j_\kappa}^{-1}| + \log\frac{\partial u'_\kappa}{\partial u_\kappa}\right) + K'_\alpha(\underline{u}') + \cdots .$$

Therefore, from the invariance of S_α, one has

$$K'_\alpha(\underline{u}') = K_\alpha(\underline{u}) + \frac{\alpha+1}{12\alpha}\sum_{\kappa=1}^{R}\log\frac{\partial u'_\kappa}{\partial u_\kappa}. \tag{5.19}$$

On the other hand, in Section 4.3 we obtained that at the critical point, when $z_{j_\kappa} = \overline{z}_{j_\kappa}^{-1}$, the entropy grows logarithmically with the size $|X|$ of the interval with a coefficient proportional to the number R of pairs of branch points that degenerate,

$$S_{\alpha,X}(\underline{u}) = \frac{(\alpha+1)R}{12\alpha}\log|X| + \mathcal{C}_\alpha(\underline{u}) + o(1). \tag{5.20}$$

The term $\mathcal{C}_\alpha(\underline{u})$ is finite in the limit $|X| \to \infty$. Its explicit expression is not known in general.

Observe that, up to constant terms, (5.20) can be obtained from (5.18) by simply replacing $\log|z_{j_\kappa} - \overline{z}_{j_\kappa}^{-1}|$ with $-\log|X| + \text{constant}$. Let us assume that, as it happened in Section 4.4, the replacement is universal in the sense that the constant does not depend on $\underline{u}$. Then, under Möbius transformations, one has

$$K'_\alpha(\underline{u}') - \mathcal{C}'_\alpha(\underline{u}') = K_\alpha(\underline{u}) - \mathcal{C}_\alpha(\underline{u}).$$

Applying in the latter identity the transformation law (5.19) of $K_\alpha(\underline{u})$, we find that $\mathcal{C}_\alpha(\underline{u})$ should change similarly,

$$\mathcal{C}'_\alpha(\underline{u}') = \mathcal{C}_\alpha(\underline{u}) + \frac{\alpha+1}{12\alpha}\sum_{\kappa=1}^{R}\log\frac{\partial u'_\kappa}{\partial u_\kappa}.$$

This leads to conclude that the change of the entanglement entropy (5.20) under an admissible Möbius transformation is identical to (5.17), that is

$$S'_{\alpha,X}(\underline{u}') = S_{\alpha,X}(\underline{u}) + \frac{\alpha+1}{12\alpha}\sum_{\kappa=1}^{R}\log\frac{\partial u'_\kappa}{\partial u_\kappa}. \tag{5.21}$$

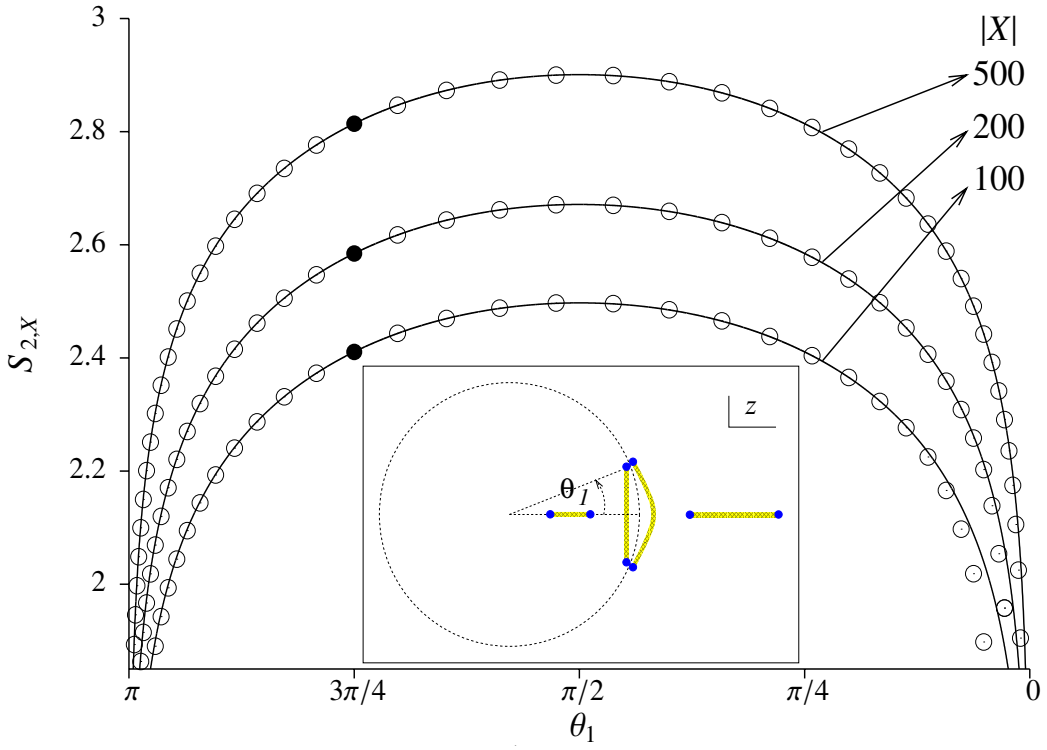

Figure 5.5: Numerical check of the transformation law (5.21) for a critical theory with $L = 2$ and pinchings at $\pm\theta_1$, as we illustrate in the inset. We have computed numerically for several sizes of X the change of the Rényi entanglement entropy for $\alpha = 2$ under $SO(1,1)$, (5.12). The solid line is the conjecture (5.21) expressed in terms of the pinching angle θ_1. The initial value of the entropy is set at $\theta_1 = 3\pi/4$ (filled dot). Under the action of $SO(1,1)$ all the branch points move following the trajectories represented in Fig. 5.2. Observe that the finite size effects are relevant when θ_1 approaches zero. In this case, all the roots of $P(z)$ are close to $z = 1$, the stable fixed point of (5.12).

From the latter expression we have that the partition function changes under an ad-

missible Möbius transformation like

$$Z'_{\alpha,X}(\underline{u}') = \prod_{\kappa=1}^{R} \left(\frac{\partial u'_\kappa}{\partial u_\kappa} \right)^{2\Delta_\alpha} Z_{\alpha,X}(\underline{u}), \tag{5.22}$$

where

$$\Delta_\alpha = \frac{1-\alpha^2}{24\alpha}.$$

Therefore $Z_{\alpha,X}$ transforms like a product of homogeneous fields of dimension $2\Delta_\alpha$ inserted at the pinchings u_κ.

In Fig. 5.5 we check numerically the validity of this transformation. For this purpose, we have considered a critical theory with range of the couplings $L = 2$ and two pinchings ($R = 2$) at the points of the unit circle $u_1 = \mathrm{e}^{\mathrm{i}\theta_1}$ and $u_2 = \overline{u}_1$ as we have depicted in the inset. In Appendix A we explain the techniques applied to calculate numerically the entanglement entropy, in particular we discuss the way to implement the branch cuts of $\mathcal{M}(z)$ and the pinchings of the Riemann surface.

Ground States breaking parity symmetry

We have arrived at the previous conjecture considering that the critical theory is the limit of a non critical one. However, there are cases in which this is not possible. Suppose a theory with a non parity invariant ground state like the one represented in Fig. 5.6. The dispersion relation $\omega(\theta)$ is negative for some intervals of θ. In the ground state all the modes with negative energy are occupied and the Dirac sea breaks the parity symmetry of the vacuum. A dispersion relation that takes negative values cannot be interpreted as the limit of a non critical one. Therefore, we must adopt another strategy in order to analyse the behaviour of the ground state entanglement entropy under admissible Möbius transformations.

In (5.22) the scaling dimension of the partition function under a Möbius transformation is related to the coefficient of the logarithmic term of the entanglement entropy. This coefficient is associated to the discontinuities of the symbol M due to the degeneration of branch points of $w^2 = P(z)$ at the unit circle. Let us examine the implications of applying this relation with full generality.

In Section 4.3 we studied in detail the different types of discontinuities that appear when the theory is critical as well as their contribution to the coefficient of the logarithmic term of the entropy. We saw that the discontinuities produced by the pinchings correspond to a global change of sign in $M(\theta)$. But when the ground state breaks parity invariance the discontinuities are of different type. In fact, remember that in this case,

$$\hat{\mathcal{G}}(\theta) = \begin{cases} -I, & \text{if } F^-(\theta) < -\omega^+(\theta), \\ M(\theta), & \text{if } |F^-(\theta)| < \omega^+(\theta), \\ I, & \text{if } F^-(\theta) > \omega^+(\theta), \end{cases}$$

with $\omega^+(\theta) = (\omega(\theta) + \omega(-\theta))/2$. In the case of Fig. 5.6 the symbol changes from $M(\theta)$ to $-I$ at the points where $\omega(\theta)$ changes its sign, i.e. at the Fermi momenta, θ_1, θ_2, and from $M(\theta)$ to I at their opposite values, $-\theta_1$, $-\theta_2$.

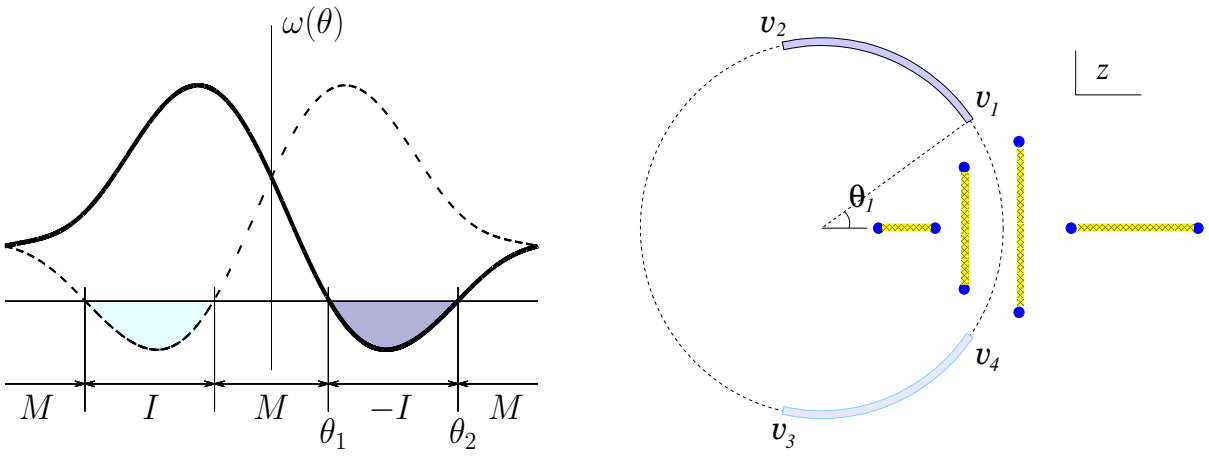

Figure 5.6: On the left, we represent the dispersion relation $\omega(\theta)$ (solid line) and its reflection $\omega(-\theta)$ (dashed line) for a critical theory with a ground state that breaks parity. In the ground state all the modes for which $\omega(\theta) < 0$ are occupied. The symbol $\hat{\mathcal{G}}(\theta)$ changes from M to $-I$ at the Fermi momenta θ_1 and θ_2 and from M to I at $-\theta_2$ and $-\theta_1$. On the right, we represent the corresponding z-plane of this theory. The dots $\bullet$ are the branch points of the curve $w^2 = P(z)$ that in this case are not degenerated. The points in the unit circle $v_1 = \mathrm{e}^{\mathrm{i}\theta_1}$, $v_2 = \mathrm{e}^{\mathrm{i}\theta_2}$, and their complex conjugates, $v_3 = \overline{v}_2$ and $v_4 = \overline{v}_1$ correspond to the discontinuities of the symbol. The transformation law (5.23) under $SO(1,1)$ of $Z_{\alpha,X}$ has insertions at these points.

We obtained there that a discontinuity from M to $\pm I$ gives a contribution to the coefficient of the logarithmic term of the entropy that is half of that corresponding to a global change of sign $\pm M$. Then, using the connection between the contribution to the logarithmic term and the scaling dimension under admissible Möbius transformations discussed above, we conjecture that the insertions related to the discontinuities from M to $\pm I$ have half the dimension of the discontinuities $\pm M$.

Let us call $v_\sigma = \mathrm{e}^{\mathrm{i}\theta_\sigma}$, $\sigma = 1, \ldots, Q$, the points of the unit circle that correspond to the Fermi momenta and their opposites, where the discontinuities from M to $\pm I$ take place. According to the above discussion, if we add them to the pinchings u_κ, the behaviour (5.22) under admissible Möbius transformations of the partition function should be modified to

$$Z'_{\alpha,X}(\underline{u}', \underline{v}') = \prod_{\kappa=1}^{R} \left(\frac{\partial u'_\kappa}{\partial u_\kappa} \right)^{2\Delta_\alpha} \prod_{\sigma=1}^{Q} \left(\frac{\partial v'_\sigma}{\partial v_\sigma} \right)^{\Delta_\alpha} Z_{\alpha,X}(\underline{u}, \underline{v}). \tag{5.23}$$

We emphasize again that the scaling dimension Δ_α of the insertions v_σ is half of the dimension $2\Delta_\alpha$ of the points u_κ. This property differentiates the parity invariant ground states from those that are not.

In Fig. 5.7 we check numerically the validity of this expression for a critical theory with a dispersion relation like that represented in Fig. 5.6.

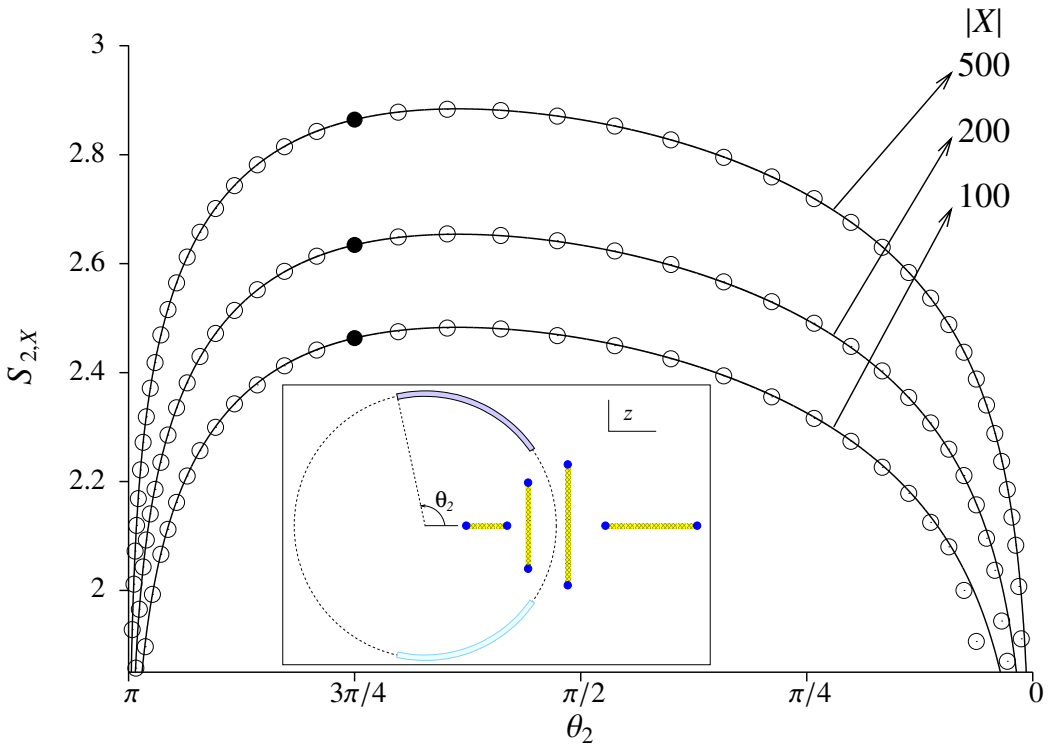

Figure 5.7: Numerical check of the transformation (5.23) for a critical theory with $L = 2$ and a dispersion relation like that in Fig. 5.6. We plot the Rényi entanglement entropy with $\alpha = 2$ for different lengths of X as a function of the Fermi momentum θ_2 under the $SO(1,1)$ group, (5.12). The solid lines represent our conjectured transformation (5.23) expressed in terms of θ_2. The initial value of the entropy is set at $\theta_2 = 3\pi/4$ and $\theta_1 = \pi/2$ (filled dots). Observe that the finite size effects are relevant when θ_2 approaches zero. In this case, all the roots of $P(z)$ are close to $z = 1$, the stable fixed point of (5.12).

The transformation in (5.23) covers the most general behaviour under admissible Möbius transformations of the entanglement entropy for an interval in the ground state of a quadratic, homogeneous fermionic chain with finite range couplings. We shall generalise it to infinite-range Hamiltonians in Section 5.5 and to subsystems composed of several disjoint intervals in the following Chapter. But before going into generalisations, we shall illustrate the previous results with their application to some examples.

5.3 Application to the XY spin chain

First we are going to study the consequences of the Möbius symmetry in the Kitaev/XY spin chain. In this system $L = 1$ and $A_0 = -h$, $A_1 = 1$ and $B_1 = \gamma$ with h, γ real and non negative. In Section 2.2.1 we solved this model and in Section 4.4 we discussed in detail the entanglement entropy of the ground state.

Since $L = 1$ the corresponding compact Riemann surface (5.6) is a torus described by the elliptic curve

$$w^2 = P(z) \equiv z^2(\Phi^+(z) + \Xi(z))(\Phi^+(z) - \Xi(z)),$$

with

$$\Phi^+(z) = \Phi(z) = z - h + z^{-1}, \quad \Xi(z) = \gamma(z - z^{-1}).$$

The roots of $P(z)$ are the points

$$z_\pm = \frac{h/2 \pm \sqrt{(h/2)^2 + \gamma^2 - 1}}{1+\gamma} \tag{5.24}$$

and their inverses $z_\pm^{-1}$. The points $z_\pm$ are the zeros of the rational function $\mathfrak{g}(z) = (\Phi(z) + \Xi(z))/(\Phi(z) - \Xi(z))$ while the inverses $z_\pm^{-1}$ are its poles.

If we now apply a transformation in $SO(1,1)$ they change as

$$z'_\pm = \frac{z_\pm \cosh\zeta + \sinh\zeta}{z_\pm \sinh\zeta + \cosh\zeta}, \tag{5.25}$$

and similarly for the inverses. This induces the following transformation in the couplings γ, h of the theory

$$\gamma' = \frac{\gamma}{(h/2)\sinh 2\zeta + \cosh 2\zeta}, \quad h'/2 = \frac{(h/2)\cosh 2\zeta + \sinh 2\zeta}{(h/2)\sinh 2\zeta + \cosh 2\zeta}. \tag{5.26}$$

According to our discussion in Section 5.1, when the theory is non-critical the entanglement entropy should be invariant under the above transformations. This implies that the asymptotic expansion of the determinant $D_X(\lambda) = \det(\lambda I - V_X)$, from which we derived the entropy using (2.36), should only depend on the branch points of $w^2 = P(z)$ through Möbius invariant functions. Since in this case we have just four branch points, any Möbius invariant function must depend on the cross-ratio of such four points.

In fact, for the non critical XY spin chain the Riemann theta functions that appear in the asymptotic expansion (4.25) of $D_X(\lambda)$ particularise to Jacobi theta functions,

$$\log D_X(\lambda) = |X| \log(\lambda^2 - 1) + \log\left(\widehat{\vartheta}[{}^{\mu}_{\nu}](\beta(\lambda)\,|\tau)\widehat{\vartheta}[{}^{\mu}_{\nu}](-\beta(\lambda)\,|\tau)\right) + o(1), \tag{5.27}$$

where τ is the modulus of the torus. In Section 4.4 we obtained that

$$\tau = \mathrm{i}\frac{I(\chi)}{I(\sqrt{1-\chi^2})} \tag{5.28}$$

where χ is precisely given by the cross-ratio of the four branch points

$$x = (z_+, z_-; z_+^{-1}, z_-^{-1}) = \frac{1-(h/2)^2}{\gamma^2} \tag{5.29}$$

such that

$$\chi = \begin{cases} \sqrt{x}, & 0 < x < 1, \quad \text{region 1a}, \\ \sqrt{x^{-1}}, & x > 1, \quad \text{region 1b}, \\ \frac{1}{\sqrt{1-x^{-1}}}, & x < 0, \quad \text{region 2}. \end{cases}$$

provided we take the branch points in the order

$$z_{a-}, z_{a+}, z_{a+}^{-1}, z_{a-}^{-1}, \quad \text{for region 1a},$$

$$z_{b+}, z_{b-}, z_{b+}^{-1}, z_{b-}^{-1}, \quad \text{for region 1b},$$

$$z_{2-}, z_{2+}^{-1}, z_{2+}, z_{2-}^{-1}, \quad \text{for region 2}.$$

We assign an index $+1$ or -1 to each branch point whether it is a zero or a pole of $\mathfrak{g}(z)$. According to the above order, the assignment is $(+1,+1,-1,-1)$ in regions 1a and 1b and $(+1,-1,+1,-1)$ in region 2. This determines the characteristics of the Jacobi theta function. They are $\mu_a = \mu_b = -1/2$, $\nu_a = \nu_b = 0$ in the regions 1a, 1b and $\mu_2 = 0$, $\nu_2 = 0$ in the region 2.

Therefore, the fact that the Rényi entanglement entropy depends solely on the parameter x can be derived as a consequence of the Möbius invariance that we uncover in this Chapter.

The curves that the transformations (5.26) induce in the plane (γ, h) are the conics $(h/2)^2 + x\gamma^2 = 1$ of constant entanglement entropy that we found in Section 4.4 by a direct inspection of the expression of the von Neumann entropy in terms of x. Hence we can conclude that these conics of constant entropy are the flow of the $SO(1,1)$ group in the space of couplings (γ, h). All these curves intersect at the essential critical point $\gamma = 0$, $h = 2$. It corresponds to the theory in which the four branch points degenerate at 1, the stable fix point of the action of $SO(1,1)$ on the Riemann sphere as we represent in Fig 5.2.

In the following, we will use the invariance under Möbius transformations to study some dualities and other relations connecting theories in the different regions of the plane of parameters of the XY spin chain, see Fig. 4.6.

Duality between regions 1a and 1b

In first place we shall explain the close connection between the expressions for the von Neumann entanglement entropy in the regions 1a and 1b,

$$S_1 = \frac{1}{6}\left[\log\left(\frac{1-x}{16\sqrt{x}}\right) + \frac{2(1+x)}{\pi} I(\sqrt{1-x}) I(\sqrt{x})\right] + \log 2 \quad \text{(region 1a)},$$

$$S_1 = \frac{1}{6}\left[\log\left(\frac{1-x^{-1}}{16\sqrt{x^{-1}}}\right) + \frac{2(1+x^{-1})}{\pi} I(\sqrt{1-x^{-1}}) I(\sqrt{x^{-1}})\right] + \log 2 \quad \text{(region 1b)}.$$

We immediately realise that the entropy is invariant under the change of x by x^{-1}. Let us try to understand this property in the light of the symmetries discovered in this Chapter.

Suppose that we start with a theory with couplings γ_a, h_a in the region 1a, $\gamma_a^2 > 1 - (h_a/2)^2 > 0$. In this region the branch points are real. The zeros of the rational function $\mathfrak{g}(z)$, $z_{a\pm}$, are inside the unit disk while the poles, $z_{a\pm}^{-1}$, are outside. We depict a sketch of this set-up in Fig. 5.8 A.

Observe that in region 1b we take the zeros $z_{a\pm}$ in reverse order with respect to that in region 1a. Hence we must permute them without permuting their inverses. That is, we take now the branch points in the order

$$z_{a+}, z_{a-}, z_{a+}^{-1}, z_{a-}^{-1}.$$

As we show in Appendix C, the permutation between branch points on the same side of the unit circle does not affect the entanglement entropy. However, the cross-ratio (5.29),

$$x_a = (z_{a+}, z_{a-}; z_{a+}^{-1}, z_{a-}^{-1}),$$

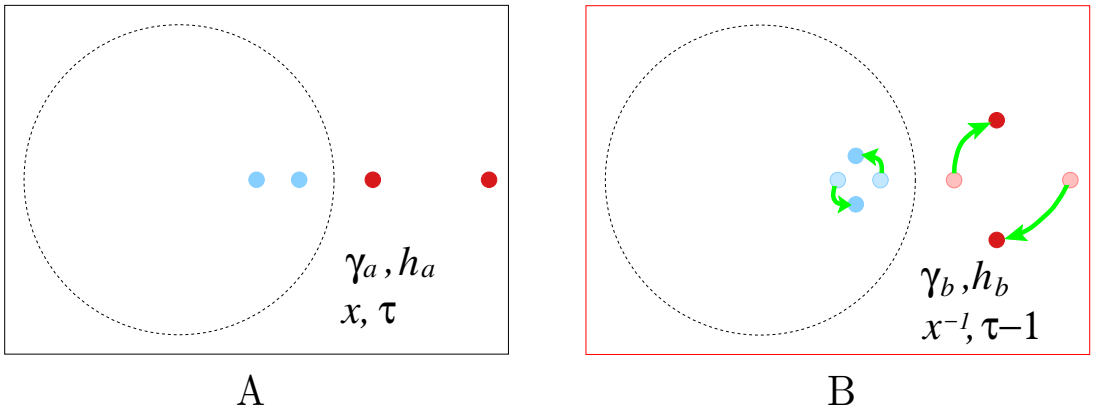

Figure 5.8: Disposition of the branch points of the curve $w^2 = P(z)$ for a non critical XY spin chain in the region 1a (panel A) and its dual in 1b (panel B). The points • are the zeros of the rational function $\mathfrak{g}(z)$ while • are its poles. The cross ratio (5.29) and the modulus of the torus are x and τ for the theory in 1a and x^{-1} and $\tau - 1$ for the dual in region 1b. Both theories have the same ground state entanglement entropy due to its invariance under Möbius transformations. The two theories are related by a permutation of the zeros of $\mathfrak{g}(z)$, that changes x and τ to x^{-1} and $\tau - 1$ and leaves the entropy invariant, plus a Möbius transformation that maps the branch points of the theory in 1a to that in 1b as it is depicted in the panel B.

is now inverted,

$$(z_{a-}, z_{a+}; z_{a+}^{-1}, z_{a-}^{-1}) = x_a^{-1}.$$

From the point of view of the corresponding Riemann surface, in this case a torus, this permutation of the branch points is equivalent to cutting the torus along the a cycle, performing a 2π rotation of one of the borders, and glueing them again. This corresponds to the modular transformation $(a, b) \mapsto (a, a + b)$ of the basic cycles a, b. Then the modular parameter changes from τ to $\tau - 1$. This is precisely one of the two Dehn twists that generate the modular group $SL(2, \mathbb{Z})$ of the torus.

Now it is when the Möbius symmetry enters into the game. By choosing a suitable Möbius transformation that does not belong to $SO(1, 1)$ it is possible to transform the two pairs z_{a+}, z_{a-} into z_{b+}, z_{b-} with the additional property $\overline{z}_{b+} = z_{b-}$ as we represent in Fig. 5.8 B. This new set of (complex) branch points corresponds to a theory in the region 1b. Considering now that the Möbius transformation leaves invariant the entanglement entropy, we can explain the duality between the entanglement entropies in regions 1a and 1b. It should be noticed that the duality, that it is manifest for von Neumann, also holds for the Rényi entropy, as it is based on the equality of the determinant $D_X(\lambda)$ for the two theories related by the transformation.

In particular, one may take as Möbius transformation the one for which

$$\frac{z_{b+} - z_{b-}}{1 + z_{b+} z_{b-}} = -\mathrm{i} \frac{z_{a+} - z_{a-}}{1 + z_{a+} z_{a-}}.$$

The new branch points correspond to a particular choice of couplings γ_b, h_b in the region 1b which are related to the original ones by

$$\gamma_b = \sqrt{1 - \left(\frac{h_a}{2}\right)^2}, \quad \frac{h_b}{2} = \sqrt{1 - \gamma_a^2}. \tag{5.30}$$

Observe that, due to the invariance under Möbius transformations of the cross-ratio and the modulus, the new theory in region 1b has to lie on the ellipse $(h/2)^2 + x_a^{-1}\gamma^2 = 1$ and it corresponds to a torus of modulus $\tau - 1$. On the other hand, the dispersion relation changes like (5.14), that is as a homogeneous field of dimension $L = 1$. Therefore, in this case the spectrum of the Hamiltonian transforms non trivially, and the symmetry in the correlation function of the vacuum is not translated to the dynamics.

Duality between regions 1a and 2

We have seen above that the exchange of the two branch points on the same side of the unit circle leaves the Riemann surface and the characteristics invariant. Consequently, the Rényi entanglement entropy does not change. Another transformation that preserves the Riemann surface is the exchange of a real branch point by its inverse. This establishes a relation between the regions 1a and 2.

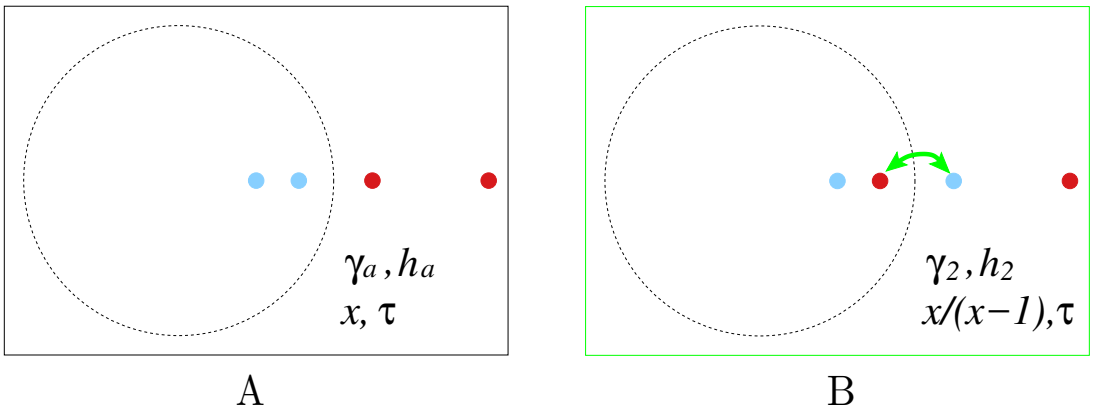

Figure 5.9: Disposition of the branch points of the curve $w^2 = P(z)$ for a non critical XY spin chain in the region 1a (panel A) and its dual theory in region 2 (panel B). The points • are the zeros of $\mathfrak{g}(z)$ while • are the poles. They are related by the exchange of a branch point by its inverse as it is shown in the panel B. This changes the cross-ratio from x to $x/(x-1)$ but leaves invariant the modulus of the torus τ. Since we are exchanging a zero and a pole of $\mathfrak{g}(z)$ the characteristics in the theta function vary and the entanglement entropy is different in each theory. On the contrary, the corresponding Hamiltonians have the same spectrum.

If we start with a theory in the region 1a, for which the branch points are arranged like in Fig. 5.9 A, the exchange of a real branch point with its inverse corresponds to identify e.g. $z_{2+} = z_{a+}^{-1}$, as it is shown in Fig. 5.9 B. The resulting theory lies in region 2. The cross ratio (5.29) changes to

$$(z_{a+}^{-1}, z_{a-}; z_{a+}, z_{a-}^{-1}) = \frac{x_a}{x_a - 1}.$$

This transformation in the cross-ratio leaves the modulus τ of the torus invariant. However, the exchange of a zero and a pole of the function $\mathfrak{g}(z)$ modifies the order in the assignment of the indices from $(+1, +1, -1, -1)$ to $(+1, -1, +1, -1)$. Thus the characteristics in $D_X(\lambda)$ vary from $\mu_a = -1/2$ to $\mu_2 = 0$ and the entropy is modified.

Under the transformation $z_{2+} = z_{a+}^{-1}$ the relation between the coupling constants γ_a,h_a

of the starting theory in 1a and γ_2, h_2 of the resulting one in region 2 is

$$\frac{h_2}{2} = \frac{2}{h_a}, \quad \frac{\gamma_2^2 - 1}{h_2} = \frac{\gamma_a^2 - 1}{h_a}. \tag{5.31}$$

Under this duality, the dispersion relation changes as

$$\omega_2(\theta) = \frac{2}{h_a}\omega_a(\theta).$$

Thus, up to a trivial rescaling, the spectrum of the Hamiltonian is unchanged. Observe that for the particular value $\gamma_a = 1$, that is the quantum Ising chain, the dual theory is also a quantum Ising model, $\gamma_2 = 1$, with magnetic field $h_2 = 4/h_a$. In this case the duality coincides with the Kramers-Wannier duality [130] that we discussed in Section 4.4.

The duality between regions 1a and 2 can be generalised to Hamiltonians of higher range L. We can exchange one real zero of $\mathfrak{g}(z)$ by its inverse, which is a pole of $\mathfrak{g}(z)$, or one complex zero of $\mathfrak{g}(z)$ and its complex conjugate by their inverses, which are poles of $\mathfrak{g}(z)$. Then both the Riemann surface and the spectrum of the Hamiltonian remain invariant. However, the characteristics change and then $D_X(\lambda)$ and the entropy vary too. Observe that two regions of the space of couplings related by one of these dualities are separated by a critical hypersurface.

We emphasize that dualities between 1a and 1b regions and between 1a and 2 are of different nature. In the former the entanglement entropy is invariant while the spectrum of the Hamiltonian changes. On the contrary, in the latter the entanglement entropy varies but the spectrum of the Hamiltonian remains invariant.

Relation between dual theories in 1a and 2 with region 1b

Although the two dual theories in regions 1a and 2 have different entanglement entropies, they can be combined to obtain the ground state entanglement entropy of a Hamiltonian in the region 1b.

This result was first noticed by Iglói and Juhász in [139] for the quantum Ising model ($\gamma = 1$). They showed that the ground state entanglement entropy $S_\alpha^T(2|X|)$ of an interval of length $2|X|$ of a XY spin chain with couplings $h_T = 0$, $\gamma_T < 1$ (in the region 1b) is exactly the sum

$$S_\alpha^T(2|X|) = S_\alpha^a(|X|) + S_\alpha^2(|X|) \tag{5.32}$$

of the ground state entanglement entropies $S_\alpha^a(|X|)$, $S_\alpha^2(|X|)$ for an interval of length $|X|$ of two quantum Ising models, $\gamma_a = \gamma_2 = 1$, with magnetic fields

$$\frac{h_a}{2} = \frac{1 - \gamma_T}{1 + \gamma_T}, \quad \frac{h_2}{2} = \frac{1 + \gamma_T}{1 - \gamma_T}.$$

Notice that the magnetic fields h_a and h_2 are related by inversion as in the duality that we have established between regions 1a and 2.

We shall extend here the previous relation. In order to proceed, it is useful to recall the following identity of Jacobi theta functions (see e.g. [140]) that combines the two dual theories in 1a and 2:

$$\widehat{\vartheta}[{}^{\mu+1/2}_{\nu}](s|\tau)\widehat{\vartheta}[{}^{\mu}_{\nu}](s|\tau) = \widehat{\vartheta}[{}^{\mu+1/2}_{\nu}](s|\tau/2).$$

If we apply this identity for $\mu = 0$ and $\nu = 0$ to the asymptotic expression (5.27) of $D_X(\lambda)$ we can conclude that the sum of the entanglement entropies of two theories with modulus τ and characteristics 1/2, 0 and 0, 0, like the two dual theories in regions 1a and 2 with couplings γ_a, h_a and γ_2, h_2 related by (5.31), gives the Rényi entanglement entropy of a third theory with modulus $\tau/2$ and characteristics 1/2, 0.

In particular, we may take that the couplings γ_T, h_T of the new theory are

$$\frac{h_T}{2} = \sqrt{1-\gamma_a^2}, \quad \gamma_T = \gamma_a \frac{1-\sqrt{1-x_a}}{1+\sqrt{1-x_a}}, \tag{5.33}$$

with

$$x_a = \frac{1-(h_a/2)^2}{\gamma_a^2}.$$

Then defining $y = \sqrt{1-x_a}$, we obtain

$$x_T = \frac{1-(h_T/2)^2}{\gamma_T^2} = \left(\frac{1+y}{1-y}\right)^2.$$

Since γ_a, h_a are the couplings of a theory in region 1a then $0 < x_a < 1$. Therefore, $x_T > 1$, and γ_T, h_T correspond to a Hamiltonian in the region 1b. Now carrying x_a and x_T to the expression (5.28) of the modulus, we respectively have

$$\tau \equiv \tau_a = \mathrm{i}\frac{I(\sqrt{1-y^2})}{I(y)}, \quad \text{and} \quad \tau_T = \mathrm{i}\frac{I\left(\frac{1-y}{1+y}\right)}{I\left(\frac{2\sqrt{y}}{1+y}\right)}.$$

Using now the Landen identities for elliptic functions [92],

$$I\left(\frac{2\sqrt{y}}{1+y}\right) = (1+y)I(y), \quad \text{and} \quad I\left(\frac{1-y}{1+y}\right) = \frac{1+y}{2}I(\sqrt{1-y^2}),$$

we obtain $\tau_T = \tau/2$ as we claimed.

Therefore, we have the following asymptotic relation between the Rényi entanglement entropies in the three non critical regions

$$S_\alpha^a + S_\alpha^2 = S_\alpha^T \tag{5.34}$$

where the superindices refer to the theories in the corresponding regions with the coupling constants defined in (5.31) and (5.33).

According to (5.33), when the theories in 1a and 2 are quantum Ising models, i.e. $\gamma_a = \gamma_2 = 1$, the theory in 1b corresponds to a XY spin chain with $h_T = 0$ and anisotropy parameter

$$\gamma_T = \frac{1-h_a/2}{1+h_a/2}.$$

This precisely corresponds to the original relation found by Iglói and Juhász. Observe that in this case the relation holds not only in the asymptotic limit but also for finite size $|X|$ as we have seen in (5.32). In fact, Iglói and Juhász showed that the ground state two-point correlation matrix of a XY spin chain with $h_T = 0$ and γ_T can actually be expressed as the direct sum of the ground state correlation matrices of two quantum Ising models with external magnetic fields h_a and $4/h_a$.

Even if in the next subsection we study the Möbius symmetry in the critical lines of the model, it is interesting to analyse here the limit in which the theories involved in the relation (5.34) become critical. The critical lines correspond to $h = 2$ (critical Ising class) and $\gamma = 0$ and $h < 2$ (critical XX chain). According to (5.31) and (5.33), if we take $h_a = 2$ (with $0 < |\gamma_a| \leq 1$) the other two related theories have coupling constants $h_2 = 2$, $\gamma_2 = \gamma_a$ and $\gamma_T = 0$, $h_T/2 = \sqrt{1-\gamma_a^2}$. The dual theories in regions 1a and 2 become the same, a critical XY spin chain belonging to the Ising universality class, while the model in region 1b corresponds to a critical XX spin chain with an external magnetic field.

Before applying the relation (5.34) notice that, since we are dealing with critical theories, the entanglement entropy grows with the logarithm of the length $|X|$ of the interval. Therefore, in order to establish the additive relation between the entropies in the critical case, we must take a finite size $|X|$. As in the exact relation found by Iglói and Juhász, we must consider different length intervals for the different theories, namely

$$S_\alpha^T(2|X|) = 2S_\alpha^a(|X|).$$

This is a very interesting relation. It relates the ground state entanglement entropies of the two critical lines of the XY spin chain. In addition, since we know the complete asymptotic expression (4.52) of the entropy for the critical XX spin chain, it allows to compute the Rényi entanglement entropy in the Ising critical line. The result is

$$S_{\alpha,X}^{\text{Ising}} = S_\alpha^a(|X|) = \frac{\alpha+1}{12\alpha}\log|X| + \frac{\alpha+1}{12\alpha}\log(4|\gamma_a|) + \Upsilon_\alpha + o(1) \tag{5.35}$$

with $0 < |\gamma_a| \leq 1$ and Υ_α the constant that we defined in (3.24).

The relation between the ground state entanglement entropies of the critical lines of the XY spin chain and the full asymptotic behaviour for entropy in the critical Ising line were first obtained by the author with Esteve, Falceto and de Queiroz in Ref. [137]. Only the case $\gamma_a = 1$ was previously known in the literature. Iglói and Juhász found it particularising their exact relation (5.32) to this case. Cardy, Castro-Alvaredo and Doyon [132] obtained this result employing field theory techniques. Kádar and Zimborás [109] realised that in this point the theory is Kramers-Wannier self-dual and the correlation matrix reduces to a Toeplitz matrix. Then they got the asymptotic expansion at this point applying the Fisher-Hartwig conjecture.

In the next section we shall study the Möbius transformations in the critical lines of the XY spin chain. In particular, in the critical Ising line, this symmetry also leads to the asymptotic expression (5.35) and it allows to extend it to any value of γ_a.

As a summary, in Fig. 5.10 we represent in the plane of parameters (γ, h) the different dualities and relations that we have found. The point $\triangle$ corresponds to a theory in the region 1a with coordinates (γ_a, h_a). The point $\triangledown$ is its dual in region 1b with

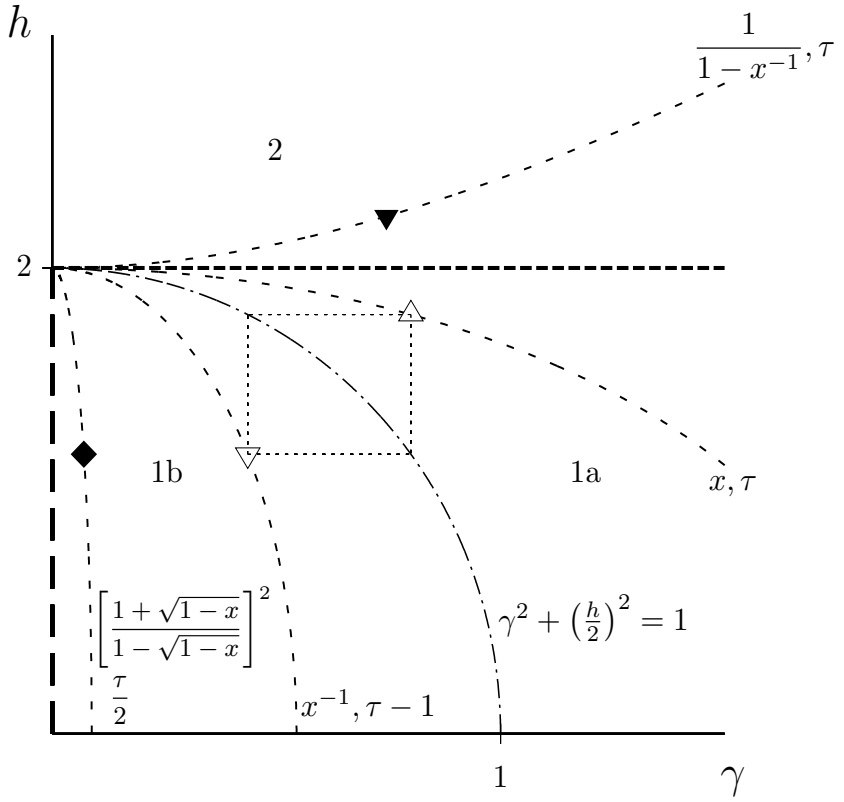

Figure 5.10: Plane of couplings (γ, h) for the XY Hamiltonian with the dualities and relations that we have obtained in the text. The dashed curves represent the induced flow of $SO(1,1)$. Therefore, they connect theories with the same entanglement entropy. The cross-ratio and the modulus of the associated torus are equal for all the points lying in the same curve of constant entropy. The point $\triangle$ corresponds to a theory with cross ratio x and modulus τ. Its dual theory in 1b is the point $\triangledown$. They have the same entanglement entropy, $S_\alpha^{\triangledown} = S_\alpha^{\triangle}$. The dual theory of $\triangle$ in 2 is $\blacktriangledown$ and, although the corresponding tori have the same modulus, the entropies are different, $S_\alpha^{\blacktriangledown} \neq S_\alpha^{\triangle}$. However, the spectrum of their Hamiltonians are equal up to a trivial rescaling. Finally, the entanglement entropy of the theory $\blacklozenge$ is given by (5.34), $S_\alpha^{\blacklozenge} = S_\alpha^{\triangle} + S_\alpha^{\blacktriangledown}$.

couplings (γ_b, h_b) given by (5.30). The point $\blacktriangledown$ is its dual theory in region 2 with the couplings (γ_2, h_2) taken according to (5.31). Finally, the point $\blacklozenge$ corresponds to the theory with couplings (γ_T, h_T) given by (5.33), so its entanglement entropy is the sum of the entanglement entropies in the points $\triangle$ and $\blacktriangledown$ according to (5.34).

Critical theories

Let us study now the Möbius transformations in the critical lines of the XY spin chain. Since the coupling constants γ, h are real the ground state is invariant under parity and the discontinuities in the symbol of the correlation matrix correspond to pairs of branch points (5.24) of the elliptic curve $w^2 = P(z)$ that merge at the unit circle. Therefore, in the transformation (5.23) of the partition function there are no insertions related to Fermi momenta and $Q = 0$

In the critical XX spin chain, $\gamma = 0$ and $h < 2$, the pairs of complex branch points z_+, z_-^{-1} and z_-, z_+^{-1} degenerate at the points of the unit circle

$$u_1 = h/2 + \mathrm{i}\sqrt{1-(h/2)^2}, \quad \text{and} \quad u_2 = \overline{u}_1$$

respectively. Since we have the complete asymptotic expansion of the entropy in this line, we can use it to check analytically the validity of the transformation law (5.23). If we write the asymptotic expression (4.52) of the entropy in terms of the pinchings u_1, u_2,

$$S_{\alpha,X}(u_1,u_2) = \frac{\alpha+1}{6\alpha}\log|X| + \frac{\alpha+1}{12\alpha}\log|u_1-u_2| + 2\Upsilon_\alpha + o(1),$$

it is immediate to conclude that the predicted transformation of the entropy under admissible Möbius transformations (5.12) is fulfilled, i.e.

$$S'_{\alpha,X}(u'_1,u'_2) = S_{\alpha,X}(u_1,u_2) + \frac{\alpha+1}{12\alpha}\log\left(\frac{\partial u'_1}{\partial u_1}\frac{\partial u'_2}{\partial u_2}\right).$$

Contrary to the case of the critical XX line, the asymptotic behaviour in the critical Ising universality class, $h = 2$, is only partially known. In the previous section we were able to determine it, see (5.35), for part of the critical line ($0 < |\gamma| \leq 1$). Here we present an alternative derivation of the same result based on the transformation of the entropy under the Möbius group.

In the critical Ising line the pair of real branch points z_+, z_+^{-1} degenerate at $u = 1$. Therefore, if we apply (5.23), the entropy should transform under an admissible Möbius transformation as

$$S'_{\alpha,X}(u') = S_{\alpha,X}(u) + \frac{\alpha+1}{12\alpha}\log\left.\frac{\partial u'}{\partial u}\right|_{u=1} \tag{5.36}$$

The coupling constants h, γ change according to (5.26). Then if we initially take $h = 2$ and $\gamma = 1$, we obtain the values

$$h' = 2, \quad \gamma' = \mathrm{e}^{-2\zeta}.$$

The set of transformed couplings corresponds to a critical Hamiltonian that belongs again to the Ising universality class.

Since

$$\left.\frac{\partial u'}{\partial u}\right|_{u=1} = \mathrm{e}^{-2\zeta},$$

if we consider $|\gamma| = \mathrm{e}^{-2\zeta}$ and apply (5.36), we have

$$S^{\gamma,h=2}_{\alpha,X} = S^{\gamma=1,h=2}_{\alpha,X} + \frac{\alpha+1}{12\alpha}\log|\gamma|.$$

Now using the known result that at the point $\gamma = 1$, $h = 2$ the entanglement entropy is

$$S^{\gamma=1,h=2}_{\alpha,X} = \frac{\alpha+1}{12\alpha}\log|X| + \frac{\alpha+1}{6\alpha}\log 2 + \Upsilon_\alpha + o(1),$$

we obtain that the entanglement entropy along the critical Ising line $h = 2$ is

$$S^{\gamma,h=2}_{\alpha,X} = \frac{\alpha+1}{12\alpha}\log|X| + \frac{\alpha+1}{12\alpha}\log(4|\gamma|) + \Upsilon_\alpha + o(1). \tag{5.37}$$

This result extends to the whole critical line the expression (5.35) that we obtained for $0 < |\gamma| \leq 1$ using the duality between the regions 1a and 2.

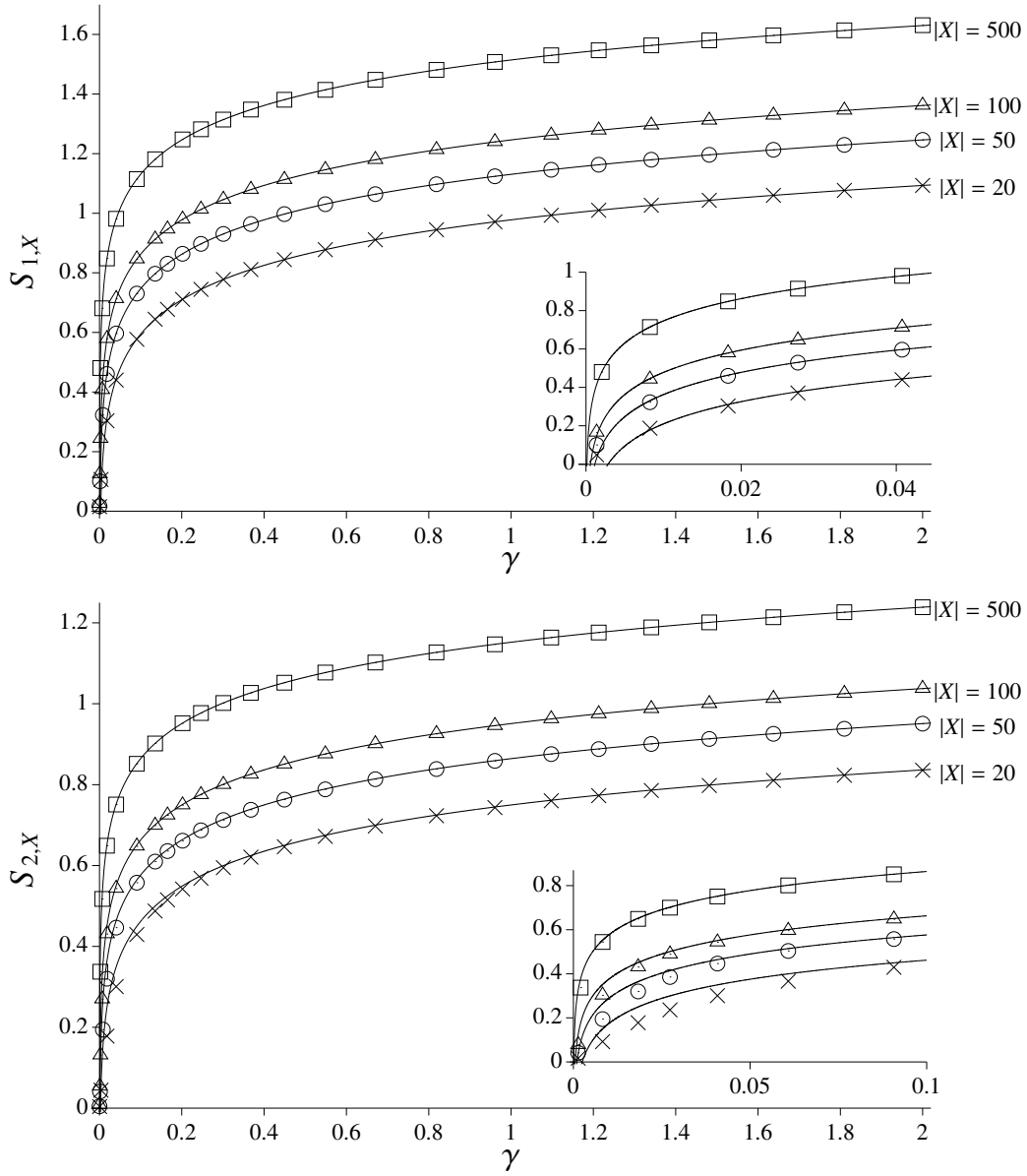

Figure 5.11: Numerical check of expression (5.37) for the entanglement entropy in the critical Ising line $h = 2$. We have computed the von Neumann entropy ($\alpha = 1$, upper plot) and the Rényi entanglement entropy with $\alpha = 2$ (lower plot) for different lengths $|X|$ of the interval and varying γ. The insets are a zoom of the plot for small values of γ where the finite size effects are more relevant, specially in the case $\alpha = 2$.

In Fig. 5.11 we check the validity of this result comparing it with numerical computations. Observe that, since it is an asymptotic result, there are finite size effects which are more important as we approach $\gamma = 0$; that is, the essential critical point, where all the branch points merge at the unit.

5.4 Application to the XY spin chain with a DM coupling

In Section 2.2.2, we saw that if we include in the Hamiltonian of the XY spin chain a Dzyaloshinski-Moriya (DM) coupling the new Hamiltonian breaks parity. In terms of the corresponding fermionic chain, the DM coupling adds an imaginary part s to the hopping $A_1 = 1 + \mathrm{i}s$. We analysed the entanglement entropy of this system in Section 4.5.

The Laurent polynomial $\Phi(z)$ has now an antisymmetric part,

$$\Phi(z) = (1+s)z - h + (1-s)z^{-1},$$

while $\Xi(z)$ is not modified. The elliptic curve $w^2 = P(z)$ that describes the associated compact Riemann surface only depends on the real part of the couplings. Hence it is the same as in the case $s = 0$.

Therefore, under an admissible Möbius transformation (5.12), the coupling constants γ, h transform in the same way (5.26) as for $s = 0$. From the behaviour of $\Phi(z)$ under the transformation,

$$\Phi'(z') = \left(\cosh 2\zeta + \frac{z + z^{-1}}{2}\sinh 2\zeta\right)^{-1} \Phi(z),$$

we determine that the coupling constant s transforms like

$$s' = \frac{s}{(h/2)\sinh 2\zeta + \cosh 2\zeta}.$$

The breaking of the parity symmetry is irrelevant when the theory is non-critical. The associated compact Riemann surface is not affected by the coupling s and the asymptotic expression of $D_X(\lambda)$ is equal to the one (5.27) for $s = 0$. Therefore all the dualities and relations that we have obtained for the non-critical XY spin chain are still valid.

The XY spin chain with a DM coupling is critical when $s^2 - \gamma^2 > 0$ and $(h/2)^2 - s^2 + \gamma^2 < 1$ (Region A) or when $\gamma > s$ and $h = 2$ (Region B). In Region B the dispersion relation,

$$\omega(\theta) = \sqrt{(h - 2\cos\theta)^2 + 4\gamma^2 \sin^2\theta} + 2s\sin\theta,$$

is always positive except at $\theta = 0$ where it is zero. Hence the ground state is invariant under parity. In this case the zero of $\omega(\theta)$ corresponds to the degeneration of the branch points z_+ and z_+^{-1} of $w^2 = P(z)$ at $u = 1$ as it happens for the critical Ising line. Therefore, the expression for the entropy (5.37) that we have obtained for the line $h = 2$ when $s = 0$ is also valid for $\gamma > s > 0$.

In Region A the dispersion relation is negative between the Fermi points θ_j, $j = 1, 2$, for which

$$\cos\theta_j = \frac{-h/2 \pm \sqrt{(s^2 - \gamma^2)(s^2 - \gamma^2 + 1 - (h/2)^2)}}{s^2 - \gamma^2 + 1}, \tag{5.38}$$

with $\theta_j \in (-\pi, 0]$ for $s > 0$. Therefore, the ground state breaks parity symmetry and the symbol has four discontinuities with lateral limits M and $\pm I$ at the points of the unit circle $v_j = \mathrm{e}^{\mathrm{i}\theta_j}$ and $v_{4-j} = \mathrm{e}^{-\mathrm{i}\theta_j}$, $j = 1, 2$.

In this region, the finite term of the ground state entanglement entropy is not known except for some particular cases. However, we can actually determine its behaviour under an admissible Möbius transformation. Since the discontinuities of the symbol correspond to the existence of Fermi points and not to degenerate branch points of $w^2 = P(z)$, in the transformation law (5.23) we have $R = 0$ and $Q = 4$ and

$$S_{\alpha,X}^{\gamma',s',h'} = S_{\alpha,X}^{\gamma,s,h} + \frac{\alpha+1}{24\alpha} \sum_{\sigma=1}^{4} \log \frac{\partial v'_\sigma}{\partial v_\sigma}. \tag{5.39}$$

For the particular case $\gamma = 0$ the symbol $\hat{\mathcal{G}}(\theta)$ is either $\pm I$ or $\pm\sigma_z$. Therefore, we can reduce the problem to a scalar symbol and apply the results of Chapter 3. We obtain

$$S_{\alpha,X}^{\gamma=0,s,h} = \frac{\alpha+1}{6\alpha} \log|X| + \frac{\alpha+1}{12\alpha} \log\left(4\frac{s^2-(h/2)^2+1}{s^2+1}\right) + 2\Upsilon_\alpha + o(1). \tag{5.40}$$

Note that this result makes sense for $s^2 - (h/2)^2 + 1 > 0$, i.e. when we are in the critical region A with $\gamma = 0$.

We can verify with the above expression the predicted transformation (5.39). The product of the complex Jacobians at the insertions v_σ is

$$\begin{aligned} \prod_{\sigma=1}^{4} \frac{\partial v'_\sigma}{\partial v_\sigma} &= \left(\frac{s^2+1}{s^2+((h/2)\sinh 2\zeta + \cosh 2\zeta)^2}\right)^2 \\ &= \left(\frac{s^2+1}{s'^2+1} \cdot \frac{s'^2-(h'/2)^2+1}{s^2-(h/2)^2+1}\right)^2 \end{aligned}$$

From the second line we can conclude that (5.40) transforms according to (5.39).

5.5 Theories with infinite range: the Long-Range Kitaev chain

We conclude this Chapter studying the Möbius symmetry when the range of the couplings in the Hamiltonian is infinite. We shall discuss the Long-Range Kitaev chain as an example of these systems.

As we have seen in Section 5.1, in order to study this symmetry we need to consider the analytical continuation of the symbol $M(\theta)$ from the unit circle $\boldsymbol{\gamma}$ to the Riemann sphere,

$$\mathcal{M}(z) = \frac{1}{\sqrt{\Phi^+(z)^2 - \Xi(z)\overline{\Xi(\overline{z})}}} \begin{pmatrix} \Phi^+(z) & \Xi(z) \\ -\overline{\Xi(\overline{z})} & -\Phi^+(z) \end{pmatrix}.$$

For finite range L, the functions $\Phi(z)$ and $\Xi(z)$ are Laurent polynomials with monomials between $-L$ and L and coefficients A_l and B_l respectively. Under a Möbius transformation (5.3) in the z-plane, they change according to (5.9). As we show in Appendix D, the Möbius transformations act on the sets $\mathbf{A} = (A_{-L}, \cdots, A_L)$ and $\mathbf{B} = (B_{-L}, \ldots, B_L)$ like the L-dimensional spin representation of the $SL(2,\mathbb{C})$ group.

On the other hand, when the couplings extend throughout all the chain and $L \to \infty$, instead of being Laurent polynomials, $\Phi(z)$, $\Xi(z)$ are the functions represented by the Laurent series

$$\Phi(z) = \sum_{l=-\infty}^{\infty} A_l z^l, \quad \Xi(z) = \sum_{l=-\infty}^{\infty} B_l z^l.$$

Therefore, under a Möbius transformation (5.3), they change as

$$\Phi'(z') = \Phi(z), \quad \Xi'(z') = \Xi(z), \tag{5.41}$$

where the resulting functions Φ' and Ξ' are represented by the Laurent series

$$\Phi'(z) = \sum_{l=-\infty}^{\infty} A'_l z^l, \quad \Xi'(z) = \sum_{l=-\infty}^{\infty} B'_l z^l$$

with new coefficients A'_l, B'_l. Therefore, the Möbius group acts on the couplings of the theory changing them from A_l, B_l to A'_l, B'_l. Observe that, if we plug the transformations (5.41) into $\mathcal{M}(z)$, we have that $\mathcal{M}'(z') = \mathcal{M}(z)$, as in the case of finite range.

This means that if the symbol of the correlation matrix is $M(\theta)$ and the entanglement entropy tends to a finite value in the limit $|X| \to \infty$ then the discussion of Section 5.1 is also valid for infinite range. Thus the Rényi entanglement entropy is, in the asymptotic limit, invariant under admissible Möbius transformations (5.12). Taking into account the analysis of Section 4.1, the entanglement entropy is finite when $|X| \to \infty$ if the symbol $M(\theta)$ is smooth enough and then the Widom theorem (4.6) applies.

We also saw in Section 4.1 that the entanglement entropy grows logarithmically with the length of the interval when the symbol is discontinuous. In particular, if it has R discontinuities at the points $\theta_1, \ldots, \theta_R$, then the entanglement entropy behaves as

$$S_{\alpha,X} = \left(\sum_{r=1}^{R} \mathcal{B}_{r,\alpha} \right) \log |X| + \mathcal{C}_\alpha + o(1). \tag{5.42}$$

The contribution $\mathcal{B}_{r,\alpha}$ of each discontinuity depends on the lateral limits at each side of the jump. It can be computed using (4.16) and then inserting the result into the contour integral (2.36).

When the Hamiltonian has finite range couplings, the discontinuities in the symbol arise due to the absence of mass gap. If the system has infinite range interactions, the symbol can be discontinuous outside the critical points, as we explicitly saw in Section 4.6 when we study the entanglement entropy in the Long-Range Kitaev chain. Moreover, we found that the lateral limits of the discontinuities originated by the long-range couplings may not commute and give a contribution to the logarithmic term different from that predicted by CFT (1.10).

In Section 5.2 we have studied the behaviour under admissible Möbius transformations of the entanglement entropy in the ground state of finite-range critical chains. We obtained in (5.23) the transformation law for the corresponding partition function. It changes as a product of homogeneous fields inserted at the discontinuity points with scaling dimension $(1-\alpha)\mathcal{B}_{r,\alpha}$, proportional to the contribution $\mathcal{B}_{\alpha,r}$ of the discontinuity to the coefficient of

the logarithmic term in the entropy. We conjecture that this result can be extended to any chain where the entanglement entropy for an interval is of the form (5.42).

Therefore, let $u_r = \mathrm{e}^{\mathrm{i}\theta_r}$, $r = 1, \ldots, R$, be the points at the unit circle $\boldsymbol{\gamma}$ of the z-plane that correspond to the discontinuity points θ_r. Thus, under an admissible Möbius transformation (5.12), they are mapped into $u'_r = \mathrm{e}^{\mathrm{i}\theta'_r}$, as Fig. 5.4 illustrates. Then, bearing in mind (5.23), we propose that the partition function for the entanglement entropy (5.42) changes as

$$Z'_{\alpha,X}(\underline{u}') = \prod_{r=1}^{R} \left(\frac{\partial u'_r}{\partial u_r} \right)^{(1-\alpha)\mathcal{B}_{r,\alpha}} Z_{\alpha,X}(\underline{u}). \tag{5.43}$$

Hence the entanglement entropy (5.42) transforms as

$$S'_{\alpha,X}(\underline{u}') = S_{\alpha,X}(\underline{u}) + \sum_{r=1}^{R} \mathcal{B}_{r,\alpha} \log \left(\frac{\partial u'_r}{\partial u_r} \right).$$

Let us check this conjecture using the results obtained in Section 4.6 for the Long-Range Kitaev chain. Remember that in this system $A_0 = h$, $A_1 = 1$, and $A_l = 0$ for $|l| \geq 2$ while the parings decay with the distance $B_l = l \cos(\phi l)/|l|^{\delta+1}$ with a dumping exponent $\delta > 0$ and $\phi \in [0, \pi)$. The functions $\Phi(z)$ and $\Xi(z)$ are in this case

$$\Phi(z) = z + h + z^{-1},$$

and

$$\begin{aligned} \Xi_{\delta,\phi}(z) &= \sum_{l=1}^{\infty} \frac{\cos(\phi l)}{l^{\delta}} (z^l - z^{-l}) \\ &= \frac{1}{2} \left[\mathrm{Li}_{\delta}(\mathrm{e}^{\mathrm{i}\phi} z) - \mathrm{Li}_{\delta}(\mathrm{e}^{\mathrm{i}\phi} z^{-1}) + \mathrm{Li}_{\delta}(\mathrm{e}^{-\mathrm{i}\phi} z) - \mathrm{Li}_{\delta}(\mathrm{e}^{-\mathrm{i}\phi} z^{-1}) \right]. \end{aligned}$$

We found that the symbol of the ground state correlation matrix,

$$M(\theta) = \frac{1}{\sqrt{(h + 2\cos\theta)^2 + |\Xi_{\delta,\phi}(\mathrm{e}^{\mathrm{i}\theta})|^2}} \begin{pmatrix} h + 2\cos\theta & \Xi_{\delta,\phi}(\mathrm{e}^{\mathrm{i}\theta}) \\ -\Xi_{\delta,\phi}(\mathrm{e}^{\mathrm{i}\theta}) & -h - 2\cos\theta \end{pmatrix}, \tag{5.44}$$

is discontinuous at the lines $h = \pm 2$ because the mass gap is zero. The long-range pairings also give rise to discontinuities when the dumping is $\delta \leq 1$. For our purposes, the most interesting theories are those in the line $\delta = 1$ since the lateral limits of the discontinuities do not commute. We have to take also into account that if $\phi = 0$ there is only one discontinuity at $\theta = 0$, and this is a fixed point of the admissible Möbius transformations. When $\phi \neq 0$ it splits into two discontinuities at $\theta = \pm\phi$, which enriches the symmetry.

In the light of the previous discussion, let us consider a chain with $\delta = 1$, $h \neq \pm 2$, and $\phi \neq 0$. Hence the mass gap is non-zero but the symbol of the correlation matrix has two discontinuities of the non commutative type at the points $\pm\phi$. According to the analysis performed in Section 4.6, each one contributes to the coefficient of the logarithmic term with

$$\mathcal{B}_{\alpha,\phi} = \frac{2}{\pi^2} \int_{\cos\frac{\Delta\xi}{2}}^{1} \frac{\mathrm{d}f_{\alpha}(\lambda)}{\mathrm{d}\lambda} \log \frac{\sqrt{1-\lambda^2}}{\sqrt{\lambda^2 - \cos^2(\Delta\xi/2)} + \sin(\Delta\xi/2)} \mathrm{d}\lambda,$$

where $\Delta\xi = \xi^+ - \xi^-$, with the angles ξ^+ and ξ^- those defined in (4.86) and (4.87). We call $u_{\pm\phi} = \mathrm{e}^{\pm \mathrm{i}\phi}$ the points in the unit circle of the z-plane corresponding to the discontinuity points $\pm\phi$.

We now perform an admissible Möbius transformation (5.12) in the symbol (5.44), then $M(\theta) \mapsto M(\theta')$, with

$$\mathrm{e}^{\mathrm{i}\theta'} = \frac{\mathrm{e}^{\mathrm{i}\theta}\cosh\zeta + \sinh\zeta}{\mathrm{e}^{\mathrm{i}\theta}\sinh\zeta + \cosh\zeta}. \tag{5.45}$$

Then the set of couplings A_l, B_l transforms to another one A'_l, B'_l according to (5.41), satisfying $A'_{-l} = A'_l$ and $B'_{-l} = -B'_l$, and the discontinuity points $u_{\pm\phi}$ move to $u'_{\pm\phi} = \mathrm{e}^{\pm \mathrm{i}\phi'}$ as we describe in the inset of Fig. 5.12.

Hence, according to the conjecture (5.43), the partition function should transform as a product of homogeneous fields inserted at the points $u_{\pm\phi}$,

$$Z'_{\alpha,X}(u'_\phi, u'_{-\phi}) = \left(\frac{\partial u'_\phi}{\partial u_\phi}\right)^{(1-\alpha)\mathcal{B}_{\alpha,\phi}} \left(\frac{\partial u'_{-\phi}}{\partial u_{-\phi}}\right)^{(1-\alpha)\mathcal{B}_{\alpha,\phi}} Z_{\alpha,X}(u_\phi, u_{-\phi}). \tag{5.46}$$

Since the two insertions have the same scaling dimension and

$$\frac{\partial u'_\phi}{\partial u_\phi} = \frac{1}{(\cosh\zeta + u_\phi \sinh\zeta)^2},$$

the transformation law of $Z_{\alpha,X}$ can be simplified to

$$Z'_{\alpha,X}(u'_\phi, u'_{-\phi}) = \left[\cosh(2\zeta) + \cos\phi \sinh(2\zeta)\right]^{2(\alpha-1)\mathcal{B}_{\alpha,\phi}} Z_{\alpha,X}(u_\phi, u_{-\phi}).$$

In conclusion, under an admissible Möbius transformation the ground state entanglement entropy $S^{\delta=1,\phi,h}_{\alpha,X}$ of a Long-Range Kitaev chain with $\delta = 1$ and $h \neq \pm 2$ changes as

$$S'_{\alpha,X} = S^{\delta=1,\phi,h}_{\alpha,X} - 2\mathcal{B}_{\alpha,\phi} \log\left[\cosh(2\zeta) + \cos\phi \sinh(2\zeta)\right]. \tag{5.47}$$

In Fig. 5.12 we have studied numerically the transformation of the von Neumann entanglement entropy for a chain with $\delta = 1$, $h = 1.2$, and $\phi = \pi/4$. If we compare the numerical points with the analytical prediction (5.47), the agreement is extraordinarily good except, perhaps, when the discontinuities of the symbol approach $\phi = 0$. As it can be observed in the plot, near this point the finite size effects are more relevant.

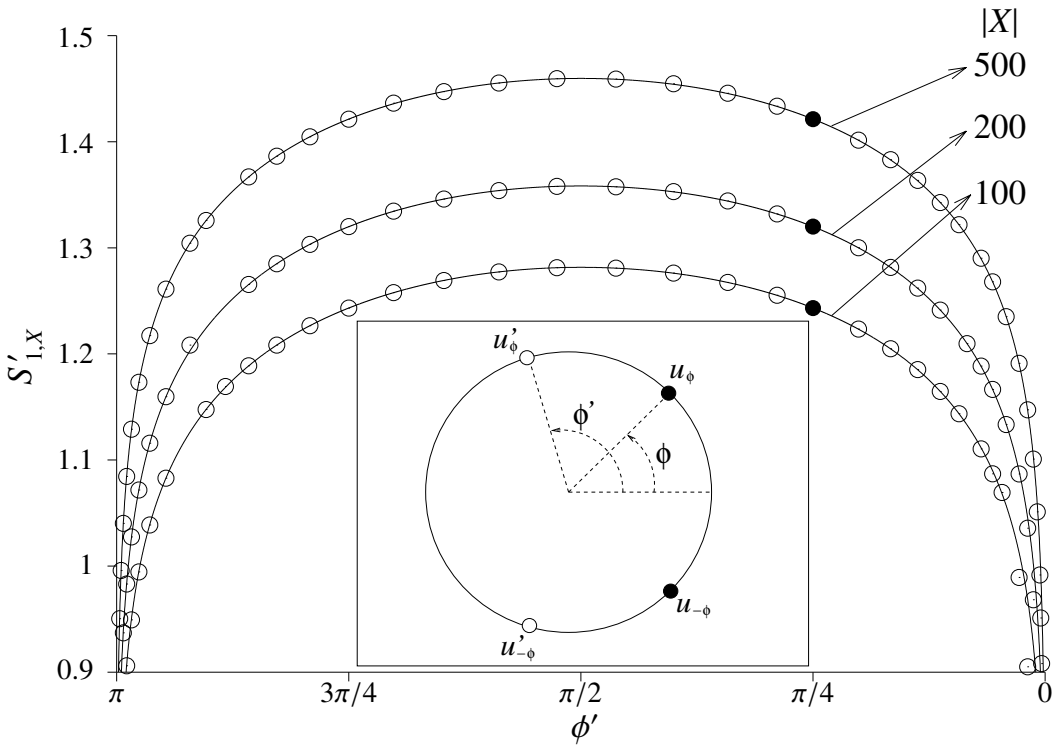

Figure 5.12: Change under admissible Möbius transformations (5.12) of the ground state entanglement entropy with $\alpha = 1$ for the Long-Range Kitaev chain (4.85) with parameters $\delta = 1$, $h = 1.2$ and $\phi = \pi/4$. The dots $\bullet$ are the numerical value of the entropy of this model for different lengths $|X|$ of the interval. The dots $\circ$ are the numerical values obtained for the entanglement entropy after the transformation. We represent the entropy in terms of the transformed angle ϕ'. The discontinuities of the symbol (5.44) are located at $\pm\phi$. Under the transformation ϕ changes to ϕ' according to (5.45) and the corresponding points $u_{\pm\phi} = \mathrm{e}^{\pm \mathrm{i}\phi}$ move along the unit circle of the z-plane as we indicate in the inset. The solid lines represent the conjecture in (5.47), taking as $S^{\delta=1,\phi,h}_{\alpha,X}$ the value at the points $\bullet$ for the different lengths of the interval.

Chapter 6

Entanglement of several disjoint intervals

In the previous chapters we have studied the asymptotic behaviour of the entanglement entropy for a single interval of contiguous sites of the chain. A natural question is what happens when the subsystem is made out of several disjoint intervals as in Fig. 6.1. This Chapter is dedicated to answer this point.

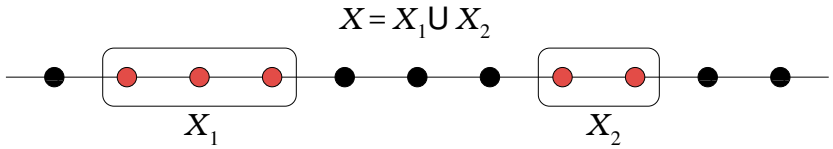

Figure 6.1: In this fermionic chain we have considered a subsystem X that consists of two disjoint intervals of sites, X_1 and X_2.

So far our analysis of the entanglement entropy has been based on the relation between this quantity and the determinant of the resolvent of the two-point correlation matrix V_X of the subsystem X,

$$S_{\alpha,X} = \frac{1}{4\pi \mathrm{i}} \lim_{\varepsilon \to 1^+} \oint_{\mathscr{C}} f_\alpha(\lambda/\varepsilon) \frac{\mathrm{d}}{\mathrm{d}\lambda} \log \det(\lambda I - V_X) \mathrm{d}\lambda. \tag{6.1}$$

Remember that V_X is a block matrix whose entries are the 2×2 matrices

$$(V_X)_{nm} = \frac{1}{2\pi} \int_{-\pi}^{\pi} \mathcal{G}(\theta) \mathrm{e}^{\mathrm{i}\theta(n-m)} \mathrm{d}\theta, \quad n, m \in X,$$

and $\mathcal{G}(\theta)$ the 2×2 matrix obtained in (2.39).

When the subsystem X is a single interval the matrix V_X is a block Toeplitz matrix. All the entries $(V_X)_{nm}$ of every subdiagonal parallel to the main one are equal, as it is represented in Fig. 6.2 A. Using the asymptotic properties of the determinants of block Toeplitz matrices we have derived the behaviour of the entanglement entropy of an interval.

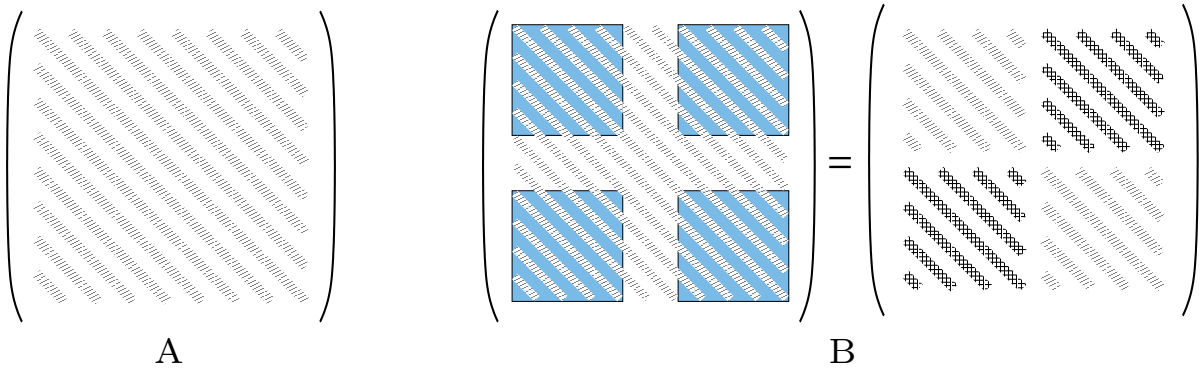

Figure 6.2: In A, we schematically represent a block Toeplitz matrix: its entries along any subdiagonal parallel to the principal one are equal. In B, we take a principal submatrix of the former. Observe that it is a block matrix in which each block is block Toeplitz but the full matrix is not.

On the other hand, if X consists of several disjoint intervals the matrix V_X is not block Toeplitz anymore, but it is the principal submatrix of a block Toeplitz matrix (in fact is a block matrix in which each block is a block Toeplitz matrix). Fig. 6.2 B provides an example of this. Therefore, the results found in the previous chapters do not apply.

In this Chapter we shall propose an asymptotic expression for the determinant of a principal submatrix of a block Toeplitz matrix. With this result we will be able to determine the behaviour of the entropy for several intervals. We shall derive the conjecture from Conformal Field Theory, that can be used to compute the entanglement entropy in the ground state of finite-range, critical theories.

We shall check numerically the proposed conjecture for different theories. The numerical results do not leave any doubt about its validity.

It is particularly interesting to analyse the Möbius symmetry studied in Chapter 5 in the case of several intervals. As we shall see it reveals a striking parallelism with the behaviour of the entanglement entropy under conformal transformations in the real space.

6.1 Entanglement entropy for disjoint intervals in Conformal Field Theory

In Chapter 4 we obtained that, for a critical fermionic chain with finite range couplings, the ground state Rényi entanglement entropy for a single interval of length $|X|$ is

$$S_{\alpha,X} = \frac{\alpha+1}{6\alpha} \mathrm{c} \log |X| + \mathcal{C}_\alpha + o(1), \tag{6.2}$$

where c is a constant proportional to the number of discontinuities of the symbol $\hat{\mathcal{G}}(\theta)$ of the two-point correlation matrix.

When the fermionic chain is critical the mass gap is zero and the correlation length diverges. In this case, the group of symmetries of the system is enlarged and it includes the conformal invariance.

We can use this symmetry to derive the asymptotic behaviour of the entanglement entropy. Actually, the transformation of the entanglement entropy under the conformal group in the real space fixes the α-dependence of the coefficient of the logarithmic term. The only free parameter is c that, from this perspective, corresponds to the central charge of the underlying conformal field theory.

Let us discuss now how the conformal symmetry determines the behaviour of the entanglement entropy in the case of several disjoint intervals. For this purpose, it will be interesting to briefly review the path integral representation of the replica trick following the works by Holzhey, Larsen and Wilczek [52] and Calabrese and Cardy [53, 141]. This procedure relates the entanglement entropy to the partition function of the CFT on a compact Riemann surface. This surface is different from the one that we have introduced in the previous chapters. Nevertheless, there are certain similarities and parallelism between them that are worth commenting.

Consider a relativistic field theory defined on a 1+1 space-time without boundaries. Suppose that the theory is in a thermal state with temperature $1/\beta$. This state is represented by the density matrix $\rho_\beta = \mathrm{e}^{-\beta H}/\operatorname{Tr}(\mathrm{e}^{-\beta H})$ where H is the Hamiltonian of the theory.

Observe that ρ_β is similar to the time evolution operator $\mathrm{e}^{-\mathrm{i}tH}$ after performing a Wick rotation $\mathrm{i}t \mapsto \tau$. The time evolution operator gives the propagator of the theory, the probability amplitude that the system evolves from a particular state to another one after a time interval t. In the path integral representation, this probability amplitude is expressed as the integral over all the possible configurations of the fields that connect the initial and the final state. Then each entry of ρ_β may be written as a path integral defined on the Euclidean space-time strip of width β represented in Fig. 6.3 (1), connecting a particular configuration at $\tau = 0$ with another one at $\tau = \beta$.

The trace of $\mathrm{e}^{-\beta H}$ is performed by setting the same initial and final configuration and integrating over all the possible states. This is equivalent to the path integral over the cylinder of circumference of length β obtained by gluing the edges of the strip at $\tau = 0$ and $\tau = \beta$.

Now let us consider in the spacial dimension a set X of P disjoint intervals

$$X = \bigcup_{p=1}^{P} [x_{2p-1}, x_{2p}],$$

where x_{2p-1} and x_{2p} denote the end-points of the p-interval. In Fig. 6.3 (1) the intervals of X correspond to the (red) segments depicted at the edges of the strip at $\tau = 0$ and $\tau = \beta$.

In order to compute the entanglement entropy of these intervals we need the reduced density matrix $\operatorname{Tr}_{\mathcal{H}_Y} \rho_\beta$. To compute this partial trace we have to set equal the configuration of the fields at $\tau = 0$ and $\tau = \beta$ at the points of the space that are not in X. In the path integral representation, this corresponds to joining together the edges of the strip at $\tau = 0$ and $\tau = \beta$ except at the points that belong to X. Then we obtain a cylinder like that in Fig. 6.3 (2), with open cuts in the intervals $[x_{2p-1}, x_{2p}]$, $p = 1, \ldots, P$, that form the subsystem X.

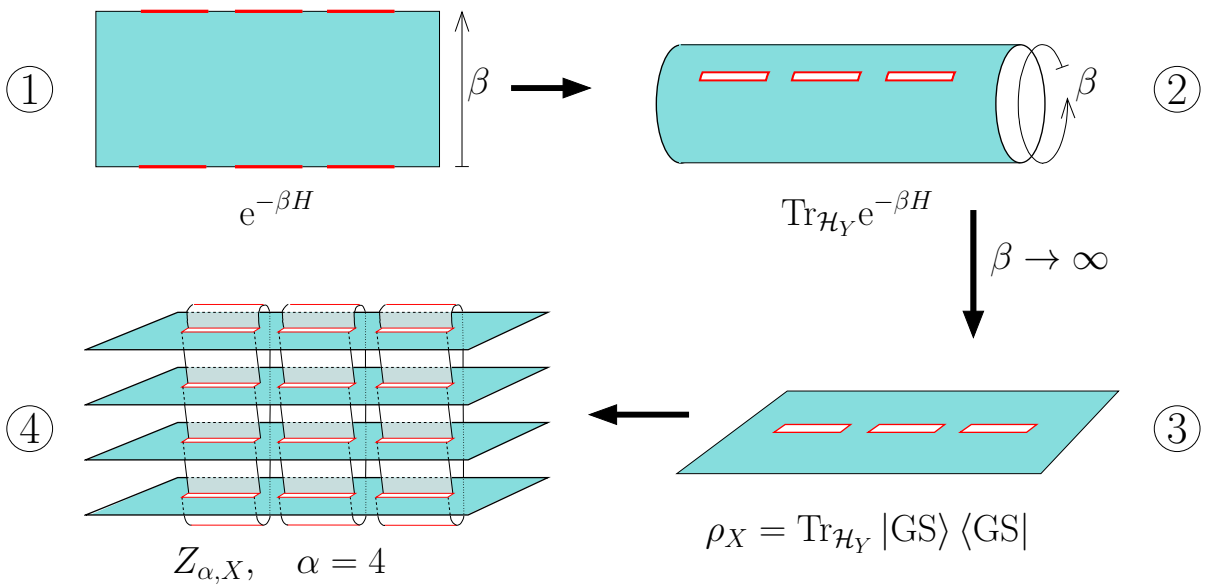

Figure 6.3: The entries of the thermal density matrix $\mathrm{e}^{-\beta H}$ can be represented as path integrals defined on the strip of the Euclidean space-time of width β represented in (1). If we consider a set $X = [x_1, x_2] \cup \cdots [x_{2P-1}, x_{2P}]$ of disjoint intervals in the real space (the red segments), the reduced density matrix $\mathrm{Tr}_{\mathcal{H}_Y}\, \mathrm{e}^{-\beta H}$ is represented by a cylinder of circumference β with open cuts along the intervals of X, like that in (2). In the limit $\beta \to \infty$ we get the ground state and the corresponding reduced density matrix ρ_X can be seen as a path integral on the plane with open cuts at the intervals of X. Then the quantity $Z_{\alpha,X} = \mathrm{Tr}(\rho_X^\alpha)$ can be interpreted as the partition function of the theory defined on the compact Riemann surface obtained by taking α copies of the plane with cuts represented in (3) and pasting them cyclically along the cuts as it is described in (4).

From the thermal state one can recover the ground state $\rho = |\mathrm{GS}\rangle \langle \mathrm{GS}|$ taking the zero temperature limit $\beta \to \infty$. In this limit the radius of the cylinder goes to infinity. Then the path integrals that give the entries of $\rho_X = \mathrm{Tr}_{\mathcal{H}_Y} |\mathrm{GS}\rangle \langle \mathrm{GS}|$ are defined on a plane similar to the one represented in Fig. 6.3 (3), with cuts along the segments $[x_{2p-1}, x_{2p}]$ corresponding to the intervals of X.

Now an integer power ρ_X^α can be computed with the replica trick. It consists in taking α copies of the path integrals that represent ρ_X and combining them as follows. Each copy is defined on a plane with P cuts like that of Fig. 6.3 (3). We paste them together along the open cuts $[x_{2p-1}, x_{2p}]$ as we illustrate in Fig. 6.3 (4). That is, if we go around the endpoints x_{2p-1} clockwise we move to the upper copy while going around the points x_{2p} clockwise we move to the lower one. Finally, the trace of ρ_X^α is obtained by joining the first and the last copies. This produces an α-sheeted Riemann surface with branch points at the endpoints $\{x_{2p-1}\}$, $\{x_{2p}\}$ of the intervals of X.

In conclusion, $Z_{\alpha,X} = \mathrm{Tr}(\rho_X^\alpha)$ is given by the path integral over the compact Riemann surface of Fig. 6.3 (4) that can be identified with the partition function of the field theory defined on this surface [1].

The von Neumann entanglement entropy can be obtained from the analytical contin-

[1]Strictly speaking, $Z_{\alpha,X}$ is the partition function $\mathcal{Z}_{\alpha,X}$ of the field theory on the compact Riemann surface normalised by the partition function $\mathcal{Z}$ of the theory defined on the Euclidean space-time so that $Z_{\alpha,X} = \mathcal{Z}_{\alpha,X}/\mathcal{Z}^\alpha$. For simplicity, we refer to $Z_{\alpha,X}$ as the partition function.

uation of $Z_{\alpha,X}$ to real values of α and then taking the limit

$$S_{1,X} = -\lim_{\alpha\to 1} \frac{\partial}{\partial\alpha} \log Z_{\alpha,X}.$$

It is interesting to compare the Riemann surface that we have described here on the context of the replica trick for several intervals with that obtained in Section 4.2 from the analytical structure of the extension of the correlation matrix symbol to the complex plane, $\mathcal{M}(z)$.

In that case, the Riemann surface is obtained in the space of momenta, where the symbol is defined, and it depends on the Hamiltonian of the theory. Actually, its genus is given by the range of the couplings and the branch points are determined by the value of the coupling constants.

On the contrary, the Riemann surface that arises in the replica trick is defined on the real space and it is universal. It does not depend on the Hamiltonian of the theory. It is univocally determined by the subsystem X and by the value of the Rényi parameter α. In fact, its genus is $(\alpha-1)(P-1)$ and it can be described algebraically by the complex curve

$$w^\alpha = \prod_{p=1}^{P}(z - x_{2p-1}) \left[\prod_{p'=1}^{P}(z - x_{2p'})\right]^{\alpha-1}. \tag{6.3}$$

Interestingly, a similar surface appears when one generalises the Wiener-Hopf factorisation problem for the 2×2 symbol $\mathcal{M}$ discussed in Section 4.2 and Appendix B to a symbol of higher dimension $\alpha\times\alpha$, see [142]. Observe that for $\alpha = 2$ the curve (6.3) is actually a hyperelliptic curve.

So far we have not made use of the conformal symmetry. The previous discussion on the replica trick is valid for all the theories, including the non-critical ones.

Cardy and Calabrese noted in [53] that the partition function of a theory defined on the Riemann surface described by the curve (6.3) may be written as the correlation function of two kinds of fields $\mathcal{T}_\alpha$ and $\overline{\mathcal{T}}_\alpha$ inserted at the branch points $\{x_{2p-1}\}$ and $\{x_{2p}\}$ respectively,

$$Z_{\alpha,X} = \langle \mathcal{T}_\alpha(x_1)\overline{\mathcal{T}}_\alpha(x_2)\cdots\mathcal{T}_\alpha(x_{2P-1})\overline{\mathcal{T}}_\alpha(x_{2P})\rangle.$$

In Ref. [132], Cardy, Castro-Alvaredo and Doyon interpreted $\mathcal{T}_\alpha$, and $\overline{\mathcal{T}}_\alpha$ as the twist fields associated to the $\mathbb{Z}_\alpha$ symmetry of the theory under the cyclic exchange of the sheets of the Riemann surface.

When the theory is massless, the conformal symmetry tells us that the branch point twist fields $\mathcal{T}_\alpha$, $\overline{\mathcal{T}}_\alpha$ are primary fields of scaling dimension $2c\Delta_\alpha$, where c is the central charge of the theory and $\Delta_\alpha = (\alpha^{-1}-\alpha)/24$.

This means that, under a global conformal transformation in the real space

$$x' = \frac{ax+b}{cx+d}, \quad \begin{pmatrix} a & b \\ c & d \end{pmatrix} \in SL(2,\mathbb{R}) \tag{6.4}$$

that moves the endpoints $\underline{x} = (x_1, \ldots, x_{2P})$ of the intervals from $\underline{x}$ to $\underline{x}'$, the partition function $Z_{\alpha,X}$ must change as

$$Z_\alpha(\underline{x}') = \prod_{\tau=1}^{2P} \left(\frac{\partial x'_\tau}{\partial x_\tau}\right)^{2c\Delta_\alpha} Z_\alpha(\underline{x}).$$

Note that, for convenience, we have changed the notation for the partition function so that $Z_\alpha(\underline{x}) = Z_{\alpha,X}$.

The above transformation law implies that the partition function should be of the form

$$Z_{\alpha,X} = K_\alpha \prod_{\tau,\tau'=1,\tau\neq\tau'}^{2P} |x_\tau - x_{\tau'}|^{(-1)^{\tau-\tau'+1}2\Delta_\alpha c} \mathcal{F}_\alpha(\underline{y}), \tag{6.5}$$

where K_α is a constant that we shall determine below and $\mathcal{F}_\alpha$ is a non universal function that depends on the details of the theory but it is invariant under the conformal transformations (6.4). Therefore, it only depends on the endpoints through the set of cross-ratios $\underline{y} = (y_1, \ldots, y_{2(P-1)})$,

$$y_s = \frac{(x_{s+2} - x_1)(x_2 - x_{2P})}{(x_{s+2} - x_2)(x_1 - x_{2P})}, \quad s = 1, \ldots, 2(P-1).$$

In Ref. [143], Casini and Huerta showed that for the ground state of critical free fermions, as it is our case, $\mathcal{F}_\alpha = 1$.

For more general theories, $\mathcal{F}_\alpha \neq 1$. For instance, Caraglio and Gliozzi [144] and Furukawa, Pasquier and Shiraishi [145] realised that $\mathcal{F}_\alpha$ is a complicated function for spin chains. One should mention that unlike for a single interval, as it was noted by Iglói and Peschel in [146], the reduced density matrix of a subsystem of disjoint intervals in a fermionic chain is different from that in the corresponding spin chain. Calabrese and Fagotti explained in [147] the reason behind this difference. We shall briefly review their arguments.

If we take for instance the two-point spin correlation $\langle \sigma_n^+ \sigma_m^- \rangle$, and we apply the Jordan-Wigner transformation (2.19) we have

$$\langle \sigma_n^+ \sigma_m^- \rangle = \langle \prod_{j=1}^{n-1} (-a_j^\dagger a_j + 1) a_n^\dagger \prod_{j'=1}^{m-1} (-a_{j'}^\dagger a_{j'} + 1) a_m \rangle = \langle a_n^\dagger \mathcal{S} a_m \rangle.$$

where

$$\mathcal{S} = \prod_{j=n}^{m-1} (-a_j^\dagger a_j + 1).$$

The correlation $\langle a_n^\dagger \mathcal{S} a_m \rangle$ can be expressed by means of the Wick theorem (2.27) in terms of the two-point correlations functions $\langle a_l^\dagger a_{l'} \rangle$, $\langle a_l a_{l'} \rangle$ with $n \leq l, l' \leq m$.

If X is a single interval of contiguous sites and $n, m \in X$, all the operators involved in the string $\mathcal{S}$ belong to X. Therefore, the two-point correlation matrix of the spin operators in the interval X is given by the two-point correlation matrix of the fermionic operators in the same subsystem. The Jordan-Wigner transformation maps the space of

states of the interval X in the spin chain into the space of states of X in the fermionic chain. Therefore, the entanglement entropy of an interval is the same in both chains.

On the contrary, suppose that the subsystem X is formed by two disjoint intervals $X = X_1 \cup X_2$. If $n \in X_1$ and $m \in X_2$, there are operators in the string $\mathcal{S}$ that do not belong to X. Hence the correlations of the spin operators between the points in X are not only given by the correlations of the fermionic operators in X, but also by those in the sites between X_1 and X_2. Hence the reduced density ρ_X is not the same for the fermionic chain and for its corresponding spin representation.

The above discussion means that when X contains several intervals the expression (6.1) of the entanglement entropy $S_{\alpha,X}$ in terms of the fermionic two-point correlation matrix V_X is valid to compute the entanglement entropy of the fermionic chain, but not that of the spin chain.

The function $\mathcal{F}_\alpha$ gives precisely the difference between the entanglement entropy of the fermionic and the corresponding spin chain. For the last years a considerable effort has been invested in order to determine $\mathcal{F}_\alpha(x)$ in several models. This is in general a difficult task. It involves applying CFT techniques on compact Riemann surfaces and sophisticated numerical methods. In particular, this function has been determined analytically for integer α in the boson compactified on a circle (that includes the critical XX spin chain) and in the Ising universality class line of the XY spin chain. Calabrese, Cardy and Tonni initially obtained the expression of $\mathcal{F}_\alpha$ for these two theories in the case of two intervals in [148] and [149]. Coser, Tagliacozzo and Tonni [150] generalised them for an arbitrary number of intervals. The expression of $\mathcal{F}_\alpha$ that they obtained shows a complicated dependence on α. This makes difficult to determine its analytical continuation to any α and, therefore, the von Neumann entropy. Some recent works [151, 152, 153] try to address this problem using different approaches. The entanglement entropy of disjoint intervals in the critical lines of the XY spin chain has been also studied numerically by several authors [144, 145, 147, 154, 155] confirming the analytical predictions.

In this thesis we shall restrict to analyse the entropy of several intervals in the fermionic chain. Therefore, for us $\mathcal{F}_\alpha = 1$.

In this case, the Rényi entanglement entropy derived from (6.5) is

$$S_{\alpha,X} = \frac{\alpha+1}{6\alpha} \mathrm{c} \log \frac{\prod_{p,p'=1}^{P} |x_{2p-1} - x_{2p'}|}{\prod_{p<p'} (x_{2p'-1} - x_{2p-1})(x_{2p'} - x_{2p})} + \frac{1}{1-\alpha} \log K_\alpha. \tag{6.6}$$

Observe that the coefficient of the logarithmic term is exactly the same than in the one interval case (6.2). In order to determine the constant term K_α we can take the limit of large separation between the intervals $|x_{2p+1} - x_{2p}| \to \infty$, $p = 1, \ldots, P-1$. In this limit the entropy should be the sum of the entropies for each interval. Therefore, the constant term is P times the constant term $\mathcal{C}_\alpha$ for a single interval.

6.2 Principal submatrix of a block Toeplitz matrix

From the expression of the entanglement entropy for several disjoint intervals that we have just obtained using conformal invariance we can propose an expression for the asymptotic behaviour of a principal submatrix of a block Toeplitz matrix.

Observe that the entanglement entropy in Eq. (6.6) can be written as a combination of that for single intervals,

$$S_\alpha(X) = \sum_{p\geq p'} S_\alpha([x_{2p'-1}, x_{2p}]) + \sum_{p<p'} \left(S_\alpha([x_{2p}, x_{2p'-1}]) - S_\alpha([x_{2p-1}, x_{2p'-1}]) - S_\alpha([x_{2p}, x_{2p'}])\right). \tag{6.7}$$

For convenience, we have slightly changed the notation for the entanglement entropy so that $S_\alpha(X) = S_{\alpha,X}$. It is immediate to show that combining the latter expression and the expansion of the entropy of a single interval (6.2) we can derive (6.6). The relation (6.7) can also be obtained applying the Holographic principle [64] as Hubeny and Rangamani did in [156]. See also [157].

The expression (6.7) has the virtue of showing more clearly the possible asymptotic behaviour of the determinant $D_X(\lambda) = \det(\lambda I - V_X)$ for several intervals. As it is explicit from the expression (6.1), the entropy $S_{\alpha,X}$ depends linearly on the logarithm of $D_X(\lambda)$. Therefore, the relation (6.7) can be derived from an analogous property for the determinant of principal submatrices of a block Toeplitz matrix.

In order to formulate this property, let us consider a block Toeplitz matrix T generated by a piecewise $d \times d$ matrix valued symbol J. For any set of indices X let us denote by $D(X) = \det(T_X)$ where T_X is the restriction of T to the set of indices X. Then the property for the determinant of a principal submatrix of T that we hypothesise can be stated as follows.

Conjecture:

$$D\left(\bigcup_{p=1}^{P}[x_{2p-1}, x_{2p}]\right) = \prod_p D([x_{2p-1}, x_{2p}]) \prod_{p<p'} \frac{D([x_{2p-1}, x_{2p'}])D([x_{2p}, x_{2p'-1}])}{D([x_{2p-1}, x_{2p'-1}])D([x_{2p}, x_{2p'}])} \left(1 + o(1)\right) \tag{6.8}$$

where $o(1)$ stands for terms that vanish when $|x_\tau - x_{\tau'}| \to \infty$ for $\tau, \tau' = 1, \ldots, 2P$. In Fig. 6.4 formula (6.8) is represented graphically for the case $P = 2$.

Notice that all the determinants of the right-hand side are of the block Toeplitz type. Therefore, we can obtain their asymptotic behaviour applying the result (4.16) that we obtained in Section 4.1. According to it,

$$\log D([x_\tau, x_{\tau'}]) = \mathcal{A}_D |x_\tau - x_{\tau'}| + \mathcal{B}_D \log |x_\tau - x_{\tau'}| + O(1), \tag{6.9}$$

for $\tau, \tau' = 1, \ldots, 2P$ and $\tau \neq \tau'$. The coefficients $\mathcal{A}_D$ and $\mathcal{B}_D$ can be determined analytically from (4.16).

This means that the new conjecture (6.8) combined with (6.9) allows to determine the expansion of the determinant of a principal submatrix of a block Toeplitz matrix. To our

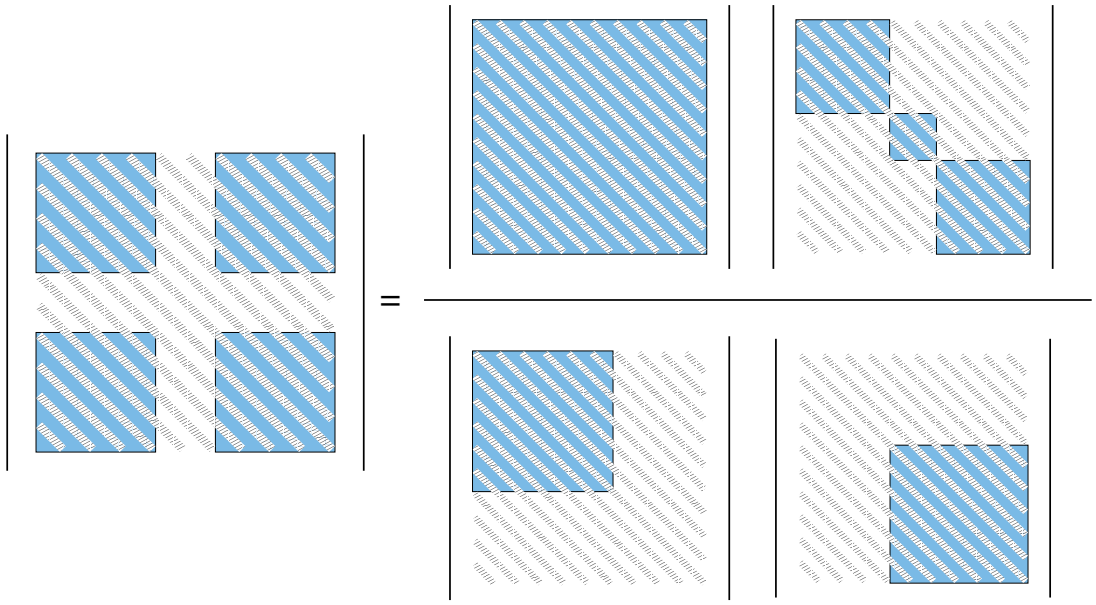

Figure 6.4: Graphical representation of the conjecture (6.8) for $P = 2$. On the left-hand side, we represent the determinant of the shadowed submatrix of T that, in general, is not block Toeplitz. On the right-hand side, however, the determinants of the shadowed submatrices are of the block Toeplitz type (or product of these).

knowledge, this result has not been considered previously in the literature until the work [158] by the author with Esteve and Falceto.

Before applying this conjecture to the computation of the entanglement entropy for several intervals, we believe that it is worth checking its validity for arbitrary piecewise symbols.

For this purpose, let us consider the case $P = 2$ (two disjoint intervals) and introduce the quantity

$$I_D([x_1, x_2] \cup [x_3, x_4]) = \log D([x_1, x_2]) + \log D([x_3, x_4]) - \log D([x_1, x_2] \cup [x_3, x_4]). \quad (6.10)$$

According to the proposed conjecture (6.4)

$$D([x_1, x_2] \cup [x_3, x_4]) \simeq \frac{D([x_1, x_4])D([x_1, x_2])D([x_2, x_3])D([x_3, x_4])}{D([x_1, x_3])D([x_2, x_4])}.$$

If we apply the expansion (6.9) to the determinants $D([x_\tau, x_{\tau'}])$ of the block Toeplitz submatrices which appear in the above expression we have

$$I_D([x_1, x_2] \cup [x_3, x_4]) \simeq -\mathcal{B}_D \log y, \quad (6.11)$$

where

$$y = \frac{(x_3 - x_2)(x_4 - x_1)}{(x_3 - x_1)(x_4 - x_2)}.$$

According to the definition in (4.57), this is the cross-ratio of the four endpoints $(x_1, x_2; x_4, x_3)$. Observe that if take this order for the endpoints in the cross-ratio then $0 < y < 1$. This will be convenient for the representation of the numerical results. The coefficient $\mathcal{B}_D$ can be obtained analytically from the discontinuities of the symbol using (4.16).

Consider now the scalar symbol ($d = 1$)

$$J^{(1)}(\theta) = \begin{cases} \frac{1}{4}\,(3 + \sin\theta)\,, & \theta \in [-\pi, 0], \\ \frac{1}{4}\,(3 + \cos\theta)\,, & \theta \in (0, \pi). \end{cases}$$

It has a jump at $\theta = -\pi$ from 3/4 to 1/2 and at $\theta = 0$ from 3/4 to 1. Then according to (4.16), the coefficient $\mathcal{B}_D^{(1)}$ is in this case

$$\mathcal{B}_D^{(1)} = \frac{1}{4\pi^2}\left[\left(\log\frac{1}{3/4}\right)^2 + \left(\log\frac{3/4}{1/2}\right)^2\right]. \tag{6.12}$$

In Fig. 6.5 we represent by dots the numerical value of I_D for this symbol while the solid line represents the logarithmic dependence (6.11) predicted by our conjecture, with the coefficient $\mathcal{B}_D^{(1)}$ computed above.

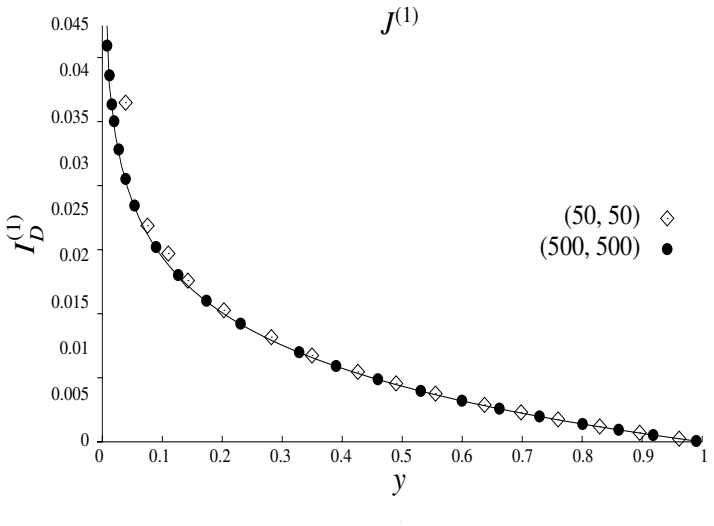

Figure 6.5: Difference between the determinants (6.10) when they are generated by the scalar symbol $J^{(1)}$. It is represented against the cross ratio of the endpoints $y = (x_1, x_2; x_4, x_3)$. The dots $\diamond$ represent the numerical value of (6.10) considering two intervals of size $|x_1 - x_2| = |x_3 - x_4| = 50$ and varying the gap between them, $|x_2 - x_3|$, from 1 up to 200. The dots $\bullet$ are obtained when we take two intervals of length 500 separated by a distance between 1 and 4500. The continuous line is the conjectured analytical expression of (6.11) using the coefficient calculated in (6.12).

As we can see in the plot, the agreement between the numerical results and the analytical curve is certainly remarkable. Due to the asymptotic nature of our formulae, the accordance with the numerical result should be poorer when the separation between the intervals is only of a few sites; that is, when y tends to zero. This is more clearly seen when we study the determinant of two small disjoint intervals.

To reinforce further the validity of our conjecture we shall check it for the 2×2 symbol

$$J^{(2)}(\theta) = \begin{cases} I + \left(\dfrac{1}{3} + \dfrac{\sin\theta}{4}\right)\sigma_x, & \theta \in [-\pi, \frac{\pi}{2}], \\ \\ I + \dfrac{\sin\theta}{2}\sigma_y + \dfrac{\cos\theta}{2}\sigma_z, & \theta \in (\frac{\pi}{2}, \pi). \end{cases}$$

It has discontinuities at $\theta = -\pi$, with lateral limits $I + 1/3\sigma_x$ and $I - 1/2\sigma_z$, and at $\theta = \pi/2$, with lateral limits $I + 7/12\sigma_x$ and $I + 1/2\sigma_y$. Notice that both are of the non commuting type. Applying (4.16) we have that the value of the coefficient $\mathcal{B}_D^{(2)}$ is in this case

$$\mathcal{B}_D^{(2)} = \frac{1}{4\pi^2}\left\{ \mathrm{Tr}\left[\log\left(I+\frac{1}{3}\sigma_x\right)\left(I-\frac{1}{2}\sigma_z\right)^{-1}\right]^2 + \mathrm{Tr}\left[\log\left(I+\frac{7}{12}\sigma_x\right)\left(I+\frac{1}{2}\sigma_y\right)^{-1}\right]^2 \right\}. \tag{6.13}$$

As for the scalar symbol, in Fig. 6.6 we compare the numerical value of I_D for $J^{(2)}$ with the predicted behaviour (6.11) by the conjecture (6.8) using the coefficient $\mathcal{B}_D^{(2)}$.

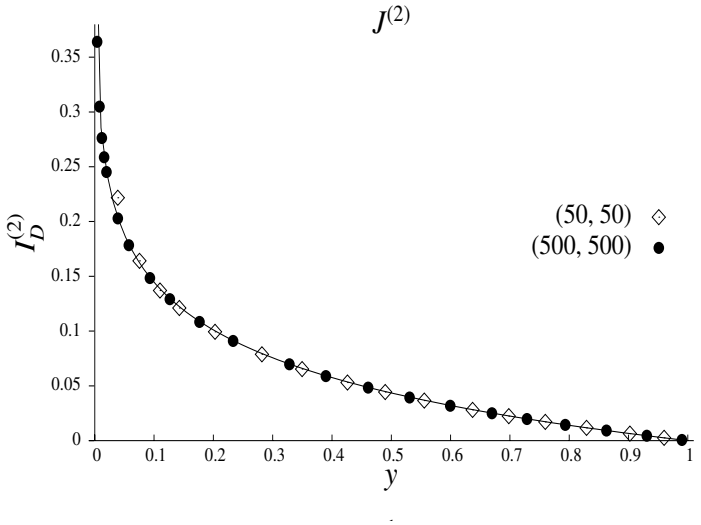

Figure 6.6: Difference between the determinants (6.10) generated by the 2×2 symbol $J^{(2)}$ as a function of the cross ratio $y = (x_1, x_2; x_4, x_3)$. The $\diamond$ represent the numerical results for two intervals of size $|x_1 - x_2| = |x_3 - x_4| = 50$. We modify the gap between them, $|x_2 - x_3|$, from 1 up to 200. The $\bullet$ correspond to two intervals of length 500 separated by a distance between 1 and 4500. The continuous line is the conjectured analytical expression of (6.11) with the coefficient obtained in (6.13).

Again our analytical prediction describes well the behaviour of the determinant of the principal submatrix. The finite size effects are more relevant when the length of the intervals considered is small and the cross-ratio y of the end-points tends to zero.

6.3 Rényi entanglement entropy for several disjoint intervals

The expansion (6.8) that we have derived for the determinant of a principal submatrix of a block Toeplitz matrix makes possible to determine the asymptotic behaviour of the entanglement entropy of several disjoint intervals for any stationary state $|\mathbf{K}\rangle = \prod_{k\in\mathbf{K}} d_k^\dagger |0\rangle$ of the fermionic chain (2.2).

As we know, for these states the entanglement entropy can be expressed in terms of

of the resolvent $D_X(\lambda)$ of the two-point correlation matrix restricted to X,

$$S_\alpha(X) = \frac{1}{4\pi \mathrm{i}} \lim_{\varepsilon \to 1^+} \oint_{\mathscr{C}} f_\alpha(\lambda/\varepsilon) \frac{\mathrm{d}}{\mathrm{d}\lambda} \log D_X(\lambda) \mathrm{d}\lambda.$$

If $X = \bigcup_{p=1}^{P} [x_{2p-1}, x_{2p}]$, applying the new conjecture (6.8) to the determinant $D_X(\lambda)$ we obtain that $S_\alpha(X)$ is a sum of the entanglement entropy of single intervals,

$$S_\alpha(X) = \sum_{p \geq p'} S_\alpha([x_{2p'-1}, x_{2p}]) + \sum_{p<p'} \left(S_\alpha([x_{2p}, x_{2p'-1}]) - S_\alpha([x_{2p-1}, x_{2p'-1}]) - S_\alpha([x_{2p}, x_{2p'}]) \right). \tag{6.14}$$

In (6.7) we already obtained this kind of relation using CFT methods, but thanks to the conjecture (6.8) we can generalise it to the entropy of any stationary state $|\mathbf{K}\rangle$. Therefore, we can extend to several intervals all the results and properties that we have obtained in the previous chapters for a single interval.

In particular, we found that the entanglement entropy for a single interval $[x_\tau, x_{\tau'}]$ behaves asymptotically as

$$S_\alpha([x_\tau, x_{\tau'}]) = \mathcal{A}_\alpha \log |x_\tau - x_{\tau'}| + \mathcal{B}_\alpha \log |x_\tau - x_{\tau'}| + \mathcal{C}_\alpha + o(1). \tag{6.15}$$

The coefficients $\mathcal{A}_\alpha$ and $\mathcal{B}_\alpha$ can always be determined. However, we only know the form of the constant term $\mathcal{C}_\alpha$ for certain cases.

Combining the previous expression with the relation (6.14), we find that for $X = \bigcup_{p=1}^{P} [x_{2p-1}, x_{2p}]$,

$$S_\alpha(X) = \mathcal{A}_\alpha \sum_{p=1}^{P} |x_{2p} - x_{2p-1}| + \mathcal{B}_\alpha \log \frac{\prod_{p,p'=1}^{P} |x_{2p-1} - x_{2p'}|}{\prod_{p<p'} (x_{2p'-1} - x_{2p-1})(x_{2p'} - x_{2p})} + P\mathcal{C}_\alpha + \cdots . \tag{6.16}$$

This result should be valid in the thermodynamic limit. The dots represent terms that vanish when the separation between the endpoints grows, i.e. $|x_\tau - x_{\tau'}| \to \infty$, $\tau, \tau' = 1, \ldots, 2P$.

The leading contribution in the expansion (6.16) reflects the extensivity of the linear term in (6.15). Remember that a linear term arises for instance in the entropy of a single interval for the ground states of the local fermionic ladders considered in Section 3.3. A particular interesting one was

$$|\mathbf{K}^{(2)}\rangle = \prod_{n=1}^{N/2} \frac{1}{\sqrt{2}} (a_n^\dagger - a_{n+N/2}^\dagger) |0\rangle ,$$

that we called State 2. This state has the special property that its entanglement entropy can be exactly computed. If $|x_{2P} - x_1| < N/2$, the reduced density matrix is proportional to the identity,

$$\rho_X^{(2)} = 2^{-|X|} I,$$

where $|X| = \sum_{p=1}^{P} |x_{2p} - x_{2p-1}|$ is the sum of the lengths of the intervals that form X. Hence

$$S_{\alpha,X}^{(2)} = |X| \log 2. \tag{6.17}$$

In Section 3.2.1 we obtained that the coefficients of the expansion (6.15) for this state are $\mathcal{A}_\alpha^{(2)} = \log 2$, $\mathcal{B}_\alpha^{(2)}, \mathcal{C}_\alpha^{(2)} = 0$. Therefore, the expression (6.16) gives in this case the exact result.

Let us check numerically the validity of (6.16) in other states for which we already studied the entropy of a single interval. It will be useful to introduce the following quantity

$$I_{\alpha,P} = \sum_{p=1}^{P} S_\alpha([x_{2p-1}, x_{2p}]) - S_\alpha\left(\bigcup_{p=1}^{P} [x_{2p-1}, x_{2p}]\right). \tag{6.18}$$

This is the analogue for P intervals of the usual mutual information for two intervals $X = [x_1, x_2] \cup [x_3, x_4]$,

$$I_{\alpha,2} = S_\alpha([x_1, x_2]) + S_\alpha([x_3, x_4]) - S_\alpha([x_1, x_2] \cup [x_3, x_4]). \tag{6.19}$$

Applying the expansions (6.15) and (6.16) we observe that in (6.18) the linear and the constant terms cancel and we obtain

$$I_{\alpha,P} \simeq -\mathcal{B}_\alpha \log \Pi \tag{6.20}$$

where

$$\Pi = \prod_{p<p'} y_{p,p'} \tag{6.21}$$

and

$$y_{p,p'} = \frac{|x_{2p'-1} - x_{2p}||x_{2p'} - x_{2p-1}|}{|x_{2p'} - x_{2p}||x_{2p'-1} - x_{2p-1}|}$$

is the cross-ratio $(x_{2p-1}, x_{2p}; x_{2p'}, x_{2p'-1})$.

In order to verify (6.20) in full lore, we shall consider systems that cannot be analysed using twist fields in CFT.

i) *Local fermionic ladder*

First, let us take the ground state of the ladder

$$H_{\text{ladder}} = \sum_{n=1}^{N} \left(A_0 a_n^\dagger a_n + A_1 a_n^\dagger a_{n+1} + A_{N/2} a_n^\dagger a_{n+N/2}\right) + \text{h.c.} \tag{6.22}$$

with $A_0 = 2A_{N/2} > 0$, $A_1 < 0$ and $2A_{N/2} > -A_1$.

We studied this state in detail in Section 3.2.1 where it was called State 3. We obtained there the expansion of the entropy for a single interval, see Eq. (3.30), using the Fisher-Hartwig conjecture. In particular, the coefficient $\mathcal{B}_\alpha^{\text{ladder}}$ of the logarithmic term is

$$\mathcal{B}_1^{\text{ladder}} = \frac{1}{8} - \frac{1}{2}\left(\frac{\log 2}{\pi}\right)^2 \tag{6.23}$$

for $\alpha = 1$, and

$$\mathcal{B}_\alpha^{\text{ladder}} = \frac{\alpha+1}{24\alpha} - \frac{1}{2\pi^2(\alpha-1)} \sum_{l=1}^{\alpha} \left(\log \sin \frac{(2l-1)\pi}{2\alpha}\right)^2 \tag{6.24}$$

for integer $\alpha \geq 2$. As it is clear $\mathcal{B}_\alpha^{\rm ladder}$ is not of the form predicted by Conformal Field Theory.

We have checked numerically the validity of (6.20) for this state taking two disjoint intervals ($P = 2$) of different sizes and changing the separation between them. In Fig. 6.7 we plot the numerical mutual information (6.19) as a function of the cross ratio $y = (x_1, x_2; x_4, x_3)$. We compare the numerical results with the analytical prediction (6.20) using the above expressions for the coefficient $\mathcal{B}_\alpha^{\rm ladder}$.

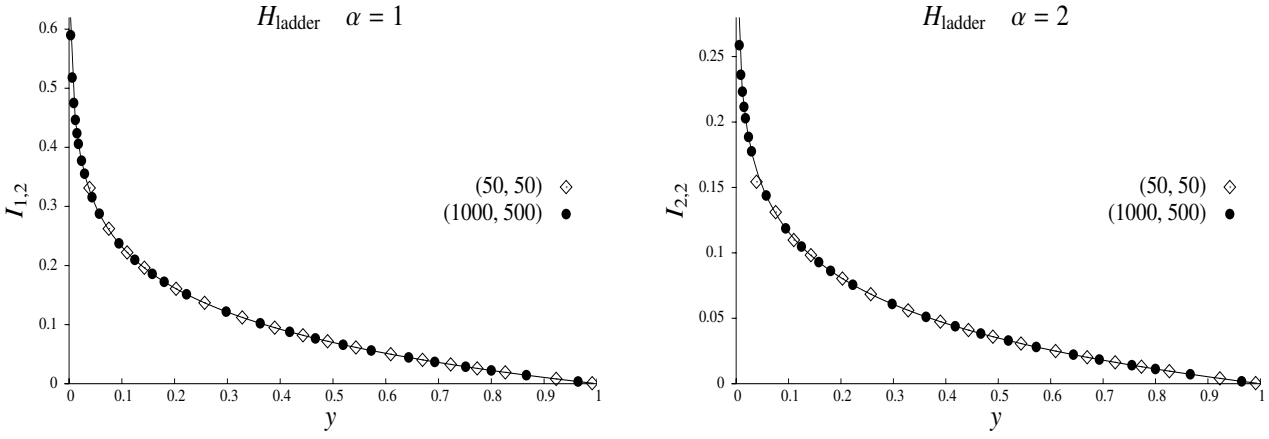

Figure 6.7: Two-intervals mutual information (6.19) for $\alpha = 1$ (left panel) and $\alpha = 2$ (right panel) as a function of the cross-ratio y for the ground state of the ladder (6.22). With $\diamond$ we represent the numerical value for two intervals made up of 50 sites each of them, varying their separation from 1 up to 500 sites. The dots $\bullet$ correspond to two intervals of length 1000 and 500 sites, separated each other between 1 and 1000 sites. The continuous line represents the function (6.20) with coefficient $\mathcal{B}_\alpha^{\rm ladder}$ that of (6.23) for $\alpha = 1$ and (6.24) for $\alpha = 2$.

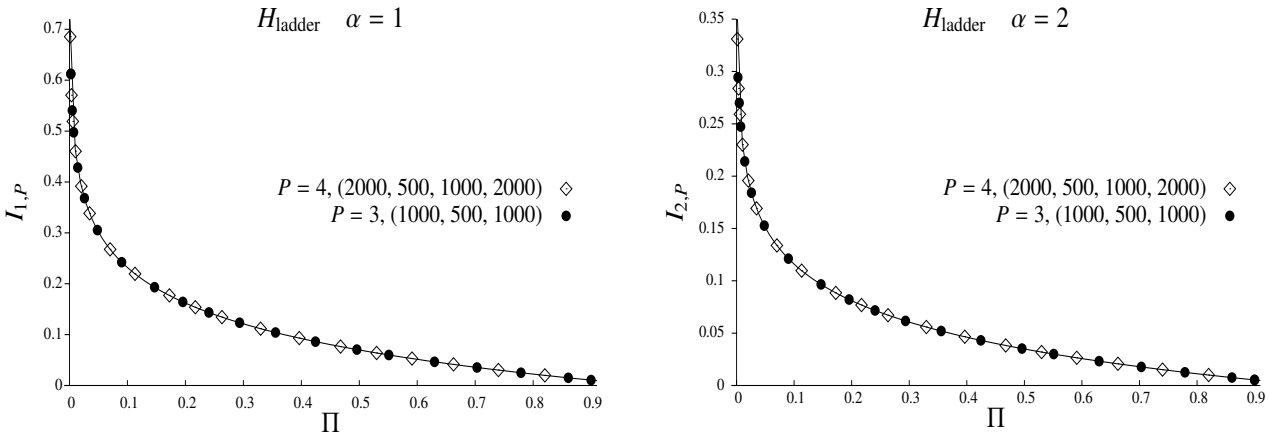

Figure 6.8: Mutual information (6.18) of three ($\bullet$) and four ($\diamond$) intervals for the ground state of the ladder (6.22). It is represented as a function of Π, see (6.21). For $P = 3$, we have chosen two intervals of 1000 sites and one of 500 sites. The separation between the latter and one of the former is 1500 sites. The distance with the other one is modified from 1 up to 99000 sites. For $P = 4$, we take intervals of lengths 2000, 500, 1000, 2000. The distance between the first couple is 1500 sites. We also fix in 5000 sites the separation between the middle intervals. The remaining distance is modified from 1 up to 99000 sites. The solid line represents the analytical conjecture (6.20) with the coefficient $\mathcal{B}_\alpha^{\rm ladder}$ given by (6.23) when $\alpha = 1$, and (6.24) for $\alpha = 2$.

In Fig. 6.8 we repeat the same calculation but choosing three and four intervals, i.e. $P = 3$ and 4. The outcome of the numerical computations is represented in terms of the product of all the possible cross-ratios of the endpoints of the intervals Π. We also plot the conjectured behaviour stated in (6.20) with the coefficient $\mathcal{B}_\alpha^{\text{ladder}}$. We obtain an outstanding agreement.

ii) *Long-Range Kitaev chain*

We have also considered the ground state of the Long-Range Kitaev chain

$$H'_{\text{LRK}} = \sum_{n=1}^{N} \left(a_n^\dagger a_{n+1} + a_{n+1}^\dagger a_n + h a_n^\dagger a_n + \sum_{|l|<N/2} \frac{l\cos(l\phi)}{|l|^{\delta+1}} (a_n^\dagger a_{n+l}^\dagger - a_n a_{n+l}) \right) - \frac{Nh}{2} \tag{6.25}$$

with $h = 1.2$, $\delta = 1$, and $\phi = \pi/4$.

In Section 4.6 we studied the entanglement entropy of a single interval for this state. There we found that although it is the ground state of a Hamiltonian with non-zero mass gap, the presence of long range interactions gives rise to a logarithmic term in the entropy of an interval. We obtained that the coefficient of this term is of the form

$$\mathcal{B}_1^{\text{LRK}} = \frac{2}{\pi^2} \int_{\cos\frac{\Delta\xi}{2}}^{1} \frac{\mathrm{d}f_1(\lambda)}{\mathrm{d}\lambda} \log \frac{\sqrt{1-\lambda^2}}{\sqrt{\lambda^2 - \cos^2(\Delta\xi/2)} + \sin(\Delta\xi/2)} \mathrm{d}\lambda \tag{6.26}$$

for $\alpha = 1$ and

$$\mathcal{B}_\alpha^{\text{LRK}} = \frac{1}{\pi^2(\alpha-1)} \sum_{l=1}^{\alpha} \left(\arctan \frac{\sin(\Delta\xi/2)}{\sqrt{\cos^2(\Delta\xi/2) + |\lambda_l|^2}} \right)^2 \tag{6.27}$$

for integer $\alpha \geq 2$. According to the analysis performed in Section 4.6, $\Delta\xi = \xi^+ - \xi^-$ where the angles ξ^+ and ξ^- are defined in (4.86) and (4.87) in terms of the parameters h, δ and ϕ. The λ_l's are given by (4.79).

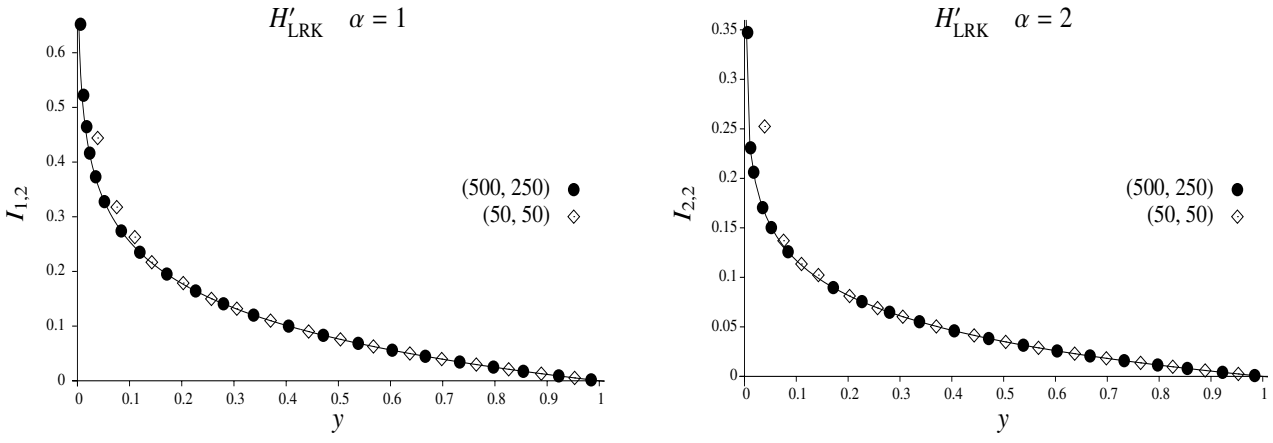

Figure 6.9: Two-intervals mutual information (6.19) for $\alpha = 1$ (left panel) and $\alpha = 2$ (right panel) as a function of y for the ground state of the long-range Kitaev chain (6.25) with $h = 1.2$, $\delta = 1$ and $\phi = \pi/4$. The dots $\diamond$ correspond to the case of two intervals with 50 sites each of them, varying their separation from 1 up to 180 sites. The dots $\bullet$ are calculated taking two intervals of lengths 500 and 250 sites and modifying their separation from 1 up to 5000 sites. The continuous line corresponds to the function (6.20) using the coefficient $\mathcal{B}_\alpha^{\text{LRK}}$ given in (6.26) if $\alpha = 1$ and (6.27) for $\alpha = 2$.

In Fig. 6.9 we present the numerical results for the two-intervals mutual information (6.19) in the ground state of this model. We take different lengths and separations for the intervals. We have also plotted the analytical prediction (6.20) with the coefficient $\mathcal{B}_\alpha^{\rm LRK}$ computed using the formulae above.

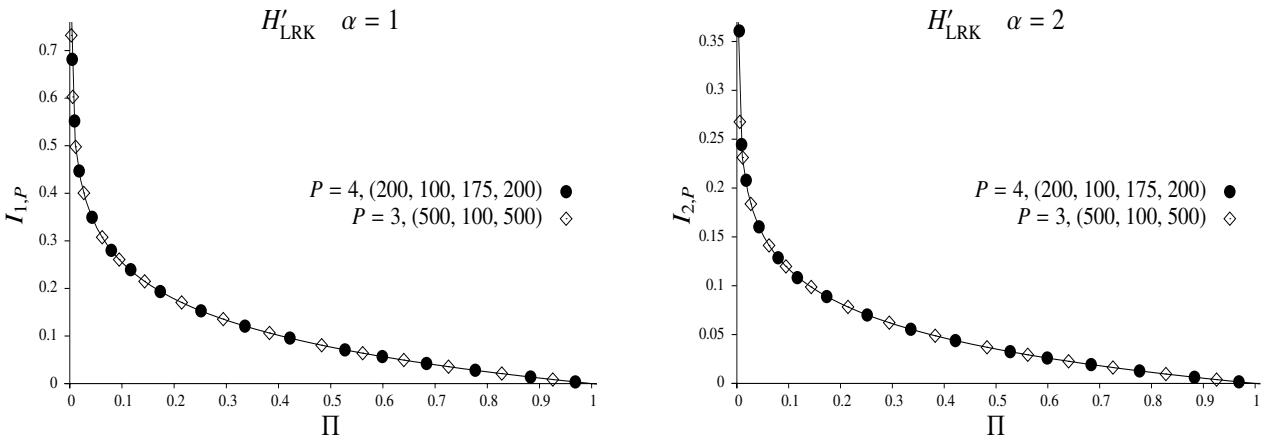

Figure 6.10: Mutual information in the ground state of the Long-Range Kitaev chain with $h = 1.2$, $\delta = 1$ and $\phi = \pi/4$ as a function of Π. We have considered three (⋄) and four (•) intervals. For $P = 3$, we have chosen two intervals of 500 sites and one of 100 sites which is separated from one of the former by 550 sites. The distance with the other one is modified from 1 up to 10^5 sites. For $P = 4$, we take intervals of lengths 200, 100, 175, 200. The distance between the first couple is 550 sites, the separation between the smallest intervals is also fixed, 5000 sites. The remaining distance is increased between 1 and 10^5 sites. The continuous line represents the function (6.20) assuming for the coefficient $\mathcal{B}_\alpha^{\rm LRK}$ the value given by (6.26) and (6.27) for $\alpha = 1$ and $\alpha = 2$ respectively.

In Fig. 6.8 we perform a similar calculation for three and four disjoint intervals. We find again a remarkable agreement between the analytical prediction and the numerical results.

6.4 Möbius symmetry for disjoint intervals

In Chapter 5 we unravelled a new symmetry of the entanglement entropy based on the Möbius group that acts on the couplings of the theory. In particular, we found that a subgroup of these transformations including the 1+1 Lorentz group,

$$z' = \frac{z\cosh\zeta + \sinh\zeta}{z\sinh\zeta + \cosh\zeta}, \tag{6.28}$$

maps the set of couplings $\mathbf{A} = (A_{-L}, \ldots, A_0, \ldots, A_L)$, $\mathbf{B} = (B_{-L}, \ldots, B_0, \ldots, B_L)$ into another set $\mathbf{A}'$, $\mathbf{B}'$ that is physically admissible in the sense that the new couplings satisfy the hermiticity condition $A'_{-l} = \overline{A'}_l$ and the antisymmetry $B'_{-l} = -B'_l$.

A natural question is what happens with this symmetry when the subsystem X is made out of several disjoint intervals. The relation (6.14) that we have obtained between the entanglement entropy for disjoint intervals and that of single intervals gives the answer.

To study the Möbius symmetry it is useful to work with the partition function,

$$Z_\alpha(X) = \mathrm{e}^{(1-\alpha)S_\alpha(X)}.$$

From the relation (6.14) one derives that, in the asymptotic limit, the partition function of $X = \bigcup_{p=1}^{2P}[x_{2p-1} - x_{2p}]$ can be expressed as

$$Z_\alpha(\underline{x}) = \prod_{1\leq\tau<\tau'\leq 2P} Z_\alpha(x_\tau, x_{\tau'})^{-\sigma_\tau\sigma_{\tau'}}, \tag{6.29}$$

where $\sigma_\tau = (-1)^\tau$. We have changed the notation so that $Z_\alpha(X) = Z_\alpha(\underline{x})$ and $\underline{x} = (x_1, \ldots, x_{2P})$. Note that on the right hand side only the partition function for a single interval appears.

If the range of coupling L is finite and the mass gap is non-zero, we showed in Section 5.1 that the asymptotic ground state Rényi entropy of an interval is invariant under Möbius transformations. Therefore, the expression (6.14) implies that the Rényi entropy of several intervals is also invariant under Möbius transformations when the distance $|x_\tau - x_{\tau'}|$, $\tau, \tau' = 1, \ldots, 2P$, between the different endpoints is large enough.

On the other hand, if the theory is critical, the symbol $\hat{\mathcal{G}}(\theta)$ of the ground state two-point correlation matrix is discontinuous. In Section 5.2 we found that the partition function of an interval transforms like the product of homogeneous fields inserted at the discontinuities of the symbol. The dimension of these homogeneous fields depends on the type of discontinuity. If it is associated to a pinching of the corresponding compact Riemann surface (i.e. located at a point where the dispersion relation $\omega(\theta)$ vanishes but does not change its sign) the dimension is $2\Delta_\alpha$. If it corresponds to a Fermi point (i.e. a mode where $\omega(\theta)$ does change its sign) the dimension is Δ_α.

Consider $u_\kappa = \mathrm{e}^{\mathrm{i}\theta_\kappa}$, $\kappa = 1, \ldots, R$, the position of the pinchings at the unit circle and $v_\sigma = \mathrm{e}^{\mathrm{i}\theta_\sigma}$, $\sigma = 1, \ldots, Q$, the points in the complex plane associated to the Fermi points and their opposites. Under the Lorentz group, $\underline{u} = (u_1, \ldots, u_R)$ and $\underline{v} = (v_1, \ldots, v_Q)$ transform according to (6.28) into $\underline{u}'$, $\underline{v}'$ and the partition function of the interval $[x_\tau, x_{\tau'}]$ changes as

$$Z'_\alpha(\underline{u}', \underline{v}'; x_\tau, x_{\tau'}) = \prod_{\kappa=1}^{R}\left(\frac{\partial u'_\kappa}{\partial u_\kappa}\right)^{2\Delta_\alpha}\prod_{\sigma=1}^{Q}\left(\frac{\partial v'_\sigma}{\partial v_\sigma}\right)^{\Delta_\alpha} Z_\alpha(\underline{u}, \underline{v}; x_\tau, x_{\tau'}),$$

Here we have written explicitly the dependence on $\underline{u}$ and $\underline{v}$ of the partition function $Z_\alpha(x_\tau, x_{\tau'})$. Now combining this result with (6.29) and taking into account that

$$\sum_{1\leq\tau<\tau'\leq 2P}\sigma_\tau\sigma_{\tau'} = -P,$$

we obtain that, under any admissible Möbius transformation (6.28),

$$Z'_\alpha(\underline{u}', \underline{v}'; \underline{x}) = \prod_{\kappa=1}^{R}\left(\frac{\partial u'_\kappa}{\partial u_\kappa}\right)^{2P\Delta_\alpha}\prod_{\sigma=1}^{Q}\left(\frac{\partial v'_\sigma}{\partial v_\sigma}\right)^{P\Delta_\alpha} Z_\alpha(\underline{u}, \underline{v}; \underline{x}) \tag{6.30}$$

in the large $|x_\tau - x_{\tau'}|$ limit.

We can compare this behaviour with the one for a conformal transformation in the real space (6.4). In Section 6.1 we saw that the latter acts on the endpoints $\underline{x} \mapsto \underline{x}'$ and the partition function of X changes as

$$Z_\alpha(\underline{u}, \underline{v}; \underline{x}') = \prod_{\tau=1}^{2P} \left(\frac{\partial x'_\tau}{\partial x_\tau} \right)^{2c\Delta_\alpha} Z_\alpha(\underline{u}, \underline{v}; \underline{x}). \tag{6.31}$$

In Section 4.3 we obtained that in a critical fermionic chain with finite range of couplings the central charge c is given by the number of pinchings and Fermi points such as

$$c = \frac{R}{2} + \frac{Q}{4}.$$

Observe the striking similarity between (6.30) and (6.31) with the role of the endpoints of the intervals, x_τ, replaced by the pinchings and the Fermi points, u_κ, v_σ.

It is actually possible to obtain a unified expression if one consider simultaneously the 1+1 Lorentz group and conformal transformations. An element of the direct product $SO(1,1) \times SL(2,\mathbb{R})$ induces a map on the space of couplings, pinchings, Fermi points and endpoints

$$(\mathbf{A}, \mathbf{B}, \underline{u}, \underline{v}, \underline{x}) \mapsto (\mathbf{A}', \mathbf{B}', \underline{u}', \underline{v}', \underline{x}')$$

where the element in the factor $SO(1,1)$ acts on $\mathbf{A}$, $\mathbf{B}$, $\underline{u}$ and $\underline{v}$ while the element in $SL(2,\mathbb{R})$ acts on $\underline{x}$. The complex Jacobian determinant in (u_κ, x_τ) and (v_σ, x_τ) is given respectively by

$$J_{\kappa\tau} = \frac{\partial u'_\kappa}{\partial u_\kappa} \frac{\partial x'_\tau}{\partial x_\tau},$$

and

$$K_{\sigma\tau} = \frac{\partial v'_\sigma}{\partial v_\sigma} \frac{\partial x'_\tau}{\partial x_\tau},$$

since the transformation of $\underline{u}$ and $\underline{v}$ do not depend on $\underline{x}$ and viceversa.

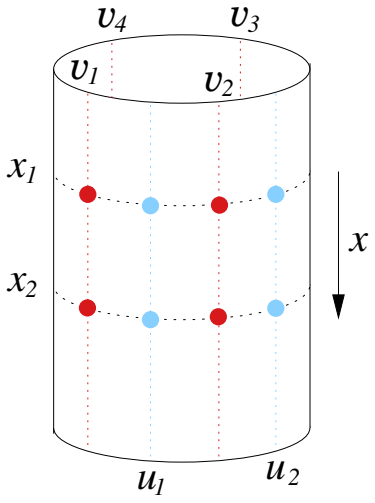

Figure 6.11: The partition function $Z_{\alpha,X}$ of an interval $X = [x_1, x_2]$ of a theory with pinchings at u_1, and u_2 and Fermi points at v_1, v_2 behaves under $SO(1,1) \times SL(2,\mathbb{R})$ as the expectation value of a product of homogeneous fields with dimension Δ_α inserted at the points (u_κ, x_τ), and with dimension $\Delta_\alpha/2$ at (v_σ, x_τ) where $\kappa = 1, 2$, $\sigma = 1, 2, 3, 4$ and $\tau = 1, 2$, with $v_3 = \overline{v}_2$ and $v_4 = \overline{v}_1$.

Hence under a general transformation in $SO(1,1) \times SL(2,\mathbb{R})$ the expressions (6.30) and (6.31) can be combined to give the following transformation law

$$Z'_\alpha(\underline{u}', \underline{v}'; \underline{x}') = \prod_{\kappa,\tau} J_{\kappa\tau}^{\Delta_\alpha} \prod_{\sigma,\tau} K_{\sigma\tau}^{\Delta_\alpha/2} Z_\alpha(\underline{u}, \underline{v}; \underline{x}).$$

This expression can be interpreted as the transformation of the expectation value, in a covariant theory in the cylinder $S^1 \times \mathbb{R}$, of homogeneous fields of dimension Δ_α inserted at the points (u_κ, x_τ) and of dimension $\Delta_\alpha/2$ inserted at (v_σ, x_τ). A particular example with $R = 2$, $Q = 4$ and $P = 1$ is represented in Fig. 6.11.

The previous picture is very attractive. It immediately suggests a generalisation of our results to larger groups containing the direct product of Möbius and conformal transformations. Also more general configurations for the insertion points could be envisaged. The form of the symbol $\hat{\mathcal{G}}(\theta)$ dictates that the discontinuities appear in pairs. If there is a discontinuity at θ there must be another similar at $-\theta$, except at $\theta = 0, -\pi$. This implies that pairs of insertions are related by inversion. An interesting point would be to break this constraint and consider a symbol with discontinuities located at arbitrary points.

However, whether the above program can be carried out, its meaning and further applications is an open question that we do no cover in this thesis.

Chapter 7

Sublogarithmic growth of the entanglement entropy

In the previous chapters we have found that the entanglement entropy of a fermionic chain may present different behaviours with the size of the chosen interval.

In Chapter 4, we saw that the entanglement entropy satisfies an area law in the ground state of a non critical chain with finite-range couplings and it saturates to a constant value in the large interval limit. On the other hand, if the mass gap becomes zero, the entanglement entropy grows with the logarithm of the length of the interval.

The presence of infinite-range couplings enriches the previous picture. In the fermionic ladders studied in Chapter 3, the leading term of the ground state entanglement entropy is proportional to the length of the interval (volume law). In Chapter 4 we found that in the Long-Range Kitaev chain the infinite-range interactions may give rise to a logarithmic growth of the entropy even when the system is non critical.

There are some recent works that address the possibility of other behaviours of the entanglement entropy with the size of the subsystem. In Ref. [159] Movassagh and Shor introduced a translational invariant, non critical and local spin chain in which the ground state entanglement entropy grows with the square root of the length of the interval. This surprising result has been extended to other spin chains, see e.g. [160, 161].

Some numerical studies [56] using Ising spin chains with long-range interactions also indicate the possibility of finding sublogarithmic terms in the entropy. This kind of behaviour is also found by Bianchini et al. in their study [162] of the entanglement entropy in non-unitary field theories. In particular, they obtained that sublogarithmic terms may arise in logarithmic conformal field theories.

In the light of those works, an interesting question is if we could engineer a fermionic chain with long-range couplings in which the entanglement entropy may display other behaviour, different from the linear or the logarithmic growth.

The basic analytical tools that we have employed to study the entanglement entropy have been the Strong Szegő Theorem and the Fisher-Hartwig conjecture for Toeplitz

determinants as well as their generalisations to the block Toeplitz case. According to these results, the entanglement entropy must grow linearly or logarithmically with the size of the subsystem, or tend to a constant value.

However, we have to bear in mind that these theorems cannot always be employed. The Strong Szegő Theorem is only valid for Toeplitz matrices generated by a smooth enough, non-zero symbol. The Fisher-Hartwig conjecture extends the former to symbols with discontinuities and/or zeros.

Therefore, an idea for looking for chains where the entanglement entropy presents other behaviours could be to study symbols that violate the hypothesis of the Strong Szegő Theorem and the Fisher-Hartwig conjecture. For example, symbols that are continuous (and therefore the Fisher-Hartwig conjecture does not apply) but not smooth enough according to the condition imposed by the Strong Szegő Theorem.

Interestingly enough, to our knowledge, there are not results in the literature that cover the asymptotic behaviour of Toeplitz determinants with a symbol of those characteristics.

In this Chapter, we shall propose a conjecture for the asymptotic behaviour of non smooth enough symbols generalising the Fisher-Hartwig conjecture. We shall check it numerically for a family of continuous symbols whose derivative diverges at a single point. We shall find that, for them, the conjecture is fulfilled and the leading term in the corresponding Toeplitz determinant is sublogarithmic. Finally, we shall apply this result to the entanglement entropy of a fermionic chain with pairing couplings that decay logarithmically with the distance.

7.1 The Fisher-Hartwig conjecture revisited

In this Section we shall see how Fisher and Hartwig arrived at their conjecture starting from the Strong Szegő Theorem (SST). This will allow us to establish a more general conjecture for the asymptotic behaviour of Toeplitz determinants with a continuous symbol that does not satisfy the smoothness condition of the SST.

We shall consider an integrable, real and positive function g defined on the unit circle S^1. We shall denote by $T_N[g]$ the Toeplitz matrix with symbol g and dimension $N \times N$. Its entries $(T_N[g])_{nm} = g_{n-m}$ are given by the Fourier coefficients of the function g,

$$g_k = \frac{1}{2\pi}\int_{-\pi}^{\pi} g(\theta)\mathrm{e}^{\mathrm{i}\theta k}\mathrm{d}\theta.$$

Let us also introduce the Fourier coefficients of $\log g$,

$$s_k = \frac{1}{2\pi}\int_{-\pi}^{\pi} \log g(\theta)\mathrm{e}^{\mathrm{i}\theta k}\mathrm{d}\theta.$$

We already enunciated the SST in Section 4.1. In the original theorem [101], Szegő considered that the symbol g must have a derivative satisfying the Hölder continuity condition for a non-zero exponent. In the following years, many mathematicians tried

to weaken this assumption. There is a plethora of papers were the SST is proved using different methods and considering more general symbols, see for instance the works by Kac [163], Baxter [164], Ibraginov [117] or Hirschman [165].

In particular, in the form due to Hirschman, the Strong Szegő Theorem establishes that the determinant $D_N[g]$ of the matrix $T_N[g]$ satisfies

$$\lim_{N\to\infty} \frac{D_N[g]}{\mathrm{e}^{Ns_0}} = \mathrm{e}^{\sum_{k=1}^{\infty} k s_k s_{-k}} < \infty \tag{7.1}$$

provided the Fourier coefficients of the symbol fulfil the condition

$$\sum_{k=-\infty}^{\infty} |g_k| + \sum_{k=-\infty}^{\infty} |k||g_k|^2 < \infty. \tag{7.2}$$

This is in some sense the weakest condition for the smoothness of the symbol g. As Devinatz showed in [166], for a real symbol such that $0 < g(\theta) < \infty$ the limit in (7.1) is finite if an only if g verifies (7.2).

It will be convenient to rewrite (7.1) in the form

$$\log D_N[g] = Ns_0 + \sum_{k=1}^{\infty} k s_k s_{-k} + o(1). \tag{7.3}$$

As we have seen in the previous chapters, in Physics we may deal with symbols that present discontinuities and, therefore, violate the smoothness condition (7.2). In fact, the work [167] by Wu on the classical Ising model and the study [168] of Lenard about impenetrable bosons led Fisher and Hartwig to conjecture a generalisation of the Strong Szegő theorem for symbols that present discontinuities and/or zeros [102]. Their conjecture was later proved by Basor in [104].

Consider that the symbol g is discontinuous at $\theta_1, \ldots, \theta_R$. According to the Fisher-Hartwig conjecture, the discontinuities contribute to $\log D_N[g]$ with a logarithmic term whose coefficient only depends on the lateral limits $g_r^{\pm} = \lim_{\theta\to\theta_r^{\pm}} g(\theta)$, $r = 1, \ldots, R$. That is,

$$\log D_N[g] = Ns_0 + \frac{\log N}{4\pi^2} \sum_{r=1}^{R} \left(\log \frac{g_r^+}{g_r^-} \right)^2 + \log E[g] + o(1). \tag{7.4}$$

Remember that we used this result in Chapters 3 and 4 to compute the asymptotic behaviour of the entanglement entropy. In section 4.1 we generalised it to the determinant of block Toeplitz matrices generated by matrix valued symbols with discontinuities.

Let us review the reasoning followed by Fisher and Hartwig in [102] to deduce the expansion (7.4) because it will be the basis of our generalisation of their conjecture for non smooth symbols.

For simplicity, and as they precisely did, we take the symbol

$$g_0(\theta) = \mathrm{e}^{\beta(\theta - \pi \mathrm{sign}(\theta))}, \quad \theta \in [-\pi, \pi), \tag{7.5}$$

that only has a discontinuity at $\theta = 0$.

The Fourier coefficients of its logarithm are

$$s_0^{(0)} = 0, \quad \text{and} \quad s_k^{(0)} = \frac{\beta}{\mathrm{i}k}, \quad \text{for} \quad k \neq 0.$$

Then if we apply to this symbol the Strong Szegő Theorem (7.3) we obtain the Harmonic series

$$\log D_N[g_0] = N s_0^{(0)} + \sum_{k=1}^{\infty} k s_k^{(0)} s_{-k}^{(0)} + o(1) = \sum_{k=1}^{\infty} \frac{\beta^2}{k} + o(1),$$

that diverges logarithmically.

Let us suppose that $\log D_N[g_0]$ can be obtained truncating the series $\sum_{k=1}^{\infty} k s_k^{(0)} s_{-k}^{(0)}$ at some $k = \lfloor N\Lambda_0 \rfloor$, with Λ_0 a positive real number. Here $\lfloor t \rfloor$ means to take the integer part of the real number t. Then we find

$$\log D_N[g_0] = \sum_{k=1}^{\lfloor N\Lambda_0 \rfloor} k s_k^{(0)} s_{-k}^{(0)} = \sum_{k=1}^{\lfloor N\Lambda_0 \rfloor} \frac{\beta^2}{k} = \beta^2 \log(N\Lambda_0) + \beta^2 \gamma_{\mathrm{E}} + o(1), \tag{7.6}$$

where γ_{E} is the Euler-Mascheroni constant.

Observe that this truncation gives precisely the Fisher-Hartwig expansion (7.4) for the symbol g_0. In fact, since $g_0(\theta)$ presents a single discontinuity ($R = 1$) with lateral limits $\mathrm{e}^{\pm\beta\pi}$, the expression in (7.4) particularises to

$$\log D_N[g_0] = \beta^2 \log N + \log E[g_0] + o(1). \tag{7.7}$$

Comparing (7.7) with (7.6) we can conclude that

$$\log E[g_0] = \beta^2(\log \Lambda_0 + \gamma_{\mathrm{E}}). \tag{7.8}$$

Fisher and Hartwig were able to fix the constant term $E[g_0]$ and, therefore, the cut-off parameter Λ_0 because they realised that the Toeplitz matrix with symbol g_0 is also a Cauchy matrix[1]. Using the properties of the determinants of Cauchy matrices they determined that

$$E[g_0] = G(1 + \mathrm{i}\beta)G(1 - \mathrm{i}\beta)$$

where $G(z)$ is the Barnes G-function. Hence we have

$$\log \Lambda_0 = 2\beta^{-2} \log |G(1 + \mathrm{i}\beta)| - \gamma_{\mathrm{E}}. \tag{7.9}$$

The same reasoning can be applied to a general symbol with R discontinuities. The asymptotic behaviour of its determinant predicted by (7.4) can be deduced from the Strong Szegő theorem (7.3) truncating the divergent terms in the series $\sum_{k=1}^{\infty} k s_k s_{-k}$.

The previous discussion suggests that one could deduce heuristically from the Strong Szegő Theorem the asymptotic behaviour of a Toeplitz determinant generated by a symbol that violates the smoothness condition (7.2). When this happens the series in (7.3) diverges. We propose that the truncation of this series at $k = \lfloor N\Lambda \rfloor$, with Λ certain positive real number, accounts for the asymptotic expansion of the Toeplitz determinant.

[1] A matrix is of Cauchy type if its entries are of the form $C_{nm} = (X_n - Y_m)^{-1}$ with $X_n - Y_m \neq 0$, and $X_n, Y_m \in \mathbb{C}$ where $n, m \in \mathbb{N}$.

That is, if the symbol g is not smooth enough, then the corresponding determinant behaves as

$$\log D_N[g] = Ns_0 + \sum_{k=1}^{\lfloor N\Lambda \rfloor} k s_k s_{-k} + o(1).$$

In the next section we shall check this conjecture for a family of continuous symbols that does not satisfy the smoothness condition of the Strong Szegő Theorem.

7.2 Generalisation of the Fisher-Hartwig conjecture

Consider the symbols of the form

$$\log g_\nu(\theta) = \beta \frac{\theta - \pi\,\mathrm{sign}(\theta)}{\left(-\log \frac{|\theta|}{2\pi}\right)^\nu}, \quad \theta \in [-\pi, \pi), \tag{7.10}$$

with $\beta < 1$ and $\nu \geq 0$.

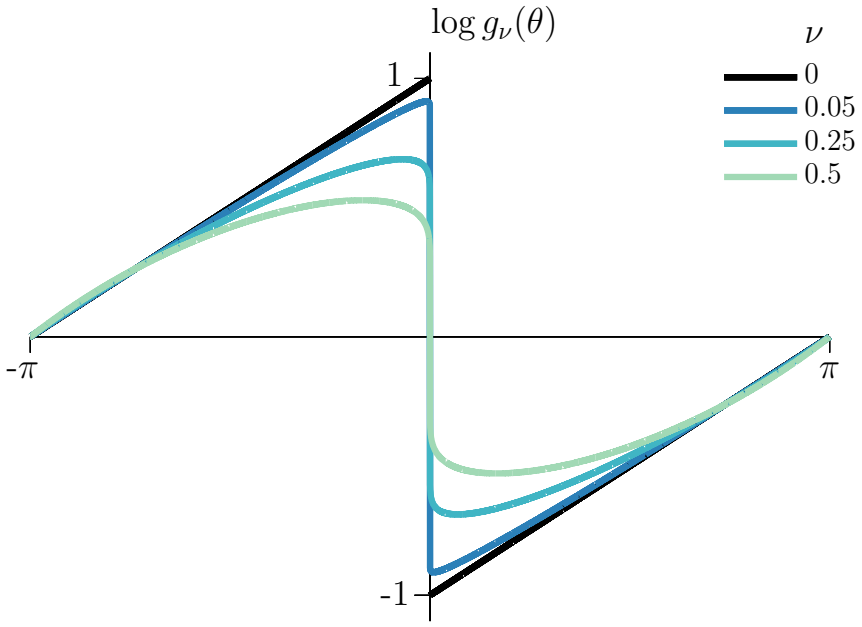

Figure 7.1: Plot of the logarithm of the symbol g_ν defined in (7.10), taking $\beta = 1/\pi$ and different values for the exponent ν. If $\nu = 0$ the function $g_0(\theta)$ is discontinuous at $\theta = 0$. When $\nu > 0$ the symbol is continuous for all θ but its derivative diverges at $\theta = 0$.

In Fig. 7.1 we plot $\log g_\nu(\theta)$ for $\beta = 1/\pi$ and different values of ν. It is a family of positive bounded functions, $0 < g_\nu(\theta) < \infty$. For $\nu \neq 0$, the function is continuous but it is non analytical at $\theta = 0$ since its derivative diverges at this point. For $\nu = 0$, it reduces to the symbol (7.5), already studied above, that has a discontinuity at $\theta = 0$. Then in this limiting case the Fisher-Hartwig conjecture can be applied.

According to the discussion in the previous section, in order to determine the asymptotic behaviour of the Toeplitz determinant generated by g_ν, we have to study the convergence of the series

$$\sum_{k=1}^{\infty} k s_k^{(\nu)} s_{-k}^{(\nu)}, \tag{7.11}$$

where $s_k^{(\nu)}$ are the Fourier coefficients of $\log g_\nu$,

$$s_k^{(\nu)} = \frac{1}{2\pi} \int_{-\pi}^{\pi} \log g_\nu(\theta) \mathrm{e}^{\mathrm{i}k\theta} \mathrm{d}\theta.$$

In Appendix E we calculate the asymptotic form of $s_k^{(\nu)}$ for large k. We find

$$s_k^{(\nu)} \sim \frac{\beta}{\mathrm{i}k(\log|k|)^\nu} \left[1 + O\left(\frac{1}{\log|k|}\right)\right]. \tag{7.12}$$

Therefore, the series (7.11) converges if and only if

$$\sum_{k=2}^{\infty} \frac{\beta^2}{k(\log k)^{2\nu}} < \infty.$$

Using for instance the integral test it is immediate to see that the latter diverges for $0 \leq \nu \leq 1/2$. Thus for these values of the exponent ν the Strong Szegő theorem (7.3) is not valid to determine the asymptotic behaviour of $D_N[g_\nu]$. We emphasize again that for $\nu \neq 0$ the function is continuous and we can neither employ the Fisher-Hartwig conjecture that only applies to symbols with discontinuities and/or zeros.

Therefore, we have to resort to the conjecture that we have proposed at the end of the previous section. According to it, there exists a positive and real number Λ_ν, that depends on ν, such that the asymptotic behaviour of the Toeplitz determinant with symbol g_ν is given by

$$\log D_N[g_\nu] = N s_0^{(\nu)} + \sum_{k=1}^{\lfloor N\Lambda_\nu \rfloor} k s_k^{(\nu)} s_{-k}^{(\nu)} + o(1).$$

Since $\log g_\nu(\theta)$ is an odd function then $s_{-k}^{(\nu)} = -s_k^{(\nu)}$. Hence $s_0^{(\nu)} = 0$, the linear term in $\log D_N[g_\nu]$ cancels, and

$$\log D_N[g_\nu] = \sum_{k=1}^{\lfloor N\Lambda_\nu \rfloor} k |s_k^{(\nu)}|^2 + o(1). \tag{7.13}$$

This conjecture predicts a sublogarithmic growth of $\log D_N[g_\nu]$ with the dimension N. In fact, if we consider the asymptotic behaviour (7.12) found for $s_k^{(\nu)}$ and we approximate the sum in (7.13) by an integral,

$$\sum_{k=1}^{\lfloor N\Lambda_\nu \rfloor} k |s_k^{(\nu)}|^2 \sim \int_{1+\epsilon}^{N\Lambda_\nu} \frac{\beta^2}{\theta(\log\theta)^{2\nu}} \left[1 + O\left(\frac{1}{\log\theta}\right)\right] \mathrm{d}\theta \tag{7.14}$$

where $\epsilon > 0$. The error that we make approximating the sum by the integral is of the order of $N^{-1}(\log N)^{-2\nu}$.

Therefore, for $0 < \nu < 1/2$ we have

$$\sum_{k=1}^{\lfloor N\Lambda_\nu \rfloor} k|s_k^{(\nu)}|^2 \;\sim\; \frac{\beta^2}{1-2\nu}(\log N\Lambda_\nu)^{1-2\nu} + O\left(\frac{1}{(\log N)^{2\nu}}\right).$$

Observe that the contribution of the subleading terms in the asymptotic behaviour (7.12) of the Fourier coefficients $s_k^{(\nu)}$ tends to zero in the limit $N \to \infty$.

If we take into account that

$$(\log N\Lambda_\nu)^{1-2\nu} = (\log N)^{1-2\nu}\left(1 + \frac{\log \Lambda_\nu}{\log N}\right)^{1-2\nu},$$

and employ the expansion $(1+z)^p = 1 + pz + O(z^2)$ for $|z| < 1$ and $p > 0$, we find

$$\sum_{k=1}^{\lfloor N\Lambda_\nu \rfloor} k|s_k^{(\nu)}|^2 \;\sim\; \frac{\beta^2}{1-2\nu}(\log N)^{1-2\nu} + o(1), \;\text{ if } \; 0 < \nu < 1/2.$$

On the other hand, for $\nu = 1/2$, the approximation in (7.14) leads to

$$\sum_{k=1}^{\lfloor N\Lambda_\nu \rfloor} k|s_k^{(\nu)}|^2 \;\sim\; \beta^2 \log\log N\Lambda_\nu + O\left(\frac{1}{\log N}\right).$$

Expressing the latter as

$$\log\log(N\Lambda_\nu) = \log\log N + \log\left(1 + \frac{\log \Lambda_\nu}{\log N}\right),$$

and applying the expansion $\log(1+z) = z + O(z^2)$ when $|z| < 1$, then

$$\sum_{k=1}^{\lfloor N\Lambda_\nu \rfloor} k|s_k^{(\nu)}|^2 \;\sim\; \beta^2 \log\log N + o(1).$$

Finally, putting these results in the conjecture (7.13) we can conclude that

$$\log D_N[g_\nu] = \frac{\beta^2}{1-2\nu}(\log N)^{1-2\nu} + o(1), \;\text{ if } \; 0 < \nu < 1/2,$$

and

$$\log D_N[g_{1/2}] = \beta^2 \log\log N + o(1), \;\text{ if } \; \nu = 1/2.$$

Observe that for $\nu = 0$ the conjecture (7.13) gives the Fisher-Hartwig expansion (7.6) with Λ_0 that given in (7.9).

Let us check (7.13) numerically. Since $\log D_N[g_\nu]$ grows sublogarithmically with the dimension N, we have to calculate it for a range of N larger than in the previous chapters. In fact, notice that $(\log 100)^{0.25} = 1.46491\ldots$ and, if we increase N two orders of magnitude, $(\log 10000)^{0.25} = 1.74208\ldots$ The problem is that if we go to larger values of N, we must diagonalise matrices of dimensions that are impossible to cope with a standard computer.

In principle, since the entries of a Toeplitz matrix only depend on the difference between the row and the column, the complete matrix is determined specifying a single row or column. However, we do not know any specific routine for computing Toeplitz determinants that makes use of this property. Hence it is needed to store the N^2 complex entries to calculate the determinant. If we work in double precision in C, each entry typically occupies 8 bytes of RAM memory. Thus, making a crude estimate, if the dimension of the matrix is $N = 20000$, we will need around 6 GB of memory, and if we take $N = 50000$, the amount of memory required increases to 37 GB.

We have bypassed that difficulty by performing the numerical calculations in the supercomputer *Memento*, managed by the Instituto de Biocomputación y Física de Sistemas Complejos, at the University of Zaragoza [169]. Each node of this cluster has 256 GB of memory. This has allowed us to reach dimensions of the order of $N = 10^5$. We have computed $\log D_N[g_\nu]$ from the spectrum of the matrix that has been obtained using the routines for Hermitian matrices provided in the *Intel MKL library* [170]. This library allows to parallelise the diagonalisation, taking advantage of the 64 cores available in each node of *Memento*. We describe the details of the numerical calculations in Appendix A.

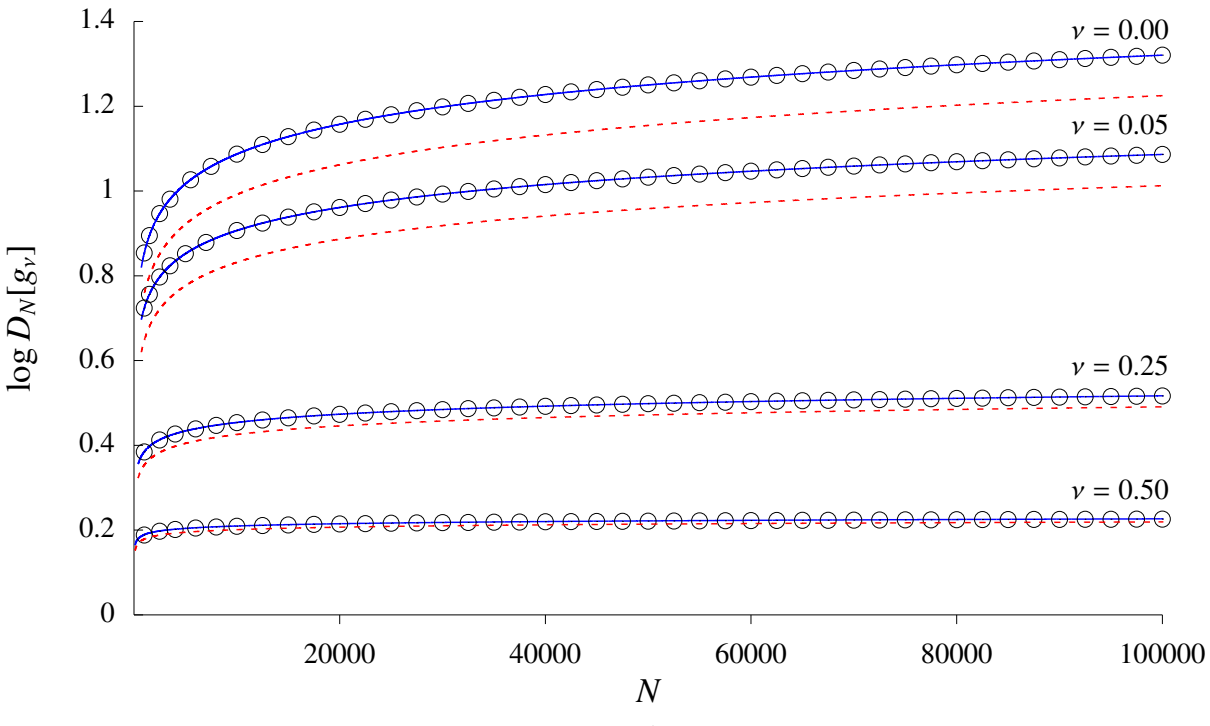

Figure 7.2: Logarithm of the Toeplitz determinant with symbol the function g_ν defined in (7.10). We represent it against the dimension N. The dots correspond to the numerical values obtained using *Memento* for different exponents ν and $\beta = 1/\pi$. When $0 \leq \nu \leq 1/2$, g_ν does not satisfy the smoothness condition (7.2) of the Strong Szegő Theorem. The solid lines represent the conjecture proposed in (7.13) for the asymptotic behaviour of $\log D_N[g_\nu]$, $\sum_{k=1}^{\lfloor N\Lambda_\nu \rfloor} k|s_k^{(\nu)}|^2$, with Λ_ν those given in Table 7.1. For $\nu = 0$ the symbol is discontinuous and we can apply the Fisher-Hartwig conjecture. In this case Λ_0 can be directly calculated using (7.9). The dashed lines correspond to the sum $\sum_{k=1}^{N} k|s_k^{(\nu)}|^2$, that is, considering $\Lambda_\nu = 1$.

In Fig. 7.2, the dots represent the numerical values calculated with *Memento* for

$\log D_N[g_\nu]$ with $\nu = 0, 0.05, 0.25$, and 0.50. The dashed lines represent the sum

$$\sum_{k=1}^{N} k|s_k^{(\nu)}|^2, \tag{7.15}$$

that is, assuming $\Lambda_\nu = 1$. The Fourier coefficients $s_k^{(\nu)}$ have been computed numerically for each ν as we explain in Appendix A. Comparing the dashed lines with the numerical points it is clear the necessity of considering a cut-off Λ_ν different from the unity. We have estimated its value for each ν as follows.

Consider the difference between taking $\Lambda_\nu = 1$ and $\Lambda_\nu > 1$,

$$\sum_{k=N}^{\lfloor N\Lambda_\nu \rfloor} k|s_k^{(\nu)}|^2.$$

For large N, if we apply the asymptotic expansion of $s_k^{(\nu)}$ up to first order corrections, see Eq. (E.3) in Appendix E,

$$s_k^{(\nu)} \sim -\frac{\mathrm{i}\beta}{k(\log|k|)^\nu} + \frac{\mathrm{i}\nu\beta(\log(2\pi)+\gamma_{\mathrm{E}})}{k(\log|k|)^{\nu+1}},$$

and we approximate the sum by an integral, we have

$$\sum_{k=N}^{\lfloor N\Lambda_\nu \rfloor} k|s_k^{(\nu)}|^2 \sim \int_N^{N\Lambda_\nu} \left(\frac{\beta^2}{\theta(\log\theta)^{2\nu}} - \frac{2\nu\beta^2(\log(2\pi)+\gamma_{\mathrm{E}})}{\theta(\log\theta)^{2\nu+1}} \right) \mathrm{d}\theta.$$

The first term in the integral gives

$$\begin{aligned} \int_N^{N\Lambda_\nu} \frac{\beta^2}{\theta(\log\theta)^{2\nu}}\mathrm{d}\theta &= \frac{\beta^2}{1-2\nu}(\log N)^{1-2\nu}\left[\left(1+\frac{\log\Lambda_\nu}{\log N}\right)^{1-2\nu} - 1\right] \\ &= \frac{\beta^2\log\Lambda_\nu}{(\log N)^{2\nu}} - \frac{\nu\beta^2(\log\Lambda_\nu)^2}{(\log N)^{2\nu+1}} + O\left((\log N)^{-2\nu-2}\right), \end{aligned}$$

where we have employed the expansion $(1+z)^p = 1+pz+p(p-1)z^2/2+O(z^3)$ for $|z|<1$.

With respect to the second term in the integral, we follow the same lines

$$\begin{aligned} \int_N^{N\Lambda_\nu} \frac{2\nu\beta^2(\log(2\pi)+\gamma_{\mathrm{E}})}{\theta(\log\theta)^{2\nu+1}}\mathrm{d}\theta &= -\beta^2(\log(2\pi)+\gamma_{\mathrm{E}})(\log N)^{-2\nu}\left[\left(1+\frac{\log\Lambda_\nu}{\log N}\right)^{-2\nu} - 1\right] \\ &= \frac{2\nu(\log(2\pi)+\gamma_{\mathrm{E}})\beta^2\log\Lambda_\nu}{(\log N)^{2\nu+1}} + O\left((\log N)^{-2\nu-2}\right). \end{aligned}$$

Putting all together, we have

$$\sum_{k=N}^{\lfloor N\Lambda_\nu \rfloor} k|s_k^{(\nu)}|^2 \sim \frac{\beta^2\log\Lambda_\nu}{(\log N)^{2\nu}} - \frac{2\nu(\log(2\pi)+\gamma_{\mathrm{E}})\beta^2\log\Lambda_\nu + \nu\beta^2(\log\Lambda_\nu)^2}{(\log N)^{2\nu+1}}. \tag{7.16}$$

Therefore, a way to estimate Λ_ν is to calculate the difference between the numerical values obtained for $\log D_N[g_\nu]$ and the sum $\sum_{k=1}^{N} k|s_k^{(\nu)}|^2$ and use the result to fit the function on the right hand side of (7.16) where Λ_ν is the only parameter to be adjusted.

In order to perform the fit, we have considered the numerical values obtained in the interval $N \in [10^4, 10^5]$. Taking into account that $\beta = 1/\pi$, in Table 7.1 we indicate the values of Λ_ν that give the best fit.

ν	Λ_ν
0.00	2.566
0.05	2.599
0.25	2.659
0.50	2.660

Table 7.1: Values of Λ_ν for different ν and $\beta = 1/\pi$ obtained by fitting the curve on the right hand side of (7.16) to the difference between the numerical values computed for $\log D_N[g_\nu]$ and the sum $\sum_{k=1}^{N} k|s_k^{(\nu)}|^2$. The case $\nu = 0.00$ has been calculated using the expression (7.9).

The solid lines in Fig. 7.2 represent the sum $\sum_{k=1}^{\lfloor N\Lambda_\nu \rfloor} k|s_k^{(\nu)}|^2$ using the values for the cut-off Λ_ν collected in Table 7.1. The agreement between them and the numerical points is outstanding.

In Fig. 7.3, we represent separately the same results for each value of ν considered. In the inset of these figures we have plotted the difference between the numerical values obtained for the determinant and our prediction,

$$\Delta(N) = \log D_N[g_\nu] - \sum_{k=1}^{\lfloor N\Lambda_\nu \rfloor} k|s_k^{(\nu)}|^2. \tag{7.17}$$

We have found that the best fit to this difference is the curve

$$\Delta(N) \approx \frac{a}{N^b},$$

with the value for the coefficients a and b indicated in Table 7.2.

ν	a $(\times 10^{-3})$	b
0.05	1.65	0.149
0.25	2.84	0.205
0.50	1.37	0.232

Table 7.2: Coefficients a and b that give the best fit of the curve a/N^b to the difference between the outcomes in the numerical calculation of $\log D_N[g_\nu]$ and the conjectured behaviour $\sum_{k=1}^{\lfloor N\Lambda_\nu \rfloor} k|s_k^{(\nu)}|^2$ using for Λ_ν the values determined in Table 7.1.

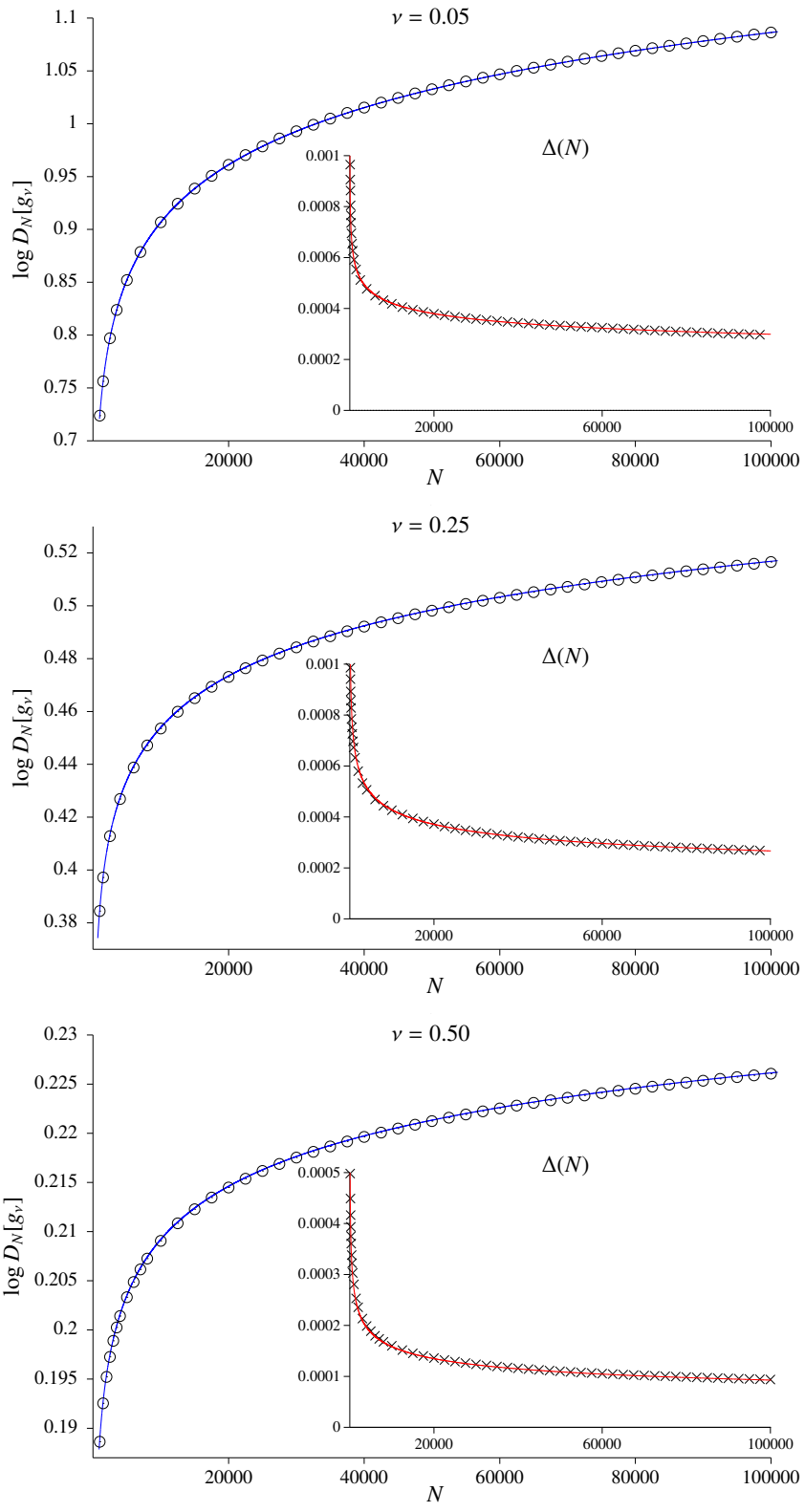

Figure 7.3: Logarithm of the Toeplitz determinant generated by the symbol g_ν defined in (7.10) for $\beta = 1/\pi$, and $\nu = 0.05$ (up), 0.25 (middle) and 0.50 (bottom). The dots correspond to the numerical results obtained for the determinant varying the dimension N while the solid line represents the conjecture $\sum_{k=1}^{\lfloor N\Lambda_\nu \rfloor} k|s_k^{(\nu)}|^2$ using as Λ_ν the values given in Table 7.1. In the inset the crosses are the difference (7.17) between the numerical values and the prediction. The solid line in the inset corresponds to the curve a/N^b with the coefficients a and b those specified in Table 7.2. This curve is the best fit that we have found for $\Delta(N)$.

In the previous chapters we found some novel properties of the asymptotic behaviour of (block) Toeplitz determinants. It is interesting to study if they are also satisfied for the symbol g_ν.

7.2.1 Determinant of a principal submatrix

In Section 6.2, we proposed and checked numerically a conjecture for the asymptotic behaviour of the determinant of a principal submatrix of a block Toeplitz matrix. We employed this result to analyse the entanglement entropy for several disjoint intervals.

Let us repeat the analysis performed in that section for the symbol g_ν. Consider the restriction of the Toeplitz matrix generated by g_ν to a subset of indices X, that we denote $T_X[g_\nu]$. For simplicity, let us assume that $X = [x_1, x_2] \cup [x_3, x_4]$. Then, according to the conjecture established in (6.8), the determinant $D(X) = \det T_X[g_\nu]$ should behave as

$$D\left([x_1, x_2] \cup [x_3, x_4]\right) \simeq \frac{D([x_1, x_4])D([x_1, x_2])D([x_2, x_3])D([x_3, x_4])}{D([x_1, x_3])D([x_2, x_4])} \tag{7.18}$$

where $\simeq$ stands for the equality of the asymptotic behaviour when $|x_\tau - x_{\tau'}| \to \infty$ for $\tau, \tau' = 1, \ldots, 4$.

The determinants on the right hand side of (7.18) correspond to Toeplitz matrices with symbol g_ν. Then we can apply to them the conjecture (7.13),

$$\log D([x_\tau, x_{\tau'}]) = \sum_{k=1}^{\lfloor N_{\tau,\tau'}\Lambda_\nu \rfloor} k|s_k^{(\nu)}|^2 + o(1), \tag{7.19}$$

where $N_{\tau,\tau'} = |x_\tau - x_{\tau'}|$.

As we did in Section 6.2, in order to check the validity of the expression (7.18) we introduce the quantity

$$I_D\left([x_1, x_2] \cup [x_3, x_4]\right) = \log D([x_1, x_2]) + \log D([x_3, x_4]) - \log D\left([x_1, x_2] \cup [x_3, x_4]\right). \tag{7.20}$$

Applying (7.18), we have

$$I_D([x_1, x_2] \cup [x_3, x_4]) \simeq -\log \frac{D([x_1, x_4])D([x_2, x_3])}{D([x_1, x_3])D([x_2, x_4])}.$$

Considering now the expected asymptotic behaviour (7.19) for the Toeplitz determinants $D([x_\tau, x_{\tau'}])$, $\tau, \tau' = 1, \ldots, 4$, we arrive at

$$I_D\left([x_1, x_2] \cup [x_3, x_4]\right) \simeq \sum_{p,p'=1}^{2} (-1)^{p+p'} \sum_{k=1}^{\lfloor N_{p,p'+2}\Lambda_\nu \rfloor} k|s_k^{(\nu)}|^2. \tag{7.21}$$

In Fig. 7.4 we have evaluated numerically I_D for the exponents $\nu = 0.05$, 0.25 and 0.50 taking $\beta = 1/\pi$. The solid line corresponds to the prediction that we have just obtained in (7.21). In order to plot it, we have computed numerically the Fourier coefficients $s_k^{(\nu)}$

and we have assumed for Λ_ν the values estimated in Table 7.1. The agreement between the numerical outcome and the expected behaviour is outstanding. This also reinforces the conjecture proposed for the Toeplitz determinants with symbol g_ν.

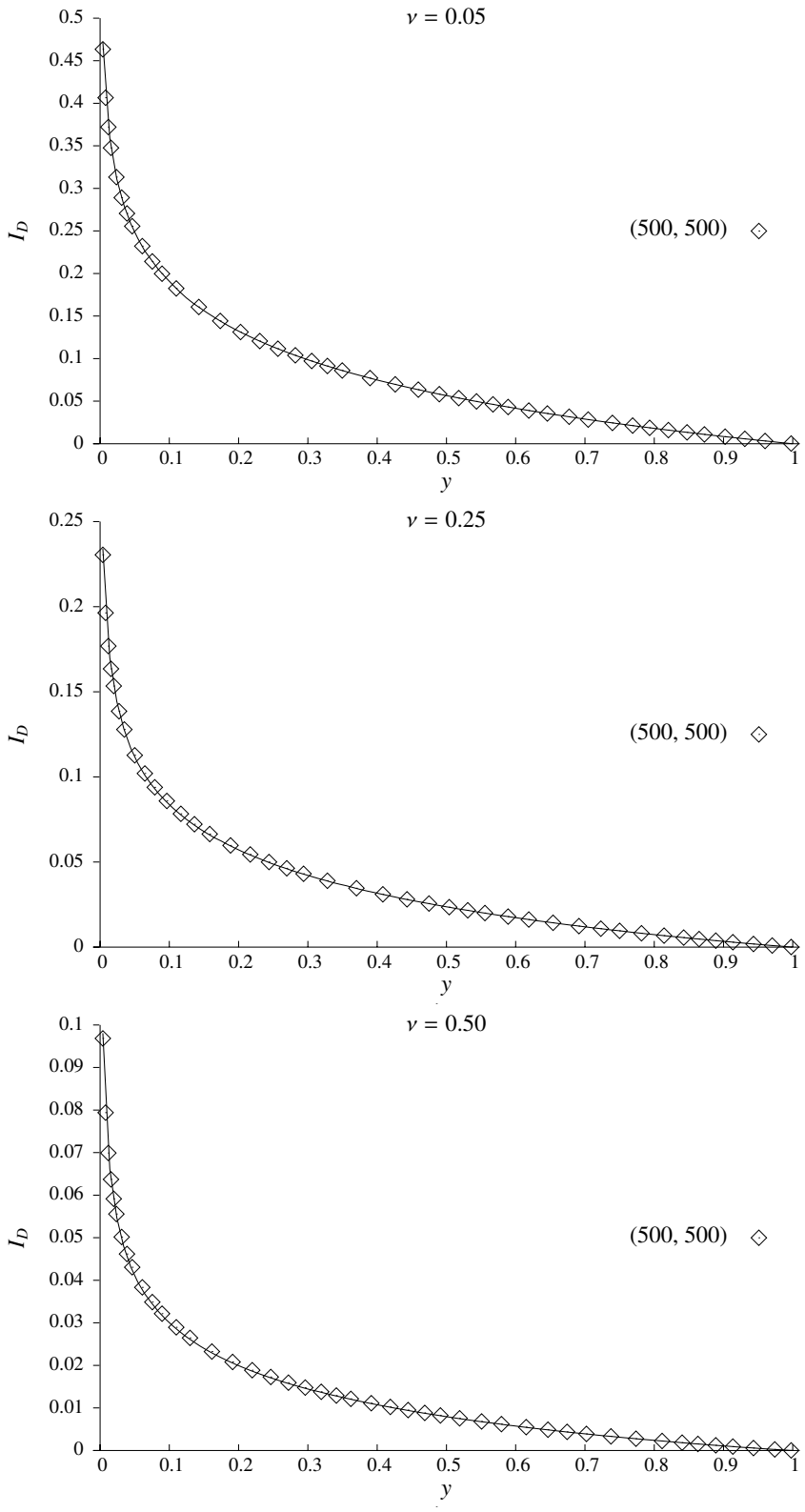

Figure 7.4: Difference between the determinants (7.20) for the symbol g_ν defined in (7.10) considering $\beta = 1/\pi$ and $\nu = 0.05$ (up), 0.25 (middle) and 0.5 (bottom). We represent it as a function of the cross-ratio (4.57) $y = (x_1, x_2; x_4, x_3)$. In all the cases we have taken $|x_1 - x_2| = |x_3 - x_4| = 500$ and we have modified the distance $|x_2 - x_3|$ from 1 up to 10000. The dots $\diamond$ are the results of the numerical calculations while the solid line corresponds to the conjecture (7.21) using as Λ_ν the values given in Table 7.1 for each ν.

7.3 Entanglement in a Kitaev chain with logarithmic decaying couplings

In this section we shall apply the mathematical results found previously to the study of the Rényi entanglement entropy in the following fermionic chain,

$$H_{\log} = \sum_{n=1}^{N} \left(h a_n^\dagger a_n + a_n^\dagger a_{n+1} + a_{n+1}^\dagger a_n \right) + \sum_{n=1}^{N} \sum_{l=-N/2}^{N/2} \frac{1}{l(\log(A|l|))^\nu} \left(a_n^\dagger a_{n+l}^\dagger - a_n a_{n+l} \right), \tag{7.22}$$

where the pairing couplings decay logarithmically with an exponent $0 \leq \nu \leq 1/2$ and $A > 1$. We shall consider $h \neq \pm 2$. The value $\nu = 0$ corresponds to the Long-Range Kitaev chain introduced in Section 2.2.3. We found in Section 4.6 that in this case the ground state entanglement entropy grows logarithmically with the size of the subsystem.

According to the general discussion of Section 2.1, in the limit $N \to \infty$, the dispersion relation of $H_{\log}$ is

$$\omega_{\log}(\theta) = \sqrt{F(\theta)^2 + |G_\nu(\theta)|^2},$$

where

$$F(\theta) = h + 2\cos(\theta),$$

and

$$G_\nu(\theta) = \sum_{l=1}^{\infty} \frac{1}{l(\log(A|l|))^\nu} \left(\mathrm{e}^{\mathrm{i}\theta l} - \mathrm{e}^{-\mathrm{i}\theta l} \right).$$

Observe that the Fourier coefficients of G_ν, $1/(l(\log A|l|)^\nu)$, are similar to the leading term in the expansion (7.12) for the Fourier coefficients $s_k^{(\nu)}$ of the function $\log g_\nu$ introduced in (7.10). Hence the behaviour of $G_\nu(\theta)$ in a neighbourhood of $\theta = 0$ is equal to that of $\log g_\nu(\theta)$. We have seen that the divergence in the derivative of $\log g_\nu(\theta)$ at $\theta = 0$ violates the smoothness condition (7.2) of the Strong Szegő Theorem when $0 < \nu \leq 1/2$. This divergence gives rise to a sublogarithmic growth of the Toeplitz determinant with symbol g_ν. Since $G_\nu(\theta)$ displays the same behaviour at $\theta = 0$, we expect that this affects the asymptotics of the ground state entanglement entropy.

We shall derive the Rényi entanglement entropy for a subsystem X of this chain using

$$S_{\alpha,X} = \frac{1}{4\pi\mathrm{i}} \lim_{\varepsilon \to 1^+} \oint_{\mathscr{C}} f_\alpha(\lambda/\varepsilon) \frac{\mathrm{d}}{\mathrm{d}\lambda} \log D_X(\lambda) \mathrm{d}\lambda, \tag{7.23}$$

where $\mathscr{C}$ is the integration contour represented in Fig. 2.5 and $D_X(\lambda) = \det(\lambda I - V_X)$ with V_X the restriction of the ground state correlation matrix to X. Remember that if the subsystem is a single interval of length $|X|$ then V_X is a block Toeplitz matrix with entries

$$(V_X)_{nm} = \frac{1}{2\pi} \int_{-\pi}^{\pi} \mathcal{G}(\theta) \mathrm{e}^{\mathrm{i}\theta(n-m)} \mathrm{d}\theta, \quad n, m = 1, \ldots, |X|,$$

and symbol $\mathcal{G}(\theta)$, the 2×2 matrix

$$\mathcal{G}(\theta) = \frac{1}{\omega_{\log}(\theta)} \begin{pmatrix} F(\theta) & G_\nu(\theta) \\ -G_\nu(\theta) & -F(\theta) \end{pmatrix}.$$

Our goal is to derive the leading term in the asymptotic expansion of the block Toeplitz determinant $D_X(\lambda)$ with symbol $\mathcal{G}_\lambda = \lambda I - \mathcal{G}$. The techniques developed in the previous section are valid for Toeplitz matrices, that is, when the symbol is a scalar function. Therefore, the first step in order to analyse the asymptotic behaviour of $D_X(\lambda)$ is to express it in terms of Toeplitz determinants.

For this purpose, let us perform the following global change of basis,

$$\mathcal{G}_\lambda(\theta) = \frac{1}{2}\begin{pmatrix} 1 & 1 \\ -1 & 1 \end{pmatrix} \mathcal{G}'_\lambda(\theta) \begin{pmatrix} 1 & -1 \\ 1 & 1 \end{pmatrix}$$

where

$$\mathcal{G}'_\lambda(\theta) = \begin{pmatrix} \lambda & \mathrm{e}^{\mathrm{i}\xi(\theta)} \\ \mathrm{e}^{-\mathrm{i}\xi(\theta)} & \lambda \end{pmatrix}.$$

and

$$\cos\xi(\theta) = \frac{F(\theta)}{\sqrt{F(\theta)^2 + |G_\nu(\theta)|^2}}, \quad \sin\xi(\theta) = \frac{\mathrm{i}G_\nu(\theta)}{\sqrt{F(\theta)^2 + |G_\nu(\theta)|^2}}. \tag{7.24}$$

The determinants of the block Toeplitz matrices with $\mathcal{G}_\lambda$ and $\mathcal{G}'_\lambda$ are equal and, therefore,

$$\log D_X(\lambda) = \log D_X[\mathcal{G}'_\lambda].$$

In the following, it will be convenient to work with the symbol $\mathcal{G}'_\lambda$ instead of $\mathcal{G}_\lambda$.

We introduce now the symbol

$$\tilde{\mathcal{G}}_\lambda(\theta) = \begin{pmatrix} \lambda & \mathrm{e}^{\mathrm{i}|\xi(\theta)|} \\ \mathrm{e}^{-\mathrm{i}|\xi(\theta)|} & \lambda \end{pmatrix}.$$

The behaviour of $|\xi(\theta)|$ in the neighbourhood of $\theta = 0$ is similar to that of $|\log g_\nu(\theta)|$. If we calculate the leading term of the Fourier coefficients $\tilde{s}_k^{(\nu)}$ of $|\log g_\nu(\theta)|$ using the same steps as in Appendix E we find

$$\tilde{s}_k^{(\nu)} = O\left(\frac{1}{k(\log|k|)^{\nu+1}}\right).$$

This means that

$$\sum_{k=1}^{\infty} k\tilde{s}_k^{(\nu)}\tilde{s}_{-k}^{(\nu)} < \infty$$

for any $\nu > 0$ and the smoothness condition (7.2) of the Strong Szegő Theorem is satisfied. Therefore, one may conclude that the symbol $\tilde{\mathcal{G}}_\lambda$ is also smooth and verifies the Widom theorem for block Toeplitz determinants (4.6).

Since $\tilde{\mathcal{G}}_\lambda$ is smooth, we can apply the Basor localisation theorem (4.9) to the product of symbols $\mathcal{G}'_\lambda\tilde{\mathcal{G}}_\lambda^{-1}$. Then we have

$$\lim_{|X|\to\infty} \frac{D_X[\mathcal{G}'_\lambda\tilde{\mathcal{G}}_\lambda^{-1}]}{D_X[\mathcal{G}'_\lambda]D_X[\tilde{\mathcal{G}}_\lambda^{-1}]} < \infty.$$

This implies that

$$\log D_X(\lambda) = \log D_X[\mathcal{G}'_\lambda] = \log D_X[\mathcal{G}'_\lambda\tilde{\mathcal{G}}_\lambda^{-1}] - \log D_X[\tilde{\mathcal{G}}_\lambda^{-1}] + O(1).$$

We can make use of Widom theorem (4.6) to derive the asymptotic behaviour of $\log D_X[\tilde{\mathcal{G}}_\lambda^{-1}]$. According to it,

$$\log D_X[\tilde{\mathcal{G}}_\lambda^{-1}] = -\log(\lambda^2-1)|X| + O(1)$$

because $\det \tilde{\mathcal{G}}_\lambda^{-1}(\theta) = (\lambda^2-1)^{-1}$. Therefore,

$$\log D_X(\lambda) = \log D_X[\mathcal{G}'_\lambda \tilde{\mathcal{G}}_\lambda^{-1}] + \log(\lambda^2-1)|X| + O(1). \tag{7.25}$$

Observe that, by the definition of $\tilde{\mathcal{G}}_\lambda$, the product $\mathcal{G}'_\lambda\tilde{\mathcal{G}}_\lambda^{-1}$ is

$$\mathcal{G}'_\lambda(\theta)\tilde{\mathcal{G}}_\lambda(\theta)^{-1} = I, \ \text{ for } \ -\pi \le \theta < 0,$$

and

$$\mathcal{G}'_\lambda(\theta)\tilde{\mathcal{G}}_\lambda(\theta)^{-1} = \frac{1}{\lambda^2-1}\begin{pmatrix} \lambda^2 - \mathrm{e}^{2\mathrm{i}\xi(\theta)} & 2\mathrm{i}\lambda\sin\xi(\theta) \\ -2\mathrm{i}\lambda\sin\xi(\theta) & \lambda^2 - \mathrm{e}^{-2\mathrm{i}\xi(\theta)} \end{pmatrix}, \ \text{ for } \ 0 \le \theta < \pi.$$

Then the unitary matrix

$$U(\theta) = \frac{1}{\sqrt{2}}\begin{pmatrix} U_+(\theta) & U_-(\theta) \\ U_-(\theta) & U_+(\theta) \end{pmatrix},$$

with

$$U_\pm(\theta) = \left(1 \pm \sqrt{1-\lambda^2\sec|\xi(\theta)|}\right)^{1/2},$$

diagonalises the symbol $\mathcal{G}'_\lambda\tilde{\mathcal{G}}_\lambda^{-1}$,

$$U(\theta)\mathcal{G}'_\lambda\tilde{\mathcal{G}}_\lambda^{-1}U(\theta)^{-1} = \begin{pmatrix} \mu_\lambda^-(\theta) & 0 \\ 0 & \mu_\lambda^+(\theta) \end{pmatrix}.$$

where the eigenvalues are

$$\mu_\lambda^\pm(\theta) = 1, \ \text{ for } \ -\pi \le \theta < 0,$$

and

$$\mu_\lambda^\pm(\theta) = \left(\frac{\sqrt{\lambda^2-\cos^2\xi(\theta)} \pm \sin\xi(\theta)}{\sqrt{\lambda^2-1}}\right)^2, \ \text{ for } \ 0 \le \theta < \pi.$$

Since $U(\theta)$ only depends on $|\xi(\theta)|$ we may conclude that it is smooth by the same reasons as those given for the symbol $\tilde{\mathcal{G}}_\lambda$. Then we can apply again the localisation theorem (4.9) to the product $U\mathcal{G}'_\lambda\tilde{\mathcal{G}}_\lambda^{-1}U^{-1}$, and

$$\log D_X[\mathcal{G}'_\lambda\tilde{\mathcal{G}}_\lambda^{-1}] = \log D_X[U\mathcal{G}'_\lambda\tilde{\mathcal{G}}_\lambda^{-1}U^{-1}] - \log D_X[U] - \log D_X[U^{-1}] + O(1).$$

Due to the smoothness of U, the Widom theorem (4.6) gives the asymptotic behaviour of $\log D_X[U]$ and $\log D_X[U^{-1}]$. Since $\det U(\theta) = 1$, the linear, dominant term of their expansion in $|X|$ vanishes and the rest of the terms tend to a finite value when $|X| \to \infty$. This leads to conclude that

$$\log D_X[\mathcal{G}'_\lambda\tilde{\mathcal{G}}_\lambda^{-1}] = \log D_X[U\mathcal{G}'_\lambda\tilde{\mathcal{G}}_\lambda^{-1}U^{-1}] + O(1). \tag{7.26}$$

Notice that the product $U\mathcal{G}'_\lambda\tilde{\mathcal{G}}_\lambda^{-1}U^{-1}$ is diagonal and, therefore, the corresponding block Toeplitz matrix can be expressed, after a global change of basis, as the direct sum

of two Toeplitz matrices with symbol the eigenvalues $\mu_\lambda^+(\theta)$ and $\mu_\lambda^-(\theta)$. This fact implies that

$$\log D_X[U\mathcal{G}'_\lambda\tilde{\mathcal{G}}_\lambda^{-1}U^{-1}] = \log D_X[\mu_\lambda^+] + \log D_X[\mu_\lambda^-], \tag{7.27}$$

that allows to apply the conjecture for Toeplitz determinants with non smooth symbol that we have proposed in Section 7.1. We suppose that the Toeplitz determinants with symbol $\mu_\lambda^\pm$ behave as

$$\log D_X[\mu_\lambda^\pm] = s_0^\pm(\lambda)|X| + \sum_{k=1}^{|X|} k s_k^\pm(\lambda)s_{-k}^\pm(\lambda) + o(1), \tag{7.28}$$

where

$$s_k^\pm(\lambda) = \frac{1}{2\pi}\int_{-\pi}^{\pi} \log \mu_\lambda^\pm(\theta)\mathrm{e}^{\mathrm{i}\theta k}\mathrm{d}\theta$$

are the Fourier coefficients of the logarithm of the eigenvalues $\mu_\lambda^\pm(\theta)$.

Since the zero modes satisfy $s_0^+(\lambda) = -s_0^-(\lambda)$ then the linear terms of the expansion (7.28) cancel in (7.27) and, therefore,

$$\log D_X[U\mathcal{G}'_\lambda\tilde{\mathcal{G}}_\lambda^{-1}U^{-1}] = \sum_{k=1}^{|X|} k\left[s_k^+(\lambda)s_{-k}^+(\lambda) + s_k^-(\lambda)s_{-k}^-(\lambda)\right] + O(1). \tag{7.29}$$

Collecting (7.25), (7.26) and (7.29), we conclude that the asymptotic behaviour of $\log D_X(\lambda)$ is given by

$$\log D_X(\lambda) = \log(\lambda^2-1)|X| + \sum_{k=1}^{|X|} k\left[s_k^+(\lambda)s_{-k}^+(\lambda) + s_k^-(\lambda)s_{-k}^-(\lambda)\right] + O(1). \tag{7.30}$$

As it happened in the previous chapters if we insert the linear term of this expansion in the contour integral (7.23) it vanishes and, therefore, the leading contribution to the entanglement entropy is given by the sum of the Fourier coefficients $s_k^\pm(\lambda)$.

We have to study now the behaviour of $s_k^\pm(\lambda)$ for large k. Since $\mu_\lambda^\pm(\theta) = 1$ for $-\pi \leq \theta < 0$, we have that

$$s_k^\pm(\lambda) = \frac{1}{\pi}\int_0^\pi \log\frac{\sqrt{\lambda^2-\cos^2\xi(\theta)} \pm \sin\xi(\theta)}{\sqrt{\lambda^2-1}}\mathrm{e}^{\mathrm{i}k\theta}\mathrm{d}\theta.$$

We can deal with this integral following the same steps as those described in Appendix E for the Fourier coefficients of $\log g_\nu$. Then we arrive at the expression

$$s_k^\pm(\lambda) = \frac{\mathrm{i}}{k\pi}\int_0^{k\pi} \log\frac{\sqrt{\lambda^2-\cos^2\xi\left(\frac{\mathrm{i}t}{k}\right)} \pm \sin\xi\left(\frac{\mathrm{i}t}{k}\right)}{\sqrt{\lambda^2-1}}\mathrm{e}^{-t}\mathrm{d}t + O(k^{-2}). \tag{7.31}$$

The functions $\cos\xi(\mathrm{i}t/k)$ and $\sin\xi(\mathrm{i}t/k)$ depend on $F(\mathrm{i}t/k)$ and $G_\nu(\mathrm{i}t/k)$ according to (7.24). In $F(\mathrm{i}t/k)$ we can perform the expansion

$$F\left(\frac{\mathrm{i}t}{k}\right) = h + 2 + O(k^{-2})$$

for large k. With respect to G_ν, since it behaves similarly to $\log g_\nu$, we make the following approximation

$$G_\nu\left(\frac{\mathrm{i}t}{k}\right) \approx -\mathrm{i}\frac{\mathrm{i}t/k-\pi}{\left(-\log\frac{\mathrm{i}t}{A|k|}\right)^\nu}, \quad \text{for} \quad 0\leq t\leq \pi k.$$

Then, for large k, we have

$$G_\nu\left(\frac{\mathrm{i}t}{k}\right) \approx \frac{\mathrm{i}\pi}{(\log|k|)^\nu}+O\left(\frac{1}{(\log|k|)^{\nu+1}}\right).$$

Plugging these expansions in $\cos\xi(\mathrm{i}t/k)$ and $\sin\xi(\mathrm{i}t/k)$, we obtain

$$\cos\xi\left(\frac{\mathrm{i}t}{k}\right) \sim 1+O\left(\frac{1}{(\log|k|)^{2\nu}}\right), \tag{7.32}$$

and

$$\sin\xi\left(\frac{\mathrm{i}t}{k}\right) \sim -\frac{\pi}{(h+2)(\log|k|)^\nu}+O\left(\frac{1}{(\log|k|)^{3\nu}}\right). \tag{7.33}$$

Finally, putting (7.32) and (7.33) in the expression (7.31) for $s_k^\pm(\lambda)$ we find that, for large k,

$$s_k^\pm(\lambda) \sim \frac{\mathrm{i}}{k\pi}\log\frac{\sqrt{\lambda^2-1}\mp\frac{\pi}{(h+2)(\log|k|)^\nu}}{\sqrt{\lambda^2-1}}. \tag{7.34}$$

Now we are ready to derive the asymptotic behaviour of the Rényi entanglement entropy taking (7.30) and (7.34), and inserting them into the contour integral (7.23). As we have already said the linear contribution vanishes and we can write

$$S_{\alpha,X} = \frac{1}{4\pi\mathrm{i}}\lim_{\varepsilon\to1^+}\oint_{\mathscr{C}} f_\alpha(\lambda/\varepsilon)\frac{\mathrm{d}}{\mathrm{d}\lambda}E_X(\lambda)\mathrm{d}\lambda,$$

where

$$E_X(\lambda) = \sum_{k=1}^{|X|} k\left[s_k^+(\lambda)s_{-k}^+(\lambda)+s_k^-(\lambda)s_{-k}^-(\lambda)\right]+O(1). \tag{7.35}$$

As usual, we perform an integration by parts,

$$S_{\alpha,X} = -\frac{1}{4\pi\mathrm{i}}\lim_{\varepsilon\to1^+}\oint_{\mathscr{C}}\frac{\mathrm{d}f_\alpha(\lambda/\varepsilon)}{\mathrm{d}\lambda}E_X(\lambda)\mathrm{d}\lambda. \tag{7.36}$$

Since $s_k^\pm(\lambda)$ is analytic outside the real interval $[-1,1]$, we can simplify the latter integral if we deform the integration contour $\mathscr{C}$ to infinity and follow the same strategy and considerations as in Section 4.2.

When $\alpha=1$, as we illustrated in Fig. 4.2, the only contribution to the integral in $S_{\alpha,X}$ is due to the change in the phase of $\mathrm{d}f_\alpha(\lambda/\varepsilon)/\mathrm{d}\lambda$ when, integrating along the branch cuts of this function, we go around its branch points $\lambda=\pm\varepsilon$. Then, for $\alpha=1$, we have

$$S_{1,X} = \frac{1}{2}\int_1^\infty E_X(\lambda)\mathrm{d}\lambda. \tag{7.37}$$

Observe that if in the latter expression we substitute $E_X(\lambda)$ for (7.35) and we apply the approximation (7.34) for the Fourier coefficients $s_k^{\pm}$ then we have to deal with the sum of two integrals of the form

$$\int_1^\infty \left[\log\left(1+\frac{\rho}{\sqrt{\lambda^2-1}}\right)\right]^2 \mathrm{d}\lambda \sim -\rho^2\log\rho + \frac{\log 2}{2}\rho^2,$$

where $\rho = \pi/(h+2)(\log|k|)^{-\nu}$.

Taking into account this behaviour in (7.37), and approximating the sum over k to an integral, we finally find

$$S_{1,X} \sim C_1^{(\nu)}(\log|X|)^{1-2\nu}\left(D_1^{(\nu)}\log\log|X|+1\right), \quad \text{for} \quad 0<\nu<1/2,$$

where the constants $C_1^{(\nu)}$ and $D_1^{(\nu)}$ depend on h and ν. They can in principle be determined through a straightforward but cumbersome procedure. Their expressions are rather involved and we think that it is no worth writing them here. They are simpler for integer $\alpha > 1$, for which we do give their explicit form.

For the limiting case $\nu = 1/2$, we obtain

$$S_{1,X} \sim C_1^{(1/2)}\log(\log|X|)(D_1^{(1/2)}\log\log|X|+1),$$

where $C_1^{(1/2)}$ and $D_1^{(1/2)}$ depend on h.

On the other hand, for integer $\alpha > 1$, the function $\mathrm{d}f_\alpha(\lambda)/\mathrm{d}\lambda$ has poles at the points of the imaginary axis

$$\lambda_l = \mathrm{i}\tan\frac{\pi(2l-1)}{2\alpha}, \quad l=1,\ldots,\alpha, \quad l\neq\frac{\alpha+1}{2}.$$

Therefore, $S_{\alpha,X}$ can be written as the sum over all the residues of the integrand in (7.36) at these points,

$$S_{\alpha,X} = \frac{1}{2(1-\alpha)}\sum_{l=1}^{\alpha} E_X(\lambda_l). \tag{7.38}$$

Observe that

$$\begin{aligned} k s_k^{\pm}(\lambda_l)s_{-k}^{\pm}(\lambda_l) &\sim -\frac{1}{k\pi^2}\left[\left(\arctan\frac{\pi\sqrt{c(\lambda_l)}}{(\log|k|)^\nu}\right)^2 + O\left(\frac{1}{(\log|k|)^{3\nu}}\right)\right], \\ &\sim -\frac{c(\lambda_l)}{k(\log|k|)^{2\nu}} + O\left(\frac{1}{k(\log|k|)^{3\nu}}\right), \end{aligned}$$

where

$$c(\lambda) = \frac{1}{(h+2)^2(|\lambda|^2+1)}.$$

If we plug this behaviour into (7.38) and approximate the sum over k by an integral, we obtain that the Rényi entanglement entropy for integer $\alpha > 1$ grows with $|X|$ as

$$S_{\alpha,X} \sim C_\alpha^{(\nu)}(\log|X|)^{1-2\nu} + O\left((\log|X|)^{1-3\nu}\right), \quad \text{for} \quad 0<\nu<1/2, \tag{7.39}$$

where

$$C_\alpha^{(\nu)} = \frac{1}{\alpha - 1} \sum_{l=1}^{\alpha} \frac{c(\lambda_l)}{1 - 2\nu}.$$

On the other hand,

$$S_{\alpha,X} \sim C_\alpha^{(1/2)} \log\log |X| + O\left(\frac{1}{\sqrt{\log |X|}}\right), \quad \text{for} \quad \nu = 1/2,$$

with

$$C_\alpha^{(1/2)} = \frac{1}{\alpha - 1} \sum_{l=1}^{\alpha} c(\lambda_l).$$

In conclusion, we expect a sublogarithmic growth of the Rényi entanglement entropy in the ground state of the Hamiltonian (7.22) with logarithmic decaying pairings. To our knowledge, this kind of behaviour has not been reported in the literature. A striking feature of our result is that the next terms in the expansion (7.39) are of the form $(\log |X|)^{1-m\nu}$ with $m = 3, 4, \ldots$. Therefore, all the terms for which $m < 1/\nu$ also diverge in the limit $|X| \to \infty$. This makes that very similar, divergent terms mix up and, therefore, it is difficult to isolate numerically the leading asymptotic behaviour. We have suffered this problem in our numerical experiments in which we are able to show the sublogarithmic behaviour of the entanglement entropy but it has been impossible for us to determine numerically its concrete form. We plan to tackle this problem in the near future.

Chapter 8

Conclusions

In this thesis, we have studied the asymptotic behaviour of the Rényi entanglement entropy in the stationary states of fermionic chains described by a general quadratic, homogeneous Hamiltonian that can present long-range couplings, and may break parity and charge conjugation symmetries.

Since the stationary states of these systems satisfy the Wick decomposition theorem, the analysis of the entanglement entropy can be performed using the two-point correlation matrix. In particular, we have been able to express the Rényi entanglement entropy in terms of the determinant of the resolvent of the correlation matrix. Then the study of the entanglement entropy is reduced to examine the determinant of a matrix.

The translational invariance of the chain implies that the correlation matrix is a block Toeplitz matrix. The asymptotic behaviour of the determinant of this kind of matrices has been the object of an intense study. However, here we have had to deal with some cases that, to our knowledge, have not been considered before in the literature. Then, motivated by our physical problem, we have investigated more deeply into the theory of block Toeplitz determinants discovering some novel results:

- We have considered block Toeplitz matrices with a symbol that has jump discontinuities. We have derived the leading contribution of the discontinuities to the determinant of these matrices as well as the expression for the coefficient of this term, that only depends on the value of the symbol at each side of the discontinuities. This result generalises the Fisher-Hartwig conjecture for Toeplitz determinants.

- Inspired by the results of Conformal Field Theory (CFT) on the entanglement entropy, we have proposed an expression for the asymptotic behaviour of the determinant of general principal submatrices of a block Toeplitz matrix. More specifically, our result relates the determinant of the submatrix to the product of several others of the block Toeplitz type. Then, combined with the result of the previous point, it provides the asymptotic scaling of the determinants of this type of submatrices. The numerical tests have confirmed the validity of this conjecture.

- We have established a conjecture to account for the asymptotic behaviour of Toeplitz determinants with a symbol that is continuous, therefore the Fisher-Hartwig con-

jecture does not apply, and besides it breaks the smoothness condition of the Strong Szegő Theorem. For these cases, we propose a new asymptotic regime that leads to the sublogarithmic growth of the logarithm of the determinant.

  - We have checked numerically this conjecture for a family of continuous symbols whose derivative diverges at a single point. For them, we have found that the logarithm of the determinant of the Toeplitz matrix depends sublogarithmically on its dimension as predicted.
  - We have seen that our conjecture for the determinant of a principal submatrix is also valid for this family of symbols.

Equipped with the previous results on block Toeplitz determinants, we have extended further the understanding of entanglement in chains of spinless fermions:

- If the Hamiltonian does not have pairing couplings and, therefore, the number of particles in the stationary states is well defined, the correlation matrix is Toeplitz. Applying the Fisher-Hartwig conjecture, we have derived the complete asymptotic behaviour of the Rényi entanglement entropy for an interval in the stationary states of these chains.

  - We have seen that the states for which the leading term in the entanglement entropy is linear can be viewed as the ground state of a local fermionic ladder. Then, this linear growth can be explained in terms of the area law. We have also shown that the results of CFT can be applied in these ladders if we take an appropriate fragment, instead of an interval, as the subsystem.

- If the Hamiltonian contains pairing couplings, the correlation matrix is, in general, block Toeplitz. In this case, we have restricted our study to the ground state.

  - For non critical chains with finite range couplings, the symbol of the correlation matrix is smooth and, according to the Widom theorem, the entanglement entropy satisfies an area law. We have reviewed the known results for this case, clearing up the beautiful geometric framework behind them. The analysis of the entanglement entropy can be formulated in terms of a compact Riemann surface given by the couplings of the Hamiltonian and genus related to the range of the interactions. Then, in systems with parity and charge conjugation symmetry, we have obtained a closed expression for the entropy in terms of the Riemann theta function with characteristics. This approach has turned out to be very useful to obtain many of the other results.
  - If the symbol is discontinuous, then we have to resort to our result for block Toeplitz determinants with discontinuous symbol. According to it, the discontinuities give rise to a logarithmic term in the entanglement entropy. We have performed a thorough analysis of the physical origin, nature and contribution to the entanglement entropy of the discontinuities.
  - In particular, we have seen that the discontinuities due to the absence of mass gap are related to pinchings of the associated compact Riemann surface if the ground state preserves parity and also to the Fermi points if it breaks this symmetry. Their contribution to the coefficient of the logarithmic term is of the form expected by CFT.

  - We have found that the presence of long-range couplings may also produce discontinuities in the symbol. This implies that the entanglement entropy may grow logarithmically outside the critical points. In addition, the two lateral limits of the discontinuities due to the long-range couplings may not commute. In this case, their contribution to the logarithmic term of the entropy is non universal and it cannot be derived from a CFT.
  - We have applied our methods to the XY spin chain with a Dzyaloshinski-Moriya term, a model that breaks parity symmetry, and to the Long-Range Kitaev chain, that contains power-law decaying pairings, determining analytically the logarithmic term of the entanglement entropy in the whole parameter space of these systems.

- Using our conjecture for the determinant of a principal submatrix of a block Toeplitz matrix and the results for a single interval, we have obtained the expansion of the Rényi entanglement entropy for subsystems made up of several disjoint intervals.

- We have discovered a new symmetry of the entanglement entropy under the Möbius group that acts on the couplings of the Hamiltonian.

  - We have shown that the spectrum of the correlation matrix is asymptotically invariant under the action of the Möbius group when its symbol is smooth. As a by-product, we have discovered that there are families of theories connected by the 1+1 Lorentz group whose ground states are different but their entanglement spectrum is the same in the asymptotic limit.
  - When the symbol has discontinuities, we have found that the exponential of the Rényi entanglement entropy, the partition function, transforms like a product of homogeneous fields inserted at the points where the symbol is discontinuous. The scaling dimension of these fields is related to the contribution of the corresponding discontinuity to the coefficient of the logarithmic term in the entanglement entropy and it is proportional to the number of intervals that form the subsystem.
  - One striking aspect of the previous behaviour is its parallelism with that of primary fields in CFT under conformal transformations in space-time. Actually, under a conformal transformation, the partition function also behaves as the product of homogeneous fields but now inserted at the endpoints of the subsystem. Their dimension depends in this case on the number of discontinuities in the correlation matrix symbol.
  - This close similarity suggests the introduction of a larger group that includes Möbius and conformal transformations. This group acts on a *phase space* obtained from the cartesian product of the space of discontinuities of the symbol (momentum space) and of the endpoints of the intervals (real space). In this scenario, we have seen that the partition function transforms like the product of homogeneous fields inserted at the points consisting of combinations of discontinuities and endpoints.
  - The Möbius symmetry can be used to find and understand relations and dualities between different theories in terms of the entanglement entropy. We have applied this idea in the XY spin chain. As a result, we have found the constant term of the entanglement entropy in the Ising critical line.

- Using our conjecture for Toeplitz determinants generated by a continuous but non smooth symbol, we have discussed the possibility of unexplored behaviours for the entanglement entropy, different from the linear and the logarithmic growth with the length of the interval.
  - In particular, we have discovered that the entanglement entropy should display a sublogarithmic growth in the ground state of a Kitaev chain with logarithmic decaying pairings.

Conclusiones

En esta tesis hemos estudiado el comportamiento asintótico de la entropía de entrelazamiento de Rényi en los estados estacionarios de cadenas fermiónicas descritas por un Hamiltoniano cuadrático y homogéneo general que puede presentar acoplos de largo alcance y romper las simetrías de paridad y conjugación de carga.

Puesto que los estados estacionarios de estos sistemas cumplen el teorema de descomposición de Wick, el análisis de la entropía de entrelazamiento puede realizarse utilizando la matriz de correlaciones entre dos puntos. En particular, hemos expresado la entropía de entrelazamiento de Rényi en términos del determinante del resolvente de la matriz de correlaciones. De este modo, el estudio de la entropía de entrelazamiento se reduce a investigar el determinante de una matriz.

La invariancia translacional de la cadena implica que la matriz de correlaciones sea una matriz *block* Toeplitz. El comportamiento asintótico del determinante de este tipo de matrices ha sido muy estudiado. Sin embargo, en esta memoria hemos tenido que tratar con algunos casos que no nos consta que hayan sido considerados previamente en la literatura. De manera que, motivados por nuestro problema físico, hemos profundizado en la teoría de determinantes *block* Toeplitz descubriendo algunos nuevos resultados:

- Hemos considerado matrices *block* Toeplitz cuyo símbolo tiene discontinuidades de salto. Hemos derivado la contribución dominante de las discontinuidades en el determinante de estas matrices así como la expresión del coeficiente de este término, que únicamente depende del valor del símbolo a cada lado de las discontinuidades. Este resultado generaliza la conjetura de Fisher-Hartwig para determinantes de matrices Toeplitz.

- Inspirados por los resultados de la Teoría de Campos Conforme (CFT) sobre la entropía de entrelazamiento, hemos propuesto una expresión para el comportamiento asintótico del determinante de submatrices principales de una matriz *block* Toeplitz. Concretamente, nuestro resultado relaciona el determinante de la submatriz con el producto de varios otros que son *block* Toeplitz. Por tanto, combinada con el resultado del punto anterior, esta conjetura proporciona el comportamiento asintótico del determinante de esta clase de submatrices. Las comprobaciones numéricas han confirmado su validez.

- Hemos establecido una conjetura que da cuenta del comportamiento asintótico de determinantes de Toeplitz cuyo símbolo es continuo, por lo que la conjetura de Fisher-Hartwig no se aplica, y además rompe la condición de suavidad del teorema

fuerte de Szegő. Para esta situación, proponemos un nuevo régimen asintótico que lleva a un crecimiento sublogarítmico del logaritmo del determinante.

  - Hemos comprobado numéricamente esta conjetura para una familia de símbolos continuos cuya derivada diverge en un punto. Para ellos, hemos encontrado que el logaritmo del determinante de la matriz de Toeplitz crece sublogarítmicamente con su dimensión como predecíamos.
  - Hemos visto que nuestra conjetura sobre el determinante de una submatriz principal también es válida para esta familia de símbolos.

Provistos de los resultados anteriores sobre determinantes *block* Toeplitz, hemos ampliado el conocimiento de la entropía de entrelazamiento en cadenas de fermiones sin spin:

- Si el Hamiltoniano no tiene acoplos de *pairing* y, por tanto, el número de partículas en los estados estacionarios está bien definido entonces la matriz de correlaciones es de Toeplitz. Aplicando la conjetura de Fisher-Hartwig, hemos derivado el comportamiento asintótico completo de la entropía de entrelazamiento de Rényi para un único intervalo en los estados estacionarios de estas cadenas.

  - Hemos visto que los estados en los que el término dominante de la entropía de entrelazamiento es lineal pueden interpretarse como el estado fundamental de una escalera local de fermiones. Así, esta dependencia lineal en la longitud del intervalo puede explicarse de acuerdo a la ley de área. También hemos demostrado que los resultados de la CFT pueden aplicarse en estas escaleras si tomamos como subsistema un fragmento apropiado en lugar de un intervalo.

- Si el Hamiltoniano contiene términos de *pairing* entonces la matriz de correlaciones es, en general, *block* Toeplitz. En este caso, hemos limitado nuestro estudio al estado fundamental.

  - En cadenas no críticas con acoplos de alcance finito el símbolo de la matriz de correlaciones es suave y, de acuerdo con el teorema de Widom, la entropía de entrelazamiento satisface una ley de área. Hemos revisado los resultados conocidos en este caso, formalizando la elegante estructura geométrica que se esconde detrás de éstos. El análisis de la entropía de entrelazamiento puede formularse mediante una superficie de Riemann compacta determinada por las constantes de acoplo del Hamiltoniano y cuyo género está dado por el alcance de las interacciones. En sistemas con simetría de paridad y conjugación de carga hemos obtenido una expresión cerrada para la entropía en términos de la función theta de Riemann con características. Este enfoque ha resultado muy útil para obtener muchos de los otros resultados.
  - Si el símbolo es discontinuo entonces tenemos que recurrir a nuestro resultado para determinantes *block* Toeplitz cuyo símbolo es discontinuo. De acuerdo al mismo, las discontinuidades dan lugar a un término logarítmico en la entropía de entrelazamiento. Hemos realizado un análisis detallado del origen físico, naturaleza y contribución a la entropía de entrelazamiento de las discontinuidades.

  - En particular, hemos visto que las discontinuidades debidas a la ausencia de *gap* de masas están relacionadas con *pinchings* o estrangulamientos de la correspondiente superficie de Riemann compacta si el estado fundamental es invariante bajo paridad y también con los puntos de Fermi si rompe esta simetría. Su contribución al coeficiente del término logarítmico es de la forma prevista por la CFT.
  - Hemos encontrado que la presencia de acoplos de largo alcance también puede producir discontinuidades en el símbolo. Esto implica que la entropía puede crecer logarítmicamente fuera de los puntos críticos. Además, los límites laterales de las discontinuidades debidas a los acoplos de largo alcance pueden no conmutar. En este caso, su contribución al término logarítmico de la entropía es no universal y no puede derivarse a partir de una CFT.
  - Hemos aplicado nuestros métodos a la cadena de spines XY con un término de Dzyaloshinski-Moriya, un modelo que rompe la simetría de paridad, y a la cadena de Kitaev de largo alcance, que contiene términos de *pairing* que decaen siguiendo una ley de potencias, determinando analíticamente el término logarítmico de la entropía de entrelazamiento en el todo el espacio de parámetros de estos sistemas.

- Utilizando nuestra conjetura para el determinante de una submatriz principal de una matriz *block* Toeplitz y los resultados para un único intervalo, hemos obtenido la expansión de la entropía de entrelazamiento de Rényi para subsistemas formados por varios intervalos disjuntos.

- Hemos descubierto una nueva simetría de la entropía de entrelazamiento bajo el grupo de Möbius que actúa sobre los acoplos del Hamiltoniano.

  - Hemos demostrado que el espectro de la matriz de correlaciones es asintóticamente invariante bajo la acción del grupo de Möbius cuando su símbolo es suave. Como resultado, hemos encontrado que existen familias de teorías conectadas por el grupo de Lorentz 1+1 cuyos estados fundamentales son diferentes pero su espectro de entrelazamiento es el mismo en el límite asintótico.
  - Cuando el símbolo tiene discontinuidades, hemos encontrado que la exponencial de la entropía de entrelazamiento de Rényi, la función de partición, transforma como un producto de campos homogéneos insertados en los puntos donde el símbolo es discontinuo. La dimensión de escala de estos campos está relacionada con la contribución de la correspondiente discontinuidad al coeficiente del término logarítmico en la entropía y es proporcional al número de intervalos que forman el subsistema.
  - Un aspecto notable del comportamiento anterior es su paralelismo con el de los campos primarios en una CFT bajo transformaciones conformes en el espaciotiempo. De hecho, bajo transformaciones conformes, la función de partición también se comporta como un producto de campos homogéneos insertados ahora en los puntos extremos de los intervalos del subsistema. Su dimensión depende en este caso del número de discontinuidades en el símbolo de la matriz de correlaciones.
  - Esta estrecha similitud sugiere la introducción de un grupo más grande que incluye a las transformaciones de Möbius y conformes. Este grupo actúa sobre

un *espacio de fases* construido a partir del producto cartesiano del espacio de discontinuidades del símbolo (espacio de momentos) y del de extremos de los intervalos (espacio real). En este escenario, hemos visto que la función de partición transforma como un producto de campos homogéneos insertados en los puntos resultantes de la combinación de discontinuidades y extremos de los intervalos.

  - La simetría de Möbius puede emplearse para hallar y entender relaciones y dualidades entre diferentes teorías en términos de la entropía de entrelazamiento. Hemos aplicado esta idea en la cadena de spines XY. Como resultado, hemos obtenido el término constante de la entropía de entrelazamiento en la línea crítica de Ising.

- Utilizando nuestra conjetura para determinantes de Toeplitz generados por un símbolo que es continuo pero no suave, hemos discutido la posibilidad de comportamientos inexplorados para la entropía de entrelazamiento, diferentes del crecimiento lineal y logarítmico con la longitud del intervalo.

  - En particular, hemos descubierto que la entropía de entrelazamiento debería mostrar un crecimiento sublogarítmico en el estado fundamental de una cadena de Kitaev con *pairings* que decaen logarítmicamente.

Appendix A

In this Appendix we give some details on how we have obtained the numerical results presented in the thesis. The source code of the programs written for the calculations can be found in the GitHub repository: `https://github.com/f-ares/entanglement`.

We have calculated the Rényi entanglement entropy using the relation found in Section 2.3 between this quantity and the restriction of the two-point correlation matrix to the chosen subsystem X,

$$S_{\alpha,X} = \frac{1}{2(1-\alpha)} \operatorname{Tr} \log \left[\left(\frac{I + V_X}{2} \right)^{\alpha} + \left(\frac{I - V_X}{2} \right)^{\alpha} \right]. \tag{A.1}$$

As we discussed in that section, this formula reduces drastically the complexity of computing $S_{\alpha,X}$ with respect to its definition in terms of the reduced density matrix ρ_X. If $|X|$ is the number of sites in X, ρ_X is a matrix of dimension $2^{|X|} \times 2^{|X|}$ while the size of V_X is $2|X| \times 2|X|$.

Therefore, the numerical computation of $S_{\alpha,X}$ consists in calculating the correlation matrix V_X, obtaining its spectrum and inserting it in the expression (A.1). In the following, we shall present the tools employed and the problems found in each of these steps.

Calculation of the correlation matrix

Remember that the entries of V_X are of the form

$$(V_X)_{nm} = \frac{1}{2\pi} \int_{-\pi}^{\pi} \mathcal{G}(\theta) \mathrm{e}^{\mathrm{i}\theta(n-m)} \mathrm{d}\theta, \quad n, m \in X$$

where $\mathcal{G}(\theta)$ is the 2×2 matrix obtained in (2.39). If the symbol $\mathcal{G}(\theta)$ is sufficiently simple, as it happens with the states studied in Section 3.2.1, the integral can be determined analytically but, in general, we have to obtain the elements $(V_X)_{nm}$ calculating the integral numerically.

We have computed the entries of V_X with *Mathematica* [171]. The numerical integration has been done employing the function `NIntegrate`. In general, it works well for the symbols considered in this thesis taking the default parameters assumed by *Mathematica*. Nevertheless, there are some points that we must take into account.

The first one concerns the symbol $M(\theta)$ defined in (4.18). As we saw in Chapter 4, its analytical continuation to the Riemann sphere,

$$\mathcal{M}(z) = \frac{1}{\sqrt{\Phi^+(z)^2 - \Xi(z)\overline{\Xi(\overline{z})}}} \begin{pmatrix} \Phi^+(z) & \Xi(z) \\ -\overline{\Xi(\overline{z})} & -\Phi^+(z) \end{pmatrix},$$

is meromorphic on the Riemann surface described by the hyperelliptic curve $w^2 = P(z)$ introduced in (4.21). Remember that $P(z)$ is a polynomial that depends on the coupling constants in the Hamiltonian of the chain and it has half of its roots inside the unit disk and the other half outside it. In Section 4.2, we established the rule that the branch cuts of the curve $w^2 = P(z)$ must be chosen such that none of them cross the unit circle. This must be also taken into account in the numerical calculations.

That rule implies that *Mathematica* has to take the square root $\sqrt{\Phi^+(z)^2 - \Xi(z)\overline{\Xi(\overline{z})}}$ continuous at the unit circle. Or, in other words, the sign of this square root must be the same for all $z = \mathrm{e}^{\mathrm{i}\theta}$. We can make sure that the sign does not change with the following trick. Taking into account that $\Xi(z^{-1}) = -\Xi(z)$, consider the logarithmic derivative

$$f'(\theta) = \mathrm{i}\mathrm{e}^{\mathrm{i}\theta} \frac{(\Phi^+)'(\mathrm{e}^{\mathrm{i}\theta})\Phi^+(\mathrm{e}^{\mathrm{i}\theta}) + \Xi(\mathrm{e}^{\mathrm{i}\theta})\overline{\Xi'(\mathrm{e}^{\mathrm{i}\theta})} + \Xi'(\mathrm{e}^{\mathrm{i}\theta})\overline{\Xi(\mathrm{e}^{\mathrm{i}\theta})}}{\Phi^+(\mathrm{e}^{\mathrm{i}\theta})^2 + |\Xi(\mathrm{e}^{\mathrm{i}\theta})|^2}.$$

We solve this differential equation numerically employing the function `NDSolveValue` in the interval $\theta \in [-\pi, \pi]$ and taking as initial condition

$$f(0) = \frac{1}{2}\log\left[\Phi^+(1)^2 + |\Xi(1)|^2\right].$$

The result is a continuous interpolating function for $f(\theta)$ in the specified interval that can be used in other *Mathematica* functions and whose exponential gives the square root $\sqrt{\Phi^+(\mathrm{e}^{\mathrm{i}\theta})^2 + |\Xi(\mathrm{e}^{\mathrm{i}\theta})|^2}$ with constant sign.

We have to pay special attention to the situation in which pairs of roots of $P(z)$ merge at the unit circle. In this case, the system is critical, the corresponding Riemann surface is pinched and there is a global change of sign in the symbol $M(\theta)$ at the points where the roots collide.

We have implemented those discontinuities in the numerical computations as follows: according to the discussions in Sections 4.2.1 and 4.3 on the degeneration of the roots at the unit circle, we can replace the symbol $M(\theta)$ with $h(\theta)\mathcal{M}_\circ(\mathrm{e}^{\mathrm{i}\theta})$. Here $\mathcal{M}_\circ(z)$ is the 2×2 matrix obtained from the analytical continuation of $\mathcal{M}(z)$ removing all the roots that degenerate. The factor $h(\theta)$ is the piecewise constant function that takes values ± 1 and it has a jump at the points where $M(\theta)$ changes the sign due to a pinching of the Riemann surface. We have applied this strategy to compute the numerical points of Fig. 5.5, where we checked the transformation law of the entanglement entropy under the Möbius group in a theory with pinchings.

We also have to be careful when we consider matrices of large dimension as in Chapters 6 and 7. Observe that, in the entries of V_X, there is an oscillating factor $\mathrm{e}^{\mathrm{i}\theta(n-m)}$. When the size of V_X is of the order of 10^3, in some entries this term oscillates so fast that the function `NIntegrate` gives a wrong result. We have solved this problem taking as

integration rule the `LevinRule` with the default options considered by *Mathematica*. This integration strategy is intended for dealing with integrands with rapidly oscillating terms as it is our case. When the dimension of V_X is large it is also necessary to increase the maximum number of recursive subdivisions of the integration region with the option `MaxRecursion`. In our case, we set this parameter to 10^4.

For the same reason, we have also used the `NIntegrate` function with the `LevinRule` and the above value for `MaxRecursion` to compute the Fourier coefficients $s_k^{(\nu)}$ of the logarithm of the symbol g_ν in the Figs. 7.2, 7.3 and 7.4 of Chapter 7.

Computation of the spectrum of the correlation matrix

Once we have calculated the elements of the correlation matrix V_X we must obtain its spectrum. We have computed it with a program written in *C* employing two different mathematical libraries: the *GNU Scientific Library* (GSL) [115] and the *Intel Math Kernel Library* (MKL) [170].

We could also obtain the eigenvalues of the matrix in *Mathematica* using the function `Eigenvalues`. However, we experienced some problems with the management of the memory when the size of the matrix is large enough and the calculation becomes slow.

The numerical results presented in chapters from 2 to 6 have been obtained using GSL while the results in Chapter 7 have been calculated with MKL. As we explained in that chapter, the reason to use MKL is that we considered matrices with dimension such that it is required an amount of RAM memory that is not available in a standard computer. This forced us to employ High Performance Computing resources. In particular, we employed the supercomputer *Memento* [169], located at BIFI, University of Zaragoza. The nodes of this cluster have enough memory to store the matrices that we needed to study. Of course, one can use GSL in a supercomputer. However, the library MKL allows to perform the diagonalisation of the matrix in parallel, and we can exploit the power that this machine offers.

The library GSL includes the routine `gsl_eigen_herm` that it is specifically designed to calculate the eigenvalues of a Hermitian matrix as it is the case of V_X. We have not found any problems when we applied it to the matrices studied in this thesis.

In MKL the analogue routine for computing the spectrum of a Hermitian matrix is `zheev`. In this case we should be cautious when we want to parallelise the process.

MKL can parallelise the calculation of the eigenvalues splitting it in several threads using *OpenMP*. In order to make use of multithreading we have to indicate it with the command `mkl_set_num_threads(int threads)` before calling the function `zheev`. This specifies the number of threads that MKL should request for parallel computation on the current execution thread. By default, MKL can dynamically change the number of *OpenMP* threads. We have disabled the dynamic adjustment with the command `mkl_set_dynamic(0)`. Then the library attempts to use the number of threads indicated in `mkl_set_num_threads`.

An important aspect in parallel computation is the scalability of the algorithm. That is, its efficiency with the number of threads employed. The ideal situation would be that the execution time of the parallel algorithm decreases with respect to the sequential one as the number of threads employed grows. But the common situation is that the efficiency of the parallel algorithm is poorer from a certain number of threads. In our case, as we show in Fig. A.1, we have determined that the optimal number is `threads=8`. From this value the execution time of the diagonalisation begins to increase.

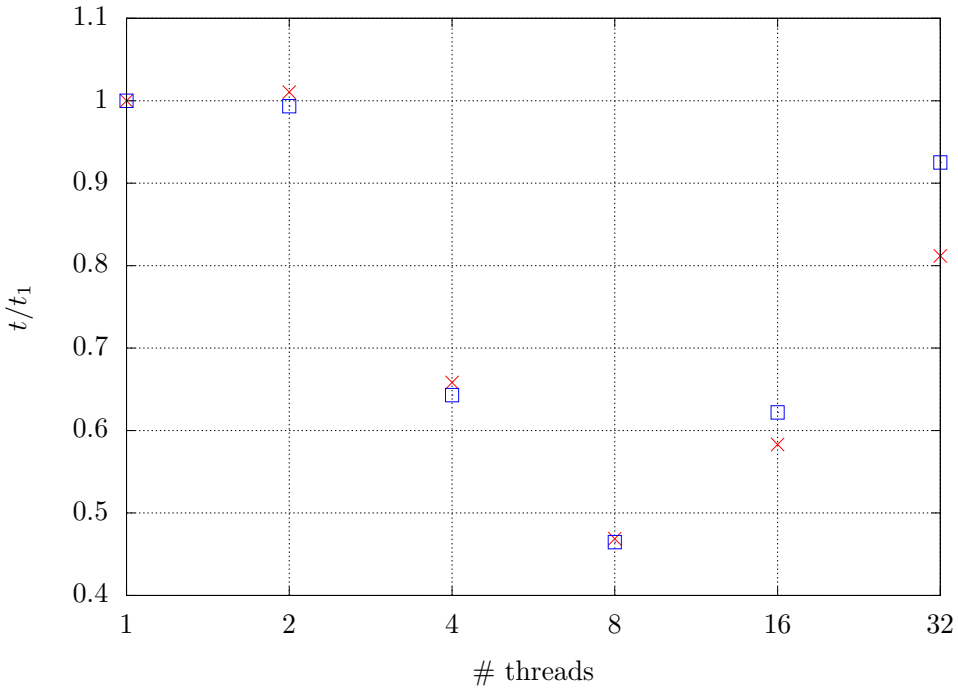

Figure A.1: In this plot we study the execution time of the diagonalisation of the Toeplitz matrix with symbol g_ν defined in (7.10), with $\nu = 0.25$ and $\beta = 1/\pi$, using the routine `zheev` included in the Intel MKL library. We represent the execution time t as a function of the number of threads in which the computation has been distributed normalised by the time t_1 spent using only one thread. For the points $\times$ the size of the matrix diagonalised is 10^4 while the points $\square$ correspond to dimension 2×10^4. The computation has been performed in a node of *Memento*, see [169], with two processors AMD Opteron 6272 (Interlagos). We have bound each thread to one core (32 in total).

Another point to take into account when we are paralellizing a routine is the affinity, or how the threads are distributed in the available CPUs. In our case, we have found that we gain a bit of performance by binding each thread to a core and banning the migration of the threads from one core to another. This can be done setting the *OpenMP* environment variable `OMP_PROC_BIND=TRUE`.

Appendix B

In this Appendix we describe the Wiener-Hopf factorisation of the matrix $\mathcal{M}_\lambda(z) = \lambda I - \mathcal{M}(z)$ where

$$\mathcal{M}(z) = \frac{1}{\sqrt{\Phi^+(z)^2 - \Xi(z)^2}} \begin{pmatrix} \Phi^+(z) & \Xi(z) \\ -\Xi(z) & -\Phi^+(z) \end{pmatrix}.$$

Here $\mathcal{M}(z)$ is the analytical continuation to the Riemann sphere $\overline{\mathbb{C}}$ of the symbol $M(\theta)$ for the ground state correlation matrix in non critical chains with PC symmetry and range of coupling L. We introduced $\mathcal{M}(z)$ in Section 4.2. The Wiener-Hopf factorisation of $\mathcal{M}_\lambda(z)$ was found in [124] by Its, Jin and Korepin for $L = 1$. The generalisation to higher values of L was done by Its, Mezzadri and Mo in [128].

The solution of the Wiener-Hopf factorisation problem for $\mathcal{M}_\lambda(z)$ is a pair of 2×2 matrices $u_+(z)$, $v_+(z)$, that are analytical inside the unit disk $|z| < 1$, and another pair $u_-(z)$, $v_-(z)$, analytical outside the unit disk, such that

$$\mathcal{M}_\lambda(z) = u_+(z)u_-(z) = v_-(z)v_+(z).$$

First of all, it is convenient to perform a change of basis and express $\mathcal{M}_\lambda(z)$ in the following form

$$\mathcal{M}_\lambda(z) = \frac{1}{2} \begin{pmatrix} 1 & 1 \\ -1 & 1 \end{pmatrix} \tilde{\mathcal{M}}_\lambda(z) \begin{pmatrix} 1 & -1 \\ 1 & 1 \end{pmatrix}$$

where

$$\tilde{\mathcal{M}}_\lambda(z) = \begin{pmatrix} \lambda & \sqrt{\mathfrak{g}(z)} \\ \sqrt{\mathfrak{g}(z)^{-1}} & \lambda \end{pmatrix}$$

with

$$\mathfrak{g}(z) = \frac{\Phi^+(z) + \Xi(z)}{\Phi^+(z) - \Xi(z)}.$$

Therefore, we shall look for the corresponding Wiener-Hopf factorisation of $\tilde{\mathcal{M}}_\lambda(z)$,

$$\tilde{\mathcal{M}}_\lambda(z) = \tilde{u}_+(z)\tilde{u}_-(z) = \tilde{v}_-(z)\tilde{v}_+(z),$$

where $\tilde{u}_+(z)$ and $\tilde{v}_+(z)$ are analytic inside the unit disk while $\tilde{u}_-(z)$ and $\tilde{v}_-(z)$ are analytic outside it.

Observe that, for $\lambda \neq \pm 1$,

$$(\lambda^2 - 1)\sigma_z \tilde{\mathcal{M}}_\lambda(z)^{-1} \sigma_z = \tilde{\mathcal{M}}_\lambda(z). \tag{B.1}$$

Using this identity we can derive $\tilde{u}_\pm(z)$ from $\tilde{v}_\pm(z)$,

$$\begin{aligned}\tilde{u}_+(z) &= (\lambda^2-1)\sigma_z\tilde{v}_+^{-1}(z)\sigma_z,\\ \tilde{u}_-(z) &= \sigma_z\tilde{v}_-^{-1}(z)\sigma_z.\end{aligned}$$

This means that we only have to find the matrices $\tilde{v}_\pm(z)$.

If we diagonalise $\tilde{\mathcal{M}}_\lambda(z)$, we have

$$\tilde{\mathcal{M}}_\lambda(z) = Q(z)DQ(z)^{-1},$$

where

$$Q(z) = \begin{pmatrix} -\sqrt{\mathfrak{g}(z)} & \sqrt{\mathfrak{g}(z)} \\ 1 & 1 \end{pmatrix}$$

and

$$D = \begin{pmatrix} \lambda-1 & 0 \\ 0 & \lambda+1 \end{pmatrix}.$$

Now, we introduce a 2×2 matrix $\Theta(z)$,

$$\tilde{\mathcal{M}}_\lambda(z) = Q(z)D\Theta(z)^{-1}\Theta(z)Q(z)^{-1}.$$

Then the problem is reduced to construct a matrix $\Theta(z)$ such that the product $\tilde{v}_+(z) = \Theta(z)Q(z)^{-1}$ is analytic inside the unit disk while $\tilde{v}_-(z) = Q(z)D\Theta(z)^{-1}$ is analytic outside it.

If we write explicitly the product $\Theta(z)Q(z)^{-1}$ we find

$$\Theta(z)Q(z)^{-1} = \frac{1}{2}\begin{pmatrix} -\sqrt{\mathfrak{g}(z)^{-1}}(\Theta_{11}-\Theta_{12}) & \Theta_{11}+\Theta_{12} \\ -\sqrt{\mathfrak{g}(z)^{-1}}(\Theta_{21}-\Theta_{22}) & \Theta_{21}+\Theta_{22} \end{pmatrix}, \tag{B.2}$$

where we have omitted the dependence of the entries of $\Theta(z)$ on z, $\Theta_{ij} = \Theta_{ij}(z)$. Therefore, the sum of the entries in each row of $\Theta(z)$ must be holomorphic inside the unit disk while the difference must cancel the discontinuities and singularities of $\sqrt{\mathfrak{g}(z)^{-1}}$ in this region.

On the other hand, for the product $Q(z)D\Theta(z)^{-1}$, we have

$$QD\Theta^{-1} = \frac{1}{\det\Theta}\begin{pmatrix} -\sqrt{\mathfrak{g}(z)}\,[(\lambda-1)\Theta_{22}+(\lambda+1)\Theta_{21}] & \sqrt{\mathfrak{g}(z)}\,[(\lambda-1)\Theta_{12}+(\lambda+1)\Theta_{11}] \\ (\lambda-1)\Theta_{22}-(\lambda+1)\Theta_{21} & (\lambda+1)\Theta_{11}-(\lambda-1)\Theta_{12} \end{pmatrix}.$$

As we explained in detail in Section 4.2, $\mathfrak{g}(z)$ is a rational function and $\sqrt{\mathfrak{g}(z)}$ is meromorphic in the compact Riemann surface described by the hyperelliptic curve

$$w^2 = P(z) = z^{2L}(\Phi^+(z)+\Xi(z))(\Phi^+(z)-\Xi(z)),$$

where $P(z)$ is a polynomial of degree $4L$. Therefore, the genus of the Riemann surface is $\mathrm{g} = 2L-1$. Let us assume that the roots of $P(z)$ are simple. Then half of them are inside the unit disk while the other half are outside it. We follow the rule established in Section 4.2, for the branch cuts of $w = \sqrt{P(z)}$. We take the $2L$ non intersecting curves Σ_ρ, $\rho = 0,\ldots,\mathrm{g}$, that join the roots of $P(z)$ $z_{2\rho+1}$ and $z_{2\rho+2}$ and do not cross the unit

circle. Hence $\sqrt{\mathfrak{g}(z)}$ is discontinuous at the points that belong to the branch cuts Σ_ρ and it has branch points at the roots of $P(z)$ z_j, $j = 1, \ldots, 4L$.

Before writing the form of $\Theta(z)$, we need to introduce several tools from the theory of compact Riemann surfaces. A nice book on this topic is for instance [172].

As in Section 4.2, we take for the homology basis of the Riemann surface described by $w = \sqrt{P(z)}$ the cycles a_r, b_r, $r = 1, \ldots, \mathrm{g}$. The cycle a_r surrounds anticlockwise the cut Σ_r in the upper sheet while the dual cycle b_r encloses clockwise the branch points $z_2, \ldots, z_{2r+1}$.

We also consider the basis of holomorphic forms

$$\mathrm{d}\eta_r = \frac{\phi_r(z)}{\sqrt{P(z)}}\mathrm{d}z,$$

where $\phi_r(z)$ is a polynomial of degree smaller than g. We normalise it demanding

$$\oint_{a_r} \mathrm{d}\eta_{r'} = \delta_{rr'}, \quad r, r' = 1, \ldots, \mathrm{g}. \tag{B.3}$$

The integration of the holomorphic forms along the b_r cycles gives the entries of the matrix of periods Π,

$$\Pi_{rr'} = \oint_{b_r} \mathrm{d}\eta_{r'}.$$

Now let us define the Abel-Jacobi map $\vec{\mathcal{A}}(z) = (\mathcal{A}_1(z), \ldots, \mathcal{A}_\mathrm{g}(z))$ taking as origin the branch point z_1,

$$\mathcal{A}_r(z) = \int_{z_1}^{z} \mathrm{d}\eta_r, \quad r = 1, \ldots, \mathrm{g}.$$

We also have to introduce the abelian differential of the third kind $\mathrm{d}\Delta$ with a simple pole at ∞ of residue $1/2$ and with the normalisation

$$\oint_{a_r} \mathrm{d}\Delta = 0, \quad r = 1, \ldots, \mathrm{g}. \tag{B.4}$$

Then we consider the map

$$\Delta(z) = \int_{z_1}^{z} \mathrm{d}\Delta.$$

In the neighbourhood of a branch point z_j, $j = 1, \ldots, 4L$, of $w = \sqrt{P(z)}$, $\vec{\mathcal{A}}(z)$ and $\Delta(z)$ can be written as

$$\vec{\mathcal{A}}(z) = \vec{\mathcal{A}}(z_j) + \sqrt{z - z_j}\, \vec{g}_{z_j}(z), \tag{B.5}$$

$$\Delta(z) = \Delta(z_j) + \sqrt{z - z_j}\, h_{z_j}(z), \tag{B.6}$$

where $\vec{g}_{z_j}(z)$ and $h_{z_j}(z)$ are holomorphic functions.

Therefore, the maps $\vec{\mathcal{A}}(z)$ and $\Delta(z)$ are discontinuous at the cuts Σ_ρ. We shall denote by $\vec{\mathcal{A}}_\pm(z)$ and $\Delta_\pm(z)$ the lateral limits of $\vec{\mathcal{A}}(z)$ and $\Delta(z)$ at each side of Σ_ρ. Thus, for a point $z \in \Sigma_\rho$ in the proximity of z_j, with $j = 2\rho + 1 + u$ and $u = 0, 1$,

$$\vec{\mathcal{A}}_\pm(z) = \vec{\mathcal{A}}(z_j) \pm \sqrt{z - z_j}\, \vec{g}_{z_j}(z),$$

$$\Delta_\pm(z) = \Delta(z_j) \pm \sqrt{z - z_j}\, h_{z_j}(z).$$

Since the origin of the Abel-Jacobi map is z_1

$$\vec{\mathcal{A}}(z_1) = \vec{0}. \tag{B.7}$$

Due to the normalisation (B.3) of the basis of holomorphic forms, for the rest of the branch points we have

$$\vec{\mathcal{A}}(z_2) = \frac{1}{2}\sum_{r=1}^{\mathrm{g}} \vec{M}_r, \tag{B.8}$$

and

$$\vec{\mathcal{A}}(z_{2r+1+u}) = \frac{\vec{N}_r - \delta_{1u}\vec{M}_r}{2} + \frac{\vec{M}_r}{2}\Pi, \quad r = 1, \dots, \mathrm{g}, \tag{B.9}$$

with $u = 0, 1$. The vectors $\vec{N}_r, \vec{M}_r \in \mathbb{Z}^{\mathrm{g}}$ have components

$$(\vec{N}_r)_{r'} = \begin{cases} 0, & r' < r \\ 1, & r' \geq r \end{cases},$$

and $(\vec{M}_r)_{r'} = \delta_{rr'}$, where $r' = 1, \dots, \mathrm{g}$.

On the other hand, for the map $\Delta(z)$ we have

$$\Delta(z_1) = 0, \quad \Delta(z_2) = \frac{\mathrm{i}\pi}{2},$$

and

$$\Delta(z_{2r+1+u}) = \frac{\mathrm{i}\pi}{2} + \mathrm{i}\pi\kappa_r, \quad r = 1, \dots, \mathrm{g}, \quad u = 0, 1,$$

where κ_r is the r-component of the vector

$$\vec{\kappa} = \frac{1}{2}\left(\oint_{b_1} \mathrm{d}\Delta, \dots, \oint_{b_{\mathrm{g}}} \mathrm{d}\Delta\right).$$

Therefore, the jumps of $\vec{\mathcal{A}}(z)$ and $\Delta(z)$ at the cuts satisfy the following equations.

For a point $z \in \Sigma_0$ close to z_1,

$$\vec{\mathcal{A}}_+(z) + \vec{\mathcal{A}}_-(z) = \vec{0},$$

$$\Delta_+(z) + \Delta_-(z) = 0.$$

For a point $z \in \Sigma_0$ close to z_2,

$$\vec{\mathcal{A}}_+(z) + \vec{\mathcal{A}}_-(z) = (1, 1, \dots, 1), \tag{B.10}$$

$$\Delta_+(z) + \Delta_-(z) = \mathrm{i}\pi. \tag{B.11}$$

For the rest of the cuts Σ_r, $r = 1, \dots, \mathrm{g}$, we have

$$\vec{\mathcal{A}}_+(z) + \vec{\mathcal{A}}_-(z) = \vec{n}_r + \vec{M}_r\Pi, \quad \vec{n}_r \in \mathbb{Z}^{\mathrm{g}}, \tag{B.12}$$

$$\Delta_+(z) + \Delta_-(z) = \mathrm{i}\pi + 2\pi\mathrm{i}\kappa_r. \tag{B.13}$$

Let us assume, without loss of generality, that z_1 is a zero of the rational function $\mathfrak{g}(z)$. Then the entries of the matrix $\Theta(z)$ can be expressed in terms of the Riemann theta function with characteristics (4.24) as follows,

$$\Theta_{11}(z) = \sqrt{z-z_1}\mathrm{e}^{-\Delta(z)}\frac{\vartheta\left[\begin{smallmatrix}\vec{\mu}\\ \vec{\nu}\end{smallmatrix}\right]\left(\vec{\mathcal{A}}(z)+\beta(\lambda)\vec{e}-\vec{\kappa}\right)}{\vartheta\left[\begin{smallmatrix}\vec{\mu}\\ \vec{\nu}\end{smallmatrix}\right]\left(\vec{\mathcal{A}}(z)\right)},$$

$$\Theta_{12}(z) = -\sqrt{z-z_1}\mathrm{e}^{\Delta(z)}\frac{\vartheta\left[\begin{smallmatrix}\vec{\mu}\\ \vec{\nu}\end{smallmatrix}\right]\left(\vec{\mathcal{A}}(z)-\beta(\lambda)\vec{e}+\vec{\kappa}\right)}{\vartheta\left[\begin{smallmatrix}\vec{\mu}\\ \vec{\nu}\end{smallmatrix}\right]\left(\vec{\mathcal{A}}(z)\right)},$$

$$\Theta_{21}(z) = -\sqrt{z-z_1}\mathrm{e}^{\Delta(z)}\frac{\vartheta\left[\begin{smallmatrix}\vec{\mu}\\ \vec{\nu}\end{smallmatrix}\right]\left(\vec{\mathcal{A}}(z)+\beta(\lambda)\vec{e}+\vec{\kappa}\right)}{\vartheta\left[\begin{smallmatrix}\vec{\mu}\\ \vec{\nu}\end{smallmatrix}\right]\left(\vec{\mathcal{A}}(z)\right)},$$

$$\Theta_{22}(z) = \sqrt{z-z_1}\mathrm{e}^{-\Delta(z)}\frac{\vartheta\left[\begin{smallmatrix}\vec{\mu}\\ \vec{\nu}\end{smallmatrix}\right]\left(\vec{\mathcal{A}}(z)-\beta(\lambda)\vec{e}-\vec{\kappa}\right)}{\vartheta\left[\begin{smallmatrix}\vec{\mu}\\ \vec{\nu}\end{smallmatrix}\right]\left(\vec{\mathcal{A}}(z)\right)},$$

with

$$\beta(\lambda) = \frac{1}{2\pi\mathrm{i}}\log\frac{\lambda+1}{\lambda-1},$$

and $\vec{e}\in\mathbb{Z}^{\mathrm{g}}$ whose first $L-1$ entries are 0 and the last L are 1.

We shall justify now why we have to take these entries for the matrix $\Theta(z)$. For this purpose we need to recall some properties of the the function $\vartheta\left[\begin{smallmatrix}\vec{\mu}\\ \vec{\nu}\end{smallmatrix}\right](z)$. It is quasi-periodic [92],

$$\vartheta\left[\begin{smallmatrix}\vec{\mu}\\ \vec{\nu}\end{smallmatrix}\right](\vec{z}+\vec{n}+\vec{m}\Pi) = \mathrm{e}^{\mathrm{i}2\pi(\vec{\mu}\cdot\vec{n}-\vec{\nu}\cdot\vec{m}-\frac{1}{2}\vec{m}\Pi\cdot\vec{m}-\vec{z}\cdot\vec{m})}\vartheta\left[\begin{smallmatrix}\vec{\mu}\\ \vec{\nu}\end{smallmatrix}\right](\vec{z})$$

for any $\vec{n},\vec{m}\in\mathbb{Z}^{\mathrm{g}}$.

The theta function also satisfies the parity property

$$\vartheta\left[\begin{smallmatrix}\vec{\mu}\\ \vec{\nu}\end{smallmatrix}\right](\vec{z}) = (-1)^{4\vec{\mu}\cdot\vec{\nu}}\vartheta\left[\begin{smallmatrix}\vec{\mu}\\ \vec{\nu}\end{smallmatrix}\right](-\vec{z})$$

if $\vec{\mu},\vec{\nu}\in(\mathbb{Z}/2)^{\mathrm{g}}$, as it will be our case.

Consider a point $z\in\Sigma_0$ in the neighbourhood of z_2. Taking into account the equations (B.10) and (B.11) for the jumps in $\vec{\mathcal{A}}(z)$ and $\Delta(z)$ and the previous properties of the theta function, we have

$$\begin{aligned}\mathrm{e}^{-\Delta_+(z)}\frac{\vartheta\left[\begin{smallmatrix}\vec{\mu}\\ \vec{\nu}\end{smallmatrix}\right]\left(\vec{\mathcal{A}}_+(z)\pm\beta(\lambda)\vec{e}-\vec{\kappa}\right)}{\vartheta\left[\begin{smallmatrix}\vec{\mu}\\ \vec{\nu}\end{smallmatrix}\right]\left(\vec{\mathcal{A}}_+(z)\right)} &= \mathrm{e}^{-\Delta_+(z)}\frac{\vartheta\left[\begin{smallmatrix}\vec{\mu}\\ \vec{\nu}\end{smallmatrix}\right]\left(-\vec{\mathcal{A}}_-(z)\pm\beta(\lambda)\vec{e}-\vec{\kappa}\right)}{\vartheta\left[\begin{smallmatrix}\vec{\mu}\\ \vec{\nu}\end{smallmatrix}\right]\left(-\vec{\mathcal{A}}_-(z)\right)}\\ &= -\mathrm{e}^{\Delta_-(z)}\frac{\vartheta\left[\begin{smallmatrix}\vec{\mu}\\ \vec{\nu}\end{smallmatrix}\right]\left(\vec{\mathcal{A}}_-(z)\mp\beta(\lambda)\vec{e}+\vec{\kappa}\right)}{\vartheta\left[\begin{smallmatrix}\vec{\mu}\\ \vec{\nu}\end{smallmatrix}\right]\left(\vec{\mathcal{A}}_-(z)\right)},\end{aligned}$$

for $z \in \Sigma_0$ close to z_2.

In the rest of the cuts Σ_r, $r = 1, \ldots, \mathrm{g}$, using the jump relations (B.12) and (B.13) for $\vec{\mathcal{A}}(z)$ and $\Delta(z)$ and the quasi-periodicity and parity of $\vartheta\left[\begin{smallmatrix}\vec{\mu}\\ \vec{\nu}\end{smallmatrix}\right]$, we find

$$\begin{aligned}
\mathrm{e}^{-\Delta_+(z)}\frac{\vartheta\left[\begin{smallmatrix}\vec{\mu}\\ \vec{\nu}\end{smallmatrix}\right]\left(\vec{\mathcal{A}}_+(z) \pm \beta(\lambda)\vec{e} - \vec{\kappa}\right)}{\vartheta\left[\begin{smallmatrix}\vec{\mu}\\ \vec{\nu}\end{smallmatrix}\right]\left(\vec{\mathcal{A}}_+(z)\right)} &= \mathrm{e}^{-\Delta_+(z) - 2\pi\mathrm{i}(\pm\beta(\lambda)\vec{e} - \vec{\kappa})\cdot\vec{M}_r}\frac{\vartheta\left[\begin{smallmatrix}\vec{\mu}\\ \vec{\nu}\end{smallmatrix}\right]\left(-\vec{\mathcal{A}}_-(z) \pm \beta(\lambda)\vec{e} - \vec{\kappa}\right)}{\vartheta\left[\begin{smallmatrix}\vec{\mu}\\ \vec{\nu}\end{smallmatrix}\right]\left(-\vec{\mathcal{A}}_-(z)\right)} \\
&= -\left(\frac{\lambda-1}{\lambda+1}\right)^{\pm e_r}\mathrm{e}^{\Delta_-(z)}\frac{\vartheta\left[\begin{smallmatrix}\vec{\mu}\\ \vec{\nu}\end{smallmatrix}\right]\left(\vec{\mathcal{A}}_-(z) \mp \beta(\lambda)\vec{e} + \vec{\kappa}\right)}{\vartheta\left[\begin{smallmatrix}\vec{\mu}\\ \vec{\nu}\end{smallmatrix}\right]\left(\vec{\mathcal{A}}_-(z)\right)},
\end{aligned}$$

for $z \in \Sigma_r$. We denote by e_r the r-component of the vector $\vec{e}$.

Given the form of the entries $\Theta(z)$, the above relations imply that they are discontinuous at the branch cuts Σ_ρ.

Observe that, since $e_r = 0$ for $r = 1, \ldots, L-1$, the lateral limits of the discontinuities in $\Theta(z)$ satisfy the relations

$$(\Theta_{11}(z))_+ = (\Theta_{12}(z))_-, \quad (\Theta_{12}(z))_+ = (\Theta_{11}(z))_-, \tag{B.14}$$

and

$$(\Theta_{22}(z))_+ = (\Theta_{21}(z))_-, \quad (\Theta_{21}(z))_+ = (\Theta_{22}(z))_-, \tag{B.15}$$

at the branch cuts Σ_ρ located inside the unit disk, i.e. $\rho = 0, \ldots, L-1$.

On the other hand, for the branch cuts outside the unit disk Σ_r, $r = L, \ldots, \mathrm{g}$, we have $e_r = 1$. Therefore, the discontinuities in $\Theta(z)$ at these cuts have lateral limits

$$(\Theta_{11}(z))_+ = \frac{\lambda-1}{\lambda+1}(\Theta_{12}(z))_-, \quad (\Theta_{12}(z))_+ = \frac{\lambda+1}{\lambda-1}(\Theta_{11}(z))_-, \tag{B.16}$$

and

$$(\Theta_{22}(z))_+ = \frac{\lambda+1}{\lambda-1}(\Theta_{21}(z))_-, \quad (\Theta_{21}(z))_+ = \frac{\lambda-1}{\lambda+1}(\Theta_{22}(z))_-. \tag{B.17}$$

Observe in (B.2) the entries of the product $\Theta(z)Q(z)^{-1}$. According to (B.14) and (B.15), $\Theta_{11}(z) + \Theta_{12}(z)$ and $\Theta_{21}(z) + \Theta_{22}(z)$ are continuous at the branch cuts inside the unit disk. Therefore, they are analytic in this region as we demanded.

On the other hand, $\Theta_{11}(z) - \Theta_{12}(z)$ and $\Theta_{21}(z) - \Theta_{22}(z)$ have a global change of sign at the cuts inside the unit disk. Therefore, in the neighbourhood of one of the branch points z_j that the cut Σ_ρ joins, they behave as

$$\Theta_{11}(z) - \Theta_{12}(z) \sim (z - z_j)^{\epsilon_j/2},$$

$$\Theta_{21}(z) - \Theta_{22}(z) \sim (z - z_j)^{\epsilon_j/2}.$$

The index ϵ_j is $+1$ if $\vec{\mathcal{A}}(z_j)$ is not a zero of the theta function $\vartheta\left[\begin{smallmatrix}\vec{\mu}\\ \vec{\nu}\end{smallmatrix}\right]$ while $\epsilon_j = -1$ if $\vec{\mathcal{A}}(z_j)$ is a zero of this function.

Since we need that $\sqrt{\mathfrak{g}(z)^{-1}}(\Theta_{11}(z)-\Theta_{12}(z))$ and $\sqrt{\mathfrak{g}(z)^{-1}}(\Theta_{21}(z)-\Theta_{22}(z))$ be analytic inside the unit disk, we have to impose that the zeros of $\vartheta\left[\begin{smallmatrix}\vec{\mu}\\ \vec{\nu}\end{smallmatrix}\right]\left(\vec{\mathcal{A}}(z)\right)$ must be the branch points that are poles of the rational function $\mathfrak{g}(z)$.

The theta function

$$\vartheta\left[\begin{smallmatrix}\vec{\mu}\\ \vec{\nu}\end{smallmatrix}\right]\left(\vec{\mathcal{A}}(z)\right)$$

has g zeros at $P_1, \ldots, P_{\mathrm{g}} \in \overline{\mathbb{C}}$ that satisfy

$$\sum_{r=1}^{\mathrm{g}} \vec{\mathcal{A}}(P_r) = \vec{\nu} + \vec{\mu}\,\Pi - \vec{K}, \tag{B.18}$$

with $\vec{\mu}, \vec{\nu} \in (\mathbb{Z}/2)^{\mathrm{g}}$ and the vector $\vec{K} \in \mathbb{C}^{\mathrm{g}}$ is the Riemann constant (see for instance [172]). The latter depends on the chosen homology basis. Let us determine it for our case.

Consider the branch points z_{2r+1}, $r = 1, \ldots, \mathrm{g}$. In (B.9) we have obtained

$$\vec{\mathcal{A}}(z_{2r+1}) = \frac{\vec{N}_r}{2} + \frac{\vec{M}_r}{2}\Pi.$$

If we take $\vec{\mu} = \vec{\nu} = 0$ and we apply the quasi-periodicity property of the theta function, we have

$$\vartheta\left[\begin{smallmatrix}\vec{0}\\ \vec{0}\end{smallmatrix}\right]\left(\vec{\mathcal{A}}(z_{2r+1})\right) = \mathrm{e}^{-\mathrm{i}\pi\vec{N}_r\cdot\vec{M}_r}\vartheta\left[\begin{smallmatrix}\vec{0}\\ \vec{0}\end{smallmatrix}\right]\left(-\vec{\mathcal{A}}(z_{2r+1})\right).$$

Since $\vec{N}_r \cdot \vec{M}_r = 1$ and due to the parity of the theta function, the above identity leads to conclude that the branch points z_{2r+1} are the zeros of $\vartheta\left[\begin{smallmatrix}\vec{0}\\ \vec{0}\end{smallmatrix}\right](\vec{\mathcal{A}}(z))$. In consequence, according to (B.18), the Riemann constant is

$$\vec{K} = -\sum_{r=1}^{\mathrm{g}} \vec{\mathcal{A}}(z_{2r+1}). \tag{B.19}$$

Once we have obtained the form of $\vec{K}$ we have to tune the characteristics $\vec{\mu}$, $\vec{\nu}$ such that the poles of $\mathfrak{g}(z)$ satisfy the condition (B.18) to be the zeros of $\vartheta\left[\begin{smallmatrix}\vec{\mu}\\ \vec{\nu}\end{smallmatrix}\right](\vec{\mathcal{A}}(z))$. Or, in other words, we have to take the condition (B.18) and to demand

$$\frac{\epsilon_2 - 1}{2}\vec{\mathcal{A}}(z_2) + \sum_{r=1}^{\mathrm{g}}\left[\frac{\epsilon_{2r+1}-1}{2}\vec{\mathcal{A}}(z_{2r+1}) + \frac{\epsilon_{2r+2}-1}{2}\vec{\mathcal{A}}(z_{2r+2})\right] = \vec{\nu} + \vec{\mu}\,\Pi - \vec{K},$$

with ϵ_j equals to $= +1$ if z_j is a zero of $\mathfrak{g}(z)$ and -1 if it is a pole.

If we apply (B.8), (B.9) and (B.19) in the latter expression we arrive at

$$\mu_r = \frac{1}{4}(\epsilon_{2r+1} + \epsilon_{2r+2}), \tag{B.20}$$

$$\nu_r = \frac{1}{4}\sum_{j=2}^{2r+1}\epsilon_j, \quad r = 1, \ldots, \mathrm{g}. \tag{B.21}$$

Coming back to the main discussion, if we take these characteristics for the theta functions in the entries of $\Theta(z)$ then $\sqrt{\mathfrak{g}(z)^{-1}}(\Theta_{11}(z)-\Theta_{12}(z))$ and $\sqrt{\mathfrak{g}(z)^{-1}}(\Theta_{21}(z)-\Theta_{22}(z))$

are analytic functions for $|z| < 1$. This allows to conclude that $\tilde{v}_+(z) = \Theta(z)Q(z)^{-1}$ is analytic inside the unit disk.

It remains to show that $\tilde{v}_- = Q(z)D\Theta(z)^{-1}$ is analytic outside the unit disk. The reasoning follows the same lines as for $\Theta(z)Q(z)^{-1}$. The only difference is that we have to employ the relations (B.16) and (B.17) for the jumps of $\Theta(z)$ at the cuts outside the unit disk. Notice that the determinant of $\Theta(z)$ also appears in this case.

Since $\det\Theta(z) = \Theta_{11}\Theta_{22} - \Theta_{12}\Theta_{21}$, it is straightforward to see using the relations for the lateral limits of the discontinuities in $\Theta(z)$ that the determinant is discontinuous at the cuts Σ_ρ, $\rho = 0, \ldots, \mathrm{g}$. The lateral limits satisfy

$$(\det\Theta(z))_+ = -(\det\Theta(z))_-, \quad z \in \Sigma_\rho.$$

Therefore, in the neighbourhood of one of the branch points z_j that is an endpoint of the cut Σ_ρ, the determinant behaves as

$$\det\Theta(z) \sim (z - z_j)^{\epsilon_j/2}.$$

Hence $\det\Theta(z)$ has the same discontinuities and singularities as $\sqrt{\mathfrak{g}(z)}$.

Appendix C

In this Appendix we shall check the consistency of the expression for $D_X(\lambda)$ that we introduced in (4.25). In particular we shall show that it does not depend on the order in which we choose the branch points of the hyperelliptic curve $w^2 = P(z)$, provided we take the first half inside and the last half outside the unit disk.

Suppose that we exchange the order of two roots z_{j_1} and z_{j_2}, with $j_\kappa = 2r_\kappa + 1 + u_\kappa, \kappa = 1, 2$ and $r_\kappa = 1, \ldots, \mathrm{g}$ and $u_\kappa = 0, 1$.

If we follow the prescriptions of Section 4.2, this induces a change in the fundamental cycles which are transformed into a'_r, b'_r, such that

$$a_r = \begin{cases} a'_r, & r \neq r_1, r_2, \\ a'_{r_1} + \Delta, & r = r_1, \\ a'_{r_2} - \Delta, & r = r_2 \end{cases} \quad , \qquad b_r = \begin{cases} b'_r, & r < r_1 + u_1, \\ b'_r + \Delta, & r_1 + u_1 \leq r \leq r_2 - 1 + u_2, \\ b'_r, & r > r_2 - 1 + u_2 \end{cases} \tag{C.1}$$

where

$$\Delta = b'_{r_2} - b'_{r_1} + \sum_{t=r_1+u_1}^{r_2-1+u_2} a'_t.$$

This transformation is a particular instance of the most general change of basis of cycles given by a modular transformation [140]

$$\begin{pmatrix} b \\ a \end{pmatrix} = \begin{pmatrix} A & B \\ C & D \end{pmatrix} \begin{pmatrix} b' \\ a' \end{pmatrix}, \qquad \begin{pmatrix} A & B \\ C & D \end{pmatrix} \in Sp_{2\mathrm{g}}(\mathbb{Z}).$$

The new period matrix is

$$\Pi' = (A - \Pi C)^{-1}(\Pi D - B).$$

While the normalized theta functions are related by

$$\widehat{\vartheta}\begin{bmatrix} \vec{p}' \\ \vec{q}' \end{bmatrix}(\vec{s}' \,|\, \Pi') = \mathrm{e}^{-\pi \mathrm{i} \vec{s} C \cdot \vec{s}'} \widehat{\vartheta}\begin{bmatrix} \vec{p} \\ \vec{q} \end{bmatrix}(\vec{s} \,|\, \Pi)$$

where

$$\vec{s}' = \vec{s}(C\Pi' + D), \tag{C.2}$$

and the characteristics verify

$$(\vec{p}', \vec{q}') \begin{pmatrix} b' \\ a' \end{pmatrix} = (\vec{p}, \vec{q}) \begin{pmatrix} b \\ a \end{pmatrix} - \frac{1}{2} \left(\mathrm{diag}(C^t A), \mathrm{diag}(D^t B) \right) \begin{pmatrix} b' \\ a' \end{pmatrix}.$$

In the particular case of the transformation (C.1), after a straightforward calculation, one obtains

$$(\vec{p}',\vec{q}')\begin{pmatrix} b' \\ a' \end{pmatrix} = (\vec{p},\vec{q})\begin{pmatrix} b \\ a \end{pmatrix} + \frac{1}{2}(u_1+u_2)(b'_{r_1}+b'_{r_2}) + \frac{1}{2}(u_1+u_2-2)\sum_{t=r_1+u_1}^{r_2-1+u_2} a'_t. \qquad \text{(C.3)}$$

We shall examine now how the arguments of the theta functions in (4.25), $\vec{s}=\pm\beta(\lambda)\vec{e}$, are modified by the transposition. Taking into account the definition of $\vec{e}$ and the form of the matrices C and D one has $\vec{e}\,C=0$ and $\vec{e}\,D=\vec{e}$ if and only if the two roots z_{j_1} and z_{j_2} that we exchange verify $j_1,j_2\le 2L$ or $j_1,j_2>2L$, which means that both roots sit at the same side of the unit circle. In this case applying (C.2) one has $\vec{s}\,'=\vec{s}=\pm\beta(\lambda)\vec{e}$.

In (4.26) we gave a prescription to obtain the characteristics for the theta functions involved in the computation of $D_X(\lambda)$. They depend on the position occupied by the poles and zeros of the rational function $\mathfrak{g}(z)$ which are labelled by a sign ϵ_j. If we exchange two of them, the original characteristics $\vec{\mu}$, $\vec{\nu}$ change into

$$\tilde{\mu}_r=\begin{cases}\mu_r, & r\neq r_1,r_2,\\ \mu_{r_1}+\frac{1}{4}\delta, & r=r_1,\\ \mu_{r_2}-\frac{1}{4}\delta, & r=r_2,\end{cases}\qquad \tilde{\nu}_r=\begin{cases}\nu_r, & r<r_1+u_1,\\ \nu_r+\frac{1}{4}\delta, & r_1+u_1\le r\le r_2-1+u_2,\\ \nu_r, & r>r_2-1+u_2,\end{cases} \qquad \text{(C.4)}$$

where $\delta=\epsilon_{j_2}-\epsilon_{j_1}$. These, in general, are different from those obtained by the application of (C.3) to $\vec{\mu}$ and $\vec{\nu}$ which we denote by $\vec{\mu}'$ and $\vec{\nu}'$. After a somehow lengthy but direct computation one obtains

$$\begin{aligned}(\vec{\tilde{\mu}}-\vec{\mu}',\vec{\tilde{\nu}}-\vec{\nu}')\begin{pmatrix} b' \\ a' \end{pmatrix} &= \left(u_1\frac{\epsilon_{j_1}-1}{2}-u_2\frac{\epsilon_{j_2}+1}{2}\right)b'_{r_2}-\left(u_1\frac{\epsilon_{j_1}+1}{2}-u_2\frac{\epsilon_{j_2}-1}{2}\right)b'_{r_1}\\ &\quad+\left((1-u_1)\frac{\epsilon_{j_1}-1}{2}-(1-u_2)\frac{\epsilon_{j_2}+1}{2}\right)\sum_{t=r_1+u_1}^{r_2-1+u_2}a'_t. \qquad \text{(C.5)}\end{aligned}$$

The important point to notice here is that, given that $u_\kappa=0,1$ and $\epsilon_j=\pm1$, one always has $\vec{\tilde{\mu}}-\vec{\mu}',\vec{\tilde{\nu}}-\vec{\nu}'\in\mathbb{Z}^{\mathrm{g}}$. This implies that

$$\widehat{\vartheta}\Big[\begin{smallmatrix}\vec{\tilde{\mu}}\\ \vec{\tilde{\nu}}\end{smallmatrix}\Big]=\widehat{\vartheta}\Big[\begin{smallmatrix}\vec{\mu}'\\ \vec{\nu}'\end{smallmatrix}\Big],$$

as one can easily check from the definitions.

Finally, putting everything together one has

$$\widehat{\vartheta}\Big[\begin{smallmatrix}\vec{\tilde{\mu}}\\ \vec{\tilde{\nu}}\end{smallmatrix}\Big](\pm\beta(\lambda)\vec{e}\,|\,\Pi')=\widehat{\vartheta}\Big[\begin{smallmatrix}\vec{\mu}'\\ \vec{\nu}'\end{smallmatrix}\Big](\pm\beta(\lambda)\vec{e}\,|\,\Pi')=\widehat{\vartheta}\big[\begin{smallmatrix}\vec{\mu}\\ \vec{\nu}\end{smallmatrix}\big](\pm\beta(\lambda)\vec{e}\,|\,\Pi),$$

where for the second equality we assume that the two branch points, whose order was exchanged, belong both to the first half of the ordering ($j_1,j_2\le 2L$) or both to the second half ($j_1,j_2>2L$).

From the equality of the normalized theta functions we deduce that a change in the order in which we take the roots does not affect the expression for the determinant, provided we do not exchange a root inside the unit disk with one outside.

Appendix D

We shall show in this Appendix that the Möbius transformations (5.3) act on the set of couplings $\mathbf{A} = (A_{-L}, \ldots, A_0, \cdots, A_L)$ and $\mathbf{B} = (B_{-L}, \ldots, B_0, \cdots, B_L)$ like the spin L representation of $SL(2, \mathbb{C})$.

For this purpose, let us see how the Laurent polynomials

$$\Phi(z) = \sum_{l=-L}^{L} A_l z^l, \quad \Xi(z) = \sum_{l=-L}^{L} B_l z^l$$

change under an arbitrary Möbius transformation. This can be done studying the representations of $SL(2, \mathbb{C})$ in the space of homogeneous polynomials of two complex variables. We shall follow Ref. [173].

To each element

$$g = \begin{pmatrix} a & b \\ c & d \end{pmatrix} \in SL(2, \mathbb{C})$$

it corresponds the linear transformation in $\mathbb{C}^2$

$$(z_1, z_2) \mapsto (az_1 + bz_2, cz_1 + dz_2).$$

Associated with this transformation we have the operator T_g which acts on the space of functions $f : \mathbb{C}^2 \to \mathbb{C}^2$ such that

$$T_g f(z_1, z_2) = f(az_1 + bz_2, cz_1 + dz_2). \tag{D.1}$$

Note that T_g is a reducible representation of $SL(2, \mathbb{C})$ in the space of functions of two complex variables. This space contains an invariant subspace under T_g: the space $\mathfrak{H}_{2L}$ of homogeneous polynomials in two variables of total degree $2L$,

$$h(z_1, z_2) = \sum_{l=-L}^{L} u_l z_1^{L+l} z_2^{L-l}.$$

The restriction of T_g to $\mathfrak{H}_{2L}$ is an irreducible representation of $SL(2, \mathbb{C})$.

There is an isomorphism between the space of Laurent polynomials $\mathfrak{L}_L$ of degree L in one (complex) variable and $\mathfrak{H}_{2L}$ given by

$$\begin{aligned} \varphi : \mathfrak{H}_{2L} &\longrightarrow \mathfrak{L}_L \\ h &\longmapsto \Upsilon(z) = z^{-L} h(z, 1), \end{aligned} \tag{D.2}$$

and

$$\begin{aligned}\varphi^{-1} : \mathfrak{L}_L &\longrightarrow \mathfrak{H}_{2L} \\ \Upsilon &\longmapsto h(z_1, z_2) = z_1^L z_2^L \, \Upsilon\left(z_1/z_2\right). \end{aligned} \tag{D.3}$$

If we call $T_g^{\mathcal{L}}$ the action of the $SL(2,\mathbb{C})$ group on the space of Laurent polynomials then we have the following commutative diagram

$$\begin{array}{ccc} \mathfrak{H}_{2L} & \xrightarrow{\varphi} & \mathfrak{L}_L \\ \Big\downarrow{\scriptstyle T_g} & & \Big\downarrow{\scriptstyle T_g^{\mathfrak{L}}} \\ \mathfrak{H}_{2L} & \xrightarrow[\varphi]{} & \mathfrak{L}_L \end{array}$$

where $T_g^{\mathfrak{L}}$ is given by

$$T_g^{\mathfrak{L}} = \varphi T_g \varphi^{-1}.$$

Then taking into account (D.1), (D.2) and (D.3) we obtain

$$T_g^{\mathfrak{L}} \Upsilon(z) = (az+b)^L (dz^{-1}+c)^L \Upsilon\left(\frac{az+b}{cz+d}\right). \tag{D.4}$$

Let us choose now as basis of $\mathfrak{L}_L$ the monomials $\{z^l\}$ with $-L \le l \le L$ and the $SU(2)$-invariant scalar product for which

$$(z^l, z^m) = \delta_{lm}, \quad -L \le l, m \le L. \tag{D.5}$$

The matrix elements of $T_g^{\mathfrak{L}}$ in this basis are

$$t_{lm}^{(g)} = (z^l, T_g^{\mathfrak{L}} z^m).$$

After a bit of algebra and using (D.4), (D.5) and Newton's binomial theorem we arrive at

$$\begin{aligned} t_{lm}^{(g)} = {} & [(L+l)!(L-l)!(L+m)!(L-m)!]^{-1/2} \\ & \sum_{j=\max(0,l-m)}^{\min(L-m,L+l)} \binom{L-m}{j} \binom{L+m}{L+l-j} a^{L+l-j} b^j c^{m-l+j} d^{L-m-j}. \end{aligned}$$

Therefore, the coefficients of the Laurent polynomial $\Upsilon(z)$ transform under $g \in SL(2,\mathbb{C})$ as

$$u_l' = \sum_{m=-L}^{L} t_{lm}^{(g)} u_m, \quad -L \le l \le L.$$

Since the coefficients of the Laurent polynomials $\Phi(z)$ and $\Xi(z)$ are precisely the couplings of the Hamiltonian, we have just found their behaviour under Möbius transformations,

$$A_l' = \sum_{m=-L}^{L} t_{lm}^{(g)} A_m; \quad B_l' = \sum_{m=-L}^{L} t_{lm}^{(g)} B_m.$$

Note that $t_{-l,-m}^{(g)} = t_{l,m}^{(g)}$ when $a = d$ and $b = c$, as it happens for the $SO(1,1)$ group. Therefore, in this case, the new couplings satisfy the required properties $A_{-l}' = \overline{A_l'}$ and $B_{-l}' = -B_l'$.

Appendix E

In this Appendix we shall determine the asymptotic behaviour of the Fourier coefficients of the function

$$\log g_\nu(\theta) = \beta \frac{\theta - \pi\,\mathrm{sign}(\theta)}{\left(-\log\frac{|\theta|}{A}\right)^\nu}, \quad \theta \in [-\pi, \pi),$$

with $\nu \geq 0$, $\beta < 1$ and $A > \pi$.

That is, the behaviour of

$$s_k^{(\nu)} = \frac{1}{2\pi}\int_{-\pi}^{\pi} \log g_\nu(\theta) \mathrm{e}^{\mathrm{i}\theta k}\mathrm{d}\theta$$

for large k.

Observe that we can express $s_k^{(\nu)}$ in the form

$$s_k^{(\nu)} = \frac{\mathrm{i}\beta}{\pi}\mathrm{Im}\int_0^{\pi} \frac{\theta - \pi}{\left(-\log\frac{|\theta|}{A}\right)^\nu}\mathrm{e}^{\mathrm{i}k\theta}\mathrm{d}\theta.$$

Consider that k is positive. If we perform the change of variables $z = k\theta$,

$$s_k^{(\nu)} = \frac{\mathrm{i}\beta}{\pi k}\mathrm{Im}\int_0^{k\pi} \frac{z/k - \pi}{\left(\log|k| - \log\frac{z}{A}\right)^\nu}\mathrm{e}^{\mathrm{i}z}\mathrm{d}z.$$

We extend now the domain of the integrand above to the complex plane. It has branch points at $z = 0$ and $z = Ak$. Then we take as branch cuts the real intervals $(-\infty, 0]$ and $[Ak, \infty)$. The integrand is analytic in the rest of the complex plane.

Then take the contour Γ represented in Fig. E.1. Applying the Cauchy residue theorem we have

$$\oint_\Gamma \frac{z/k - \pi}{\left(\log|k| - \log\frac{z}{A}\right)^\nu}\mathrm{e}^{\mathrm{i}z}\mathrm{d}z = 0. \tag{E.1}$$

Therefore,

$$\begin{aligned} s_k^{(\nu)} &= \frac{\mathrm{i}\beta}{k\pi}\mathrm{Im}\left[\lim_{\varepsilon\to 0^+}\int_\varepsilon^{k\pi} \frac{z/k - \pi}{\left(\log|k| - \log\frac{z}{A}\right)^\nu}\mathrm{e}^{\mathrm{i}z}\mathrm{d}z\right] \\ &= -\frac{\mathrm{i}\beta}{k\pi}\mathrm{Im}\left[\lim_{\varepsilon\to 0^+}\int_{\Gamma_1\cup\Gamma_2} \frac{z/k - \pi}{\left(\log|k| - \log\frac{z}{A}\right)^\nu}\mathrm{e}^{\mathrm{i}z}\mathrm{d}z\right] \end{aligned}$$

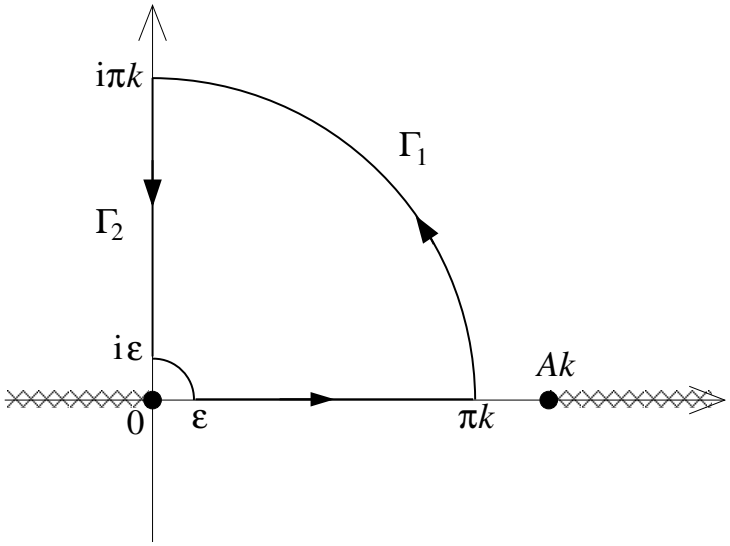

Figure E.1: Contour of integration, cuts and branch points for the computation of the Fourier coefficients of $\log g_\nu$ using the contour integral (E.1). The integrand has branch points at 0 and Ak with $A > \pi$ and $k > 0$. The branch cuts are the real intervals $[Ak, \infty)$ and $(-\infty, 0]$.

where Γ_1 and Γ_2 are the curves indicated in Fig. E.1.

With respect to the integral along the arc Γ_1,

$$I_1 = \frac{\mathrm{i}\beta}{k\pi}\mathrm{Im}\int_{\Gamma_1}\frac{z/k-\pi}{\left(\log|k|-\log\frac{z}{A}\right)^\nu}\mathrm{e}^{\mathrm{i}z}\mathrm{d}z,$$

if we take $z = k\pi\mathrm{e}^{\mathrm{i}\varphi}$ then

$$I_1 = \mathrm{i}\beta\pi\,\mathrm{Im}\int_0^{\pi/2}\frac{\mathrm{e}^{\mathrm{i}\varphi}-1}{\left(\log\frac{A}{\pi}-\mathrm{i}\varphi\right)^\nu}\,\mathrm{e}^{\mathrm{i}k\pi\cos\varphi}\mathrm{e}^{-k\pi\sin\varphi}\mathrm{i}\mathrm{e}^{\mathrm{i}\varphi}\mathrm{d}\varphi.$$

Hence

$$|I_1| \le \beta\pi\int_0^{\pi/2}\frac{|\mathrm{e}^{\mathrm{i}\varphi}-1|}{\left|\log\frac{A}{\pi}-\mathrm{i}\varphi\right|^\nu}\mathrm{e}^{-k\pi\sin\varphi}\mathrm{d}\varphi = \beta\pi\int_0^{\pi/2}\sqrt{\frac{2-2\cos\varphi}{\left(\left(\log\frac{A}{\pi}\right)^2+\varphi^2\right)^\nu}}\mathrm{e}^{-k\pi\sin\varphi}\mathrm{d}\varphi.$$

Since the integrand in the latter expression decays exponentially with k for $0 < \varphi \le \pi/2$, the only non-neglectible contribution when k is large enough to the integral is due to the points close to $\varphi = 0$. Therefore, taking into account that $\cos\varphi \approx 1-\varphi^2/2$ and $\sin\varphi \approx \varphi$ for $\varphi \ll 1$, we can approximate the integral above as

$$\int_0^{\pi/2}\sqrt{\frac{2-2\cos\varphi}{\left(\left(\log\frac{A}{\pi}\right)^2+\varphi^2\right)^\nu}}\mathrm{e}^{-k\pi\sin\varphi}\mathrm{d}\varphi \approx \int_0^{\pi/2}\frac{\varphi}{\left(\log\frac{A}{\pi}\right)^\nu}\mathrm{e}^{-k\pi\varphi}\mathrm{d}\varphi = \frac{1-\mathrm{e}^{-k\pi^2}(1+k\pi^2/2)}{\left(\log\frac{A}{\pi}\right)^\nu\pi^2k^2}.$$

Thus we can conclude that

$$|I_1| = O(k^{-2})$$

and, therefore,

$$s_k^{(\nu)} = -\frac{\mathrm{i}\beta}{k\pi}\mathrm{Im}\left[\lim_{\varepsilon\to0^+}\int_{\Gamma_2}\frac{z/k-\pi}{\left(\log|k|-\log\frac{z}{A}\right)^\nu}\,\mathrm{e}^{\mathrm{i}z}\mathrm{d}z\right] + O(k^{-2}). \tag{E.2}$$

Consider now

$$I_2 = \frac{\mathrm{i}\beta}{k\pi}\mathrm{Im}\int_0^{\mathrm{i}k\pi} \frac{z/k-\pi}{\left(\log|k| - \log\frac{z}{A}\right)^{\nu}}\,\mathrm{e}^{\mathrm{i}z}\mathrm{d}z.$$

If we perform the change of variables $t = -\mathrm{i}z$,

$$I_2 = \frac{\mathrm{i}\beta}{k\pi}\mathrm{Re}\int_0^{k\pi} \frac{\mathrm{i}t/k-\pi}{\left(\log|k| - \log\frac{\mathrm{i}t}{A}\right)^{\nu}}\,\mathrm{e}^{-t}\mathrm{d}t.$$

Assuming $k > 1$, let us express the integral above in the form

$$I_2 = \frac{\mathrm{i}\beta}{k\pi(\log|k|)^{\nu}}\mathrm{Re}\int_0^{k\pi} (\mathrm{i}t/k-\pi)\left(1 - \frac{\log\frac{t}{A} + \mathrm{i}\pi/2}{\log|k|}\right)^{-\nu}\mathrm{e}^{-t}\mathrm{d}t,$$

and expand the denominator using

$$(1+a)^{-\nu} = 1 - \nu a + O(a^2), \quad \text{if} \quad |a| < 1.$$

Therefore

$$I_2 = \frac{\mathrm{i}\beta}{k\pi(\log|k|)^{\nu}}\mathrm{Re}\int_0^{k\pi} (\mathrm{i}t/k-\pi)\left[1 + \nu\frac{\log\frac{t}{A} + \mathrm{i}\pi/2}{\log|k|} + O\left(\frac{1}{(\log|k|)^2}\right)\right]\mathrm{e}^{-t}\mathrm{d}t.$$

If we restrict the expansion of the integrand in terms of $1/\log|k|$ to first order and we take the real part then

$$I_2 = -\frac{\mathrm{i}\beta}{k(\log|k|)^{\nu}}\int_0^{k\pi} \mathrm{e}^{-t}\left(1 + \frac{\nu\log\frac{t}{A}}{\log|k|} + O\left(\frac{1}{(\log|k|)^2}\right)\right)\mathrm{d}t.$$

Hence

$$I_2 = -\frac{\mathrm{i}\beta}{k(\log|k|)^{\nu}}\left[1 - \nu\frac{\log A + \gamma_{\mathrm{E}}}{\log|k|} + O\left(\frac{1}{(\log|k|)^2}\right)\right].$$

Applying this result in (E.2) we find that

$$s_k^{(\nu)} \sim -\frac{\mathrm{i}\beta}{k(\log|k|)^{\nu}} + \frac{\mathrm{i}\beta\nu(\log A + \gamma_{\mathrm{E}})}{k(\log|k|)^{\nu+1}} + O\left(\frac{1}{k(\log|k|)^{\nu+2}}\right) \tag{E.3}$$

when k is large enough.

Bibliography

[1] E. Schrödinger, *Discussion of probability relations between separated systems*, Math. Proc. Cambridge Philos. Soc. 31 (1935) 555–563.

[2] E. Schrödinger, *Probability relations between separated systems*, Math. Proc. Cambridge Philos. Soc. 32 (1936) 446–451.

[3] A. Peres, D. Terno, *Quantum Information and Relativity Theory*, Rev. Mod. Phys. 76, 93 (2004), `arXiv:quant-ph/0212023`

[4] A. Einstein, B. Podolski, N. Rosen, *Can quantum-mechanical description of physical reality be considered complete?*, Phys. Rev. 47, 777 (1935)

[5] J. S. Bell, *On the Einstein Podolski Rosen paradox*, Physics, 1, 195-200 (1964)

[6] S. J. Freedman, J. F. Clauser, *Experimental Test of Local Hidden-Variable Theories*, Phys. Rev. Lett 28, 938 (1972)

[7] A. Aspect, P. Grangier, G. Roger, *Experimental tests of realistic local theories via Bell's theorem*, Phys. Rev. Lett. 47, 460 (1981)

[8] B. Hensen et al., *Loophole-free Bell inequality violation using electron spins separated by 1.3 kilometres*, Nature 526, 682–686 (2015), `arXiv:1508.05949 [quant-ph]`

[9] M. Giustina et al., *Significant-loophole-free test of Bell's theorem with entangled photons*, Phys. Rev. Lett. 115, 250401 (2015), `arXiv:1511.03190[quant-ph]`

[10] L. K. Shalm et al., *A strong loophole-free test of local realism*, Phys. Rev. Lett. 115, 250402 (2015), `arXiv:1511.03189[quant-phys]`

[11] J. Yin et al., *Satellite-based entanglement distribution over 1200 kilometers*, Science 356, Issue 6343, 1140-1144 (2017), `arXiv:1707.01339v1 [quant-ph]`

[12] R. Horodecki, P. Horodecki, M. Horodecki, K. Horodecki, *Quantum Entanglement*, Rev. Mod. Phys. 81, 865 (2009), `arXiv:quant-ph/0702225`

[13] R. P. Feynman, *Simulating Physics with Computers*, Int. J. Theor. Phys. 21, 467 (1982)

[14] M. A. Nielsen, I. L. Chuang, *Quantum Computation and Quantum Information*, Cambridge Univ. Press, Cambridge, 2000

[15] R. Jozsa, *Entanglement and Quantum Computation*, Geometric Issues in the Foundations of Science, Oxford University Press 1997, arXiv:quant-ph/9707034

[16] C. H. Bennett, D. P. DiVincenzo, *Quantum information and computation*, Nature 404, 247-255 (2000)

[17] X.-S. Ma et al., *Quantum teleportation over 143 kilometres using active feed-forward*, Nature 489, 269-273 (2012), arXiv:1205.3909 [quant-ph]

[18] L. Amico, R. Fazio, A. Osterloh, V. Vedral, *Entanglement in many-body systems*, Rev. Mod. Phys. 80, 517 (2008), arXiv:quant-ph/0703044

[19] N. Laflorencie, *Quantum entanglement in condensed matter systems*, Phys. Rep. 643, 1 (2016), arXiv:1512.03388 [cond-mat.str-el]

[20] P. Calabrese, J. Cardy, B. Doyon (Editors), *Entanglement entropy in extended quantum systems*, J. Phys. A: Math. Theor. 42 500301 (2009)

[21] A. Kitaev, J. Preskill, *Topological entanglement entropy*, Phys. Rev. Lett. 96, 110404 (2006), arXiv:hep-th/0510092

[22] A. Osterloh, L. Amico, G. Falci, R. Fazio, *Scaling of Entanglement close to a Quantum Phase Transitions*, Nature 416, 608-610 (2002), arXiv:quant-ph/0202029

[23] T. J. Osborne, M. A. Nielsen, *Entanglement in a simple quantum phase transition*, Phys. Rev. A 66, 032110 (2002), arXiv:quant-ph/0202162

[24] G. Vidal, J. I. Latorre, E. Rico, A. Kitaev, *Entanglement in quantum critical phenomena*, Phys. Rev. Lett. 90, 227902 (2003), arXiv:quant-ph/0211074

[25] S. R. White, *Density matrix formulation for quantum renormalization groups*, Phys. Rev. Lett. 69, 2863 (1992)

[26] G. Vidal, *Class of Quantum Many-Body States That Can Be Efficiently Simulated*, Phys. Rev. Lett. 101, 110501 (2008), arXiv:quant-ph/0610099

[27] J. I. Cirac, F. Verstraete, *Renormalization algorithms for Quantum-Many Body Systems in two and higher dimensions*, arXiv:cond-mat/0407066

[28] J. I. Cirac, F. Verstraete, *Renormalization and tensor product states in spin chains and lattices*, J. Phys. A: Math. Theor. 42, 504004 (2009), arXiv:0910.1130 [cond-mat.str-el]

[29] C. Monroe, J. Kim, *Scaling the Ion Trap Quantum Processor*, Science 339, Issue 6124, 1164–1169 (2013)

[30] A. Micheli, G.K. Brennen, P. Zoller, *A toolbox for lattice-spin models with polar molecules*, Nature Physics 2, 341-347 (2006), arXiv:quant-ph/0512222

[31] J. Zhang, G. Pagano, P. W. Hess, A. Kyprianidis, P. Becker, H. Kaplan, A. V. Gorshkov, Z.-X. Gong, C. Monroe, *Observation of a Many-Body Dynamical Phase Transition with a 53-Qubit Quantum Simulator*, Nature 551, 601-604 (2017), arXiv:1708.01044 [quant-ph]

[32] J. I. Cirac, P. Zoller, *Quantum computation with cold trapped ions*, Phys. Rev. Lett. 74, 4091 (1995)

[33] M. Plenio, S. Virmani, *An introduction to entanglement measures*, Quant. Inf. Comput. 7 1-51 (2007), arXiv:quant-ph/0504163

[34] A. Rényi, *On Measures of Entropy and Information*, Proc. Fourth Berkeley Symp. Math. Stat. and Probability, Vol. 1. Berkeley, CA: University of California Press, 547-561 (1961)

[35] C. H. Bennett, H. J. Bernstein, S. Popescu, B. Schumacher, *Concentrating partial entanglement by local operations*, Phys. Rev. A 53, 2046 (1996), arXiv:quant-ph/9511030

[36] H. Li, F.D.M. Haldane, *Entanglement Spectrum as a Generalization of Entanglement Entropy: Identification of Topological Order in Non-Abelian Fractional Quantum Hall Effect States*, Phys. Rev. Lett. 101, 010504 (2008), arXiv:0805.0332 [cond-mat.mes-hall]

[37] P. Calabrese, A. Lefevre, *Entanglement spectrum in one-dimensional systems*, Phys. Rev. A 78, 032329 (2008), arXiv:0806.3059 [cond-mat.str-el]

[38] L. Fidkowski, *Entanglement spectrum of topological insulators and superconductors*, Phys. Rev. Lett. 104, 130502 (2010), arXiv:0909.2654 [cond-mat.str-el]

[39] F. Franchini, A. R. Its, V. E. Korepin, L. A. Takhtajan, *Entanglement Spectrum for the XY Model in One Dimension*, Quantum Information Processing 10: 325-341 (2011), arXiv:1002.2931 [quant-ph]

[40] G. De Chiara, L. Lepori, M. Lewenstein, A. Sanpera, *Entanglement Spectrum, Critical Exponents, and Order Parameters in Quantum Spin Chains*, Phys. Rev. Lett. 109, 237208 (2012), arXiv:1104.1331 [cond-mat.stat-mech]

[41] X. Chen, E. Fradkin, *Quantum Entanglement and Thermal Reduced Density Matrices in Fermion and Spin Systems on Ladders*, J. Stat. Mech. (2013) P08013, arXiv:1305.6538 [cond-mat.str-el]

[42] J. Cardy, E. Tonni, *Entanglement hamiltonians in two-dimensional conformal field theory*, J. Stat. Mech. (2016) 123103, arXiv:1608.01283 [cond-mat.stat-mech]

[43] V. Alba, P. Calabrese, E. Tonni, *Entanglement spectrum degeneracy and Cardy formula in 1+1 dimensional conformal field theories* J. Phys. A: Math. Theor. 51 024001 (2018), arXiv:1707.07532 [hep-th]

[44] E. Tonni, J. Rodríguez-Laguna, G. Sierra, *Entanglement hamiltonian and entanglement contour in inhomogeneous 1D critical systems*, J. Stat. Mech. (2018) 043105, arXiv:1712.03557 [cond-mat.stat-mech]

[45] J. D. Bekenstein, *Black Holes and Entropy*, Phys. Rev. D 7, 2333 (1973)

[46] S. Hawking, *Particle creation by black holes*, Comm. Math. Phys. 43, 3, 199 (1975)

[47] L. Bombelli, R. K. Koul, J. Lee, R. D. Sorkin, *Quantum source of entropy for black holes*, Phys. Rev. D 34, 373 (1986)

[48] M. B. Hastings, *An area law for one-dimensional quantum systems*, J. Stat. Mech. (2007) P08024, arXiv:0705.2024 [quant-ph]

[49] F.G.S.L. Brandao, M. Horodecki, *An area law for entanglement from exponential decay of correlations*, Nature Physics 9, 721 (2013), arXiv:1309.3789 [quant-ph]

[50] F.G.S.L. Brandao, M. Horodecki, *Exponential Decay of Correlations Implies Area Law*, Comm. Math. Phys. 333, 761 (2015), arXiv:1206.2947 [quant-ph]

[51] A. A. Belavin, A. M. Polyakov, A. B. Zamolodchikov, *Infinite conformal symmetry in two-dimensional quantum field theory*, Nucl. Phys. B 241, 333-380 (1984)

[52] C. Holzhey, F. Larsen, F. Wilczek, *Geometric and renormalized entropy in conformal field theory*, Nucl. Phys. B 424, 443-467 (1994), hep-th/9403108

[53] P. Calabrese, J. Cardy, *Entanglement Entropy and Quantum Field Theory*, J. Stat. Mech. (2004) P06002, arXiv:hep-th/0405152

[54] A-X. Gong, M. Foss-Feig, F.G.S.L. Brandao, A. V. Gorshkov, *Entanglement area laws for long-range interacting systems*, Phys. Rev. Lett. 119, 050501 (2017), arXiv:1702.05368 [quant-ph]

[55] X.-L. Deng, D. Porras, J. I. Cirac, *Effective spin quantum phases in systems of trapped ions*, Phys. Rev. A 72, 063407 (2005), arXiv:quant-ph/0509197

[56] T. Koffel, M. Lewenstein, L. Tagliacozzo, *Entanglement Entropy for the Long-Range Ising Chain in a Transverse Field*, Phys. Rev. Lett. 109, 267203 (2012), arXiv:1207.3957 [cond-mat.str-el]

[57] M. G. Nezhadhaghighi, M. A. Rajabpour, *Quantum entanglement entropy and classical mutual information in long-range harmonic oscillators*, Phys. Rev. B 88, 045426 (2013), arXiv:1306.0982 [cond-mat.stat-mech]

[58] D. Vodola, L. Lepori, E. Ercolessi, A. V. Gorshkov, G. Pupillo, *Kitaev chains with long-range pairing*, Phys. Rev. Lett. 113, 156402 (2014), arXiv:1405.5440 [cond-mat.str-el]

[59] D. Vodola, L. Lepori, E. Ercolessi, and G. Pupillo, *Long-Range Ising and Kitaev Models: Phases, Correlations and Edge Modes*, New J. Phys. 18, 015001 (2016), arXiv:1508.00820 [cond-mat.str-el]

[60] J. Eisert, M. Cramer, M. B. Plenio, *Area laws for the entanglement entropy-a review*, Rev. Mod. Phys. 82, 277 (2010), arXiv:0808.3773 [quant-ph]

[61] G. 't Hooft, *Dimensional Reduction in Quantum Gravity*, arXiv:gr-qc/9310026

[62] L. Susskind, *The World as a Hologram*, J. Math. Phys. 36, 6377 (1995), arXiv:hep-th/9409089

[63] J. M. Maldacena, *The large N limit of superconformal field theories and supergravity*, Adv. Theor. Math. Phys. 2, 231 (1998), arXiv:hep-th/9711200

[64] S. Ryu, T. Takayanagi, *Holographic Derivation of Entanglement Entropy from AdS/CFT*, Phys. Rev. Lett. 96, 181602 (2006), arXiv:hep-th/0603001

[65] M. Van Raamsdonk, *Lectures on Gravity and Entanglement*, arXiv:1609.00026 [hep-th]

[66] I. Peschel, *Calculation of reduced density matrices from correlation functions*, J. Phys. A: Math. Gen., L205 (2003), arXiv:cond-mat/0212631

[67] P. Jordan, E. P. Wigner, *About the Pauli exclusion principle*, Zeitschrift fur Physik, 47,631–651 (1928)

[68] M. M. Wolf, G. Ortiz, F. Verstraete, J. I. Cirac, *Quantum Phase Transitions in Matrix Product Systems*, Phys. Rev. Lett. 97, 110403 (2006), arXiv:cond-mat/0512180

[69] W. Son, L. Amico, R. Fazio, A. Hamma, S. Pascazio, V. Vedral, *Quantum phase transition between cluster and antiferromagnetic states*, Europhys. Lett. 95, 50001 (2011), arXiv:1103.0251 [quant-ph]

[70] A. Deger, T.-C. Wei, *Geometric Entanglement and Quantum Phase Transition in Generalized Cluster-XY models*, arXiv:1702.01800 [quant-ph]

[71] A. Kitaev, *Unpaired Majorana fermions in quantum wires*, Phys.-Usp. 44 131, (2001), arXiv:cond-mat/0010440

[72] E. Lieb, T. Schulz, D. Mattis, *Two soluble models of an antiferromagnetic chain*, Annals of Physics, 16, 407-466 (1961)

[73] E. Barouch, B. M. McCoy, M. Dresden, *Statistical Mechanics of the XY Model. I*, Phys. Rev. A 2, 1075 (1970)

[74] E. Barouch, B. M. McCoy, *Statistical Mechanics of the XY Model. II. Spin-Correlation Functions*, Phys. Rev. A 3, 786 (1971)

[75] J. Kurmann, H. Thomas, G. Müller, *Antiferromagnetic Long-Range Order in the Anisotropic Quantum Spin Chain*, Physica A 112, 235 (1982)

[76] P. Zanardi, N. Paunković, *Ground state overlap and quantum phase transitions*, Phys. Rev. E 74, 031123 (2006), arXiv:quant-ph/0512249

[77] R. Islam, E. E. Edwards, K. Kim, S. Korenblit, C. Noh, H. Carmichael, G.-D.Lin, L.-M. Duan, C.-C. Joseph Wang, J. K. Freericks, C. Monroe, *Onset of a Quantum Phase Transition with a Trapped Ion Quantum Simulator*, Nature Commun. 2, 377 (2011), arXiv:1103.2400 [quant-ph]

[78] J. W. Britton, B. C. Sawyer, A. C. Keith, C.-C. J. Wang, J. K. Freericks, H. Uys, M. J. Biercuk, J. J. Bollinger, *Engineered two-dimensional Ising interactions in a trapped-ion quantum simulator with hundreds of spins*, Nature 484 , 489 (2012), arXiv:1204.5789 [quant-ph]

[79] H. Labuhn, D. Barredo, S. Ravets, S. de Léséleuc, T. Macrì, T. Lahaye, A. Browaeys, *Realizing quantum Ising models in tunable two-dimensional arrays of single Rydberg atoms*, Nature 534, 667 (2016), arXiv:1509.04543 [cond-mat.quant-gas]

[80] I. Dzyaloshinski, *A thermodynamic theory of "weak" ferromagnetism of antiferromagnetics*, J. Phys. Chem. Solids 4, 241 (1958)

[81] T. Moriya, *Anisotropic Superexchange Interaction and Weak Ferromagnetism*, Phys. Rev. 120, 91 (1960)

[82] S. Hernández-Santana, C. Gogolin, J. I. Cirac, A. Acín, *Correlation decay in fermionic lattice systems with power-law interactions at non-zero temperature*, Phys. Rev. Lett. 119, 110601 (2017), arXiv:1702.00371 [quant-ph]

[83] L. Lepori, D. Vodola, G. Pupilo, G. Gori, A. Trombettoni, *Effective Theory and Breakdown of Conformal Symmetry in a Long-Range Quantum Chain*, Annals of Physics 374, 35-66 (2016), arXiv:1511.05544 [cond-mat.str-el]

[84] M. van Regemortel, D. Sels, M. Wouters, *Information propagation and equilibration in long-range Kitaev chains*, Phys. Rev. A, 93, 032311 (2016), arXiv:1511.05459 [cond-mat.stat-mech]

[85] L. Lepori, A. Trombettoni, D. Vodola, *Singular dynamics and emergence of nonlocality in long-range quantum models*, J. Stat. Mech. 033102 (2017), arXiv:1607.05358 [cond-mat.str-el]

[86] K. Patrick, T. Neupert, J. K. Pachos, *Topological Quantum Liquids with Long-Range Couplings*, Phys. Rev. Lett. 118, 267002 (2017), arXiv:1611.00796 [cond-mat.str-el]

[87] L. Lepori, L. Dell'Anna, *Long-range topological insulators and weakened bulk-boundary correspondence,* New. J. Phys. 19, 103030 (2017), arXiv:1612.08155 [cond-mat.str-el]

[88] A. Alecce, L. Dell'Anna, *Extended Kitaev chain with longer-range hopping and pairing*, Phys. Rev. B 95, 195160 (2017), arXiv:1703.10086 [cond-mat.str-el]

[89] O. Viyuela, D. Vodola, G. Pupillo, M. A. Martín-Delgado, *Topological Massive Dirac Edge Modes and Long-Range Superconducting Hamiltonians*, Phys. Rev. B 94, 125121 (2016), arXiv:1511.05018[cond-mat.str-el]

[90] P. Cats, A. Quelle, O. Viyuela, M. A. Martín-Delgado, C. Morais-Smith, *Staircase to Higher Topological Phase Transitions*, Phys. Rev. B 97, 121106 (2018), arXiv:1710.05691[cond-mat.stat-mech]

[91] N. Sedlmayr, P. Jäger, M. Maiti, J. Sirker, *A bulk-boundary correspondence for dynamical phase transitions in one-dimensional topological insulators and superconductors*, Phys. Rev. B 97, 064304 (2018), arXiv:1712.03618 [cond-mat.stat-mech]

[92] *NIST Digital Library of Mathematical Functions*, `http://dlmf.nist.gov/`, Release 1.0.18 of 2018-03-27. F. W. J. Olver, A. B. Olde Daalhuis, D. W. Lozier, B. I. Schneider, R. F. Boisvert, C. W. Clark, B. R. Miller, and B. V. Saunders, eds.

[93] M.-C. Chung, I. Peschel, *Density-matrix spectra of solvable fermionic systems*, Phys. Rev. B 64, 064412 (2001), `arXiv:cond-mat/0103301`

[94] I. Peschel, V. Eisler, *Reduced density matrices and entanglement entropy in free lattice models*, J. Phys. A: Math. Theor. 42 (2009) 504003, `arXiv:0906.1663 [cond-mat.stat-mech]`

[95] I. Peschel, M.-C Chung, *On the relation between entanglement and subsystem Hamiltonians*, Europhys. Lett. 96 50006 (2011), `arXiv:1105.3917 [cond-mat.stat-mech]`

[96] I. Peschel, V. Eisler, *Analytical results for the entanglement Hamiltonian of a free-fermion chain*, J. Phys. A: Math. Theor. 50 284003 (2017), `arXiv:1703.08126 [cond-mat.stat-mech]`

[97] V. Eisler, I. Peschel, *Properties of the entanglement Hamiltonian for finite free-fermion chains*, `arXiv:1805.00078 [cond-mat.stat-mech]`

[98] B.-Q. Jin, V.E. Korepin, *Quantum Spin Chain, Toeplitz Determinants and Fisher-Hartwig Conjecture*, J. Stat. Phys. 116 (2004) 157-190, `arXiv:quant-ph/0304108`

[99] B. Kaufman, L. Onsager, *Crystal Statistics, III. Short-Range Order in a Binary Ising Lattice*, Phys. Rev. 76 1244 (1949)

[100] P. Deift, A. Its, I. Krasovsky, *Toeplitz matrices and Toeplitz determinants under the impetus of the Ising model. Some history and some recent results*, Comm. Pure Appl. Math. 66 (2013), 1360-1438, `arXiv:1207.4990v3 [math.FA]`

[101] G. Szegő, *On certain hermitian forms associated with the Fourier series of a positive function*, Festschrift Marcel Riesz, Lund (1952), 228–238

[102] M. E. Fisher, R. E. Hartwig, *Toeplitz determinants, some applications, theorems and conjectures*, Adv. Chem. Phys. 15, 333-353 (1968)

[103] A. Böttcher, B. Silbermann, *Analysis of Toeplitz Operators*, 2nd edition, Springer-Verlag, (2006)

[104] E. L. Basor, *A localization theorem for Toeplitz determinants*, Indiana Math. J. 28, 975 (1979)

[105] F. Ares, J. G. Esteve, F. Falceto, E. Sánchez-Burillo, *Excited state entanglement in homogeneous fermionic chains*, J. Phys. A: Math. Theor. 47 (2014) 245301, `arXiv:1401.5922 [quan-phys]`

[106] J. P. Keating, F. Mezzadri, *Random Matrix Theory and Entanglement in Quantum Spin Chains*, Commun. Math. Phys. 252 (2004), 543-579, `arXiv:quant-ph/0407047`

[107] J.P. Keating, F. Mezzadri, *Entanglement in Quantum Spin Chains, Symmetry Classes of Random Matrices, and Conformal Field Theory*, Phys. Rev. Lett. 94, 050501 (2005), arXiv:quant-ph/0504179

[108] V. Alba, M. Fagotti, P. Calabrese, *Entanglement entropy of excited states*, J. Stat. Mech. (2009) P10020, arXiv:0909.1999 [cond-mat.stat-mech]

[109] Z. Kádar, Z. Zimborás, *Entanglement entropy in quantum spin chains with broken reflection symmetry*, Phys. Rev. A 82, 032334 (2010), arXiv:1004.3112[quant-ph]

[110] V. Eisler, Z. Zimborás, *Area law violation for the mutual information in a nonequilibrium steady state*, Phys. Rev. A 89, 032321 (2014), arXiv:1311.3327[cond-mat.stat-mech]

[111] J. Hutchinson, N. G. Jones, *Fisher–Hartwig determinants, conformal field theory and universality in generalised XX models*, J. Stat. Mech. (2016) 073103, arXiv:1603.05612 [cond-mat.stat-mech]

[112] J. A. Carrasco, F. Finkel, A. González-López, M. A. Rodríguez, P. Tempesta, *Critical behavior of $su(1|1)$ supersymmetric spin chains with long-range interactions*, Phys. Rev. E 93, 062103 (2016), arXiv:1603.03668 [quant-ph]

[113] J. A. Carrasco, F. Finkel, A. González-López, M. A. Rodríguez, *Supersymmmetric spin chains with non-monotonic dispersion relation: criticality and entanglement entropy*, Phys. Rev. E 95, 012129 (2017), arXiv:1610.03989 [quant-ph]

[114] P. Calabrese, F. H. L. Essler, *Universal corrections to scaling for block entanglement in spin-1/2 XX chains*, J. Stat. Mech. (2010) P08029, arXiv:1006.3420 [cond-mat.stat-mech]

[115] M. Galassi et al, *GNU Scientific Library Reference Manual*, (3rd Ed.), ISBN 0954612078. http://www.gnu.org/software/gsl/

[116] G. Szegő, *Ein Grenzwertsatz über die Toeplitzschen Determinanten e iner reellen positiven Funktion*, Math Ann. 76 (1915), 490-503.

[117] I. A. Ibraginov, *A theorem of Gabor Szegő*, Mat. Zametki 3 (1968), 693–702 (In Russian, English translation: Math. Notes 3 (1968), 6, 442–448)

[118] B. Gyires, *Eigenwerte verallgemeinerter Toeplitzschen Matrizen*, Publ. Math. Debrecen 4 (1956), 171–179.

[119] I. I. Hirschman, *Matrix-valued Toeplitz operators*, Duke Math. J. 34, (1967), 403-415

[120] H. Widom, *Asymptotic Behavior of Block Toeplitz Matrices and Determinants*, Adv. in Math. 13, 284-322 (1974)

[121] H. Widom, *Asymptotic Behavior of Block Toeplitz Matrices and Determinants II*, Adv. in Math. 21:1 (1976), 1–29

[122] H. Widom, *On the Limit of Block Toeplitz Determinants*, Proceedings of the American Mathematical Society, Volume 50, 1, 167-173 (1975)

[123] A. R. Its, *The Riemann-Hilbert Problem and Integrable Systems*, Notices Am. Math. Soc. 50, 11 (2003)

[124] A. R. Its, B. Q. Jin, V. E. Korepin, *Entropy of XY spin chain and block Toeplitz determinants*, Fields Institute Communications, Universality and Renormalization, vol 50, page 151, (2007), arXiv:quant-ph/06066178

[125] F. Ares, J. G. Esteve, F. Falceto, A. R. de Queiroz, *Entanglement in fermionic chains with finite range coupling and broken symmetries*, Phys. Rev. A 92, 042334 (2015), arXiv:1506.06665 [quant-ph]

[126] F. Ares, J. G. Esteve, F. Falceto, A. R. de Queiroz, *Entanglement entropy in the Long-Range Kitaev chain*, Phys. Rev. A 97, 062301 (2018), arXiv:1801.07043 [quant-ph]

[127] P. Deift, A. R. Its, X. Zhou, *A Riemann-Hilbert approach to asymptotic problems arising in the theory of random matrix models, and also in the theory of integrable statistical mechanics*, Annals of Mathematics, 146 (1997), 149-235

[128] A. R. Its, F. Mezzadri, M. Y. Mo, *Entanglement entropy in quantum spin chains with finite range interaction*, Comm. Math. Phys. Vo. 284 117-185 (2008), arXiv:0708.0161v2 [math-ph]

[129] J. I. Latorre, E. Rico, G. Vidal, *Ground state entanglement in quantum spin chains*, Quant.Inf.Comput. 4 (2004) 48-92, arXiv:quant-ph/0304098

[130] H. A. Kramers, G. H. Wannier, *Statistics of the two-dimensional ferromagnet. Part 1.*, Phys. Rev. 60, 252 (1941); *Statistics of the Two-Dimensional Ferromagnet. Part II*, Phys. Rev. 60, 263 (1941)

[131] J. B. Kogut, *An introduction to lattice gauge theory and spin systems*, Rev. Mod. Phys. 51, 4 (1979)

[132] J.L. Cardy, O.A. Castro-Alvaredo, B. Doyon, *Form factors of branch-point twist fields in quantum integrable models and entanglement entropy*, J. Stat. Phys. 130:129-168 (2008), arXiv:0706.3384 [hep-th]

[133] I. Peschel, *On the entanglement entropy for an XY spin chain*, J. Stat. Mech. (2004) P12005, arXiv:cond-mat/0410416

[134] F. Franchini, A. R. Its, V. E. Korepin, *Rényi entropy of the XY spin chain*, J. Phys. A: Math. Theor. 41 (2008) 025302, arXiv:0707.2534 [quant-ph]

[135] F. Franchini, A. R. Its, B.-Q. Jin, V. E. Korepin, *Ellipses of Constant Entropy in the XY Spin Chain*, J. Phys. A: Math. Theor. 40 (2007) 8467-8478 arXiv:quant-ph/0609098

[136] F. Pientka, L. I. Glazman, F. von Oppen, *Topological superconducting phase in helical Shiba chains*, Phys. Rev. B 88, 155420 (2013), arXiv:1308.3969 [cond-mat.mes-hall]

[137] F. Ares, J. G. Esteve, F. Falceto, A.R. de Queiroz, *On the Möbius transformation in the entanglement entropy of fermionic chains*, J. Stat. Mech. (2016) 043106, arXiv:1511.02382 [math-ph]

[138] F. Ares, J. G. Esteve, F. Falceto, A. R. de Queiroz, *Entanglement entropy and Möbius transformations for critical fermionic chains*, J. Stat. Mech. (2017) 063104, arXiv:1612.07319 [quant-ph]

[139] F. Iglói, R. Juhász, *Exact relationship between the entanglement entropies of XY and quantum Ising chains*, Europhys. Lett. 81, 57003 (2008), arXiv:0709.3927 [cond-mat.stat-mech]

[140] J. Igusa, *Theta Functions*, Die Grundlehren der mathematischen Wissenschaften 194, Springer-Verlag (1972)

[141] P. Calabrese, J. Cardy, *Entanglement entropy and conformal field theory*, J. Phys. A: Math. Theor. 42 504005 (2009), arXiv:0905.4013 [cond-mat.stat-mech]

[142] V. Z. Enolski, T. Grava, *Singular $\mathbb{Z}_N$ -Curves and the Riemann-Hilbert Problem*, International Mathematics Research Notices 2004, No. 32, 1619–1683

[143] H. Casini, M. Huerta, *Reduced density matrix and internal dynamics for multicomponent regions*, Class. Quant. Grav. 26 185005 (2009), arXiv:0903.5284 [hep-th]

[144] M. Caraglio, F. Gliozzi, *Entanglement Entropy and Twist Fields*, JHEP 11 (2008) 076, arXiv:0808.4094 [hep-th]

[145] S. Furukawa, V. Pasquier, J. Shiraishi, *Mutual Information and Boson Radius in a c=1 Critical System in One Dimension*, Phys. Rev. Lett. 102, 170602 (2009), arXiv:0809.5113 [cond-mat.stat-mech]

[146] F. Iglói, I. Peschel, *On reduced density matrices for disjoint subsystems*, EPL 89, 40001 (2010), arXiv:0910.5671 [cond-mat.stat-mech]

[147] M. Fagotti, P. Calabrese, *Entanglement entropy of two disjoint blocks in XY chains*, J. Stat. Mech. P04016 (2010), arXiv:1003.1110 [cond-mat.stat-mech]

[148] P. Calabrese, J. Cardy, E. Tonni, *Entanglement entropy of two disjoint intervals in conformal field theory*, J. Stat. Mech. P11001 (2009), arXiv:0905.2069 [hep-th]

[149] P. Calabrese, J. Cardy, E. Tonni, *Entanglement entropy of two disjoint intervals in conformal field theory II*, J. Stat. Mech. P01021 (2011), arXiv:1011.5482 [hep-th]

[150] A. Coser, L. Tagliacozzo, E. Tonni, *On Rényi entropies of disjoint intervals in conformal field theory*, J. Stat. Mech. P01008 (2014), arXiv:1309.2189 [hep-th]

[151] M. Rajabpour, F. Gliozzi, *Entanglement entropy of two disjoint intervals from fusion algebra of twist fields*, J. Stat. Mech. P02016 (2012), arXiv:1112.1225 [hep-th]

[152] C. Nobili, A. Coser, E. Tonni, *Entanglement entropy and negativity of disjoint intervals in CFT: Some numerical extrapolations*, J. Stat. Mech. P06021 (2015), arXiv:1501.04311 [cond-mat.stat-mech]

[153] P. Ruggiero, E. Tonni, P. Calabrese, *Entanglement entropy of two disjoint intervals and the recursion formula for conformal blocks*, arXiv:1805.05975 [cond-mat.stat-mech]

[154] P. Facchi, G. Florio, C. Invernizzi, S. Pascazio, *Entanglement of two blocks of spins in the critical Ising model*, Phys. Rev. A 78, 052302 (2008), arXiv:0808.0600 [quant-ph]

[155] M. Fagotti, *New insights into the entanglement of disjoint blocks*, Europhys. Lett. 97 17007 (2012), arXiv:1110.3770 [cond-mat.stat-mech]

[156] V. E. Hubeny, M. Rangamani, *Holographic entanglement entropy for disconnected regions*, JHEP 03 (2008) 006, arXiv:0711.4118 [hep-th]

[157] H. Casini, M. Huerta, *Remarks on the entanglement entropy for disconnected regions*, JHEP 03 (2009) 048, arXiv:0812.1773 [hep-th]

[158] F. Ares, J. G. Esteve, F. Falceto, *Entanglement of several blocks in fermionic chains*, Phys. Rev. A 90, 062321 (2014), arXiv:1406.1668 [quant-ph]

[159] R. Movassagh, P. W. Shor, *Power law violation of the area law in quantum spin chains*, PNAS (2016): 201605716, arXiv:1408.1657 [quant-ph]

[160] O. Salberger, V. E. Korepin, *Fredkin Spin Chain*, arXiv:1605.03842 [quant-ph]

[161] O. Salberger, T. Udagawa, Z. Zhang, H. Katsura, I. Klich, V. E. Korepin, *Deformed Fredkin spin chain with extensive entanglement*, J. Stat. Mech. (2017) 063103, arXiv:1611.04983 [cond-mat.stat-mech]

[162] D. Bianchini, O. Castro-Alvaredo, B. Doyon, E. Levi, F. Ravanini, *Entanglement entropy of non-unitary conformal field theory*, J. Phys. A: Math. Theor. 48 04FT01, arXiv:1405.2804 [hep-th]

[163] M. Kac, *Toeplitz matrices, translation kernels and a related problem in probability theory*, Duke Math. J. 21, 501–509 (1954)

[164] G. Baxter, *A convergence equivalence related to polynomials orthogonal on the unit circle*, Trans. Amer. Math. Soc. 99 471–487 (1961)

[165] I. I. Hirschman, *On a theorem of Szegő, Kac and Baxter*, J. d'Analyse Math. 14, 225-234 (1965)

[166] A. Devinatz, *The Strong Szegő Limit Theorem*, Illinois J. Math. 11, 160-175 (1967)

[167] T. T. Wu, *Theory of Toeplitz Determinants and the Spin Correlations of the Two-Dimensional Ising Model. I*, Phys. Rev. 149 (1966), 380–400

[168] A. Lenard, *Momentum Distribution in the Ground State of the One-Dimensional System of Impenetrable Bosons*, J. Math. Phys. 5 (7) (1964), 930–943

[169] http://www.bifi.es/scientific-equipment/,

http://old.bifi.es/en/infrastructures/scientific-equipment/memento-caesaraugusta

[170] *Intel Math Kernel Library (MKL)*, `https://software.intel.com/en-us/mkl`

[171] Wolfram Research, Inc., *Mathematica*, `https://www.wolfram.com/mathematica/`

[172] H. M. Farkas, I. Kra, *Riemann Surfaces*, Springer, New York, 1992

[173] N. Ja. Vilenkin, *Special functions and the theory of group representations*, Translations of Mathematical Monographs, 22, AMS (1968)